Dissertation
submitted to the
Combined Faculties for the Natural Sciences and for Mathematics
of the Ruperto-Carola University of Heidelberg, Germany
for the degree of
Doctor of Natural Sciences

presented by

Anna Marta Pryszlak, Biologist (Diploma)

born in Gdańsk (Danzig), Poland

Oral-examination:

Functional Crosstalk between Human Papillomaviruses and Lentiviruses

Referees: Prof. Dr. Martin Müller
Prof. Dr. Felix Hoppe-Seyler

Creativity

is intelligence

having fun.

— Albert Einstein

Mojej rodzinie - za ich miłość i wsparcie
i Marco - za cierpliwość i wyrozumiałość

To my family - for their love and support
and to Marco - for his patience and understanding

TABLE OF CONTENTS

SUMMARY

Human papillomaviruses (HPVs) and human immunodeficiency virus-1 (HIV-1) are human pathogens of high biomedical significance worldwide. Interestingly, increasing epidemiological evidence indicates that individuals with active HPV infections possess an enhanced risk of being infected by HIV-1. These findings raise the possibility that HPVs may directly or indirectly increase the pathogenicity of lentiviruses, such as HIV-1.

Using a Vesicular Stomatitis Virus-G-(VSV-G)-pseudotyped vector as an experimental model system, and subsequently extending these analyses to HIV-1, this study defines a possible scenario which could account for the epidemiological association between HPV and HIV-1 infections. These results provide first insights into the interplay of two important human pathogens which may have profound clincial implications. Moreover, the findings of this study support the idea that the HPV vaccination may have a preventive effect against HIV-1 infections.

ZUSAMMENFASSUNG

Humane Papillomviren (HPVs) und das Human Immunodeficiency Virus-1 (HIV-1) sind humane Pathogene mit einer weltweit hohen biomedizinischen Relevanz. Interessanterweise gibt es zunehmend epidemiologischen Anhalt dafür, dass Individuen mit einer akuten HPV-Infektion ein erhöhtes Risiko tragen, HIV-1-Infektionen zu erwerben.

Dies weist darauf hin, dass HPVs direkt oder indirekt die Pathogenität von HIV-1 steigern könnten. Mittels eines Vesicular Stomatitis Virus-G-(VSV-G)-pseudotypisierten Vektors als experimentelles Modellsystem, und anschließender Ausweitung der Analysen auf HIV-1, erarbeiten die vorliegenden Untersuchungen ein mögliches Szenario, mit dem der epidemiologische Zusammenhang zwischen HPV- und HIV-1-Infektionen erklärt werden könnte. Diese Ergebnisse ermöglichen Einblicke in die Wechselwirkungen zweier bedeutsamer menschlicher Pathogene, mit wichtigen klinischen Implikationen. Darüber hinaus unterstützen die Resultate dieser Studie die Hypothese, daß die Vakzinierung gegen HPV möglicherweise einen präventiven Effekt gegenüber einer HIV-1-Infektion besitzen könnte.

ACKNOWLEDGMENTS

The following thesis was conducted at the German Cancer Research Center in Heidelberg, Germany, in the group “Molecular therapy of virus-associated cancers” under the supervision of and reviewed by Professor Felix Hoppe-Seyler.

This PhD work has been, for me, an exciting journey across many borders: the borders of countries and cultures, the borders of maturity - independence and the borders of knowledge. I would like to warmly thank all the people who accompanied me on this life-changing voyage. First of all, I would like to thank my supervisor and referee Professor Felix Hoppe-Seyler for the opportunity to work in his group on this exciting research topic. His critical evaluation taught me a great deal about good scientific practice. I am also grateful to Professor Karin Hoppe-Seyler for her didactic support, patience and understanding.

I would like to acknowledge my thesis referee, Professor Martin Müller (German Cancer Research Center), whose suggestions helped me a lot during my thesis advisory committee meetings. Professor Stephan Frings (University of Heidelberg) and Dr. Karin Müller-Decker (German Cancer Research Center) kindly agreed to join the thesis defense committee. I am also grateful to Professor Oliver Keppler (University of Frankfurt) for his enthusiasm and feedback during my TAC meetings.

I want to express my gratitude to all scientists who shared their skills and expertise with me. Our group members Julia Bulkescher, Claudia Lohrey and Angela Holzer helped me with their technical support. I am obliged to Dr. Eileen Reinz for her time and stimulating discussions. Without my fellow PhD students Anja Honegger, Jenny Leitz and Christina Stutz, the lab would be a much emptier place. I will especially warmly remember Christina, with whom I shared not only office space but also many inspiring talks. Thomas Holz solved all my computer problems. Claudia Tessmer guided my first steps in protein purification. Marco Raffaele Cosenza shared his expertise in confocal microscopy and this work is much more colorful thanks to him. Lis Müller and others from Prof. Martin Müller’s group supplied me with materials and all the help needed for HPV experiments.

This research would not have been possible without our collaboration partners. I would like to acknowledge the group of Prof. Oliver Keppler (University of Frankfurt). Our cooperation led to the confirmation of the E4 effect in infection by HIV-1 and other human viruses. Dr. Karsten Richter from the Imaging and Cytometry Core Facility (German Cancer Research Center) helped me with my first trial in preparing electron microscopy specimens and performed most of the imaging.

These three years of my PhD were filled by amazing people who always supported me. All the international friendships I made opened my eyes to new cultures, places and tastes. Many of my friends took time to read this thesis and shared suggestions, Janet and Anja in particular.

Finally, I want to thank those people without whom I wouldn’t be where I am now - my understanding and supporting parents, especially my mom, who will always be my best friend. During this time abroad, my brother has grown up to be a young man I am proud of. Here, in Germany, Marco become my partner, companion and friend and allowed me to always take science home and discuss it for hours. At last, words fail…

CHAPTER 1

INTRODUCTION

1.1 EPIDEMIOLOGICAL EVIDENCE OF A CROSSTALK BETWEEN HPV AND HIV

1.1.1 THE HPV LIFE CYCLE

Human papillomaviruses (HPVs) belong to the large family of *Papillomaviridae.* More than one hundred members of this family able to infect humans, have been described so far (de Villiers et al. 2004). The HPV genetic material consists of a double stranded DNA of approximately 8 kb. It contains eight open reading frames coding for six early (E) and two late (L) structural proteins. The HPV genome forms chromatin-like complexes by association with cellular histones (Favre et al. 1977, Howley 1996). Seventy-two star-shaped L1 pentamers assemble together with a much smaller and variable number of L2 proteins to form a non-enveloped viral capsid (Buck et al. 2008, Finnen et al. 2003) (Fig. 1).

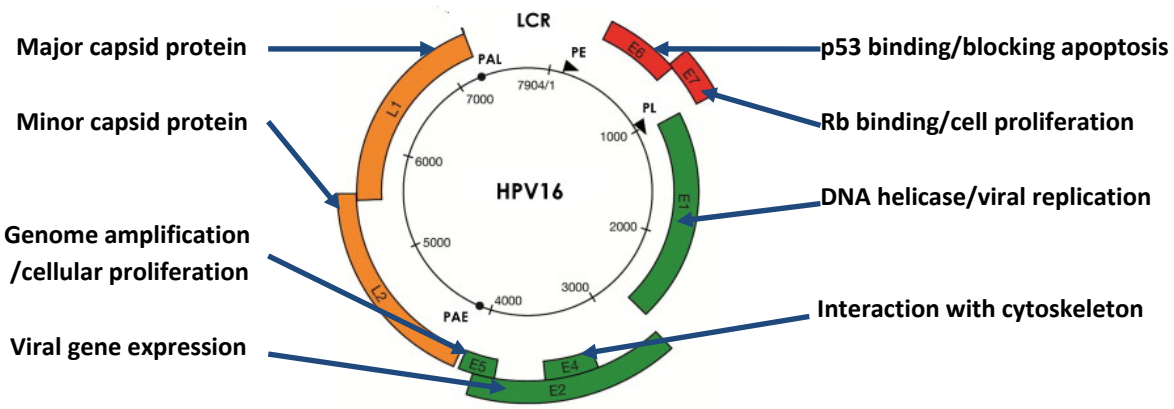

Figure 1: Organization of the HPV16 genome.
The circular HPV DNA genome (8 kb) contains eight open reading frames under the control of a long control region (LCR). Genes encoding early proteins (E) are shown in green, including two viral oncoproteins (red). Late proteins (L) are marked in orange. Major functions for each protein are indicated. Modified from (Doorbar et al., 2012).

The HPV life cycle is strictly connected to the differentiation program of epithelial cells. The exact receptor for viral entry is still unknown. However, this step of viral life cycle appears to involve interaction with cellular heparin sulfate proteoglycans (HSPG, Johnson et al. 2009, Culp et al. 2006). Virus attachment leads to structural changes in the capsid, including L2 cleavage by furin, interaction with a secondary receptor and virus internalization (Kines et al. 2009). HPV uncoats within endosomes inside the cell. The viral genome - L2 complex is transported to the nucleus, while the L1 protein is retained in endosomes and finally degraded in lysosomes (Bergant Marusic et al. 2012).

In the nucleus, early gene transcription is driven by cellular transcription factors binding to sequences in the long control region (LCR). The newly synthetized E1 protein forms hexamers exhibiting ATPase and 3’ - 5’ helicase activities. The E2 protein assembles into dimers that bind to E1 multimers. These E1 - E2 complexes interact with cellular DNA polymerase and recruit the host replication machinery to the viral origin of replication, thereby facilitating HPV genome amplification (Conger et al. 1999, Hughes and Romanos 1993).

In HPV infected basal keratinocytes, the viral genomes are partitioned into the two daughter cells after mitosis. One daughter cell will migrate toward the upper layers of the epithelium and undergo terminal differentiation. This would normally lead to an exit from the cell cycle into the G_0 phase. Conversely, HPV requires the cells to be in the S-phase to promote replication of the viral genome by the cellular replication machinery. Therefore, two viral proteins, E7 and E6, drive keratinocytes back to the cell cycle. E7 binds to members of the Rb-pocket family (including Rb, p107, and p130), leading to the disassociation of Rb-HDAC (histone deacetylase) from E2F/DP-1 transcription complexes. The E2F release results in the transcription of genes involved in progression into S-phase (Dyson et al. 1989, Riley et al. 2003, Felsani et al. 2006). Re-entry into the cell cycle is additionally promoted by E7 association with and stabilization of cyclins A and E (Tommasino et al. 1993, McIntyre et al. 1996). HPV is able to further deregulate the cell cycle and block cellular apoptosis via the action of the viral E6 protein. E6 binds to the cellular tumor suppressor protein p53, which is an important regulator for the expression of proteins involved in the G_1/S and G_2/M checkpoints. A complex of E6 - p53 binds to the ubiquitin ligase E6AP and leads to p53 ubiquitinylation and proteosomal degradation. This decreases expression of the p53 transcriptional target p21. Lack of p21 blocks senescence and apoptosis (Fu et al. 2010, Hubbert et al. 1992).

There are many functional differences between the E6 and E7 proteins of low-risk (LR) and high-risk (HR) HPV types. The characteristics described above are best studied for the HPV16 and HPV18 serotypes. E6 and E7 from HR-HPV types are considered the major viral oncoproteins and their expression leads to cellular transformation. Persistent infection with HR HPVs is linked to the development of a number of cancers, including cervix, vulvar, vaginal, anal, penile, and head and neck cancers (Pim and Banks 2010, zur Hausen 2009).

During a productive HPV infection, genome amplification is followed by expression of the structural proteins L1 and L2. Finally, in the most superficial keratinocytes, the viral genome is packaged into capsids and mature viral particles are released (Buck et al. 2005). Most HPV infections are cleared as a result of a cell-mediated immune response within two years of acquisition (Schiffman et al. 2007).

1.1.2 THE HIV LIFE CYCLE

The first cases of severe acquired cellular immunodeficiency were described in 1981 (Gottlieb et al. 1981, Siegal et al. 1981). Two years later, the human immunodeficiency virus (HIV) was isolated from patients with acquired immunodeficiency syndrome (AIDS) and shown to be the causative agent of the disease (Popovic et al. 1984, Gallo et al. 1984, Sarngadharan et al. 1984). Since then, in less than 35 years, more than 70 million people have been diagnosed with HIV infection and half of them died of AIDS (Ruelas and Greene 2013, Reid et al. 2013).

HIV belongs to the *Lentivirus* genus of the *Retroviridae* family. Two major types, HIV-1 and HIV-2, have been recognized. HIV-1 is subdivided into three major groups: M (main), O (outlier), and N (non-M/non-O). The M group, consisting of 10 subtypes or clades (A to K), is responsible for more than 90% of infections (Kantor et al. 2005). The HIV virion carries two copies of identical single-stranded RNA (ssRNA) associated with the p6 and p7 nucleocapsid proteins in a cone-shaped capsid made by the p24 protein. The viral matrix is composed of the p17 protein. The matrix is surrounded by a viral envelope that is derived from the cellular membrane when the virus particle buds from the cell. The

envelope contains the viral glycoproteins p120 and p41 (Watts et al. 2009, Zhao et al. 2013, Frankel and Young 1998).

The viral genome is flanked by long terminal repeats (LTRs) and encodes nine different gene products. *Gag* encodes for the Gag polyprotein, which is cleaved into the structural proteins of the core and matrix. *Pol* encodes for the Pol polyprotein, which is cleaved into the viral replication enzymes and protease. *Env* encodes for the viral envelope glycoproteins. Tat binds to the transactivation response element (TAR) and stimulates the transcription of viral genes. Rev is essential for the export of genomic viral RNA from the nucleus to the cytoplasm. Vpr is involved in the arrest of the cell cycle. Vif enhances the infectivity of progeny viruses by suppressing cellular defense mechanisms. Nef controls cellular signal transduction and down-regulates the CD4, MHCI and MHCII receptors on the cell surface. Vpu plays a role in viral particle release (Emerman and Malim 1998, Bayer et al. 1995, Foti et al. 1997) (Fig. 2).

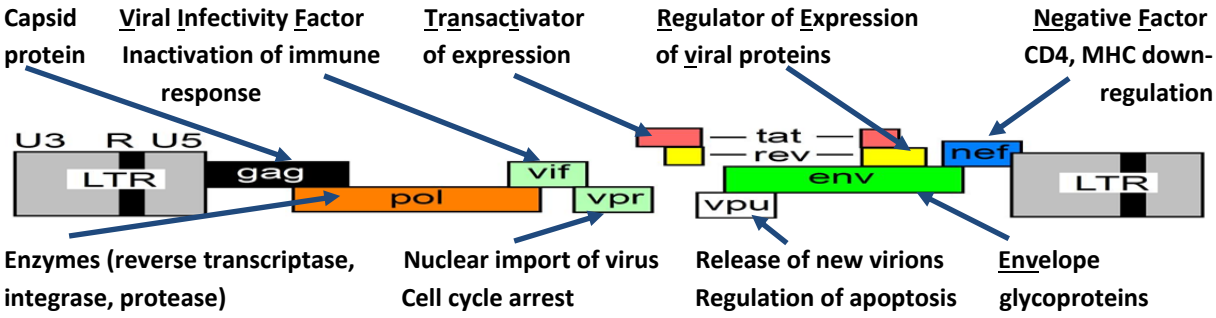

Figure 2: Organization of the HIV genome.
The linear ssRNA (9 kb) genome is flanked by long terminal repeats (LTRs) and contains nine open reading frames. Main functions of the viral proteins are marked. Modified from (Rubbert et al. 2011).

The HIV life cycle can be divided into six main steps: (I) Binding and entry occurs when gp120 binds to the cellular CD4 receptor present on the surface of immune cells. This interaction causes structural changes in the virion and facilitates binding to the co-receptors CCR5 (activated T-lymphocytes, monocytes/macrophages, dendritic cells) or CXCR4 (mainly T-lymphocytes). As a result, gp41 penetrates through the cellular membrane, enabling virus entry. Next, (II) the virion undergoes trafficking toward the nucleus and uncoats. (III) HIV RNA is converted into proviral DNA by reverse transcription. (IV) The provirus is integrated into the cellular genome through the activity of viral integrase. (V) Transcription of HIV regulatory, structural, and enzymatic genes is followed by the assembly of immature viral particles. (VI) Virions migrate toward the cell surface, where the large precursor proteins are cleaved by the HIV protease. Finally, mature virus particles bud through the host cell membrane (Miller et al. 1997, Konig et al. 2008, Hladik and McElrath 2008).

HIV infection eventually leads to a reduction of the level of CD4+ T helper cells in blood below 200 cells/µL, the clinical definition of AIDS. The gradual deterioration of immune system functions results in the development of opportunistic infections, higher occurrence of particular types of cancer, severe body weight loss (HIV wasting syndrome) and, in many cases, death (Langford et al. 2007).

1.1.3 COMMON HPV AND HIV INFECTION SITES

HPVs are one of the most common sexually transmitted infections (STI) worldwide. They infect both men and women and it is estimated that above 80% of the total population will become infected with at least one HPV type during their lifetime (Bruni et al. 2010, de Sanjose et al. 2007). From over 100 HPV genotypes described so far, around 40 are detected in the epithelium of the anogenital tract (Trottier and Franco 2006). In the mucosa of genital areas, HPV infects basal cells of the stratified squamous epithelium exposed by micro-abrasions or other minor traumas (Fig. 3B, Chow et al. 2010, Kines et al. 2009).

HIV is, in most cases, acquired through the genital or rectal mucosa. To establish infection, the virus must first cross the epithelial barrier. Several different pathways of invasion have been described, including transcytosis, penetration through the gaps between the cells, and diffusion through physical abrasions (Fig. 3A, Alfsen et al. 2005, Bomsel 1997, Dorosko and Connor 2010, Herfs et al. 2011, Zussman et al. 2003). Moreover, Langerhans cells residing in the epithelium have dendrites which can extend even to the surface of the mucosa (Nishibu et al. 2006), allowing contact and internalization of HIV (Fig. 3, Tschachler et al. 1987). In the stroma, the virus encounters its target cells, the CD4+ T lymphocyts, dendritic cells and macrophages, leading to a productive infection (Miller and Shattock 2003, Shen et al. 2011).

As described above, both HPVs and HIV are sexually transmitted. The infections can occur in cervical and anal squamocolumnar junctions, where both pathogens cross the epithelial tissue barrier (Fig. 3). This common site of infection opens the possibility of crosstalk between the two pathogens (Herfs et al. 2011, Syrjanen 2011).

A **B**

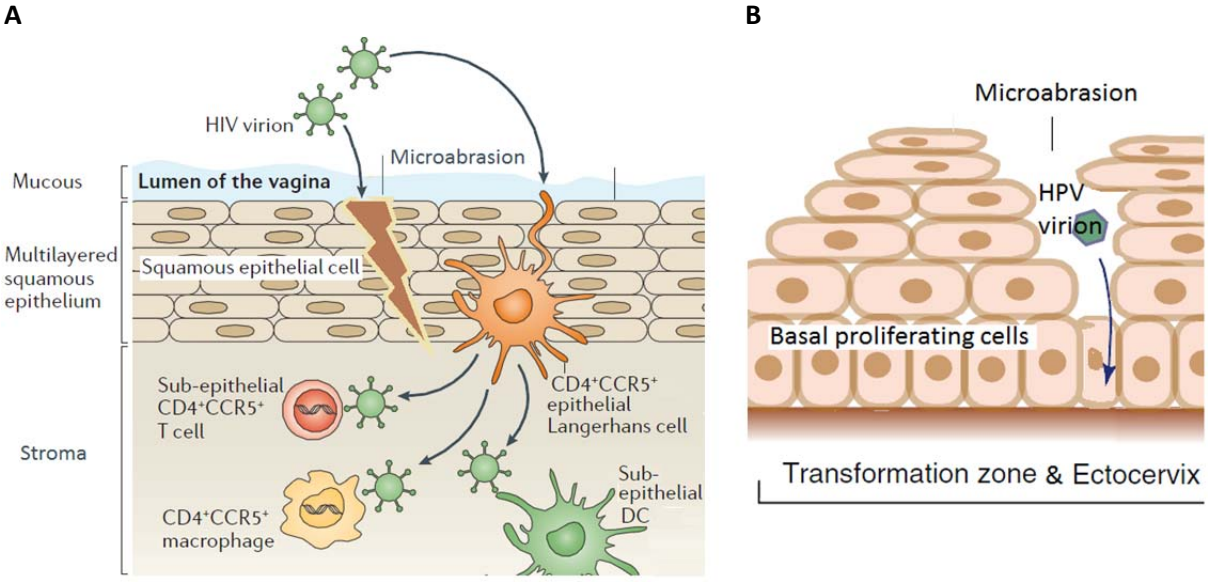

Figure 3: Common HIV and HPV infection sites.
(A) HIV transmission through the genital epithelium and infection of target cells in stroma. HIV crosses the epithelium barrier by transcytosis, through the gaps between the cells, or through physical abrasions. The virus infects CD4+ T cells, dendritic cells and macrophages residing in stroma or epithelial Langerhans cells, which have dendrites extended to the surface of epithelium (based on (Lederman et al. 2006)).
(B) HPV infection of the genital epithelium cells. HPV crosses stratified squamous epithelium through microabrasions and infects basal proliferating cells (based on (Bodily and Laimins 2011)).

1.1.4 EPIDEMIOLOGICAL STUDIES OF HPV ASSOCIATION WITH HIV-1 ACQUISITION

HIV acquisition has been previously described to be associated with certain STIs such as that caused by *Neisseria gonorrhoea*, *Chlamydia trachomatis*, *Trichomonas vaginalis*, *Treponema pallidum* and herpes simplex virus-2 (HSV-2) (Freeman et al. 2006, Fleming and Wasserheit 1999, Korenromp et al. 2005, Ward and Ronn 2010). In recent years, a number of epidemiological studies have shown that a pre-existing infection of the anogenital mucosa with HPVs increases the risk of HIV-1 acquisition (Auvert et al. 2010, Averbach et al. 2010, Chin-Hong et al. 2009, Smith et al. 2010, Smith-McCune et al. 2010, Veldhuijzen et al. 2010). Two meta-analyses with 12,750 and 6,567 participants have been performed. Both studies identified a direct association between these two pathogens. The risk of HIV-1 acquisition approximately doubled when a prior HPV infection was diagnosed (Fig. 4, Houlihan et al. 2012, Lissouba et al. 2013).

Interestingly, when clearance and persistence of the HPV virus were analyzed, two studies reported a 5-fold or 2-fold increase in the risk of HIV acquisition in the case of non-persistent HPV infection (Averbach et al. 2010, Smith-McCune et al. 2010). One suggested explanation was that a new HPV infection leads to a strong local immune response. This, in turn, would cause migration and activation of HIV-1 target immune cells.

Data regarding the association of particular HPV serotypes with an increased risk of HIV infection remain contradictory. Some studies have shown stronger association of HR-HPV types with HIV infection while others suggested an opposite trend (Houlihan et al. 2012). Overall, the oncogenic potential of the virus does not seem to have a significant impact on the risk of HIV acquisition. Studies performed by Auvert, Averbach, Chin-Hong and colleagues have indicated that the risk of HIV acquisition is elevated with infection by several concomitant HPV types (Auvert et al. 2010, Averbach et al. 2010, Chin-Hong et al. 2009, Smith et al. 2010), while data from Smith and colleagues did not find this association (Auvert et al. 2010, Averbach et al. 2010, Chin-Hong et al. 2009, Smith et al. 2010).

Importantly, although both pathogens share the same route of transmission, the positive association between HPV and HIV remains strong after accounting for behavioral and biological covariates such as sexual practices, number of partners and circumcision. Moreover, results were corrected for the STI status. Again, a HPV - HIV correlation was still apparent after adjustment for additional co-infections (Averbach et al. 2010, Chin-Hong et al. 2009, Rositch et al. 2013). Though differences in the strength of the HPV-HIV association have been reported (Fig. 4), the available data gives strong evidence that HPV infection is a cofactor for HIV acquisition.

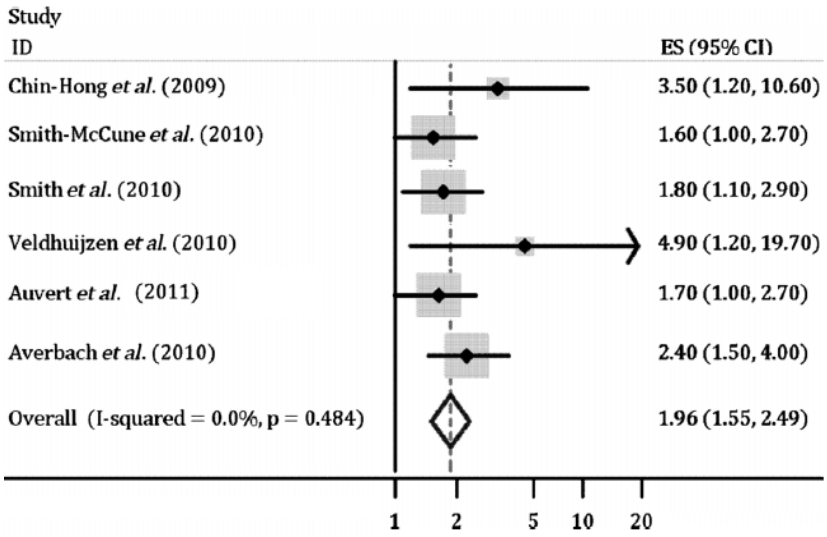

Figure 4: Combined estimate of the association between HPV infection and HIV acquisition.
The random-effect meta-analysis was used to calculate the weights and combined estimate. The x- axis (natural log scale) represents estimates from individual studies and the combined estimate (adapted from (Lissouba et al. 2013)).

1.1.5. THE CROSSTALK BETWEEN HPV AND HIV

A possible indirect interaction between HPVs and HIV-1 has been proposed based on the idea that a HPV infection leads to recruitment and activation of HIV target cells (Herfs et al. 2011, Syrjanen 2011). Moreover, it has been suggested that HPV-infected mucosa, where microabrasions and lesions often develop, is possibly more vulnerable and therefore more likely to be infected by HIV during sexual intercourse (Chin-Hong et al. 2009). However, strong evidence for this hypothesis is so far unavailable.

It is still unknown whether there is a more direct, functional crosstalk between HPV and HIV-1. The only functional interaction between HPV and HIV reported so far is the ability of HIV tat to enhance synthesis of the HPV oncoproteins and the HPV structural protein L1. Tat is a transactivator protein that can promote transcription from the HPV LCR, leading to an increase in E7, E1, and L1 expression (Kim et al. 2008). No direct interaction of any HPV protein with HIV has been reported so far.

1.2 THE HPV E4 PROTEIN

1.2.1 E4 EXPRESSION

The HPV *E4* open reading frame (ORF) lies entirely within the hinge region of the *E2* sequence (Fig. 1). Although the size of *E4* may vary between different HPV types, it is usually one of the shortest genes of HPV, around 300 bp long for the mucosal HPV types. The primary *E4* transcript undergoes splicing. The mature *E4* mRNA encodes the first five amino acids (including the initiation codon) derived from the *E1* ORF fused to the *E4* ORF. For HPV16, one classical splice acceptor site, conserved among different HPV types, and one known splice donor site in the 5' segment of the *E2* gene have been described (Doorbar et al. 1986, Doorbar et al. 1990, Nasseri et al. 1987). Additional *E4* transcripts are identified in other HPV types. In HPV18, for example, *E4* contains an additional splice donor site that leads to the expression of a chimeric E2^E4 protein (Tan et al. 2012).

Expression of E4 is tightly connected with both the HPV life cycle and the differentiation program of epithelial cells (Wang et al. 2004). Although E4 is classified as an early HPV protein, it is synthesized relatively late during viral infection. Accordingly, E4 is first detected when amplification of the viral genome begins. Its expression shortly precedes synthesis of the viral structural proteins L1 and L2 (Fig. 5A, Peh et al. 2002). In the middle layers of HPV-infected epithelium, HPV16 E4 is mainly expressed from the early promoter p97. When infected cells progress through S and G_2 phase, before exiting the cell cycle to undergo terminal differentiation, the HPV16 differentiation-dependent promoter p670 becomes activated. This leads to a dramatic upregulation of E4 expression and protein accumulation in the upper part of the epithelium (Fig. 5 A and B, Bryan et al. 1998, Wilson et al. 2005).

In the cells, E4 mostly localizes in the cytoplasm. However, in some HPV types E4 can also be detected in the nucleus (Brown et al. 2004, Pray and Laimins 1995, Roberts et al. 1993). In the granular layer of the epithelium and in the *stratum corneum*, E4 mRNA and protein become the most abundant HPV products (Fig. 5B, Bryan et al. 1998, Griffin et al. 2012, Supchokpul et al. 2011, Wilson et al. 2005). Astonishingly, HPV E4 accounts for 20 – 30% of the total cellular proteins produced in HPV-induced warts (Breitburd and Croissant 1987).

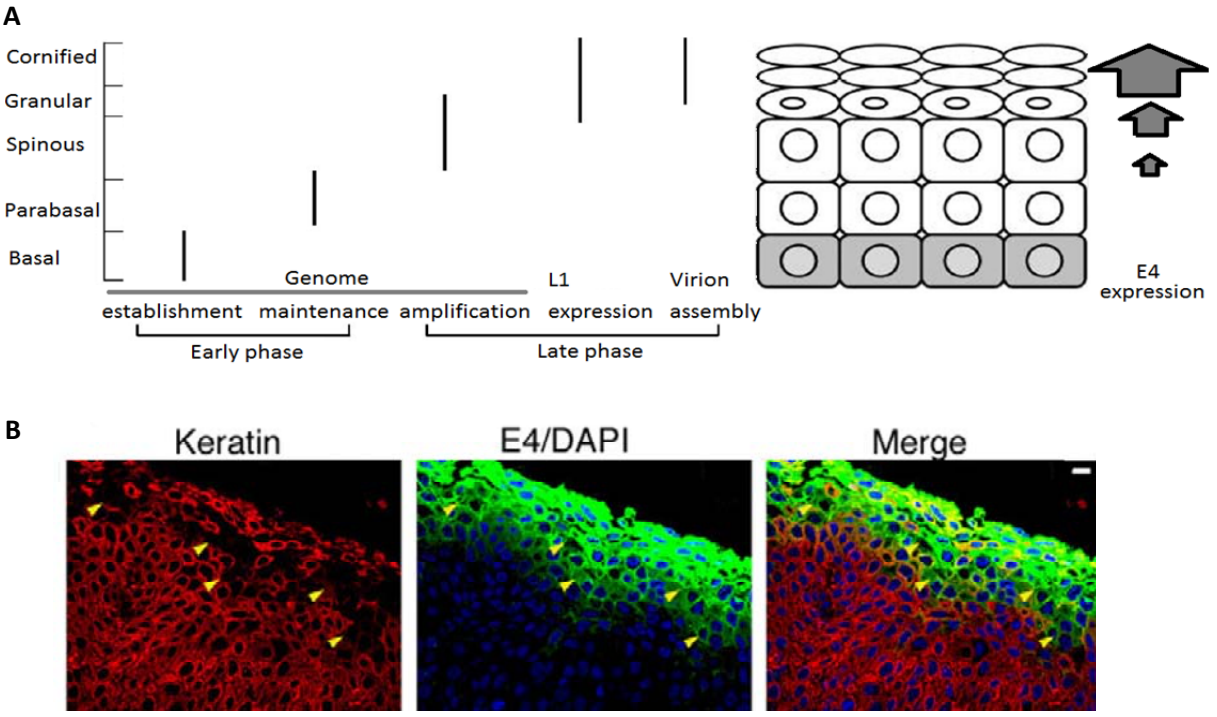

Figure 5: E4 expression during the HPV life cycle and accumulation in the upper layers of the epithelium.
(A) E4 distribution in HPV-infected stratified squamous epithelium during the productive viral life cycle. Arrow thickness corresponds to the amount of expressed E4. E4 is first detected at the onset of viral genome amplification and accumulates in the late phase. (Modified from (Knight et al. 2004)).
(B) Analysis of E4 expression in HPV-infected tissue sections. HPV16-positive cervical epithelium was immunostained against keratin (red) and E4 (green). Nuclei are visualized by DAPI (blue). Scale bar represents 10 µm. (Adapted from (McIntosh et al. 2010)).

Because of its high level of expression, E4 has been suggested as an effective HPV infection biomarker. This protein is synthesized in all cells that support viral genome amplification and in most low-grade lesions (Griffin et al. 2012). Nonetheless, E4 cannot be used as a cervical cancer biomarker because HPV integration into the host genome, frequently observed during oncogenic transformation, results in the preferential deletion of the *E2* and, consequently, *E4* gene. Using type-specific antibodies, HPV-16/18/58 E4 is rarely detected in high-grade lesions (Choo et al. 1987, Griffin et al. 2012).

1.2.2 E4 PROTEIN STRUCTURE

Alignment of the *E4* sequences from different HPV types reveals limited homology. Moreover, the E4 protein from different HPVs is highly divergent at the amino acid (aa) level. E4 proteins vary considerably in size, ranging from 92 aa or 87 aa for HPV16 and HPV18, respectively, to 221 aa for HPV25. This variation in the E4 length is mainly due to an extension of the central hinge region of the protein (Doorbar and Myers 1996, Doorbar 2013). Evolutionary analysis of the *E4* ORF led to the conclusion that neutral selection is dominant and mostly silent mutations accumulate in the *E4* gene (Doorbar et al. 1989, Tsakogiannis et al. 2012).

HPV16 E4 is classified as an intrinsically disordered protein which means that it lacks a stable tertiary structure. However, E4 contains some elements of regular local folds. Beside 42% of random coil, HPV16 E4 consists of 32% of beta-strands, 15% of turns and 11% of alpha helices (Fig. 6). The charge distribution in the protein partially restrains conformational freedom of the C- and N-terminal ends. As a result, E4 is suggested to form a limited fold structure resembling a hairpin with a central region of the protein coiled into a loop (Fig. 6, McIntosh et al. 2008).

As mentioned above, the E4 proteins from different HPV types are not conserved at the level of the primary amino acid sequence, yet they share a common modular organization. They consist of several characteristic structural domains: (I) an N-terminal leucine-rich motif, (II) a proline-rich region, (III) a central loop region, and (IV) a C-terminal domain (Fig. 7). The central loop domain is preceded by a cluster of positively charged aa and followed by negatively charged aa, which forms a pattern of a charge redistribution that contributes to the hairpin structure of E4. This region also contains the major immune-dominant epitopes of the E4 protein (Doorbar 2013, Nakahara et al. 2005, Roberts et al. 1994).

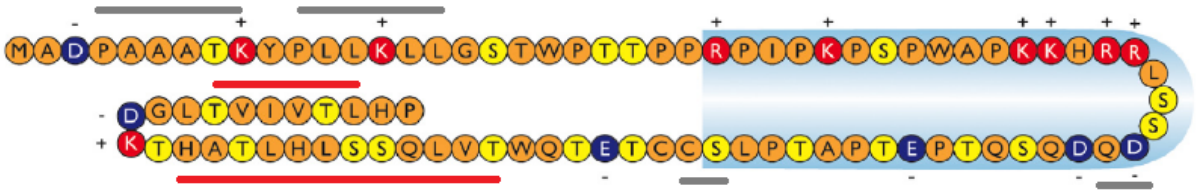

Figure 6: Amino acid sequence and proposed arrangement of the E4 protein with the predicted secondary structure.
Model of polypeptide arrangement based on tryptophan fluorescence data (McIntosh et al. 2008). Red lines indicate the beta strand and grey lines indicate helical regions. (Modified from (Doorbar 2013, McIntosh et al. 2008)).

1.2.3 E4 FUNCTION

The observation that the E4 modular structure is found in divergent HPV types suggests conserved protein function. Studies using a large array of E4 mutants have shown that the structural domains of E4 indeed correspond to characteristic functional regions and E4 proteins from different papillomavirus types share a number of functions.

ASSOCIATION WITH KERATIN AND REORGANIZATION OF THE KERATIN CYTOSKELETON

The E4 N-terminal end of a large number of alpha-group HPV types contains a conserved leucine cluster motif, LLXLL. This domain has been described to mediate E4 association with differentiation-dependent and primary cellular keratins (Roberts et al. 1994). E4 acts as a crosslinker, strongly impairing keratin network dynamics both *in vivo* and *in vitro*. The interaction with the keratin cytoskeleton is based on direct physical binding and results in a decrease of keratin subunits mobility between soluble and insoluble fractions. Inhibition of cytoskeleton dynamics triggers a response similar to that of stress stimuli with activation of p38 mitogen-activated protein kinase (MAPK), c-Jun N-terminal kinase (JNK), followed by the induction of stress-activated protein kinases (SAPKs) and finally resulting in the phosphorylation of keratin. In uninfected cells, phosphorylation of keratin intermediate filaments allows binding of the cellular 'solubility factor' 14-3-3 and solubilization of keratin monomers. In cells expressing E4, keratin remains insoluble despite hyperphosphorylation and accumulates in keratin-E4 aggregates. Those nonfunctional keratin deposits become ubiquitinated, however, they cannot be degraded because of saturation of the proteasome system (McIntosh et al. 2008, McIntosh et al. 2010, Wang et al. 2009).

The final consequence of E4-mediated reorganization of the keratin intermediate filament network is functional keratin depletion. Accordingly, expression of E4 from HPV2, -11, -16, -18, -31, -35, and -45 in keratinocytes leads to aggregated or partially reorganized keratin filaments that may eventually collapse and form perinuclear bundles (McIntosh et al. 2010, Wang et al. 2004).

ASSOCIATION WITH MITOCHONDRIA

The E4 leucine cluster is also responsible for the interaction with mitochondria although the affinity of this binding is lower than that to cytokeratin. If E4 is still expressed after the complete collapse of the keratin cytoskeleton, it forms punctuate structures in the cytoplasm that colocalize with mitochondria. Initially, these E4-mitochondria aggregates are evenly distributed in the cells (Raj et al. 2004). Over time, E4 detaches the mitochondria from the microtubule network without destroying the latter. As a result, E4-mitochondria aggregates assemble into clustered bundles that localize around the nucleus. Moreover, E4 binding to mitochondria causes a strong drop in the mitochondrial membrane potential. This induces apoptosis by a mechanism independent of pore formation in mitochondrial membranes (Raj et al. 2004).

BLOCKING CELL CYCLE PROGRESSION AND DNA SYNTHESIS

Another function of E4 conserved among different HPV types is the ability to block the cell cycle and suppress cellular DNA synthesis. In HPV16 this effect is mediated by the proline-rich region between residues 17 and 35 (Davy et al. 2002). E4 sequesters cyclin-dependent kinases 2 (CDK2)/cyclin A and CDK1/cyclin B complexes by binding them to cytokeratin (Davy et al. 2005). Consequently, this depletion of cyclin-CDK prevents the progression of cells into mitosis, leading to cell cycle arrest in the G_2 cell cycle phase. A characteristic feature of cells stopped in an E4-induced G_2-like phase is endoreduplication with a DNA content of 4N or more (Knight et al. 2004, Nakahara et al. 2002).

E4 is also able to inhibit initiation of DNA replication. An arginine located close to the proline-rich domain is indispensable for this effect. E4 prevents recruitment of replication licensing factors (RLFs) onto chromatin, thus impairing binding of Mcm2 and Mcm7 helicases and blocking chromosomal replication (Knight et al. 2004, Roberts et al. 2008).

Finally, E4 seems to be able to block differentiation of keratinocytes in the superficial spinous and granular layers. In this part of the epithelium, cells become positive for the epithelial differentiation marker, keratin K10. Expression of E4 in keratinocytes leads to appearance of a differentiation-defective phenotype without the synthesis of K10 (Nakahara et al. 2005, Wilson et al. 2005).

INTERACTION WITH DEAD-BOX PROTEIN

HPV16 E4 protein has been shown to interact with the 66 kDa DEAD-box protein termed E4-DBP (E4-DEAD box protein, Doorbar et al. 2000). DEAD-box proteins belong to a family of ATP-dependent RNA helicases. These helicases can shuttle between the nucleus and the cytoplasm and are involved in almost every aspect of RNA processing including ribosome biogenesis, splicing, translation initiation, RNA transport, and mRNA stability (Cordin et al. 2006). E4-DBP binding occurs between the last 27 aa residues of the E4 C-terminal end and the E4-DBP GXGXT motif. The GXGXT domain is suggested to be involved in ATP hydrolysis rather than RNA association, which means that E4 binding may interfere with the catalytic activity of DEAD-box helicase (Doorbar et al. 2000).

ROLE IN HPV REPLICATION AND LIFE CYCLE

Despite the fact that E4 is the most highly expressed product of HPV infection, its exact role in viral replication is still mainly speculative and can only be deduced from E4's effect on the host cell. The appearance of E4 in the upper, differentiating layers of the epithelium suggests that the protein is involved in late stages of the viral life cycle.

It has been proposed that E4-mediated disruption of the cellular cytokeratin network may lead to cell collapse and support virus release (McIntosh et al. 2010). Moreover, E4 may also disrupt the cornified cell envelope in the upper layers of the epithelium (Wilson et al. 2007). Because E4 expression shortly precedes synthesis of the structural HPV proteins, it was suggested that E4 may play a role in virus assembly, but evidence for this function is still lacking (Burd 2003).

An HPV mutant carrying a nonfunctional E4 gene showed a significant decrease in transcription of late HPV genes. Moreover, this mutant had a lower level of viral genome amplification (Wilson et al. 2005). Expression of HPV16 late genes is mostly controlled on the post-transcriptional level. The main regulatory mechanism is the control of mRNA processing and stability (Cumming et al. 2008). It seems plausible that the association of E4 with the DEAD-box protein described above (Doorbar et al. 2000) may play a role in the promotion of papillomavirus late-gene synthesis.

Nuclear dot 10 (ND10) is a sub-nuclear structure functioning as the replication site of many DNA viruses, including HPVs (Rivera-Molina et al. 2013). High E4 expression leads to reorganization of ND10. Together with E4-induced G_2 arrest, these cellular conditions are postulated to be advantageous for papillomavirus genome amplification and gene expression (Roberts et al. 2003).

Finally, E4 may act as an antagonist of E6 and E7 proteins, preventing uncontrolled proliferation of HPV-infected keratinocytes. E4 from cutaneous HPV types (mu, beta and gamma) and some mucosal types (e.g. HPV18) forms aggregates with characteristics of aggresomes (described in more detail below, Gross et al. 1982, Kajitani et al. 2013). E4 aggresome-like structures assemble in upper layers of the epithelium. These structures bind HPV oncoproteins and decrease their concentration in the cell. In the absence of E6 and E7 keratinocytes undergo terminal differentiation, which is required for capsid protein expression and virion assembly (Kajitani et al. 2013). Indeed, HPV maturation can take place only in terminally differentiated keratinocytes. The most superficial epithelial cells lose mitochondrial oxidative phosphorylation. The cytoplasm then converts from a reducing to an oxidizing environment. This promotes formation of disulphide bonds between the L1 proteins, leading to the production of mature capsids and, finally, complete infectious virions (Buck et al. 2005).

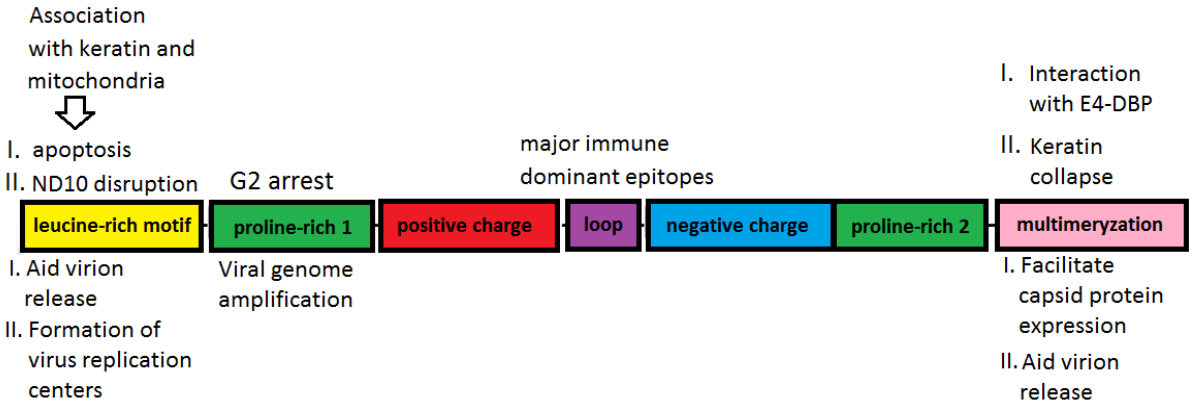

Figure 7: Functional domains of the HPV16 E4 protein.
A schematic representation of the E4 protein with indicated known functional domains. For each domain the postulated function is listed above the scheme. The proposed roles for the viral life cycle are described below the scheme.

1.2.4 POST-TRANSLATIONAL MODIFICATION OF E4 AND MULTIMERIZATION

During the viral life cycle, E4 is structurally and functionally modified as the cells migrate toward the uppermost layer of the epithelium. Post-translational modifications of HPV E4 include phosphorylation, ubiquitination, oligo- and multimerization, and proteolytic cleavage (Knight et al. 2004).

E4 PHOSPHORYLATION

E4 activity is primarily regulated by phosphorylation. Cellular kinases are activated by both viral gene products that drive cell proliferation and affect normal cell signaling (e.g. E6, E7 and E5) and by cellular environment changes in terminally differentiated cells of the epithelium (Bell et al. 2007, Bryan et al. 2000). In the middle layer of the epithelium, differentiating cells in the S-like phase support viral genome amplification. E5 then stimulates E4 phosphorylation within residues 35 to 59 by MAPK. Phosphorylation on threonine 57 results in the addition of a negative charge to a region of the protein already rich in acidic aa. This leads to futher structural changes. The central loop of E4 becomes more compact and exposes the leucine-rich motif on the surface of E4, thereby strongly enhancing keratin binding (Wang et al. 2009).

When HPV-infected cells move to the middle and upper layers of the epithelium they enter E4-induced G_2-like phase. Then E4 becomes phosphorylated by CDKs on serine 32. The presence of a negative charge in a generally positively-charged region relaxes the hairpin structure, thus enhancing E4 cleavage by calpain (described in detail below). Moreover, opening of the loop region in the upper layer of the epithelium is promoted by the dephosphorylation of threonine 57 due to MAPK absence (Davy et al. 2006, McIntosh et al. 2010).

In the upper layers of the epithelium, where keranocytes exit the cell cycle, E4 is phosphorylated by protein kinase A and protein kinase C. Accumulation of negative charge in the loop region aids E4 stabilization and enhances protein accumulation (Wang et al. 2009).

PROTEOLYTIC CLEAVAGE OF E4

The accumulation of E4 in the upper layers of the epithelium and its phosphorylation by CDKs result in E4 proteolytic cleavage. The enzyme mediating the truncation of the E4 N-terminus is the cysteine protease calpain (Khan et al. 2011). Calpains are a family of structurally and functionally related enzymes that require calcium for proteolytic activity. Unlike degradative proteases that lead to complete proteolysis of their substrates, calpain cleavage is usually very specific, resulting in a product with new activity. Vertebrates have two calpains, μ- and m-calpain, that depend on μM and mM concentrations of Ca^{2+}, respectively (Takahashi and al. 1990). In the upper layers of the epithelium, calpains become activated in keratinocytes and are involved in processing of profilaggrin to filaggrin (Resing et al. 1993).

HPV16 E4 is cleaved between residues 14 and 15 or 17 and 18. The later cleavage form becomes predominant over time. The resulting C-terminal fragment lacks the domain required for the E4 association with keratin and mitochondria and interaction with ND10. Calpain cleavage causes

changes of the E4 structure, exposing a C-terminal multimerization domain that is otherwise folded inside the E4 hairpin structure. This allows formation of multimers (Khan et al. 2011). Importantly, HPV16 E7 was shown to decrease the calcium requirement of μ-calpain. This finding suggests that HPV infection results in calpain activation (Darnell et al. 2007). Moreover, the calpain cleavage site is conserved among HPV types (Fig. 8A), indicating that multimerization is important for the HPV life cycle. N-terminal truncated forms of E4 have been detected in cells infected with HPV16, -18 or -33 (Doorbar 2013, Khan et al. 2011).

FORMATION OF MULTIMERS BY E4

Another post-transcriptional modification of E4 is its multimerization. *In vitro* expressed full length HPV16 E4 protein can be detected as monomers, dimers, and hexamers. Interestingly, a mutant HPV16 E4 protein with a partial deletion of the C-terminal multimerization domain (E4d86-92) still forms dimeric, trimeric, tetrameric, pentameric and hexameric structures. E4 proteins from other HPV types, e.g. HPV1, have been observed to form hexamers or even higher-order structures, up to 24-mers (Wang et al. 2004).

Besides multimers, bigger aggregates of E4 protein were also described. The E4 protein from cutaneous HPV types HPV1 and HPV63 (mu genus), HPV4 and HPV65 (gamma genus) and HPV5 and HPV8 (beta genus), can form inclusion granules. These inclusion granules are cytoplasmic or sometimes nuclear and contain large amounts of E4 aggregates (Gross et al. 1982, Doorbar et al. 1996). HPV11 E4 has additionally been shown to associate into large, perinuclear localized multimers (Bryan et al. 1998).

In cells infected with HPV18, E4 is deposited into aggresome-like compartments. These E4 aggregates form at the microtubule organizing center (MTOC) and have all the characteristics of aggresomes, including the presence of polyubiquitinated proteins, proteasomes, molecular chaperones, histone deacetylase 6 (HDAC6) and vimentin cages (Kajitani et al. 2013).

FORMATION OF AMYLOIDS

E4 calpain cleavage leads to further structural changes, opening the hairpin and exposing the C-terminal multimerization domain. This region of HPV16 E4 contains 18 amino acids folded into a long beta-strand with a high hydrophobicity and a low net charge. This beta-strand can be extended or arranged in an antiparallel beta sheet conformation (McIntosh et al. 2008). In the absence of N-terminal residues, the multimerization domain becomes accessible for self-association (Khan et al. 2011). An N-terminal-truncated E4d2-5 mutant forms high molecular weight structures of unbranched fibrils (McIntosh et al. 2008), while an HPV16 E4 fragment encompassing residues 18 - 92 spontaneously assembles into amyloid-like fibrils (Fig. 8B, Khan et al. 2011).

Amyloids have been traditionally described as insoluble fibril deposits in the extracellular spaces of tissues and organs formed through defective protein folding, eventually leading to a pathological condition known as amyloidosis. Recently, a large number of naturally occurring and synthetic polypeptides, many unconnected with diseases, have been shown to form amyloids *in vivo* or *in vitro* (Sipe et al. 2010, Maji et al. 2009). Therefore, a new definition was conceived to identify amyloids

based on their structure and physical characteristics. Criteria that must be fulfilled for protein assemblies to be classified as amyloid include: (I) Structure of non-branching fibrils approximately 5 to 25 nm in diameter and several hundred nm in length that (II) possess a repeated cross-β-sheet structure parallel to the fibril axis, (III) binds specific dyes, such as Thioflavin T (ThT) or Congo red and (IV) exhibits green bi-refringence in polarisation microscopy (Eisenberg et al. 2012, Pedersen et al. 2010). Importantly, amyloids can be formed by many structurally and functionally unrelated proteins of astonishingly divergent aa sequences and yet they all possess common structural and physical characteristics (Foley et al. 2013, Toyama and Weissman 2011).

The interface between the cross-β-sheets forms a ‘‘dry steric zipper” held together by a number of interactions, both polar (hydrogen-bonds and alternating charges) and nonpolar (Van der Waals and aromatic stacking). This results in the extreme stability of amyloids, making them resistant to dissolution in 5% SDS, 4 M urea or formic acid (Chiti et al. 1999, Eisenberg et al. 2012, Nilsson 2004, Pedersen et al. 2010). Formation of amyloids is a multistep process starting with a nucleation. Fibrils grow by the addition of monomers or profilaments to ends, while breaking and branching of these fibrils leads to nucleation of new amyloids (Pedersen et al. 2010). Mature amyloids are preceded by short protofilaments and curly, irregular (wormlike) thin (2 - 5 nm) structures, termed protofibrils (Greenwald and Riek 2010, Jimenez et al. 2001, Toyama and Weissman 2011).

Noncovalent hydrophobic interactions between partially folded proteins appear to be necessary for amyloid formation (Chiti et al. 1999). Therefore, E4 assembly into amyloids is, most likely, mediated by hydrophobic interactions between beta-strand multimerization domains. HPV16 E4 forms amyloid fibrils with characteristic, flexible, unbranched ribbon-like morphology (Fig. 8C, McIntosh et al. 2008). Individual fibrils, 100 - 300 nm long and 7 nm wide, can assemble over time into twisted bundles up to several micrometers long (Khan et al. 2011).

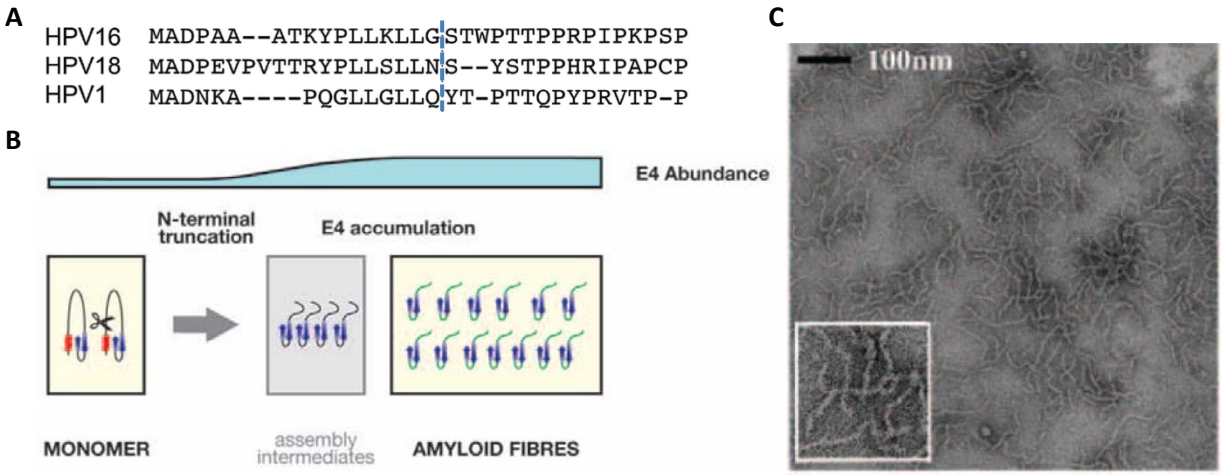

Figure 8: Conservation of E4 calpain cleavage sites and model of E4 assembly into amyloid-like fibers.
(A) Alignment of the amino acid sequences of HPV16, HPV18, and HPV1 E4 N-terminal ends using CLUSTALW. Vertical dotted line shows known calpain cleavage sites in HPV types 16 and 1 and the predicted site in type 18.
(B) Following calpain cleavage, E4 forms amyloid-like fibers. The existence of hexameric E4 intermediates has been suggested.
(C) Electron micrograph of amyloid-like fibers formed by HPV16 E4d2-5 (inset magnified x2).
(Adapted from (Khan et al. 2011, McIntosh et al. 2008)).

Within the HPV-infected cell, E4 amyloid-like fibers may be heterogenous and consist of both truncated and full-length E4, either free or keratin-bound. It has been proposed that the calpain-cleaved E4 form acts as a template for fibril formation. The E4 fibers aid E4-mediated disruption of the keratin network. Even though calpain cleavage removes the leucine-rich motif, the formation of heterogeneous fibers, containing full length protein, causes crosslinking of cytokeratin, thereby increasing its fragility (Khan et al. 2011).

Although the E4 protein is not evolutionally conserved, the sequences from the most prevalent, HR alpha group viruses have a high degree of homology at the C-terminal end. Some of the hydrophobic residues in the multimerization domain (HPV16 84 - 92; LTVIVTLHP) are found among different HPV types. Moreover, the tertiary structure of the E4 C-terminal beta-strand seems to be common among HPV subtypes (Khan et al. 2011, Roberts et al. 1997), suggesting that E4 amyloid formation is likely a general property of this protein. Accordingly, E4 protein was detected by amyloid imaging probes in monolayer cells infected with HPV16, HPV18 or HPV33, as well as in HPV16-positive biopsy materials (McIntosh et al. 2008).

1.3 AMYLOIDS AND HIV INFECTION

An interesting property of amyloids, in the context of fibril structure formation by E4, is their ability to enhance infection of enveloped viruses, including HIV-1.

1.3.1 INFLUENCE OF AMYLOIDS ON LENTIVIRAL INFECTION

β-AMYLOIDS ENHANCE LENTIVIRAL INFECTION

The ability of amyloids to enhance lentiviral infection has been first described for two β-amyloid (Aβ) isoforms (Wojtowicz et al. 2002). β-amyloid peptides are the main components of the amyloid plaque deposits found in the brains of Alzheimer's disease patients. These amyloid fibrils consist of 36 - 43 aa long peptides that are derived from the amyloid precursor protein (APP). Similar to many other amyloids, formation of fibrils is triggered by proteolytic cleavage of the precursor. In this case, β- and γ- secretases cut the transmembrane glycoprotein APP, leading to formation of several isoforms of amyloidogenic peptides including $A\beta_{40}$ and $A\beta_{42}$. Although the shorter peptide is much more abundant, $A\beta_{42}$ is more amylogenic (Bitan et al. 2003, Seilheimer et al. 1997, Seubert et al. 1993).

$A\beta_{40}$ and $A\beta_{42}$ have been shown to enhance the infection rate of multiple HIV-1 isolates, HSV, and viruses pseudotyped with the envelope glycoproteins of vesicular stomatitis virus (VSV). $A\beta_{40}$ forms shorter and thinner fibrils and increases the infection rate stronger than $A\beta_{42}$. In the case of HIV-1, $A\beta_{40}$ and $A\beta_{42}$ fibrils do not bypass the requirement for the appropriate receptors and augment infection only in cells expressing CD4 and an appropriate co-receptor. The Aβ effect on infection with VSV-G-pseudotyped virus, which binds to unspecific and ubiquitously expressed receptors, is independent of the cell type used (Wojtowicz et al. 2002).

SEVI

The ability of amyloids to enhance HIV infection has been best described for different fibrils found in seminal fluid. The first example is prostatic acid phosphatase (PAP). PAP is a 100 kDa homodimeric glycoprotein produced in the prostate and secreted into the seminal plasma in high quantity. After expression, PAP undergoes proteolytic cleavage that removes the signal peptide and leads to the creation of the mature, active form of the enzyme. PAP is a non-specific histidine phosphomonoesterase that catalyzes dephosphorylation in acidic conditions. Its physiological function is not clearly understood and only few substrates have been identified so far. PAP is one of the most abundant proteins found in semen and also a marker for diagnosis and follow-up of prostatic cancer (Brillard-Bourdet et al. 2002, French and Makhatadze 2012, Muniyan et al. 2013).

Naturally occurring, short polypeptides derived from the PAP C-terminal end (PAP 248 - 286) self-assemble into amyloid fibrils, termed semen-derived enhancer of virus infection (SEVI). SEVI strongly augments the HIV-1 infection rate in a dose-dependent manner both *in vitro* - in human immune cells and *in vivo* - in a rat model. Both, isolated SEVI and SEVI-containing semen are general enhancers of HIV-1 infection. Their effect is independent of the viral geno- or serotype. SEVI augments HIV-1 infection of various cell types expressing the HIV receptor and co-receptors. Additionally, the PAP fragment corresponding to the N-terminal end (PAP 85 - 120) also forms fibrils that significantly enhance HIV-1 infection (Arnold et al. 2012, Munch et al. 2007).

SEMs

Further amyloid-forming proteins found in semen are the semenogelins (SEMs). Two variants, SEM I (50 kDa) and SEM II (63 kDa), constitute together the major structural proteins of human semen. Following linkage to fibronectin, SEMs form the gel semen coagulum. SEMs are cleaved by prostate-specific antigen (PSA). The resulting peptide fragments readily assemble into amyloids (Brillard-Bourdet et al. 2002, Lilja et al. 1987). SEM fibrils, analogous to SEVI, interact with HIV-1 virions and increase the fusion of CXCR4- and CCR5- tropic HIV-1 variants with $CD4^+$ T lymphocytes (Roan et al. 2011).

AMYLOIDS AS GENERAL ENHANCERS OF HIV-1 INFECTION

In addition to naturally occurring amyloids, artificial amyloid-like fibrils can also enhance the infection rate of enveloped viruses. General, amphipathic, cationic peptides with a sequence of Ac-Kn(XKXE)2-NH2 form cross-β-sheet fibtilar structures. Those fibrils strongly boost HIV-1 transduction (Easterhoff et al. 2011). Therefore, it appears that the sequence of the amyloid precursor does no influence the effect on the lentiviral infection rate.

1.3.2 PROPOSED MECHANISMS OF AMYLOID-MEDIATED ENHANCEMENT OF LENTIVIRAL INFECTION

The exact mechanism by which amyloids enhance lentiviral infection is not defined. However studies on factors influencing Aβ- and SEVI-mediated augmentation of infection resulted in several proposed scenarios. Amyloids seem to facilitate early steps of infection, e.g. virus attachment or entry into the cell. This interaction is not mediated by improvement of syncytia formation (Wojtowicz et al. 2002), a common feature induced by HIV-1 in T-lymphocytes and facilitating viral entry to cells (Fouchier et al. 1995, Watkins et al. 1997). Moreover, phagocytosis is not critical for the SEVI-mediated increase of HIV-1 infection (Martellini et al. 2011).

High molecular weight fibrils may trap virus particles facilitating HIV-1 aggregation, thereby enhancing the rate of virus sedimentation onto cells (Easterhoff et al. 2011). HIV-amyloid assemblies are suggested to have a higher probability of attachment to the mucosa of the genital surfaces and penetration through the tissue barrier (Martellini et al. 2011, Munch et al. 2007).

Furthermore, SEVI and SEMs have high isoelectric points (pI), above 10 in the case of SEVI. The positive charge of amyloid fibrils could reduce the electrostatic repulsion between the cell membrane and the virion surface, both of which are negatively charged. Thanks to its highly cationic nature, SEVI can bind to both the virus envelope and HSPG, naturally occurring anionic carbohydrate polymers present on the surface of target cells. The creation of an amyloid bridge between HIV-1 and the cells subsequently elevates the likelihood of receptor-mediated viral entry and promotes receptor-independent adsorption (Easterhoff et al. 2011, Olsen et al. 2010, Roan et al. 2011, Martellini et al. 2011). In this way, fibrils may enhance the interaction between cellular and viral surfaces, subsequently assisting a physical association of viral envelopes with the cellular lipid membrane (Wojtowicz et al. 2002).

1.4. RESEARCH OBJECTIVES

A better understanding of the factors that promote HIV transmission is critical for a more effective control of the emerging AIDS pandemic. Recent epidemiological studies suggest a possible role of HPV infections for increasing HIV acquisition. In light of the documented enhancement of lentiviral infection rate by amyloid fibrils, we hypothesize that the amyloid forms of HPV E4 may be able to increase HIV-1 uptake and infection. If so, the high prevalence of HPV infections, the substantial amounts of E4 expression, and the likely release of this protein onto the surface of the anogenital mucosa could make E4 a very potent enhancer of HIV-1 acquisition.

Thus, the overall aim of these studies is to examine a possible direct functional crosstalk between HPVs and HIV. It will be tested whether the HPV E4 protein can enhance the infection rate of VSV-G-pseudotyped lentiviruses, which serve as a model system. These analyses will be complemented by mechanistic studies. Analogous studies will then be extended to other viruses, including HIV-1.

Specifically, the work will focus on:

(I) Expression and purification of HPV16 E4 protein variants, including full-length E4, a truncated version corresponding to the naturally-occurring calpain cleavage product, and mutants with deletions of structurally or functionally pre-defined domains. Investigation of E4 assembly into multimers and validation of amyloid formation by means of specific staining and visualization of E4 using microscopic techniques, including electron microscopy.

(II) Testing the influence of E4 on the transduction rate of Vesicular Stomatitis Virus-G-(VSV-G)-pseudotyped vector as a model of enveloped virus infection by both fluorescence microscopy and quantitative flow cytometry analysis. This includes characterization and optimization of experimental conditions that influence the effect of E4 on lentiviral transduction. Investigation of the mechanisms by which E4 may affect lentiviral infection rates.

(III) Comparative analyses of the E4 protein activities from additional HPV types, including high-risk and low-risk HPVs.

(IV) Investigation of the effects of HPV16 E4 on the HPV infection rate.

(V) Examination of the influence of E4 on other enveloped viruses, including HIV-1, if E4 is confirmed to enhance lentiviral infection rates in our model. This latter part will be done in cooperation with the group of Prof. Dr. O. Keppler, Department of Virology, University of Frankfurt.

CHAPTER 2

RESULTS

2.1 PREPARATION OF HPV E4 PROTEINS

In order to investigate a possible direct functional crosstalk between HPV and lentiviruses a number of HPV proteins, including E4, E7 and L1, were prepared, all of them containing the hexahistidine tag (6xHis-tag). In addition to the full length HPV16 E4, a wide range of protein mutants was constructed. These variants corresponded to the naturally occurring HPV16 E4 isoforms, were based on alanine substitutions, or on deletions of known E4 functional domains. A comprehensive list of all HPV16 E4 constructs and their aa sequence alignment is presented in Table 1.

Table 1: List of HPV16 E4 constructs.

Name	Abbreviation	Description
E4WT	**E4WT**	HPV16 E4 full-length sequence
E4d2-17	**E4dN**	a truncated version of E4 corresponding to the naturally occurring calpain cleavage form (Khan et al. 2011)
E4d2-5	**E4dN'**	mutated form of E4WT lacking the first five amino acids from the N-terminal domain and described to form amyloid fibrils *in vitro* (McIntosh et al. 2008)
E4d86-92	**E4dC'**	mutated form of E4 with a partial deletion of the C-terminal domain which should not form amyloid fibrils *in vitro* (McIntosh et al. 2008)
E4d87-92	**E4dC**	mutated form of E4 with a partial deletion of the C-terminal domain which should not form amyloid fibrils *in vitro* (McIntosh et al. 2008, Wang et al. 2004)
E4d2-17d87-92	**E4dNdC**	a truncated version of E4 corresponding to the naturally occurring calpain cleavage product but with a partial deletion of the C-terminal multimerization domain
E4d2-17 Ala	**E4ala**	a mutant version of E4d2-17 where all positively-charged amino acids were substituted with alanine
E4d70-92	**E4d70**	mutated form of E4 with a complete deletion of the C-terminal multimerization domain
E4d36-41	**E4d36**	mutated version of E4 with a deletion of the cluster of positively charged amino acids in a central loop region involved in assembly of E4 structure (Doorbar 2013)
E4(66-92)	**E4C**	Synthetic peptide corresponding to the E4 C-terminus (aa 66 to 92) described to form short fibrilar structures (McIntosh et al. 2008)
E4(66-92)Ala	**E4Cala**	Synthetic peptide corresponding to the E4 C-terminus (aa 66 to 92) with the only positive aa in this region, lysine, substituted with alanine

```
E4
WT    MADPAAATKYPLLKLLGSTWPTTPPRPIPKPSPWAPKKHRRLSSDQDQSQTPETPATPLSCCTETQWTVLQSSLHLTAHTKDGLTVIVTLHP
dN    ----------------STWPTTPPRPIPKPSPWAPKKHRRLSSDQDQSQTPETPATPLSCCTETQWTVLQSSLHLTAHTKDGLTVIVTLHP
dN'   ----MAATKYPLLKLLGSTWPTTPPRPIPKPSPWAPKKHRRLSSDQDQSQTPETPATPLSCCTETQWTVLQSSLHLTAHTKDGLTVIVTLHP
dC'   MADPAAATKYPLLKLLGSTWPTTPPRPIPKPSPWAPKKHRRLSSDQDQSQTPETPATPLSCCTETQWTVLQSSLHLTAHTKDGLT-------
dC    MADPAAATKYPLLKLLGSTWPTTPPRPIPKPSPWAPKKHRRLSSDQDQSQTPETPATPLSCCTETQWTVLQSSLHLTAHTKDGLTV------
dNdC  ----------------STWPTTPPRPIPKPSPWAPKKHRRLSSDQDQSQTPETPATPLSCCTETQWTVLQSSLHLTAHTKDGLTV------
ala   ----------------STWPTTPPAPIPAPSPWAPAAHAALSSDQDQSQTPETPATPLSCCTETQWTVLQSSLHLTAHTADGLTVIVTLHP
d70   MADPAAATKYPLLKLLGSTWPTTPPRPIPKPSPWAPKKHRRLSSDQDQSQTPETPATPLSCCTETQWTVL----------------------
d36   MADPAAATKYPLLKLLGSTWPTTPPRPIPKPSPWA------LSSDQDQSQTPETPATPLSCCTETQWTVLQSSLHLTAHTKDGLTVIVTLHP
C     ------------------------------------------------------------QWTVLQSSLHLTAHTKDGLTVIVTLHP
Cala  ------------------------------------------------------------QWTVLQSSLHLTAHTADGLTVIVTLHP
```

The lower part of the table shows a protein sequence alignment by CLUSTALW. The calpain cleavage site is indicated by the green line. The multimerization domain is marked in blue, and positively charged residues, in red. For simplicity, the indicated abbreviation will be used in the text.

Constructed HPV protein variants were expressed in bacterial systems, purified using Nickel affinity chromatography and refolded. The standardized protocols for bacterial protein expression and purification were adapted and optimized to allow preparation of proteins differing in size and physiochemical characteristics (Graslund et al. 2008). All steps were tested and improved to ensure high yield of protein production. The final established E4 preparation protocol is summarized in Fig. 9, while the strategies applied for the optimization of each step are described in the appendix (see 5.1-5.2).

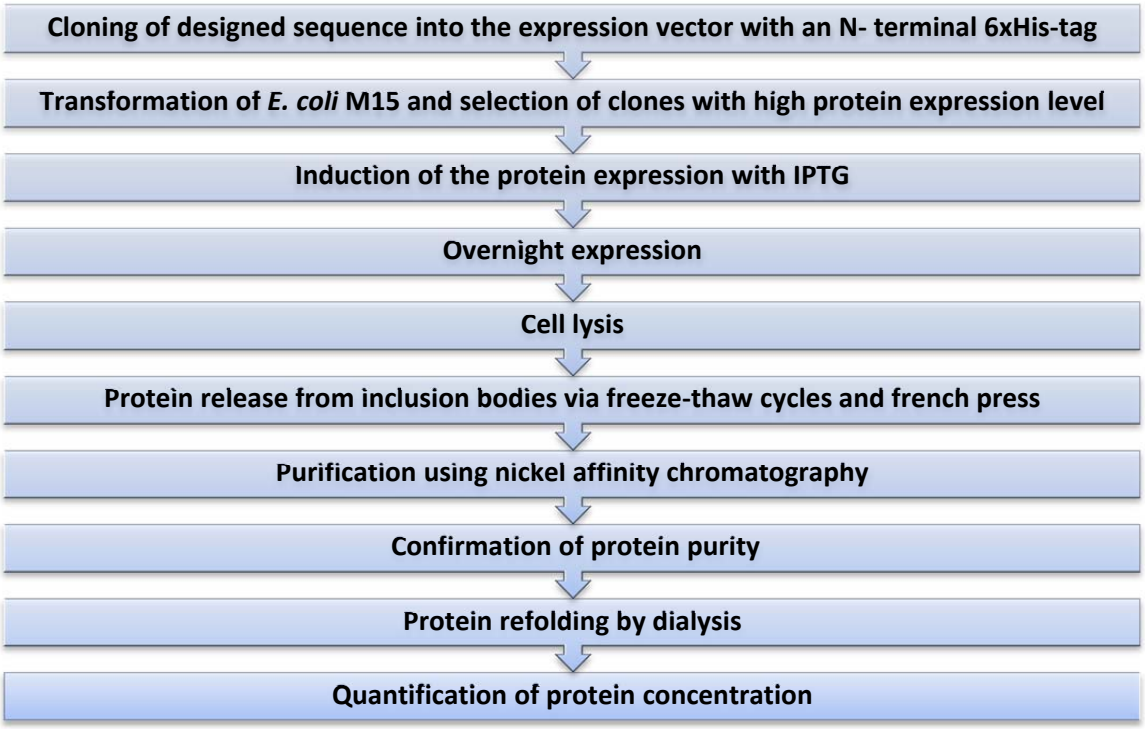

Figure 9: Schematic flowchart of protein preparation.

To obtain protein stocks with high activity, E4 refolding and storage conditions were optimized (see appendix 5.3). Time, temperature and pH were tested to define the most reproducible conditions. Protein refolding was carried out by dilution of individual E4 variants to a desired final concentration, followed by dialysis in the refolding buffer. Upon refolding, the E4 protein solution became turbid and even contained macroscopically visible clots. Turbidity is an early indications of protein assembly into multimers or polymers (Bruggink et al., 2012) and is one of the criteria used to characterize the formation of active SEVI preparations (Roan et al. 2011).

To visualize the macromolecular structures of E4, an E4dN solution was analyzed using confocal microscopy. A globular bovine serum albumin (BSA) protein was used as a negative control. The amyloid-specific dye ThT (Biancalana and Koide 2010, Khurana et al., 2005, Nilsson 2004) was utilized to test for the presence of fibrils. Proteins were analyzed using light transmission and different fluorescence spectra. It was noticed that at an excitation and emission of around 400 nm and 550 nm, respectively, E4 possessed detectable autofluorescence (Fig. 13 and data not shown). As E4 autofluorescence could not be easily distinguished from ThT signal, thus this staining approach did not allow for conformation of amyloid formation. Nevertheless it was established that the E4 solution contained complex macromolecular assemblies. In the sample containing BSA, no visible

structures were found and no fluorescence signal was recorded (Fig. 10). E4dN formed large, amorphous structures as well as thin, fine fibrils (Fig. 10). E4 assemblies evenly covered the entire coverslip surface and filaments were repeatedly found together with aggregates. When fluorescence was analyzed, both aggregates and fibrils exhibited fluorescence in the green emission spectrum (Fig. 10).

The presence of visible structures indicates that, upon refolding, E4 assembles into high-order structures, such as multi- and possibly polymers or aggregates. This is not caused due to the applied conditions, as BSA present in the same buffer remains dissolved without any macroscopic aggregates.

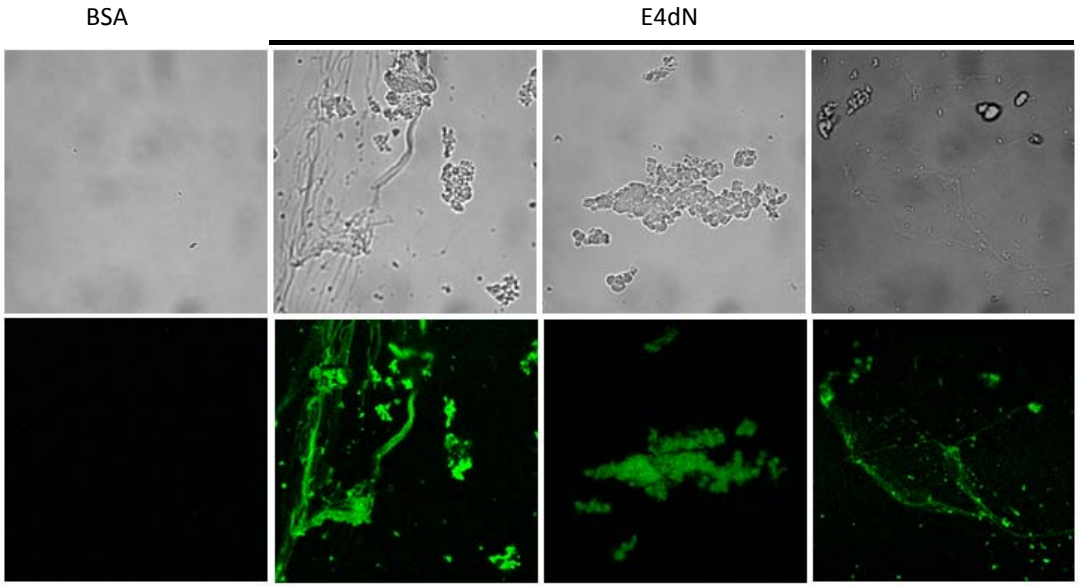

Figure 10: E4dN forms macroscopically visible structures upon refolding.
Refolded E4dN solution (3.5 mg/ml) was dried on coverslips, fixed with 4% PFA and stained with ThT (16 µg/ml). Coresponding volume of BSA (3.5 mg/ml) was used as a negative control. E4dN was visualized using confocal microscopy. Representative white light transmission images (upper panel), and corresponding fluorescence images in green spectrum (lower panel) are shown. [Magnification 40X].

The first set of experiments dealt with a technical difficulty associated with measuring the E4 concentration. Amyloids are known to assemble into fibrils of different sizes and lengths, up to several hundred nanometers long (Greenwald and Riek 2010). As described above (Fig. 10), E4 formed complex macromolecular structures during refolding that were not homogenously solubilized /solvated. For this reason, the concentration of refolded protein stocks could not be measured accurately using the NanoDrop or Bradford assays. Therefore in initial experiments protein concentrations were estimated from the concentration of E4 determined before refolding (experiments presented in chapter 2.2 and appendix 5.3 – 5.4).

To overcome this problem, in later experiments (data presented from chapter 2.3 onwards), a BSA standard curve was used to estimate the final concentration of E4. Proteins were separated using SDS-PAGE and stained with Instant Blue, a Coomassie Blue-based reagent. This dye primarily stains basic aa (arginine, lysine and histidine), which constitute 17% of the residues in BSA. The E4 variants contain around 18% basic residues, with the exception of alanine mutant E4ala, with a basic residue

content of 12%. Therefore, the relative Instant Blue binding to BSA and E4 per mg of protein is comparable, allowing for reasonably accurate quantification of the E4 concentration (Fig. 11A).

The E4 variants were also analyzed with different antibodies. E4d36 could not be detected here with either the commercial antibody against E4 (α-TVG) or a rabbit polyclonal anti-E4 antibody (α-RPE4) (prepared in collaboration with the group of Prof. Oliver T. Keppler). This finding may reflect the fact that the domain described as an immunogenic epitope was deleted in this mutant. Both E4d70 and E4ala were poorly detected with α-TVG and α-RPE4, although Instant Blue staining confirmed that all proteins were present in similar amounts. Therefore, a panel of monoclonal mouse antibodies against E4 (prepared in collaboration with the group of Prof. Oliver T. Keppler) was evaluated. Two out of the six tested antibodies detected most E4 variants (Fig. 11B).

Instant Blue staining and immunoblot analysis has shown that three of the E4 variants, E4dC, E4d70 and E4ala, were always detected, as small multimers, in addition to the monomer (Fig. 11). The E4 dimers and trimers were very resistant to denaturing conditions and could not be fully disassembled even in the presence of reducing agents and after boiling. This was especially apparent for the E4d70 variant, where the band corresponding to the size of a monomer (predicted molecular weight of approximately 9 kDa) was only occasionally observed. Depending on the protein stock, the monomer-multimer ratio was variable, with larger forms predominating in some protein preparations. Moreover, it appeared that denaturation-resistant multimers accumulate during E4 storage.

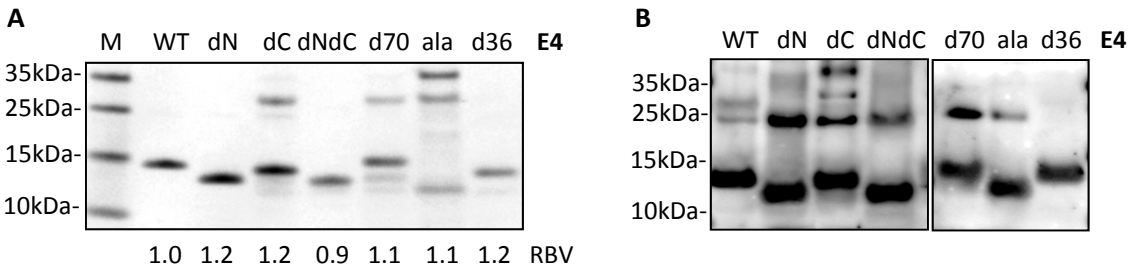

Figure 11: Quantification of the E4 protein concentrations.
(A) E4 variants were refolded at 1 mg/ml and visualized using Instant Blue staining. Protein concentration was calculated by comparing relative band volumes (RBV) of E4 variants to a BSA standard (1 mg/ml) using BIO-ID software.
(B) Immunoblot analysis was performed using α-E4-mouse monoclonal antibodies: EC8-BE2 IgM (left panel) and C8-DC3 IgM (right panel).

2.2. E4dN ENHANCES LENTIVIRAL INFECTION RATE

2.2.1 ANALYSIS OF THE CYTOTOXIC EFFECT OF E4 PROTEINS

When expressed in mammalian cells, HPV E4 alters the cell cycle and viability of cells. However, to the best of our knowledge, the effect of E4 protein treatment of cells has not been tested. For this reason, the cytotoxic effect of two different E4 variants (E4WT and E4dN) was examined to exclude changes in viability of HeLa and SupT1 CCR5 cells (a lymphocyte-derived cell line), during infection experiments. Therefore, cells were incubated with E4 for 24 h, followed by washing. Cellular viability

was measured after 72 h to mimic the conditions of a lentiviral infection in the presence of E4. To estimate the number of metabolically active HeLa and SupT1 CCR5 cells, water-soluble tetrazolium salt (WST-1)-based cytotoxicity test was performed. Wells incubated with medium only, taken as reference for 100% viability, were used as positive control.

At concentrations ranging from 1 - 200 µg/ml, E4WT and E4dN had no detectable effect on viability of HeLa or SupT1 CCR5 cell lines (Fig. 12). Nevertheless, later microscopic observations (see chapter 2.9) revealed that E4 treatment causes changes in the general cell appearance. Therefore, it cannot be excluded that administration of E4 to cells causes alterations in viability or metabolism that cannot be measured with the WST-1 assay at this time point.

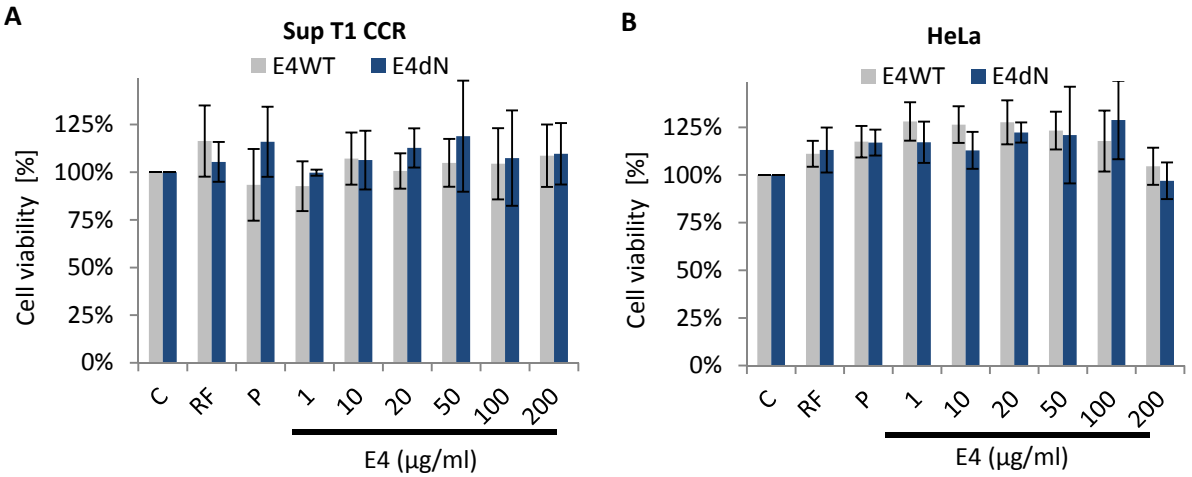

Figure 12: E4WT and E4dN do not affect viability of SupT1 CCR5 and HeLa cells.
WST-1-based cytotoxicity assay. E4 protein variants were added to SupT1 CCR5 **(A)** or HeLa **(B)** cell cultures. Cells were washed after 24 h incubation. The metabolic activity of cells was measured 72 h post-treatment. Control treated with medium only (C); refolding buffer (RF); 8 µg/ml Polybrene (P); Graphs represent data from three independent experiments, error bars reflects standard deviation (SD).

2.2.2 THE E4 PROTEIN ENHANCES THE LENTIVIRAL INFECTION RATE OF HeLa AND SupT1 CCR5 CELLS

The influence of E4dN on the lentiviral infection rate was tested in two cell lines – adherent HeLa cells and suspension SupT1 CCR5 cells. Vesicular Stomatitis Virus-G-(VSV-G)-pseudotyped lentiviral vector was used as a general model for infection with enveloped viruses, including HIV-1. This lentiviral vector has very wide tropism and enters the cells by binding to unspecific and ubiquitously expressed receptors. To allow easy detection of transduced cells, a vector expressing GFP under the control of the EF1-α promoter was used.

E4dN was mixed with the virus and added to HeLa cells. Following an overnight incubation, cells were washed. Two controls were used: cells were either incubated with the virus alone or with E4dN alone, in order to assess the effect of the E4 auto-fluorescence on the experimental readout. Additionally, as positive control, cells were infected with virus treated with polybrene (a cationic polymer commonly used to increase the efficiency of lentiviral infections).

In the initial experiments, GFP expression was examined by fluorescence microscopy. A significant increase in the infection rate was observed for E4-treated virus compared to control cells infected

with either virus alone or with polybrene-treated virus (Fig. 13). In a control containing E4 without virus, small auto-fluorescent protein aggregates were observed. However, they differed considerably in size from GFP-positive cells and therefore could not be mistaken for a false positive background.

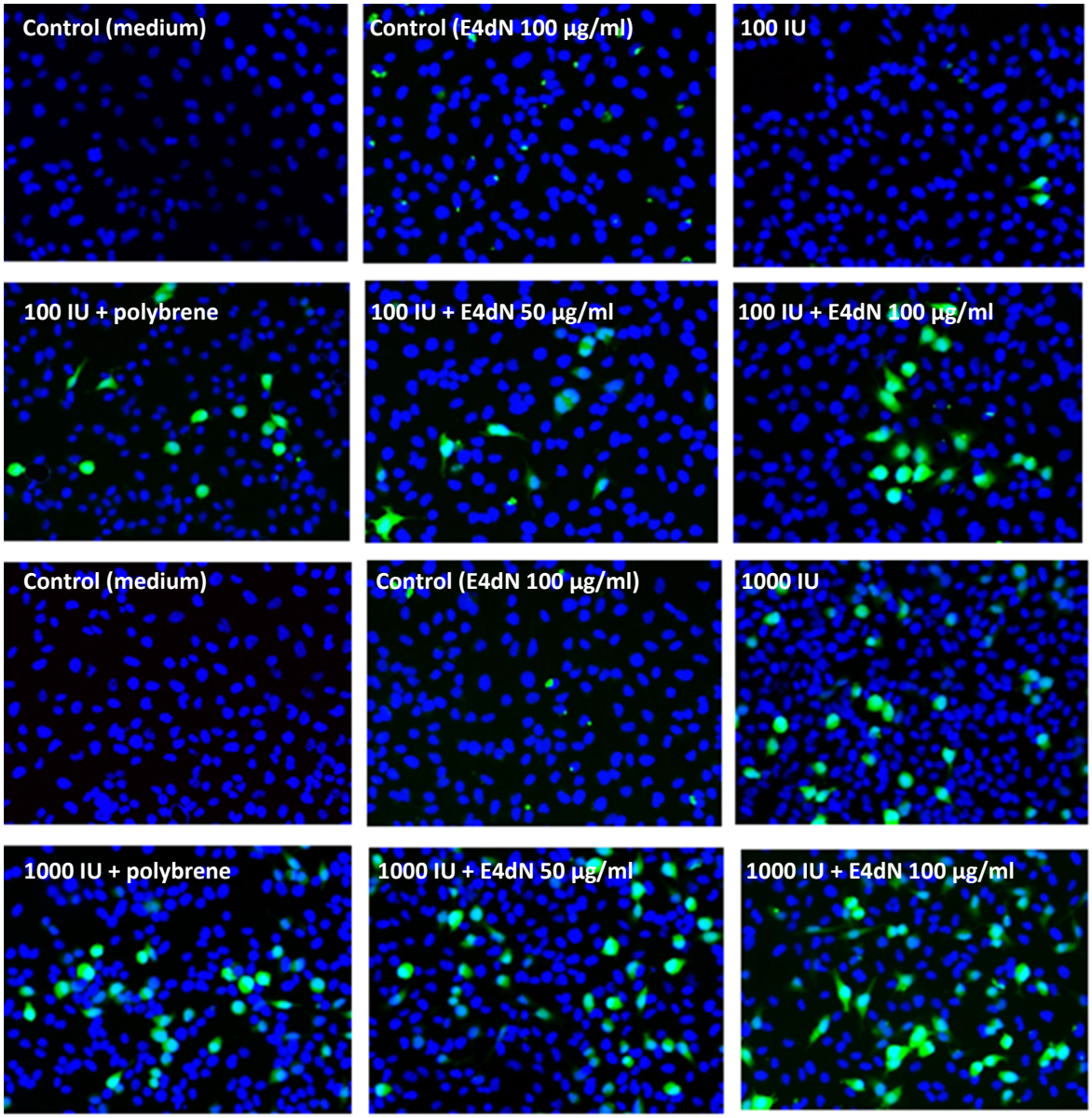

Figure 13: E4dN enhances the lentiviral infection rate.
HeLa cells were infected with 100 or 1000 infection units (IU) of VSV-G-pseudotyped lentiviral vector in the presence or absence of E4dN or polybrene. Cells were washed after overnight incubation. GFP expression was analyzed 72 h post infection by fluorescence microscopy. Representative results are shown. The experiment was independently repeated four times. [Magnification 20X].

For better quantification of the number of infected cells, GFP expression was subsequently measured by flow cytometry. E4dN augmented the lentiviral infection rate of HeLa cells up to 9-fold (Fig. 14 A and B) and of SupT1 CCR5 cells up to 12-fold (Fig. 14C). Cells treated with E4dN in the absence of virus did not exhibit any measureable fluorescence in the GFP spectrum. E4-mediated enhancement of infection was dose-dependent but reached a plateau at high concentrations. The most pronounced effect was observed for E4 at a concentration of 50 - 100 µg/ml (Fig. 14). Moreover, it was observed that, after reaching a maximum enhancement of infection, the addition of higher

amounts of E4dN (200 µg/ml) led to a gradual suppression of the E4 effect (Fig. 14C). Several explanations can be proposed. For example, even though WST-1 based tests of E4 cytotoxicity (2.2.1) revealed no changes in cellular viability, it cannot be excluded that treatment with high protein concentration leads to alterations in cellular function resulting in lower enhancement of infection.

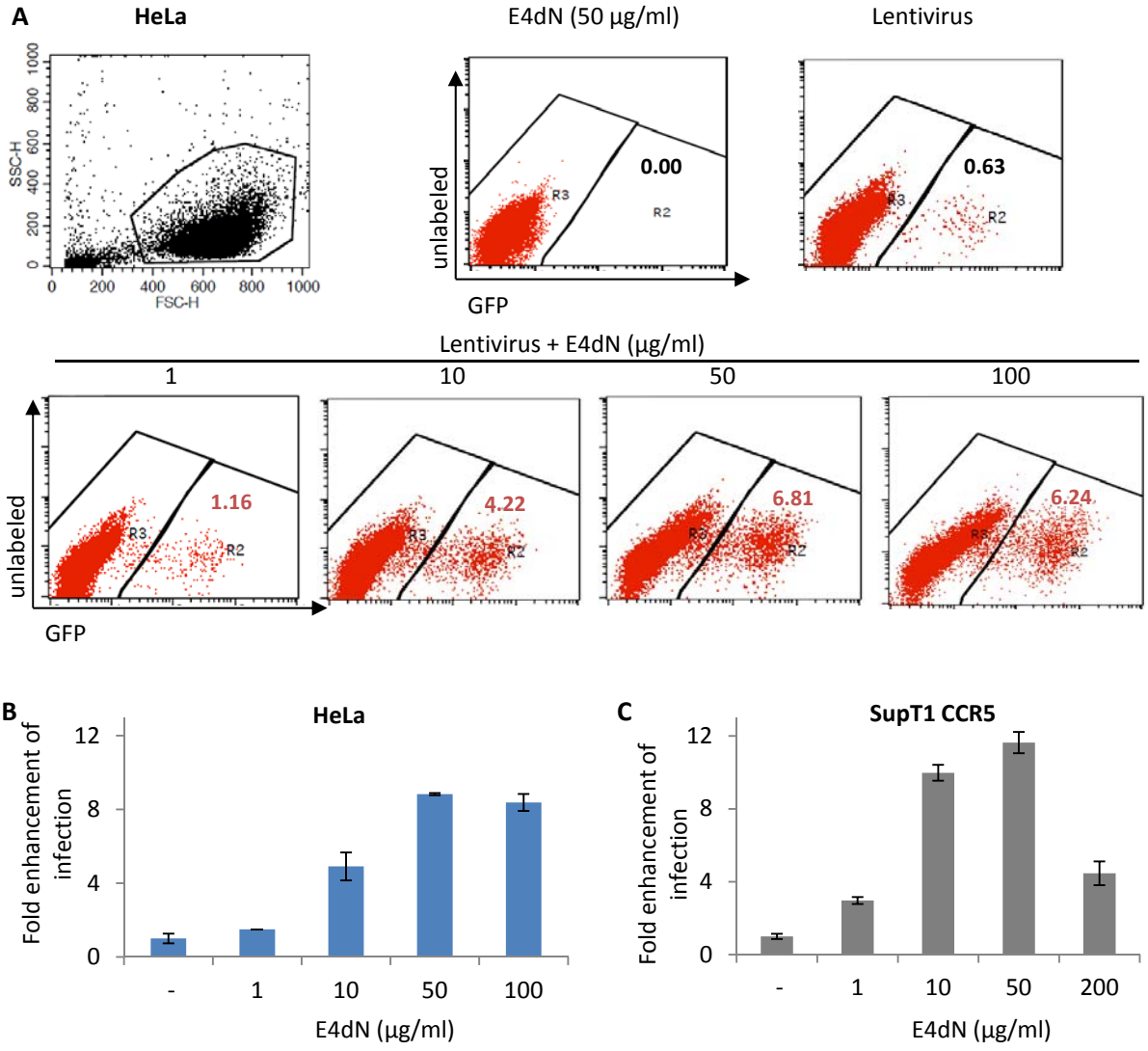

Figure 14: E4dN enhances the lentiviral infection rate in a dose-dependent manner.
HeLa **(A and B)** or SupT1 CCR5 **(C)** cells were infected with VSV-G-pseudotyped lentiviral vector (lentivirus) in the absence (-) or the presence of E4dN. Cells were washed after overnight incubation. GFP expression was measured 72 h post infection using flow cytometry.
(A) Representative dot plots for HeLa cells are shown. The numbers indicate the percentage of infected cells.
(B and C) Graphs show fold enhancements of infection. Fold enhancement of infection was calculated relative to the number of cells infected with virus without E4 (arbitrarily set as 1.0). Representative results are shown. Error bars reflect the SD of two replicates.

2.2.3 INFLUENCE OF E4 PREPARATION AND HANDLING ON AUGMENTATION OF INFECTION

The HPV E4 protein has been described to form amyloids both *in vitro* and *in vivo* (Knight et al. 2004, McIntosh et al. 2008). Amyloidogenic proteins can assemble into fibrils with different structures and biophysical characteristics depending on the conditions. *In vitro* preparation of amyloids is challenging and factors influencing this process are not well-understood (Eisenberg and Jucker 2012, Pedersen et al. 2010, Fezoui et al. 2000, Toyama and Weissman 2011). Moreover, every amyloidogenic peptide needs customized and carefully optimized handling procedures to ensure high quality of results (Chiti et al. 2001, Chiti et al. 1999, Fezoui et al. 2000, Jahn et al. 2006, Toyama and Weissman 2011). Therefore, the guidelines for handling of amyloidogenic fibrils were followed in the design of all experiments.

Details of the optimization of E4 handling conditions as well as the influence of infection settings on the E4-mediated effect are described in appendix (see 5.3.1 - 5.3.8). The most important findings are summarized below.

(I) The most stable E4 stocks were obtained if the protein was filtered to remove aggregated structures and refolded up to 3 days at 4°C.
(II) Repeated freeze-thaw cycles reduced the ability of E4 to enhance lentiviral infection.
(III) Refolded HPV16 E4 protein was active for months when stored at -20°C.
(IV) Sonication of E4 before its application resulted in a moderate enhancement of the effect on virus infection.
(V) The best results were observed when E4 was pre-incubated with the virus for 15 - 45 min at 37°C.
(VI) An optimal increase of the viral infection rate was observed when E4 was pre-incubated with the virus in a small volume before adding to cells, then in decreasing order: E4 mixed with the virus and added directly onto cells > E4 incubated with cells and virus added after 15 min > cells incubated with virus for 15 min before adding E4. This effect reflects the observation that,
(VII) the maximal concentration of E4 present with the virus prior to infection, not the final concentration of protein, determined the increase of infection;

When these findings were taken into account during protein preparation and design of experimental settings, the enhancement of the infection rate of SupT1 CCR5 cells increased above 30-fold (Fig. 15).

In these experiments, it was observed that the enhancement of infection rate is approximately 2-fold higher for suspension (SupT1 CCR5) than for adherent (HeLa) cells (see appendix 5.3.1-5.3.8). In HeLa cells, contact with E4 occurs only on the surface of the cell monolayer, while E4 can bind to suspension cells in all three dimensions. This may allow for a higher likelihood of E4-virus-cell interactions explaining stronger enhancement of lentiviral transduction.

E4dN strongly enhanced the lentiviral infection rate, but still the degree of enhancement differed from protein preparation to preparation. Several possible explanations may be proposed. First, high molecular weight structures formed by E4 are surprisingly heterogeneous, as observed using microscopy (see chapter 2.1 and 2.7). E4 multimers differ both in size and shape, ranging from thin filaments to large fibril assemblies and non-structural aggregates in a single sample. E4 is known to form heterogeneous structures (Khan et al. 2011) and the amyloid/multimer/monomer ratio in

solution depends on the protein preparation conditions (Antzutkin et al. 2002, Jimenez et al. 2001). Therefore, the same amount of protein from different batches or even different aliquots of the same batch may differ in the amount of functional protein. Moreover, E4 appears to readily interact with all types of surfaces, adhering to both glass and plastic of tips and pipets. This may lead to accidental loss of protein during handling, decreasing E4 concentration and influencing the final infection outcome.

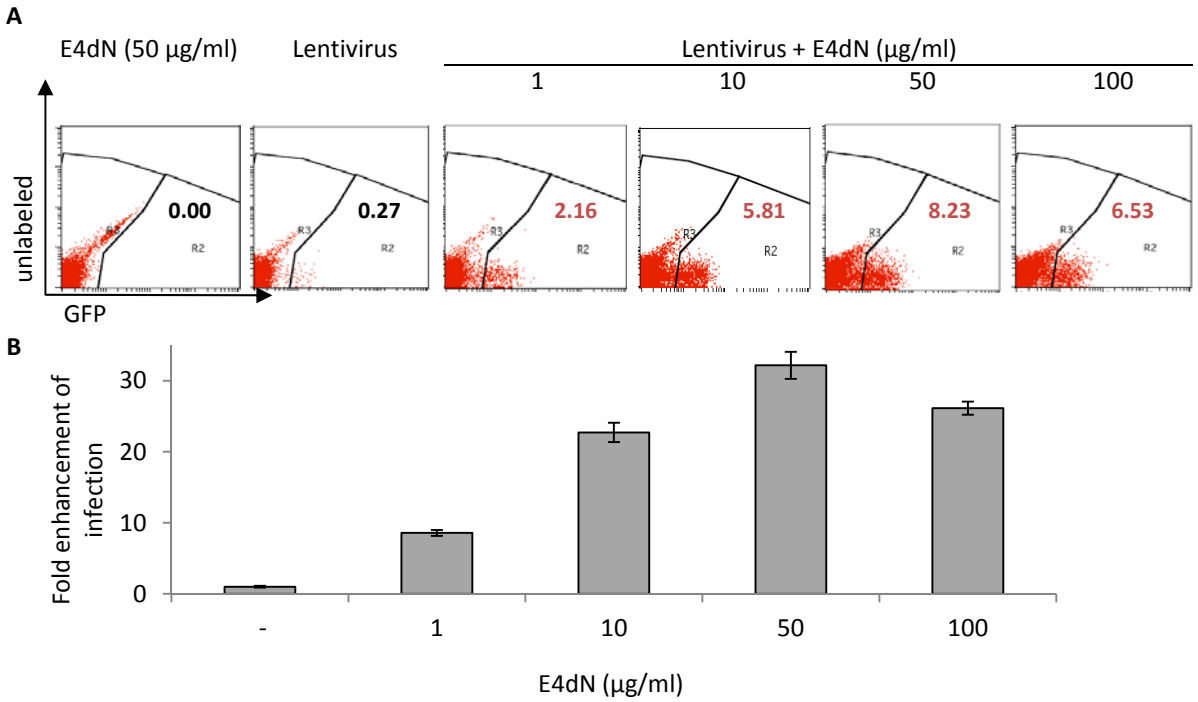

Figure 15: Optimization of E4 handling led to an augmentation of the E4-mediated effect.
Sup T1 CCR5 cells were infected with VSV-G pseudotyped lentiviral vector (lentivirus) in the absence (-) or the presence of E4dN. GFP expression was measured 72 h post-infection using flow cytometry.
(A) Representative FACS dot plots. Numbers indicate the percentage of infected cells.
(B) Fold enhancement of infection was calculated relative to the number of cells infected with virus without E4 (arbitrarily set as 1.0). The results of a single representative experiment are shown. Error bars reflect the SD of three replicates.

2.2.4 LOW pH DOES NOT INFLUENCE E4 ACTIVITY

It is known that different pH conditions can promote the formation of fibrils with altered morphology (Pfefferkorn et al. 2010, Zhu et al. 2003). *In vivo*, E4 fibrils form in female reproductive tracts, an environment that is characterized by acidic conditions (Linhares et al. 2011, Witkin et al. 2007). For this reason, the influence on lentivirus transduction was analyzed when E4dN was refolded either at neutral pH 7.0 or at an acidic pH of 5.5 and 4.5, matching the pH of the female genital system.

No significant difference in the effect of E4dN proteins prepared at different pH values was detected. Importantly, low pH during refolding did not cause E4 protein inactivation and had no observable effect on E4-mediated enhancement of the lentiviral infection rate (Fig. 16).

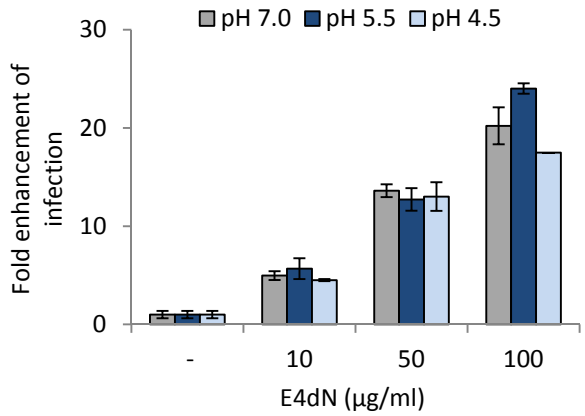

Figure 16: pH of E4 refolding has no significant effect on E4 activity.
E4dN was refolded at indicated pH. SupT1 CCR5 cells were infected with VSV-G-pseudotyped lentiviral vector in the absence (-) or the presence of E4dN. GFP expression was measured 72 h post-infection using flow cytometry. Fold enhancement of infection was calculated relative to the number of cells infected with virus without E4 (arbitrarily set as 1.0). The results of a single representative experiment are shown. Error bars reflect the SD of three replicates.

2.2.5 THE E4-MEDIATED ENHANCEMENT OF INFECTION IS BEST OBSERVED AT LOW INFECTION UNITS

During sexual transmission of HIV, the concentration of virus deposited in the anogenital track is very low. As a consequence, only few virus particles succeed in establishing the primary infection (Keele et al. 2008, Parker et al. 2013, Shaw and Hunter 2012). Hence, the influence of E4 on the infection rate in the presence of different amounts of virus was investigated. SupT1 CCR5 cells were incubated with increasing amount of VSV-G-pseudotyped lentiviral vector, 10 - 2000 infection units, in the presence or absence of E4dN. Quantitative measurements of GFP expression was performed with flow cytometry.

In agreement with the previous microscopic observations (Fig. 13), the highest enhancement of infection, more than 100-fold, was observed at the lowest viral doses used, when only approximately 0.01% of cells were infected in the absence of E4. The fold change gradually decreased with increasing infection units (Fig. 17). A similar correlation was observed for HeLa cells (data not shown).

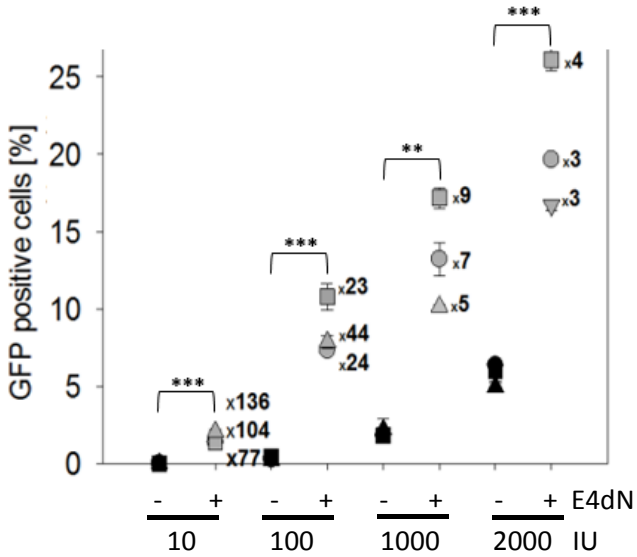

Figure 17: The strongest E4 effect is observed at infection with low viral doses.
SupT1 CCR5 cells were infected with VSV-G-pseudotyped lentiviral vector in the presence or absence of E4dN (100 µg/ml). GFP expression was measured by flow cytometry 72 h post-infection. The diagram shows the percentage of GFP positive cells. Each dot/triangle/square represents the mean of one independent experiment performed in triplicates (error bars reflect the SD). For significance calculations the mean of the three independent experiments was formed. Numbers indicate the enhancement of the infection rate calculated relative to the respective control (cells infected in the absence of E4 set as 1.0).

At the lowest amount of virus tested only around 1% of cells become infected, even in the presence of E4 (Fig. 17). In these conditions the number of cells infected without E4 was close to 0. Such a small population of cells can be easily influenced by additional factors, independent of E4 function. Therefore, although the E4-mediated increase of infection is most pronounced at very low infection

units (10 IU), future experiments were performed with a higher infection rate (100 IU or more) to ensure more robust experimental settings.

2.3 FUNCTIONAL CHARACTERIZATION OF E4 DOMAINS MEDIATING THE ENHANCEMENT OF LENTIVIRAL INFECTION

2.3.1 E4 VARIANTS WITH MUTATIONS IN FUNCTIONAL DOMAINS ENHANCE THE INFECTION RATE TO DIFFERENT DEGREES

To characterize the contribution of different, E4 structural-functional domains on the lentiviral infection rate an array of E4 mutants (Table 1) was analyzed. Surprisingly, all tested E4 variants enhanced the lentiviral infection rate in a dose-dependent manner. The strongest effect was observed for the truncated version of E4 (E4dN), corresponding to the naturally occurring calpain cleavage form (up to 40-fold enhancement). The full-length protein (E4WT) also strongly enhanced the infection rate up to 20-fold. Partial deletion of the C-terminal multimerization domain (E4dC) weakened the E4 effect and an enhancement of up to 15-fold was observed. When an E4 variant with both N-terminal and partial C-terminal truncations (E4dNdC) was tested, the infection enhancement within the similar range as for the E4dC was seen. All variants augmented the lentiviral infection, reaching an optimal enhancement effect at 50-100 mg/ml (Fig. 18).

Since the deletion in the multimerization domain appeared to interfere with the E4-mediated enhancement of the infection rate, a mutant lacking the whole C-terminal domain (E4d70) was also tested. This deletion further reduced the E4 effect, leading to an increase of infection of only maximaly up to 10-fold (Fig. 18). Moreover, the effect of E4d70 reached saturation at a relatively low protein concentration compared with other E4 variants and could not be improved by further addition of protein (Fig. 18).

Finally, a mutant with the deletion of the positively charged amino acids clustered in the central loop (E4d36) was tested. This domain is postulated to be involved in structural changes of E4, including assembly into amyloid fibrils (Doorbar, 2013). Nevertheless this mutant still increased the infection rate up to 10-fold (Fig. 18).

In summary, all tested deletion mutants and wild type E4 protein augmented the lentiviral infection rate, although to a lesser degree than E4dN. Unexpectedly, none of the designed deletions of functionally pre-defined domains was able to completely abolish E4-mediated enhancement of infection.

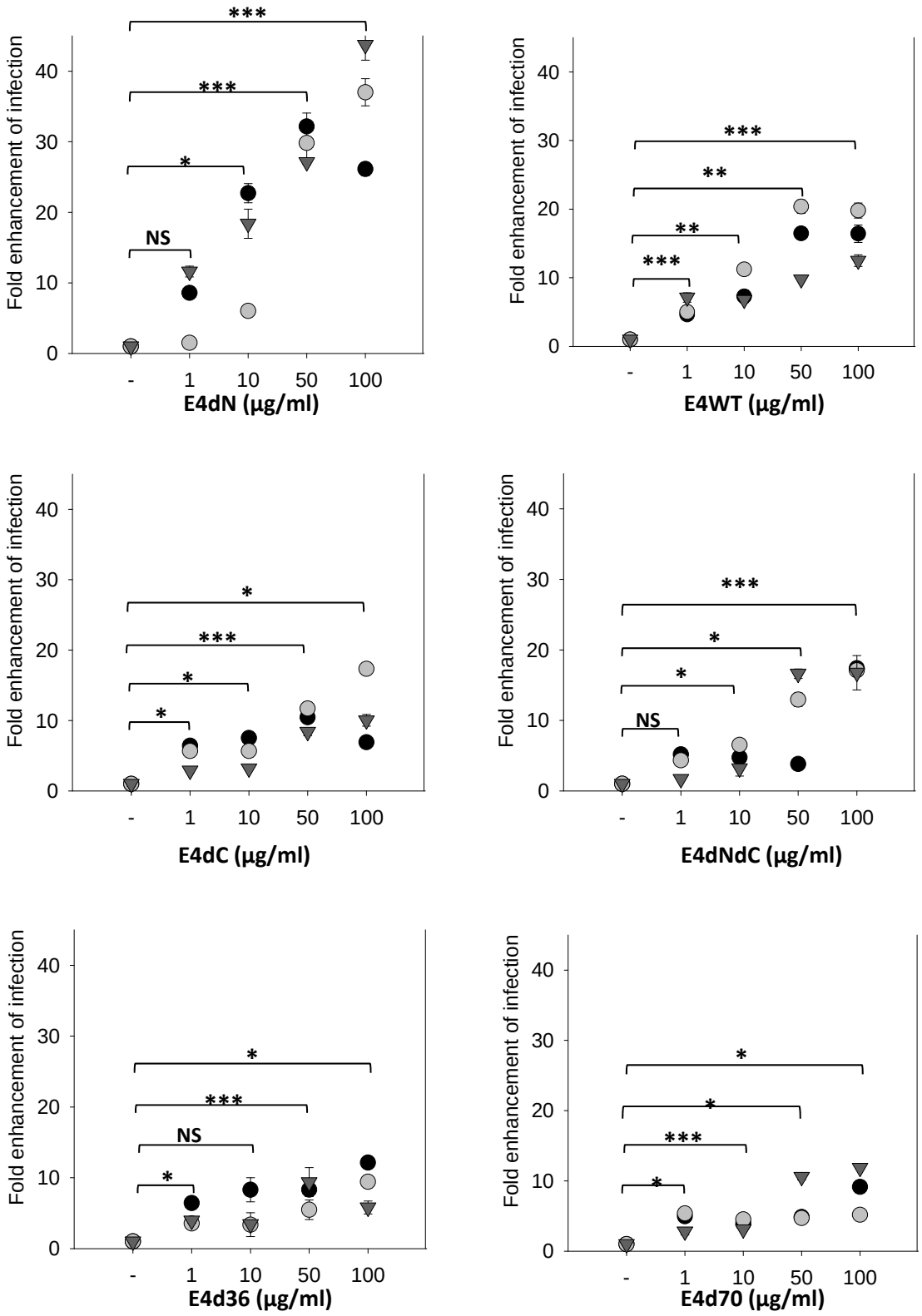

Figure 18: E4 variants with deletions of structural domains enhance the lentiviral infection rate.
SupT1 CCR5 cells were infected with VSV-G-pseudotyped lentivirus in the absence (-) or presence of different E4 variants. GFP expression was measured 72 h post-infection using flow cytometry. Fold enhancement of infection was calculated relative to the number of cells infected with virus without E4 (arbitrarily set as 1.0). Each dot/triangle represents the mean of one independent experiment performed in triplicates (error bars reflect the SD). For significance calculations the mean of the three independent experiments was formed; not significant (NS).

2.3.2. THE E4 MULTIMERIZATION DOMAIN (66-92) ENHANCES THE INFECTION RATE

As presented above, all of the tested E4 mutants, even the one with deletions of the multimerization domain, enhanced lentiviral transduction. The multimerization domain is described to be necessary for amyloid formation, moreover on its own it assembles into short fibrils (McIntosh et al. 2008). Therefore, the effect of the E4 multimerization domain (E4C) on the lentiviral infection rate was analyzed. A synthetic peptide consisting of residues 66 - 92 was refolded in PBS and resulted in a turbid solution.

Addition of the E4C peptide increased the lentiviral infection rate up to 15-fold. This effect was, as with the other E4 variants, protein concentration-dependent, with the most prominent enhancement at 50 - 100 µg/ml (Fig. 19). Although the E4C-mediated enhancement of infection was approximately one-third lower than the effect normally observed for E4dN, it was shown that the multimerization domain alone has a significant potential to augment infection.

Both the C-terminal multimerization domin (E4C) and the E4 variant lacking it (E4d70), increased the lentiviral infection rate. This suggests that the E4-mediated effect may be largely sequence-independent and rather based on the particular structural properties of the protein. Accordingly, similar observation was made for two amyloid forming peptides derived from the opposite ends of PAP (Arnold et al. 2012, Munch et al. 2007).

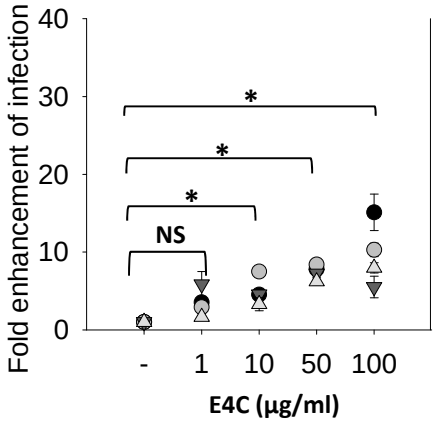

Figure 19: The E4 multimerization domain enhances the lentiviral infection rate.
SupT1 cells were infected with VSV-G-pseudotyped vectors in the absence (-) or presence of E4C. GFP expression was measured 72 h post-infection by flow cytometry. Fold enhancement of infection was calculated relative to the number of cells infected with virus without E4 (arbitrarily set as 1.0). Each dot/triangle represents the mean of one independent experiment performed in triplicates (error bars reflect the SD). For significance calculations the mean of the four independent experiments was formed; not significant (NS)

Surprisingly, none of the designed mutations abolished the E4 effect on the infection rate. And even mutants that should not be able to form amyloids augmented lentiviral transduction. This finding was unexpected and required further evaluation. Several controls were prepared to exclude the possibility that the observed effect was caused by: (I) the refolding buffer itself, (II) co-purification of other bacterial proteins that could influence the infection rate or (III) the presence of the 6xHis-tag.

To check for the first possibility the VSV-G-pseudotyped lentiviral vector was pre-incubated with E4 or the corresponding volume of refolding buffer. When the percentage of GFP-positive cells was measured, the refolding buffer on its own had no observable effect (Fig. 20A).

Co-purification of bacterial compounds such as toxins and other contaminations could influence the infection rate and cause a false positive result. To test for this possibility a control bacterial lysate with an empty pQc8 vector was prepared following the procedure described in chapter 4.5. In the

purified control lysate, no protein was detected by Instant Blue staining and the protein concentration was below the detection limit when measured by NanoDrop (not shown). Using the same infection settings, E4 strongly enhanced the lentiviral infection, above 30-fold, while the control lysate had no detectable effect (Fig. 20B).

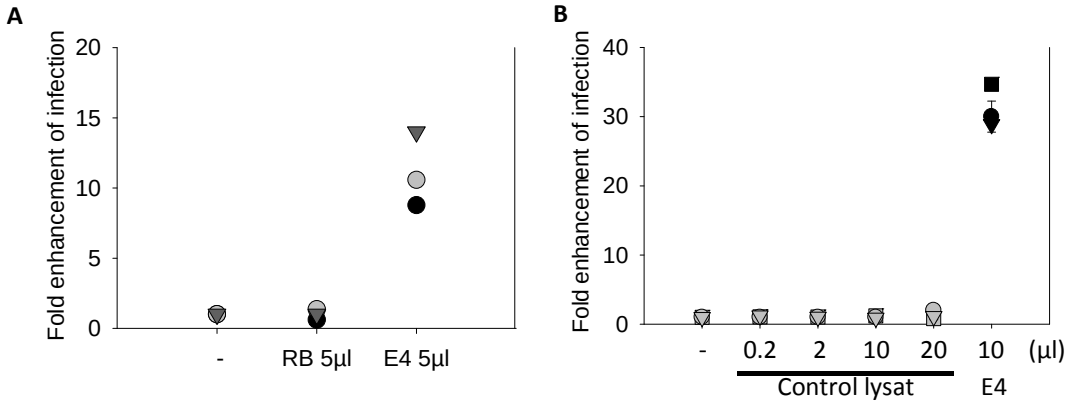

Figure 20: The refolding buffer and a control lysate have no detectable effect on the lentiviral infection rate. SupT1 CCR5 cells were infected with VSV-G-pseudotyped lentiviral vector in in the absence (-) or the presence of E4dN (E4) and either refolding buffer **(A)** or control bacterial lysate **(B)**. When protein concentration could not be determined due to experimental settings (e.g. in refolding buffer) corresponding volumes of tested solutions were used. GFP expression was measured 72 h post-infection by flow cytometry. Fold enhancement of infection was calculated relative to the number of cells infected with virus without E4 (arbitrarily set as 1.0). Each dot/triangle/square represents the mean of one independent experiment performed in triplicates (error bars reflect the SD).

The majority of the protein variants used in this work was bacterially expressed (see 2.1). To enable purification by affinity chromatography all proteins had a 6xHis-tag that binds to the Nickel ion triads (Cheung et al. 2012). To confirm that the observed effects are mediated by E4 itself, and are not influenced by the presence of the 6xHis-tag in the protein, a synthetic E4dN polypeptide without the His-tag was tested.

As the E4-mediated enhancement of the infection rate strongly depends on the protein amount, the concentrations of the two proteins, bacterially expressed and synthetic, were adjusted using SDS-PAGE and Instant Blue staining. Both proteins were present in comparable amounts (Fig. 21A). Upon refolding, the synthetic E4 became turbid, revealing microscopic visible aggregate-like structures, similar to those observed in bacterially expressed E4. Synthetic E4 significantly enhanced lentiviral infection rate in a dose-dependent manner to a similar extent as bacterially expressed E4 (Fig. 21B).

Summarizing, the augmentation of lentiviral infection was not caused by co-purification of other bacterial proteins or the refolding buffer. Moreover, the 6xHis-tag does not play a role in the E4-mediated enhancement of infection, as the synthetic E4dN polypeptide lacking the tag increased infection to the same degree as bacterially expressed E4dN. These results strongly support the finding that E4 is required and sufficient for the enhancement of the lentiviral infection rate.

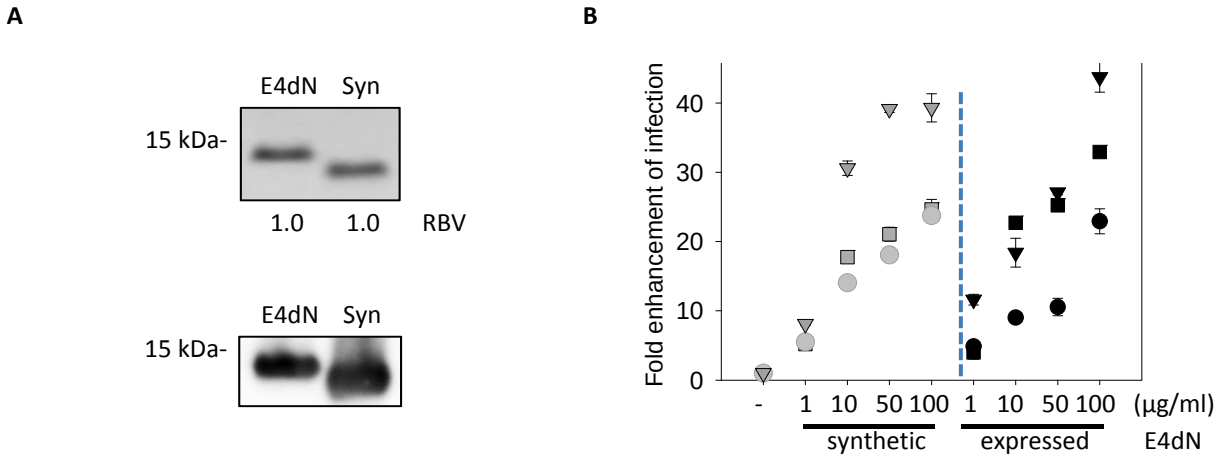

Figure 21: Synthetic E4 enhances the infection rate to the same degree as bacterially expressed protein.
(A) Comparison of the protein amounts. Bacterial-expressed (E4dN) and synthetic E4dN (Syn) were refolded at a concentration of 1 mg/ml and visualized using Instant Blue (upper panel) or α-RPE4 (lower panel). The protein concentration was compared using Bio-ID software based on relative band volumes (RBV).
(B) VSV-G-pseudotyped lentiviral vector was pre-incubated in the absence (-) or presence of bacterially expressed or synthetic E4dN. SupT1 CCR5 cells were infected. GFP expression was measured 72 h post-infection by flow cytometry. Fold enhancement of infection was calculated relative to the number of cells infected with virus without E4 (arbitrarily set as 1.0). Each dot/triangle/square represents the mean of one independent experiment performed in triplicates (error bars reflect the SD).

Fetal bovine serum (FBS) may affect the lentiviral infection efficiency. Additionally, it was shown that E4dN augmented lentiviral infection in the serum free medium (see appendix 5.4). This indicates that no serum cofactor is required for the E4-mediated enhancement of the infection rate.

2.3.3. COMPARISON OF THE E4 EFFECT WITH THAT OF OTHER HPV PROTEINS: E7 AND L1

Next the E4 effect was compared with that of other HPV proteins: E7 and a mutant L1. E7 is an oncoprotein that *in vivo* forms mostly monomers and dimers, although some multimeric structures can form *in vitro* (Petrone et al. 2011). The mutant L1 protein can assemble into pentamers but is deficient in forming capsids (L1 construct was a kind gift from Prof. Martin Müller, Schadlich et al. 2009). Both proteins were expressed in the bacterial system and purified using nickel affinity chromatography. As with E4, refolded L1 became turbid, while the E7 solution remained clear. The purity and the concentration of proteins was measured as described for E4. The amount of mutant L1 could not be reliably quantified, because this protein was detected in form of a ladder. The presence of the L1 products of different length may be caused either by degradation or abortive transcription/translation (Fig. 22A).

Both, E7 and mutant L1 were tested in infection assays and their effect was compared with that of E4. E7 had no detectable effect on the lentiviral infection rate, even at the highest tested concentration of 100 µg/ml. Under the same conditions, E4 enhanced the infection rate up to 40-fold (Fig. 22B). The L1 mutant increased the infection rate of the VSV-G-pseudotyped lentivirus up to 10-fold. L1-mediated enhancement of infection was approximately 25% of that seen for E4 (Fig. 22C).

The relative ability of L1 to augment infection was further confirmed using virus-like particles (VLPs) consisting of the HPV16 capsid L1 protein (a kind gift from Prof. Martin Müller). A VLP stock of

1 mg/ml was dialyzed in PBS and the L1 protein concentration was confirmed by SDS-PAGE and Instant Blue staining. Unlike the bacterially expressed mutant L1 protein, L1 from VLPs was detected as a single band of approximately 55 kDa (Fig. 23D). VLPs enhanced the infection rate up to 20-fold, half of the effect observed for E4dN (Fig. 23E).

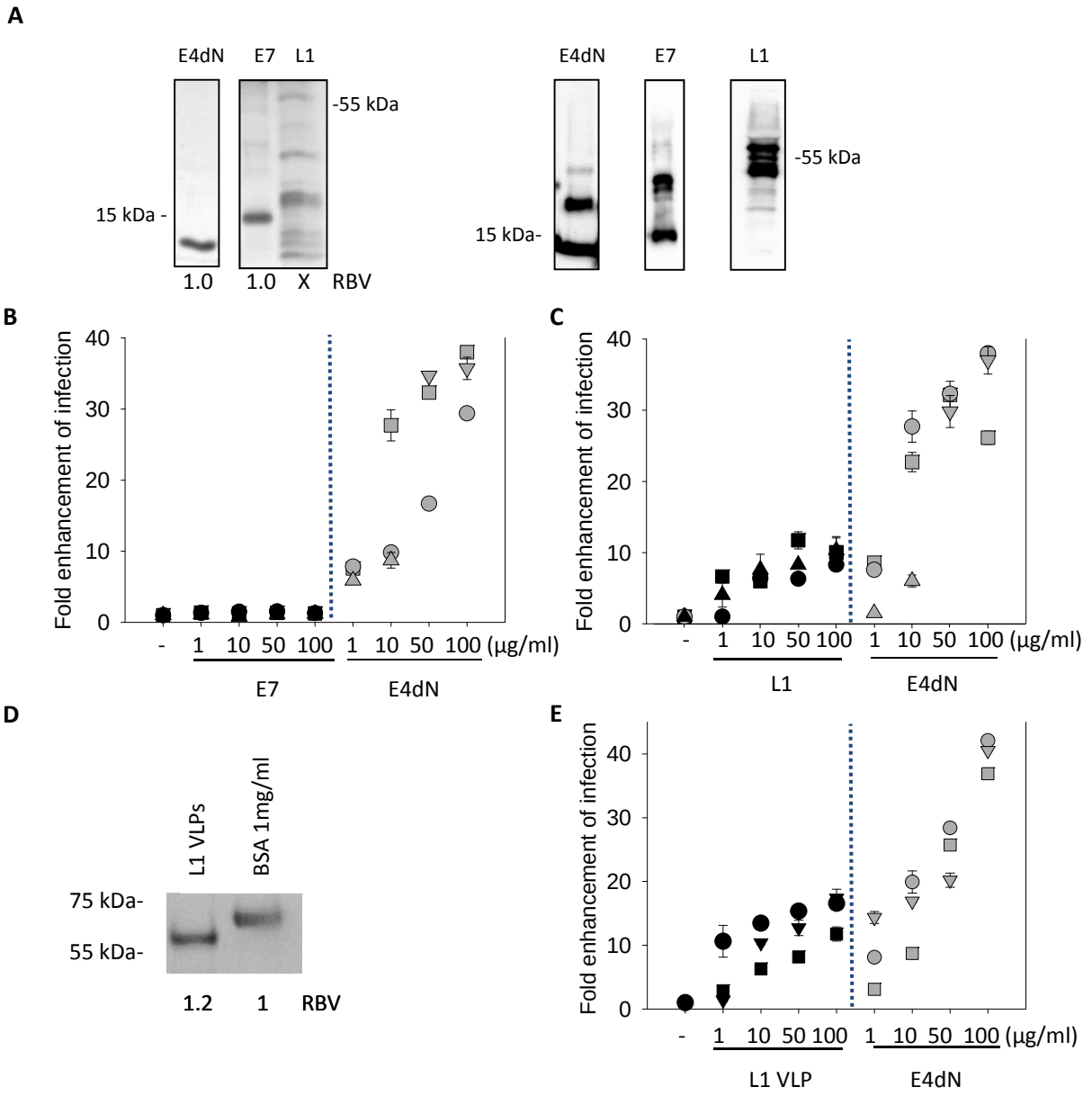

Figure 22: HPV16 L1 protein enhances lentiviral infection rate while HPV16 E7 has no observable effect.
E4, E7, L1 **(A)** and VLPs **(D)** were visualized using SDS-PAGE and Instant Blue staining. Protein concentrations were compared using Bio-ID software based on relative band volumes (RBV). Immunoblot analysis was performed using an α-His-tag antibody (**A** right panel).
SupT1 CCR5 cells were infected with VSV-G-pseudotyped lentiviral vector in the absence (-) or presence of E7 **(B)**, L1 **(C)** or VLPs **(E)**. E4, at the same concentration range, was used as a positive control. GFP expression was measured 72 h post-infection by flow cytometry. Fold enhancement of infection was calculated relative to the number of cells infected with virus without E4 (arbitrarily set as 1.0) Each dot/triangle/square represents the mean of one independent experiment performed in triplicates (error bars reflect the SD).

These results lead to the interesting possibility that the observed augmentation of the lentiviral infection may not be restricted to only amyloids, but rather represents a broader phenomenon based on the formation of multimers by proteins.

2.4 THE E4 EFFECT IS COMPARABLE WITH OTHER ENHANCERS OF LENTIVIRAL INFECTION

2.4.1 THE E4-MEDIATED ENHANCEMENT OF INFECTION IS STRONGER THAN THE EFFECT OF POLYBRENE

Cationic polymers such as polybrene are commonly used to increase the efficiency of retrovirus-mediated gene transfer. Polybrene is an unspecific enhancer of infection and its effect is both virus- and cell type- independent. It is suggested that, due to its positive charge, polybrene augments receptor-independent virus absorption. The recommended concentration of polybrene is ~8 µg/ml (Denning et al. 2013, Davis et al. 2002). In these experiments the effect of E4 was compared with an optimized amount of polybrene. For this purpose, VSV-G-pseudotyped lentiviral vectors were pre-incubated with E4dN or polybrene for 15 min and added to cells. GFP expression was measured 72 h post-infection by flow cytometry.

Polybrene-mediated enhancement of infection was not greater than 12-fold (Fig. 23). The effect of E4dN was much stronger and increased of the lentiviral infection rate more than 40-fold (Fig. 23).

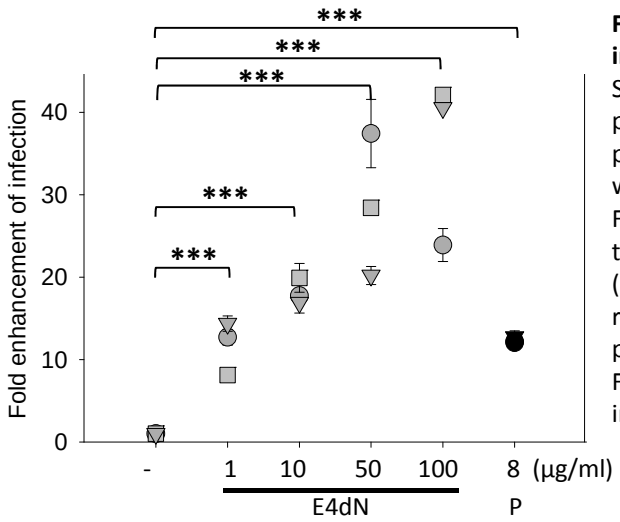

Figure 23: E4-mediated enhancement of lentiviral infection is stronger than the effect of polybrene. SupT1 CCR5 cells were infected with VSV-G-pseudotyped lentiviral vector in the absence (-) or presence of E4dN or polybrene (P). GFP expression was measured 72 h post-infection by flow cytometry. Fold enhancement of infection was calculated relative to the number of cells infected with virus without E4 (arbitrarily set as 1.0). Each dot/triangle/square represents the mean of one independent experiment performed in triplicates (error bars reflect the SD). For significance calculations the mean of the three independent experiments was formed.

2.4.2 THE E4-MEDIATED ENHANCEMENT OF INFECTION IS COMPARABLE WITH THE EFFECT OF SEVI

The effect of E4 was next compared with other amyloid forming peptides. SEVI and $A\beta_{40}$ were chosen as known enhancers of the lentiviral infection rate (Arnold et al. 2012, Capule et al. 2012, Munch et al. 2007, Olsen et al. 2010, Wojtowicz et al. 2002).

Both SEVI and $A\beta_{40}$ synthetic peptides were refolded as described in respective publications showing their influence on the infection rate of enveloped viruses (Munch et al. 2007, Wojtowicz et al. 2002). Briefly, peptides were resuspended in PBS and refolded while shaking overnight at 37°C. After

refolding, the SEVI solution turned turbid with macroscopically visible clots. The $A\beta_{40}$ solution remained clear. To compare the effect of all proteins on VSV-G-pseudotyped lentiviral infection rate, SupT1 CCR5 cells were infected in the absence or presence of increasing concentrations of SEVI, $A\beta_{40}$ and E4dN pre-incubated with virus, according to the standard protocol.

SEVI enhanced the lentiviral infection rate up to 20-fold and, in the tested conditions, this effect was comparable to that of E4dN (Fig. 24A). $A\beta_{40}$ had no observable effect on the lentiviral infection rate in either HeLa or SupT1 CCR5 cells while, under the same experimental settings, E4dN enhanced the infection rate (data not shown). It cannot be excluded that, under the described conditions, protein refolding was suboptimal and/or the Alzheimer peptide quality was not sufficient. It is known that amyloid formation may be highly accelerated by seeding. The addition of a precursor amyloid can act as a nucleus for the formation of new fibrils. Moreover, previous literature has described cross-seeding with one type of amyloid as a trigger for the formation of fibrils from different precursor protein (Eisenberg et al. 2012). Thus, 200 µl of $A\beta_{40}$ solution was spiked with 1 µl of SEVI and refolded by shaking overnight at 37°C. No change of turbidity was noticed and no visible structures were observed by microscopy. When tested in functional assays, $A\beta_{40}$ enhanced the lentivira infection rate up to 2-fold while E4dN increased infection by 20-fold (Fig. 24B). Nevertheless, it cannot be excluded that the observed activity was caused by the presence of SEVI (added to promote cross-seeding) rather than by $A\beta_{40}$ itself.

Importantly, the effect of E4 was shown to be similar in strength to that observed for SEVI. Under the tested conditions, $A\beta_{40}$ was not functional. Notably, this result agrees with previous studies where SEVI-mediated enhancement of HIV-1 infection was compared with $A\beta_{40}$ and the latter showed no activity (Munch et al. 2007).

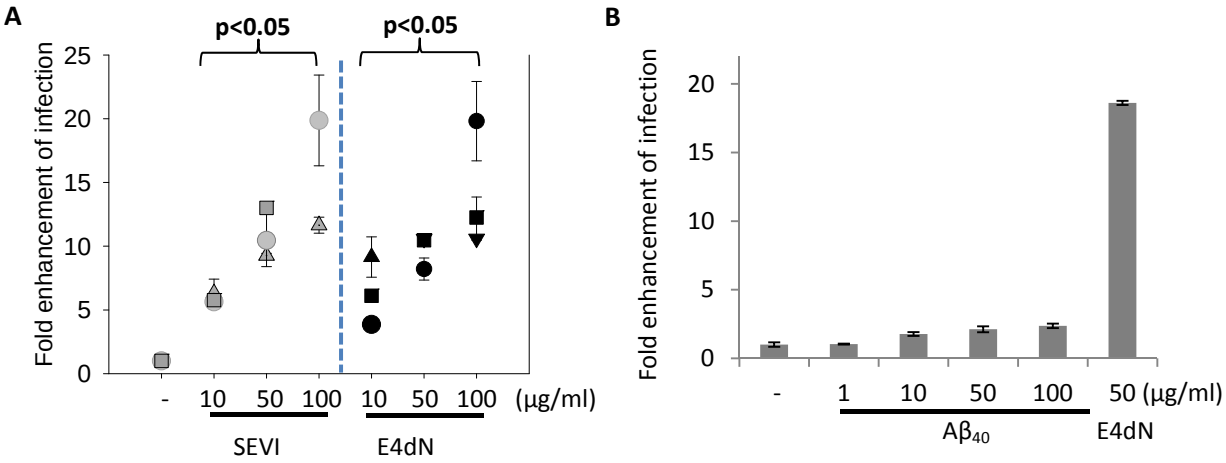

Figure 24: E4dN increases the lentiviral infection rate to the same degree as SEVI.
SupT1 CCR5 cells were infected with VSV-G-pseudotyped lentiviral vector in the absence (-) or presence of E4dN and either SEVI **(A)** or $A\beta_{40}$ **(B)**. GFP expression was measured 72 h post-infection by flow cytometry. Fold enhancement of infection was calculated relative to the number of cells infected with virus without E4 (arbitrarily set as 1.0).
(A) Each dot/triangle/square represents the mean of one independent experiment performed in triplicates (error bars reflect the SD). For significance calculations the mean of the three independent experiments was formed and compared with the control (-).
(B) The results of a single representative performed in triplicates experiment are shown. Error bars reflect the SD.

2.5 E4 PROTEINS FROM DIFFERENT HPV TYPES ENHANCE LENTIVIRAL INFECTION

Epidemiological studies have reported a strong association of various, not only oncogenic, HPV types with an elevated HIV-1 infection rate. Our results from the lentiviral model indicate that HPV16 E4 may mediate this effect. Based on epidemiological reports (Houlihan et al. 2012, Lissouba et al. 2013) five additional HPV types were chosen to test the effect of the different E4 proteins on the lentiviral infection. We included the high-risk HPV18 and HPV58 genotypes and low-risk HPV11, HPV42 and HPV70 genotypes, which cause common genital warts. Two variants of E4 from each HPV type were prepared (a kind gift from Julia Bulkescher), wild-type E4 corresponding to the full-length protein and a mutant version with an N-terminal truncation (E4dN). E4dN mutants were designed based on known (HPV11 and HPV18) or predicted (based on conserved LLXLLX sequence) calpain cleavage sites (Table 2).

Table 2: E4 constructs from different HPV types.

E4 variant	Sequence
HPV16	MADPAAATKYPLLKLLGSTWPTTPPRPIPKPSPWAPKKHRRLSSDQDQSQTPETPATPLSCCTETQWTVLQSSLHLTAHTKDGLTVIVTLHP
HPV18	MADPEVPVTTRYPLLSLLNSYSTPPHRIPAPCPWAPQRPTARRRLLHDLDTVDSRRSSIVDLSTHFSVQLHLQATTKDGNVVVTLRL
HPV11	MADDSALYEKYPLLNLLHTPPHRPPPLQCPPAPRKTACRRRLGSEHVDRPLTTPCVWPTSDPWTVQSTTSSLTITTSTKEGTTVTVQLRL
HPV42	MADDTAPHPPTQRYPLLDLLSWYNKCAPQTHCTPQRPLTTTTQTVQTEQHTTCPSKPHRHENDTDSVDSRHHSTCSTQTPASPASPAHPWTLDC VGSELTVKTVTSDGTTVEVRLRL
HPV58	MDDPEVIKYPLLKLLTQRPPRPPTTKVHRGQSDDDSIYQTPETTPSTPQSIQTAPWTVDHEEEDYTVQLTVHTKGGTCVVLKFHLSCI
HPV70	MANCEVPVTTQYPLLSLLQNYNTPPRPIPPQQPHAPKKLSRRRLASVESPDPQKQTECSWTLLQVKAATNDGTSVVVTLHL

Conserved amino acids at the calpain cleavage site are marked in green. The calpain cleavage site, which marks the N-terminus of the E4dN variants is indicated with a green arrow. Positively charged amino acids are marked in red. Conserved amino acids, according to ClustalW multiple aligiment, are underlined.

The E4 proteins from different HPV types were bacterially expressed with an N-terminal 6xHis-tag and purified using nickel affinity chromatography. After refolding, all E4 protein preparations became turbid and also developed macroscopic clots, characteristic for HPV16 E4. The protein concentration was adjusted after E4 refolding using SDS-PAGE and Instant Blue staining (Fig. 25A). To test the effect of the chosen E4 variants on the infection rate, SupT1 CCR5 cells were infected with VSV-G-pseudotyped lentivirus in the absence or presence of increasing concentrations of E4WT and E4dN.

Both E4WT and the truncated E4dN from all tested HPV types (HPV11, HPV16, HPV18, HPV42, HPV58, HPV70) augmented the VSV-G-pseudotyped lentiviral infection rate. No significant difference between proteins from low- and high-risk HPV types was observed. The E4-mediated enhancement of the lentiviral infection was dose-dependent. Moreover, in accordance with previous data, truncated E4 variants (E4dN) appeared to be more effective in increasing the infection rate, up to 30-fold, while E4WT variants increased the infection rate up to approximately 25-fold (Fig. 26 B and C).

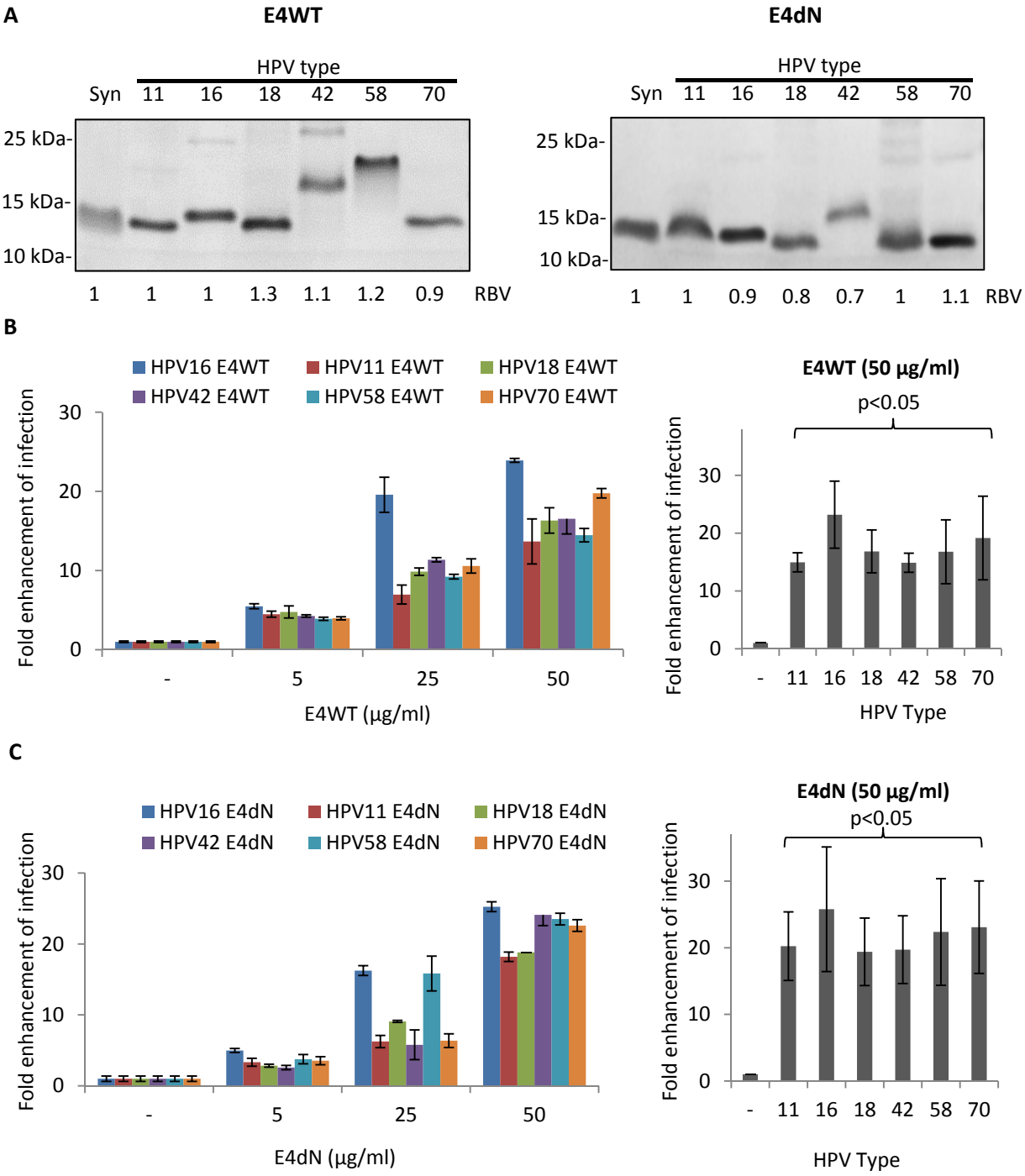

Figure 25: E4 proteins from different HPV types enhance lentiviral infection.
(A) Quantification of purified protein concentrations. E4 protein variants from different HPV types were refolded at 1 mg/ml and visualized using SDS-PAGE and Instant Blue staining. Synthetic (Syn) E4dN (1 mg/ml) was used as a concentration standard. Protein concentrations were compared with Syn standard using Bio-ID software based on relative band volumes (RBV).
SupT1 CCR5 cells were infected with VSV-G-pseudotyped lentiviral vector in the absence (-) or presence of E4WT **(B)** and E4dN **(C)** from indicated HPV types. GFP expression was measured 72 h-post infection using flow cytometry. Fold enhancement of infection was calculated relative to the number of cells infected with virus without E4 (arbitrarily set as 1.0). Example of protein titration of a single experiment (left) and the mean of three independent experiments performed in triplicates (right). Error bars represent the SD.

These experiments showed that the E4-mediated enhancement of lentiviral infection is a widespread phenomenon, not only limited to HPV16 but also mediated by the E4 protein from other HPV types. The extremely robust effect observed with E4 proteins of divergent sequence and length argues in favor of a more general, perhaps structure based, property of E4 as a possible explanation for this function.

2.6 HPV16 E4 HAS NO SIGNIFICANT EFFECT ON THE HPV INFECTION RATE

Both SEVI and the Alzheimer peptides $A\beta_{40}$ and $A\beta_{42}$ have been previously shown to enhance the infection rate of enveloped viruses (Munch et al. 2007, Wojtowicz et al. 2002). No effect of those amyloid fibrils on non-enveloped viruses has been described so far. Nevertheless, the E4-mediated enhancement of viral transduction could be very beneficial for a HPV secondary infection. Therefore, we addressed the question of whether HPV E4 is able to augment the infection rate of HPV.

The influence of E4 on the HPV infection rate was tested using HPV16 and HPV18 pseudovirions containing a GFP reporter gene (kind gift from Prof. Martin Müller). The infection efficiency was tested and the amount of virus stock used was optimized to obtain ~0.5% - 1% infected cells in the absence of E4. Increasing amounts of HPV16 E4WT or E4dN were mixed with HPV16 and HPV18 pseudovirions. As negative controls, cells were either incubated with the virus alone or E4 alone, to exclude false positive results due to the observed auto-fluorescence of E4.

No significant change in the HPV16 or HPV18 pseudovirion infection rate was observed in the presence of E4. Neither E4WT nor E4dN had any measureable effect even at the highest concentration used, 50 µg/ml (Fig. 26). Importantly, the E4 preparations tested here enhanced lentiviral infection in a parallel experiment indicating that E4 protein was functional.

In conclusion, no effect of the E4 variants on the HPV infection rate was observed. It appears that HPV E4, does not enhance the infection rate of the virus by which it is encoded.

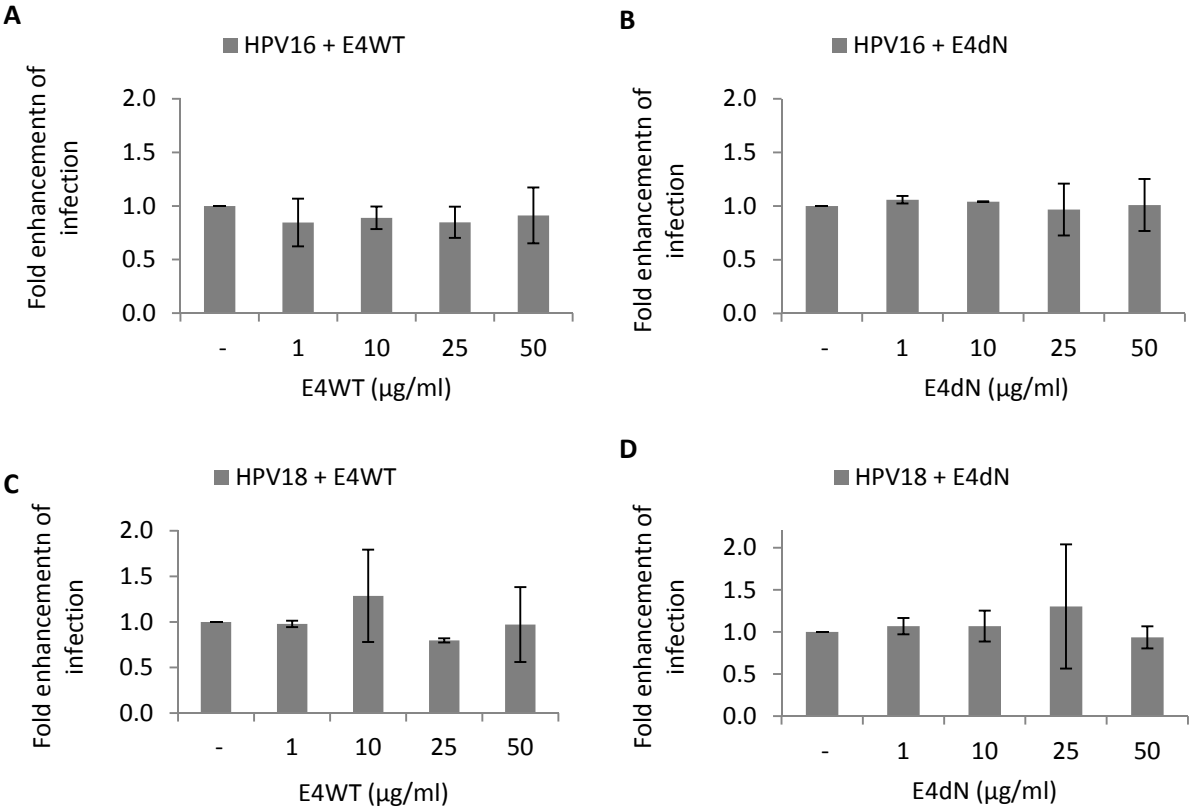

Figure 26: HPV16 E4WT and E4dN do not enhance HPV infection.
HeLaT cells were infected with HPV16 **(A and B)** or HPV18 **(C and D)** pseudovirions in the absence (-) or presence of E4WT **(A and C**) or E4dN **(B and D)**. Increasing amounts of E4WT or E4dN were mixed with HPV16 and HPV18 pseudovirions, incubated for 15 min and added to HeLaT. Cells were washed after overnight incubation and GFP expression was measured 72 h post-infection by flow cytometry. Fold enhancement of infection was calculated relative to the number of cells infected with virus without E4 (arbitrarily set as 1.0). SDs of two independent experiments are indicated.

2.7 STRUCTURAL ANALYSIS OF E4

SEVI-mediated augmentation of enveloped viruses' infection is believed to be mediated by the formation of amyloid fibrils. As shown in chapters 2.2 - 2.6, E4 also strongly enhances the lentiviral infection rate (while not affecting the infection rate of non-enveloped viruses, such as HPV) in a dose-dependent manner. However, not only the truncated variant of E4 (E4dN), described to form amyloid-like structures, but also the full-length E4 (E4WT) and several E4 mutants, containing partial or complete deletions of the multimerization domain showed a significant effect (Fig. 18). These E4 proteins should not form amyloid fibrils. Two explanations for these observations were proposed. First, E4dN, E4WT and the C-terminal mutants could all still be capable of assembling into fibrils. Alternatively the formation of amyloids may not be a prerequisite for the E4-mediated augmentation of infection. To test the first hypothesis, E4 was structurally analyzed, with particular emphasis on the formation of multimers, protofilaments, protofibrils and/or mature amyloids.

2.7.1 E4 VARIANTS FORM MULTIMERS

E4 was first analyzed by immunofluorescence analysis using a set of antibodies recognizing either a particular sequence or protein conformation. Besides antibody against the 6xHis-tag, two antibodies against E4, α-TVG and α-RPE4, were used. Two antibodies designed to study amyloid formation, α-A11, described to detect pre-fibrillar amyloid structures, and α-OC, described to detect amyloid structures (Kayed et al. 2007), were also tested.

The α-TVG, α-RPE4 and α-His-tag antibodies detected monomers and dimers of E4WT and E4dN (Fig. 27). Surprisingly, the α-A11 antibody also recognized monomers and dimers of both E4 variants (Fig. 27). The α-A11 antibody is described to recognize structural motives characteristic for an early step of fibril formation without recognizing mature fibers. The α-A11 antibody is not E4 specific and should not recognize the protein sequence but the cross β-sheets structure. One possible explanation is that α-A11 may detect β-strand regions described to be present at the E4 C-terminus (McIntosh et al. 2008). The α-OC amyloid specific antibody did not recognize E4, giving only unspecific staining (Fig. 27).

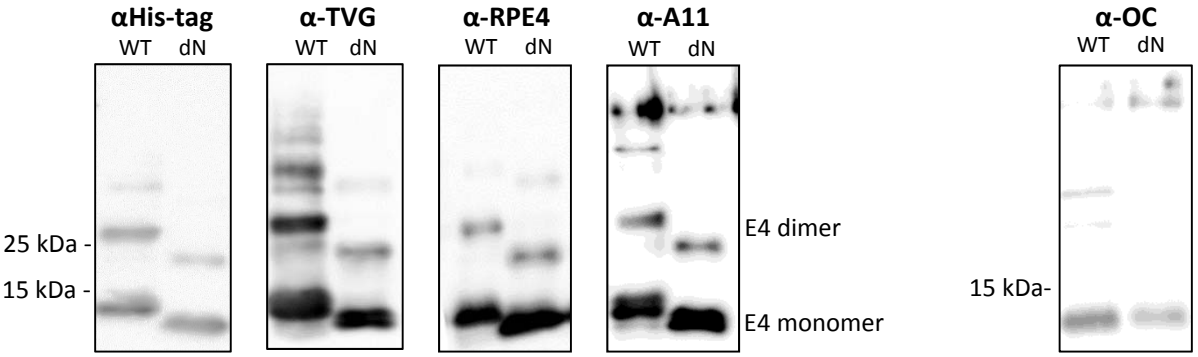

Figure 27: E4 analysis with a set of sequence or conformation specific antibodies.
SDS-PAGE and immunoblot analysis of E4WT (WT) and E4dN (dN) was performed using an α -His-tag, α-TVG, α-RPE4, α-A11 and α-OC antibodies. Monomeric and dimeric forms of the protein are indicated.

Next, it was investigated whether the E4 variants form multimers. Refolded E4WT and E4dN were analyzed using SDS-PAGE in non-reducing conditions. Loading buffer without β-mercaptoethanol was used to preserve disulfide bonds and protein cross-links. Alternatively, E4 was analyzed in non-reducing conditions with 0.05% SDS (half of the standard amount). The lower concentration of SDS was used in the loading buffer, polyacrylamide gels and the running buffer for electrophoresis. These conditions should lead to only partial protein unfolding and limited disassembly of protein complexes resulting in better preservation of higher multimer structures (Klodmann et al. 2011, Yoshiike et al. 2008).

Under non-reducing conditions, additional bands with sizes ranging from 35 - 70 kDa were observed for both E4WT and E4dN (Fig. 28A). The higher molecular weight forms were also detected when proteins were separated in the presence of 0.05% SDS (Fig. 28B). Moreover multimer species, ranging from dimers up to a size corresponding to trimers -tetramers were detected for other E4 variants (E4dC, E4dNdC, E4d70 and E4d36) (Fig 28B).

Detection of bands with molecular weights corresponding to dimers and bigger multimers strongly suggests that the E4 variants, even those with deletions in the multimerization domain, form high molecular weight assemblies. Results from SDS-PAGE under non-reducing conditions and low SDS concentration indicate that all E4 mutants form high molecular weight structures that can be partially disassembled in the presence of reducing agent and ionic detergent.

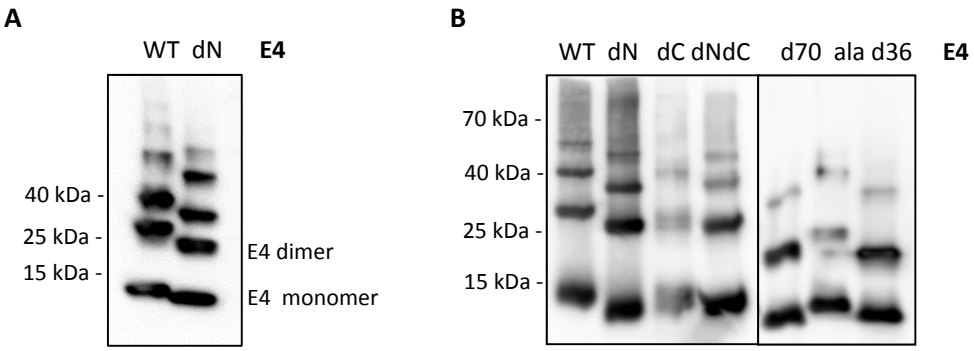

Figure 28: HPV16 E4 forms high molecular weight multimers.
(A) SDS-PAGE in non-reducing conditions (in the absence of β-mercaptoethanol). Immunoblot analysis was performed using an α -His-tag antibody. Monomeric and dimeric forms of the protein are indicated.
(B) Non-reducing SDS-PAGE gel with 0.05% SDS. Immunoblot analysis was performed using an α-His-tag antibody.

2.7.2. E4 VARIANTS BIND THIOFLAVIN T (THT)

To test whether E4 contains cross β-sheet-rich structures, characteristic for amyloids, ThT staining was used. This fluorescent dye is considered "the gold standard" for staining and identification of amyloids both *in vivo* and *in vitro*. Upon binding to the grooves formed by the side chains of amino acids composing β-sheets, ThT fluorescence increases. The drawback of this technique is the detection of aggregates of disorganized β-sheets structures (Biancalana and Koide 2010, Nilsson 2004).

As described in chapter 2.1, the ThT signal could not be distinguished from E4 autofluorescence in fluorescence microscopic analysis. Therefore, a more quantitative approach based on the spectroscopic assay was tested. The amounts of both protein and dye were titrated to determine the optimal conditions. The fluorescence intensity was measured with an excitation of 440 nm and a characteristic ThT maximum emission of 482 nm, which differs from the spectrum used in fluorescence microscopy. As a negative control, a BSA solution in refolding buffer with the same concentration as E4 was used. Globular BSA protein does not contain β-sheet structures and should not bind the ThT dye. Relative fluorescence intensity was calculated by subtracting baseline readings of protein-free refolding buffer from the signal of the ThT-stained protein solution.

As seen in the microscopy analysis of E4 (Fig. 10 and Fig. 13), this protein possesses detectable autofluorescence. First, it was tested whether the E4 autofluorescence would interfere with the spectroscopic measurement of protein binding to ThT. To this end, samples with and without dye were compared. In the absence of ThT, the autofluorescence of E4WT and E4dN was below 1 fluorescence unit (Fig. 29A), indicating that, at the measurement wavelength, E4 is not significantly autofluorescent and will not interfere with the analysis. In the presence of both E4WT and E4dN the

ThT signal intensity increased 20- to 36- fold (Fig. 29A). This indicates the presence of cross-β-sheet structures.

In a second series of experiments, the E4 concentration was first confirmed by Instant Blue staining (Fig. 29B). As a control non-refolded E4 (in 8 M urea) was tested to determine ThT binding to monomeric E4 protein. SEVI is known to enhance ThT fluorescence (Munch et al. 2007) and was used as a positive control. A mutant HPV L1 capsid protein that assembles into pentamers (described in 2.3.3), was used to asses ThT binding to multimers.

Non-refolded E4 did not significantly increase the ThT fluorescence signal. In samples containing refolded E4WT and E4dN the fluorescence signal exceeded 20 arbitrary units (Fig. 29C). Fluorescence also increased above 20 arbitrary units with other E4 variants: E4dC and E4dNdC. SEVI enhanced the ThT fluorescence much stronger than E4, up to 80 units. The signal obtained from the pentameric L1 protein was similar to BSA and non-refolded E4 protein (Fig. 29C).

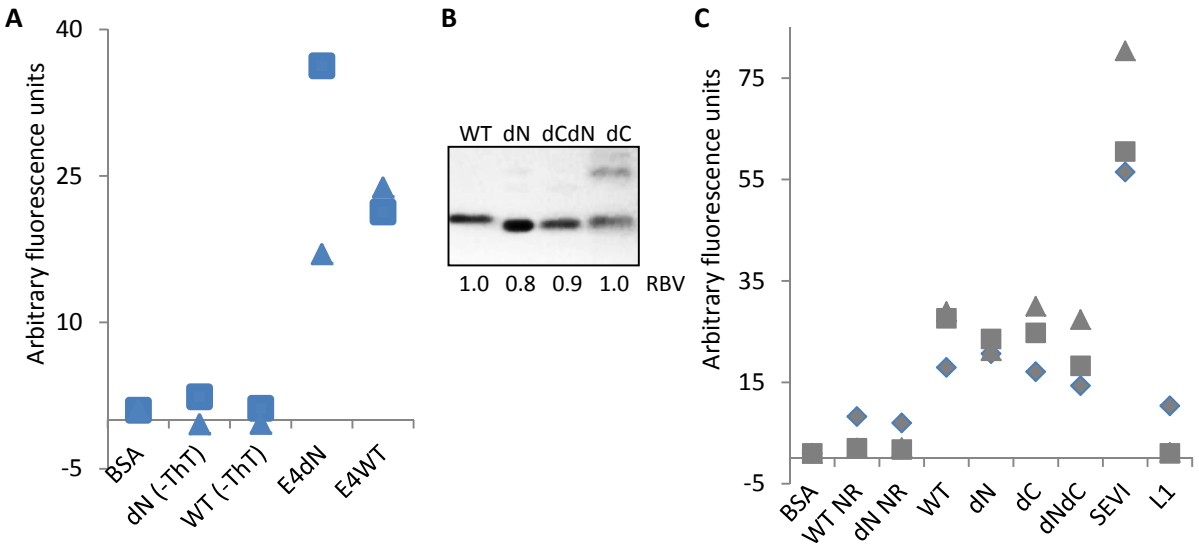

Figure 29: E4 variants increase the fluorescence of Thioflavin T (ThT).
(A) E4WT and E4dN (1 mg/ml) were stained with ThT solution (16 µg/ml) or mixed with an appropriate volume of ThT buffer without ThT (- ThT). The ThT signal was measured with an excitation of 440 nm and emission of 482 nm. Fluorescence units of measured samples were compared with BSA (arbitrarily set as 1.0). Results from two independent experiments are shown.
(B) Comparison of the concentration of the E4 variants. E4 variants were visualized using SDS-PAGE and Instant Blue staining. The protein concentration was calculated by comparing relative band volumes (RBV) of E4 variants to a BSA standard (1mg/ml) using the BIO-ID software.
(C) Comparison of ThT binding by different E4 variants. Refolded and non-refolded (NR) E4 variants, SEVI, and mutant L1 protein solutions (all 1 mg/ml) were stained with ThT (16 µg/ml). The ThT signal was measured with an excitation of 440 nm and emission of 482 nm. Fluorescence units of measured samples were compared with BSA (arbitrarily set as 1.0). Results from three independent experiments are shown.

In summary, the enhancement of the ThT signal indicates that all tested E4 variants form a cross-β-sheet structure upon refolding. Moreover, ThT did not bind to L1 pentamers, therefore it can be postulated that the higher fluorescence signal observed in E4 samples is not caused by unspecific binding of this dye to protein multimers. Finally, the ThT signal from E4 variants was relatively lower

compared to SEVI. This may be due to the lower molar concentration of E4 compared to synthetic SEVI, poorer refolding efficiency, resulting in a lower concentration of actual fibrils, or unspecific binding of ThT to E4 β-sheet aggregates without substantial amyloid formation (Nilsson 2004).

2.7.3 E4 FORMS FIBRILS

The formation of amyloid fibrils should be confirmed by at least two different techniques (Sipe et al. 2010, Bruggink et al. 2012). To exclude the possibility that the ThT binding was a false positive result caused by unspecific staining of amorphous β-sheet aggregates and to further investigate the details of E4 structures, electron microscopy (EM) was used. EM is widely applied for the ultrastructural characterization of amyloids. The major advantage of EM is the high, nanometer-scale resolution that allows distinction between mature amyloid fibrils and protofilaments or protofibrils (Nielsen et al. 1999).

E4WT, E4dN, E4dC and E4C were fixed using glutardehyde, negatively stained with uranyl acetate and visualized using EM (imaging was performed together with Dr. Karsten Richter from the Imaging and Cytometry Core Facility (German Cancer Research Center)). All protein preparations used for EM analysis were tested in parallel in functional studies and were highly active in enhancing lentiviral infection.

To exclude the presence of bacterial contaminants in the microscopy samples (resulting from purification procedures), the appearance of bacterially expressed E4dN was compared with that of synthetic E4dN. Synthetic SEVI, described to form characteristic amyloid structures (Munch et al. 2007, Roan et al. 2011), was used as a positive control.

All tested E4 variants formed ordered structures of considerable size. Thin filaments, ragged ribbon-like filaments of approximately 100 - 200 nm in length, assemblies of filaments and thick fibrils were observed in both synthetic and bacterially expressed E4dN (Fig. 30). E4WT formed assemblies of filaments and thick fibrils (Fig. 30), while E4dC was observed only as thin, apparently rotated filaments of several hundred nanometers (Fig. 30). In some samples of protein expressed in bacteria, additional non-structural aggregates were present. These structures represent either background from residual impurities or not-properly refolded E4.

Furthermore, bacterially expressed E4WT and E4dN as well as synthetic E4dN formed large, compact assemblies of fibrils (Fig. 30). These structures had various sizes, up to several µm, and appeared to consist of agglomerates of thick fibrils. They were well-distinguishable from amorphous aggregates and had a filamentous internal structure with dozens of fibrils aligned parallel to each other in thick bundles (Table 3).

Ribbon-like filaments found in E4dN preparations had the characteristics of profibrils. The long, thin filaments observed in most E4 samples resemble protofilaments, the first stage of amyloid formation. The immense assemblies of fibrils were difficult to classify, however, they did not meet the general criteria for mature amyloid fibrils (Chiti et al. 1999, Gras et al. 2011, Shirahama and Cohen 1967).

A synthetic fragment of E4 corresponding to the E4 C-terminus (E4C) formed an extensive network covering the whole surface of the grid (Fig. 30). The E4C network consisted of short, straight, rod-like, up to 100 nm long filaments. These highly abundant structures resembled one type of fibrils also found in E4dN samples just present at a high abundance (Fig. 30).

SEVI formed distinguishably different structures. Straight, needle-like fibrils several hundred nanometers long were observed. Ordered SEVI particles had coarse striations in the direction of the main axis and fine transverse striations. SEVI fibrils resembled crystals and had a tendency to bundle and associate into thicker filaments (Fig. 30). Observed SEVI structures corresponded to data published previously (Munch et al. 2007)

These structural studies confirm that E4 undoubtedly forms ordered, high molecular weight structures. Different forms corresponding to protofilaments, protofibrils and structures of fibril assemblies were found in a single protein preparation and in different preparations, indicating that the E4 solutions were not homogenous. Truncated E4, corresponding to the calpain-cleaved form, and wild-type protein assembled into similar structures. Truncation of the C-terminus appeared to partially inhibit E4 structure formation, as only thin filaments were found in the E4dC mutant. Additionally, the multimerization domain alone was sufficient to form short fibrils. E4 formed structures clearly distinguishable from SEVI. In our hands E4 most likely assembles primarily into intermediate amyloid forms and structurally organized protein assemblies.

Table 3: Summary of structures formed by different E4 variants and SEVI.

	E4WT	**E4dN**	**E4dC**	**E4dN synthetic**	**E4C synthetic**	**SEVI**
Fibril assemblies **(A)**	+	+		+		
Ribbon-like filaments (100 nm) **(B)**		+		+		
Filament assemblies **(C)**	+	+		+		
Thick fibrils **(D)**	+	+		+		
Thin filaments **(E)**		+	+	+		
Network form of nodes **(F)**		+			+	
Non-structural aggregates **(G)**	+	+	+		+	
Amyloids **(H)**						+

Based on electron microscopy results (Fig. 30).

E4dN

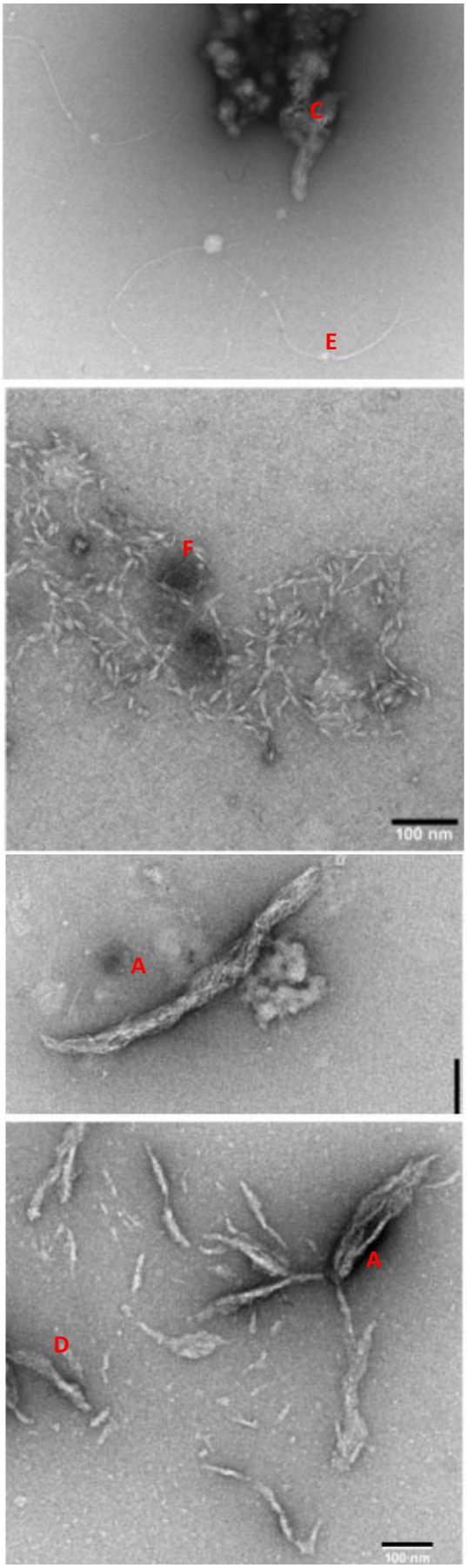

E4WT

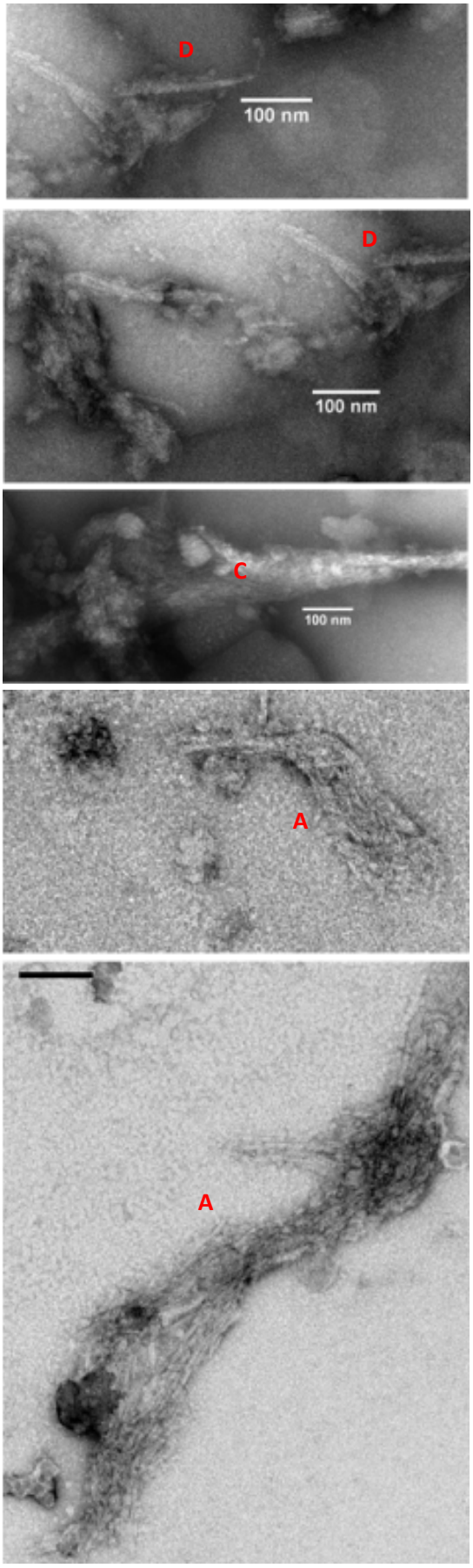

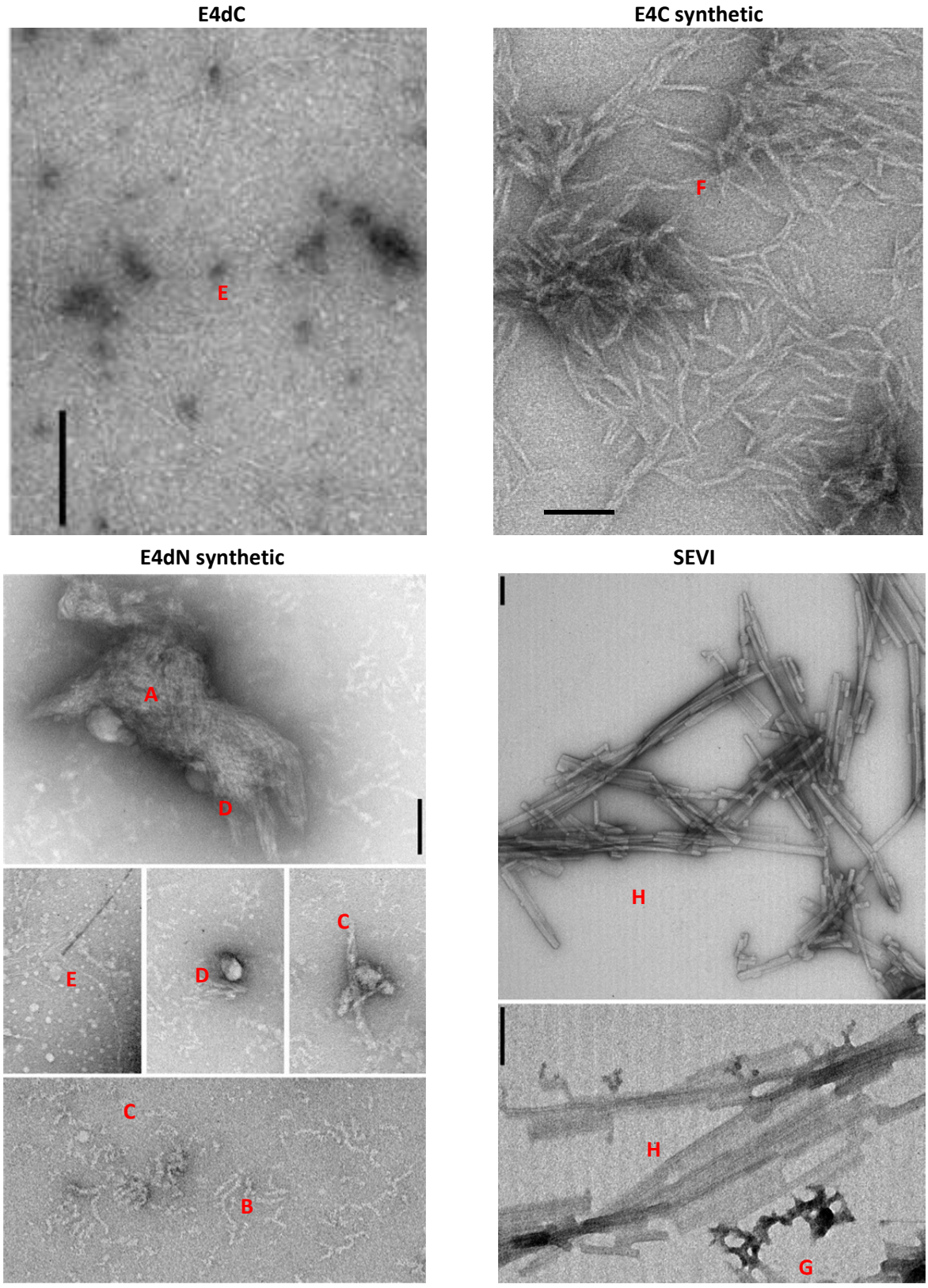

Figure 30: Electron micrographs of different E4 variants and SEVI.
Solutions of E4 variants or SEVI were negatively stained with uranyl acetate. Different types of structures are shown. Amyloid assemblies (A); ribbon-like filaments (100 nm) (B); filament assemblies (C); thick fibrils (D); thin filaments (E); network form of nodes (F); non- structural aggregates (G); and amyloids (H). Scale bars represent 100 nm.

An alternative fixation technique was also tested. To prevent structural changes during the preparation process, E4WT and E4dN were embedded in methylcellulose and negatively stained with uranyl acetate. When analyzed by electron microscopy, E4dN formed a network of worm-like tubular structures, 1 nm wide and approximately 100 nm long (Fig. 31). Identical structures have previously been described for E4 (McIntosh et al. 2008). Mostly aggregates were observed in E4WT samples, though occasionally long, straight fibers were also found (Fig. 31).

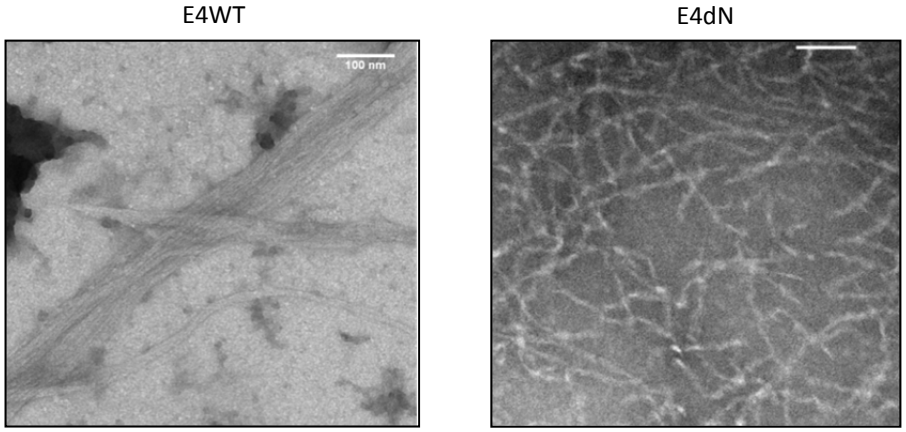

Figure 31: Electron micrographs of E4WT and E4dN.
E4 protein solution (1 mg/ml) was embedded in methylcellulose and negatively stained with uranyl acetate. Scale bars represent 100 nm.

In summary, non-reducing and low percentage of SDS in SDS-PAGE analysis as well as EM data showed that all E4 variants, even mutants with a partial deletion of the multimerization domain, formed high molecular weight structures. A high level of heterogeneity within a given sample and between different samples was observed. The E4WT and E4dN proteins seem to consist of the most ordered forms, including thick fibrils. Importantly, deletion of the multimerization domain did not completely inhibit the formation of organized structures and thin fibrils were detected in E4dC samples. Moreover, the multimerization domain (E4C) on its own assembled into a network of short, straight fibrils. The observed E4 structures resembled pro-filaments and pro-fibrils but most probably no mature amyloid fibrils are formed. Finally, E4 variants only moderately enhanced ThT fluorescence compared with SEVI, strongly indicating lower amounts of cross-β-sheet-rich structures.

No strong evidence for the formation of mature amyloids by E4 was presented. Importantly, these results indicate that formation of amyloids by E4 is not a necessary prerequisite for the enhancement of lentiviral transduction. Therefore, other possible mechanisms for the E4-mediated increase of lentiviral infection were considered.

2.8 MECHANISMS OF E4-MEDIATED ENHANCEMENT OF LENTIVIRAL INFECTION

Amyloid fibrils like SEVI and $A\beta_{40}$ have been proposed to augment the infection rate of enveloped viruses by several mechanisms. Viral particles could be captured by large amyloid structures, subsequently enhancing their sedimentation velocity and increasing the likelihood of attachment to the epithelium (Easterhoff et al. 2011, Martellini et al. 2011, Munch et al. 2007). Amyloids could shield the electrostatic repulsion between virus and cells (Olsen et al. 2010, Roan et al. 2011). Amyloids may also enhance the physical interaction between the cellular membrane and viral envelope (Wojtowicz et al. 2002). Hence, we investigated whether these mechanisms are also a prerequisite for the E4 function.

2.8.1 THE POSITIVE CHARGE OF E4 IS REQUIRED FOR THE ENHANCEMENT OF INFECTION

Studies on the SEVI-dependent increase of the infection by enveloped viruses revealed that the cationic properties of amyloids are indispensable for their activity (Roan et al. 2009). SEVI possesses a high isoelectric point above 10.2. E4 is less cationic and the isoelectric points of the tested E4 variants vary between 6.23 for E4d36, a mutant with the deletion of a positively charged central domain, and 9.2 for E4WT, E4dC and E4d70. The isoelectric point (pI) of L1 lies at around 8.3 and is within the pI range of the different E4 variants (Table 4).

Table 4: Isoelectric points of E4 variants, SEVI and L1

	E4									SEVI	L1
	WT	dN	dC	dNdC	d70	36-41	ala	C	Cala		
Isoelectric Point	9.14	8.8	9.14	8.8	9.18	6.23	4.75	7.02	6.25	10.21	8.27

Isoelectric points (pIs) of E4 variants, SEVI and L1 were predicted based on the respective aa sequence. The computation of the theoretical pI was done using tools from the SIB Bioinformatics Resource Portal ExPASy. Positively charged polypeptides are marked in red; negatively charged polypeptides, in blue.

POLYANIONS HAVE NO DETECTABLE CYTOTOXIC EFFECT ON THE TESTED CELLS

To study the contribution of positive charge to the E4-mediated enhancement of the infection rate two polyanionic compounds- heparin and dextran sulfate - were utilized. They were used to neutralize positively charged amino acids residues of E4 multimers.

First, we examined the effect of the polyanions on the viability of HeLa and SupT1 CCR5 cells. Polyanions were dissolved in PBS. Increasing concentrations of tested compounds, ranging from 1 - 200 mg/ml, were added to the cells. As a negative control, PBS without polyanions was used. The metabolic activity of cells was measured 72 h post-treatment using the WST-1-based cytotoxicity test. Thise time point was chosen to account for the conditions of the lentivirus infection. Untreated cells in medium only, assumed to be 100% viable were used as reference.

At concentrations ranging from 1 - 200 mg/ml, heparin and dextran sulfate had no detectable cytotoxic effect on SupT1 CCR5 or HeLa cells (Fig. 32). Moreover, no obvious changes in cell appearance, size or shape were observed under the microscope.

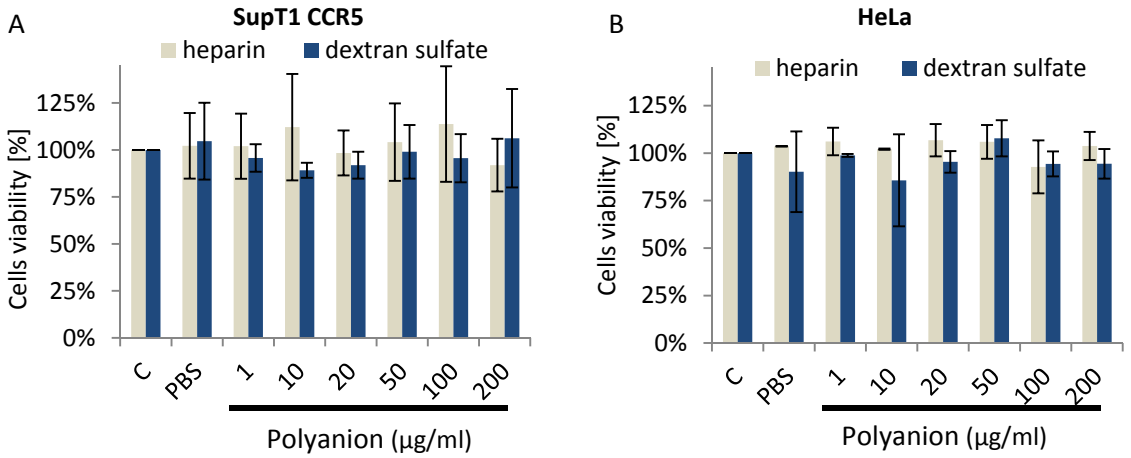

Figure 32: Heparin and dextran sulfate have no detectable cytotoxic effect on SupT1 CCR5 and HeLa cells. WST-1-based cytotoxicity assay. Heparin and dextran sulfate were added to the cell culture medium. Cells were washed after 24 h incubation. The metabolic activity of cells was measured after 72 h. Control (C) cells were treated with medium only. Graphs represent data from two independent experiments, error bars reflects the SD.

POLYANIONS STRONGLY DECREASE THE E4-MEDIATED AUGMENTATION OF THE INFECTION RATE

It was tested whether treatment of E4 with polyanions may influence the infection rate. Two E4 variants E4WT, with a pI of 9.14, and E4dN, with a pI of 8.8, were chosen. In a preliminary experiment, E4 was pre-incubated with virus for 15 min at 37°C, mixed with heparin or dextran sulfate and added to the cells. At these conditions, only a moderate decrease of the E4-mediated enhancement of the infection rate was observed (not shown).

It was hypothesized that, if an electrostatic interaction between E4-virus had already taken place beforehand, the addition of polyanions could be insufficient to disturb existing complexes. Thus, E4 was pre-treated with heparin or dextran sulfate and incubated for 15 min at RT before the addition of virus. This procedure attenuated the E4-mediated enhancement of infection but, at the tested polyanion concentrations of up to 100 µg/ml, lentiviral infection itself was decreased. The inhibitory effect of heparin and dextran sulfate on retrovirus (HIV-1) infection is well-known (Ito et al. 1987). To avoid false positive results caused by reduction of infection, lower concentrations of polyanions, up to 25 µg/ml were evaluated. This amount of polyanions did not significantly influence the VSV-G-pseudotyped infection rate in the absence of E4 (Fig. 33). Consequently, the E4 concentration was also adjusted to avoid oversaturation of the polyanion effect.

E4WT and E4dN at concentrations of 30 µg/ml were mixed with either heparin or dextran sulfate at concentrations ranging from 0.1 - 25 µg/ml. After 15 min, VSV-G-pseudotyped lentivirus vector was added and samples were further incubated for 15 min at 37°C. SupT1 CCR5 cells were infected, and the percentage of infected, GFP-positive cells was measured after 72 h by flow cytometry.

Pre-treatment with both heparin and dextran sulfate strongly reduced the E4-mediated enhancement of infection, decreasing it virtually back to control levels. At the same time, at the highest concentration used in the experiment, polyanions had no detectable effect on the lentiviral infection in the absence of E4 (Fig. 33). The ability of polyanions to considerably impair the effect of

full-length and truncated E4 versions strongly indicates that a positive charge is essential for the E4-mediated enhancement of the infection rate.

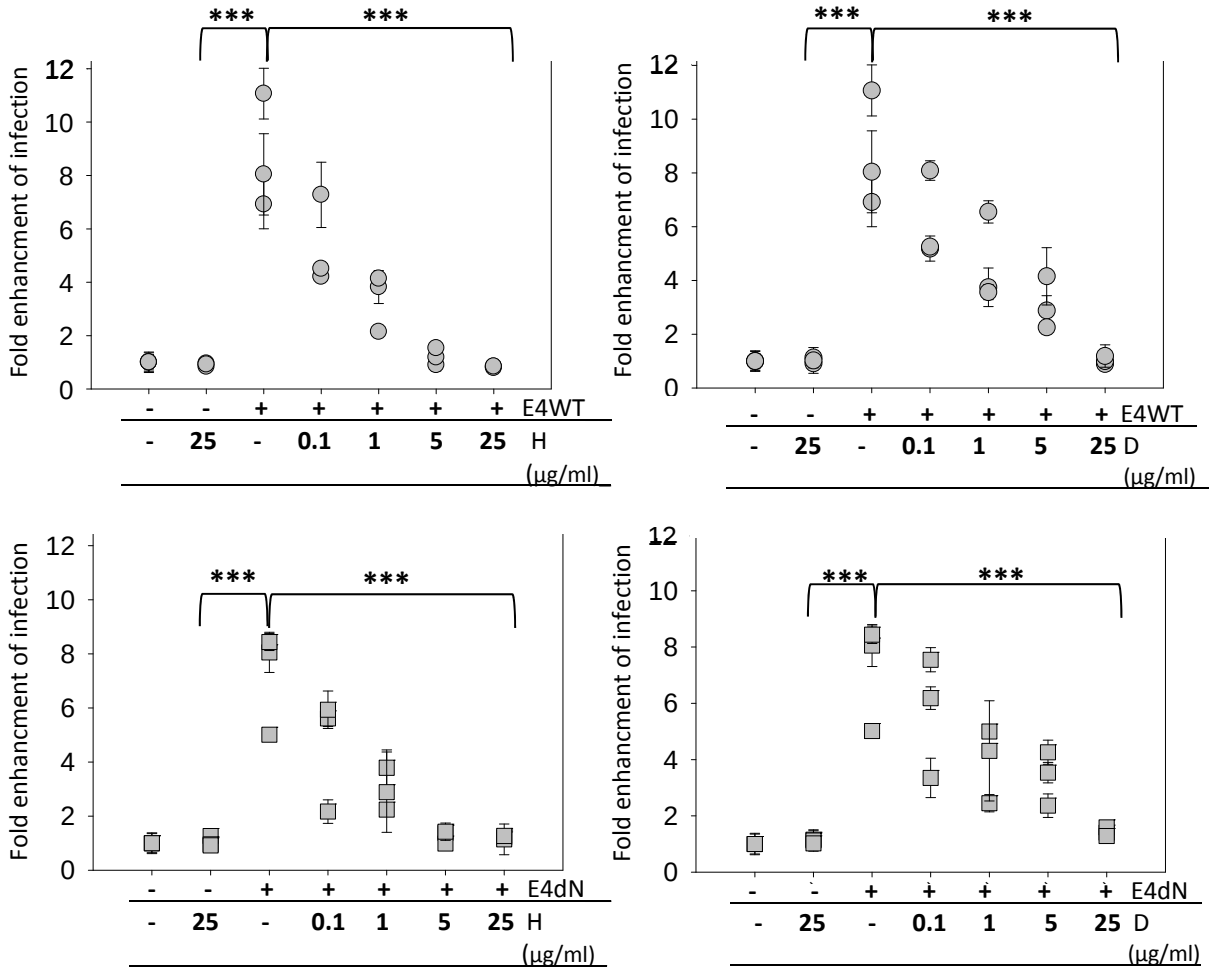

Figure 33: Polyanions strongly decrease the E4-mediated augmentation of infection.
E4WT and E4dN (30 µg/ml) were pre-treated with polyanions (heparin (H) or dextran sulfate, (D)) for 15 min at RT and incubated with VSV-G-pseudotyped lentiviral vectors (15 min, 37°C) before adding to cells. SupT1 CCR5 cells were infected in the absence (-) or presence of E4 and/or polyanions. GFP expression was measured 72 h post-infection using flow cytometry. Fold enhancement of infection was calculated relative to the number of cells infected with virus without E4 (arbitrarily set as 1.0). Each dot /square represents the mean of one independent experiment performed in triplicates (error bars reflect the SD). For significance calculations the mean of the three independent experiments was formed.

To exclude the possibility that the observed effect is cell type dependent HeLa cells were also tested and showed similar results. Again, E4 was pre-treated with 0.1 - 25 µg/ml of polyanions and incubated with virus before addition to HeLa cells. In agreement with the results observed for suspension SupT1 CCR5 cells, both heparin and dextran sulfate decreased the E4-mediated augmentation of the infection of adherent HeLa cells back to control levels (Fig. 34).

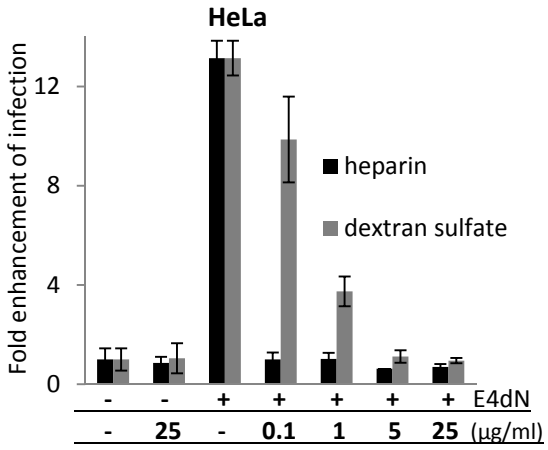

Figure 34: Polyanions block the E4-mediated augmentation of lentiviral infection rate of the adherent cells.
E4dN (30 µg/ml) was pre-treated with polyanions (heparin or dextran sulfate) for 15 min at RT and incubated with VSV-G-pseudotyped lentiviral vectors (15 min, 37°C) before addition to cells. HeLa cells were infected in absence (-) or presence of E4 and/or polyanions. GFP expression was measured 72 h post-infection using flow cytometry. Fold enhancement of infection was calculated relative to the number of cells infected with virus without E4 (arbitrarily set as 1.0). The results of a single representative experiment are shown. Error bars reflect the SD of three replicates.

To further verify the role of charge for E4 function, all protein variants described in earlier chapters were analyzed using the same conditions as with E4WT and E4dN. In accordance with earlier observations, both polyanions suppressed the effect of the E4 variants with partial or complete deletion of the multimerization domain, E4dC, E4dNdC and E4d70, and the E4 mutant lacking the positively charged central domain, E4d36, back to control levels (Fig. 35 A-D).

Compared to other E4 variants (except E4d36), the multimerization domain has a much lower, almost neutral pI of 7.02 (Table 4). Moreover, only one positively charged aa is present in this HPV16E4 fragment, K81. Surprisingly, addition of both polyanions decreased the E4C-mediated enhancement of the infection rate only by 50% (from a 6-fold enhancement to 3-fold enhancement) (Fig. 35E). Another protein variant, tested in parallel to E4C, was strongly affected by polyanion addition, indicating that the observed low effectiveness was not caused by lack of activity of heparin and dextran sulfate. This result suggests that, at the concentrations tested, polyanions are not able to completely block the E4C effect.

Finally, we tested whether the L1-mediated enhancement of the lentiviral infection rate could also be blocked by the negative charge of polyanions. Experiments were performed as described for E4. Again, augmentation of the infection rate was abolished in the presence of heparin and dextran sulfate (Fig. 35F).

Taken together, this data indicates that blocking of positive charges abolishes the E4-mediated enhancement of the infection rate. This effect was observed for all E4 variants, and was independent of the type of infected cells and the protein sequence. Moreover, the augmentation of infection mediated by pentamer-forming HPV16 L1 mutant was also blocked by polyanions.

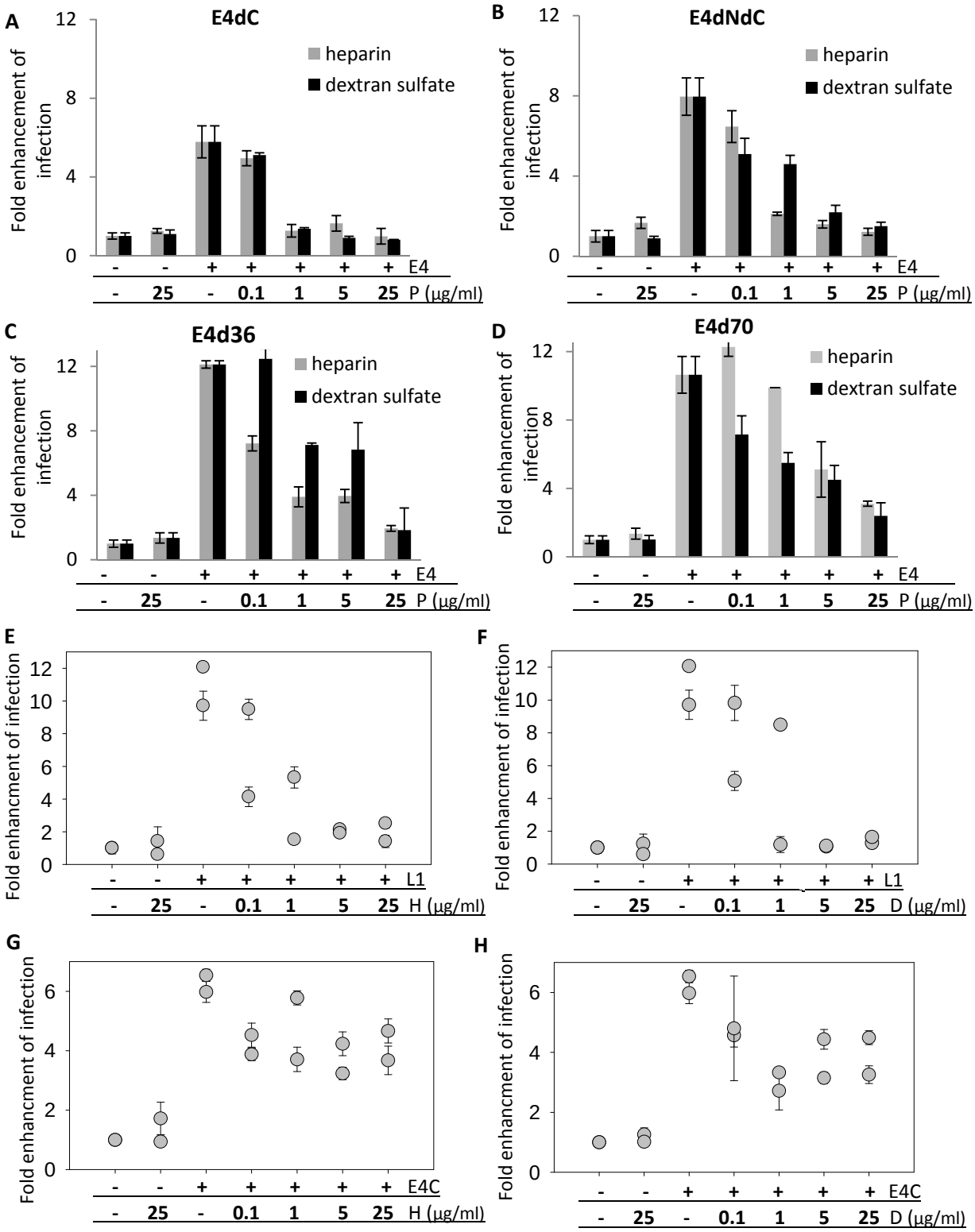

Figure 35: Polyanions decrease the E4- and L1- mediated augmentation of the lentiviral infection rate.
E4 variants (30 µg/ml) or L1 (30 µg/ml) were pre-treated with polyanions (P): heparin (H) or dextran sulfate (D), for 15 min at RT and incubated with VSV-G-pseudotyped lentiviral vectors (15 min, 37°C) before addition to cells. SupT1 CCR5 cells were infected in the absence (-) or presence of E4 and/or polyanions. GFP expression was measured 72 h post-infection using flow cytometry. Fold enhancement of infection was calculated relative to the number of cells infected with virus without E4 (arbitrarily set as 1.0). **(A-D)** Results of single experiments performed in triplicates are shown. **(E-H)** Each dot represents the mean of one independent experiment performed in triplicates (error bars reflect the SD).

E4 ALANINE MUTANTS DO NOT ENHANCE LENTIVIRAL INFECTION

All findings presented above emphasize the importance of a positive charge in the E4-mediated enhancement of the infection rate. Two additional E4 mutants were designed, E4ala and E4Cala. E4ala is an N-terminally truncated version of E4 in which all positively charged amino acids have been substituted with alanine (Table 1). This mutation led to a low, anionic pI of 4.75, despite the presence of a 6xHis-tag. E4ala was expressed in bacteria and purified with nickel affinity chromatography. E4Cala constitutes the C-terminal multimerization domain of E4 and contains a single K81A substitution. E4Cala has a near-neutral pI of 6.81 and was generated by chemical synthesis. After resuspension, refolding and agitation, both protein solutions became turbid and macroscopic aggregates were observed. The alanine mutants were tested to exclude the possibility that polyanions block the E4 effect not by shielding the charge but rather by interfering with the protein structure, and/or leading to disassembly of E4 complexes.

The effect of alanine mutants on the infection rate was measured as described previously. E4ala from two different purifications was used. No significant changes in the lentiviral infection rate were observed. Under the same conditions, E4dN increased the infection up to 40-fold (Fig. 36A). Similarly, the E4Cala also had no strong effect on the infection rate (Fig. 36B). This finding further confirms the hypothesis that the presence of positively charged amino acids is required for the E4-mediated enhancement of the lentiviral infection rate.

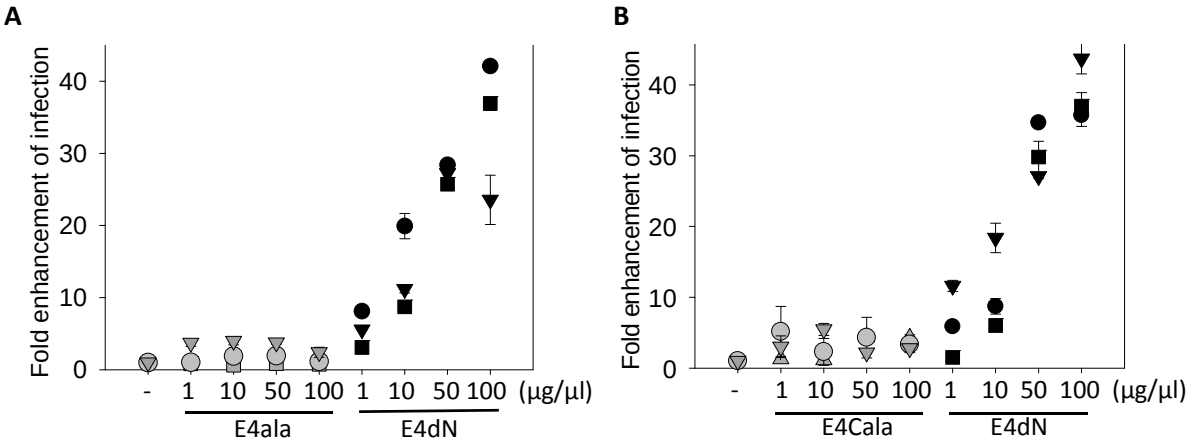

Figure 36: E4 alanine mutants do not enhance the lentiviral infection rate.
SupT1 CCR5 cells were infected with VSV-G-pseudotyped vectors in the absence (-) or presence of E4ala **(A)** or E4Cala **(B)**. E4dN at the same concentration range was used as a positive control. GFP expression was measured 72 h post-infection by flow cytometry. Fold enhancement of infection was calculated relative to the number of cells infected with virus without E4 (arbitrarily set as 1.0) Each dot/triangle/square represents the mean of one independent experiment performed in triplicates (error bars reflect the SD).

We conclude that the positive charge of E4 is important for the augmentation of the infection. Mutant forms in which lysines and arginines were replaced with alanine could not increase the infection rate. In addition, the effect of the E4 variants is strongly and, in most cases, completely abrogated in the presence of anionic polymers. These findings suggest that E4 boosts viral infectivity by decreasing charge repulsion between host cells and lentiviruses. This charge shielding could in turn facilitate virion attachment to the cellular membrane.

To compare the effect of different E4 variants and gain even more reliable insight into the relevance of charge and structure, all E4 mutants were tested in parallel. This approach eliminates variations in experimental settings, e.g. differences of the in cells culture conditions. It was nfirmed that E4dN is the strongest enhancer of the lentiviral infection rate, followed by E4WT. Partial deletion, as in E4dC and E4dNdC, or complete deletion, as in E4d70, of the multimerization domain further impaired the enhancement. The E4 multimerization domain (E4C) enhanced the infection rate to the same degree as mutants lacking this part of protein. E4d36, a mutant lacking a positively charged cluster of amino acids had effect compared with other deletion mutants. The alanine mutants, missing all positively charged amino acids, E4ala and E4Cala did not significantly enhance the infection rate. Moreover, E7 had no effect on infection. Finally, the mutant L1 protein exhibited moderate but significant activity (Fig. 37). Taken together these results strongly support all findings presented in previous chapter (see 2.2, 2.3 ans 2.8.1)

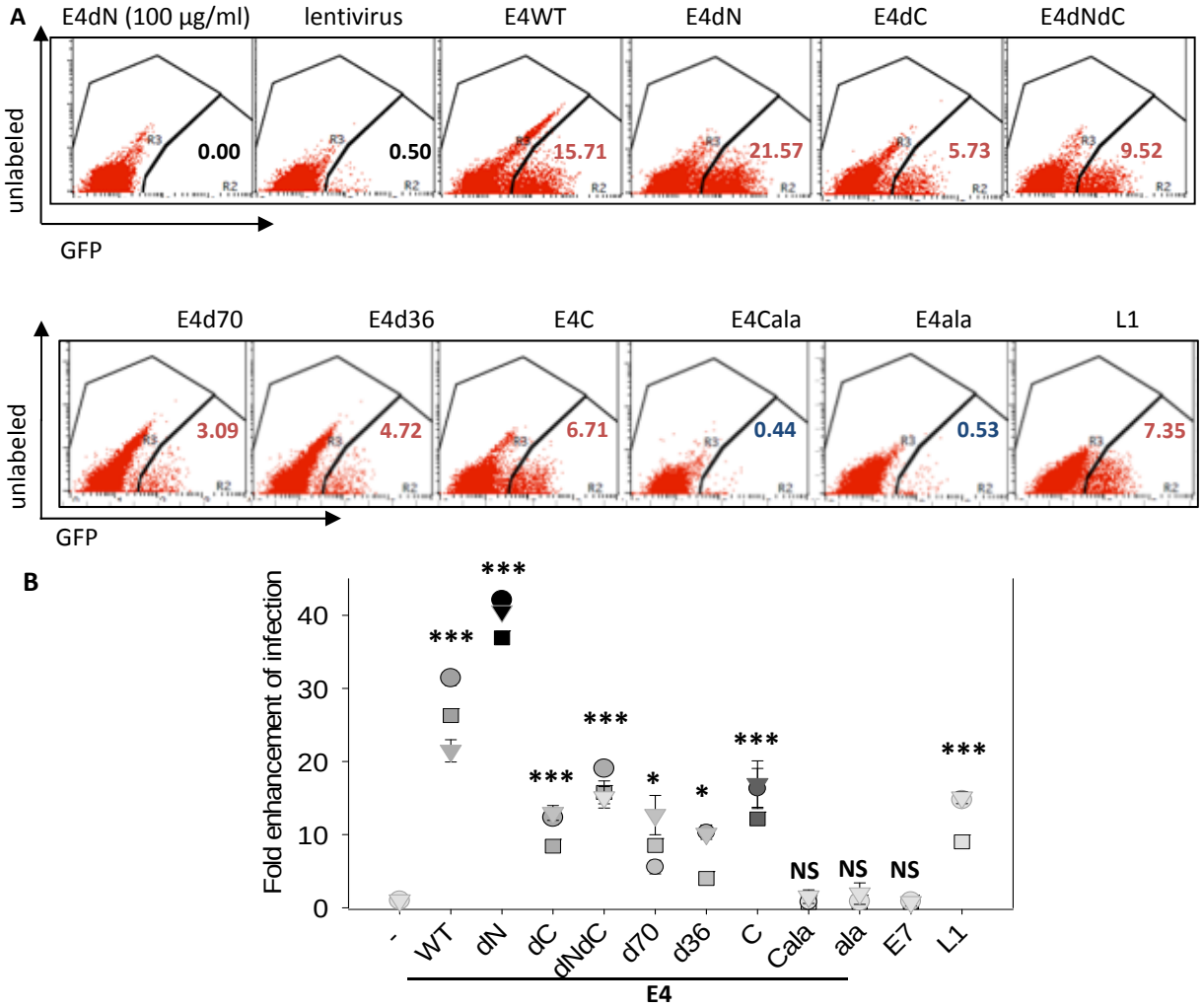

Figure 37: Influence of the E4 variants, E7 and L1 on the lentiviral infection rate.
SupT1 CCR5 cells were infected with VSV-G-pseudotyped lentiviral vectors (lentivirus) in the absence (-) or presence of E4 variants, E7 or mutant L1 (all 100 µg/ml). GFP expression was measured 72 h post-infection using flow cytometry.
(A) Representative dot plots are shown. Numbers indicate percentages of infected cells.
(B) Fold enhancement of infection was calculated relative to the number of cells infected with virus without E4 (arbitrarily set as 1.0). Each dot/triangle/square represents the mean of one independent experiment performed in triplicates (error bars reflect the SD). For significance calculations the mean of the three independent experiments was formed and compared with control (-); not significant (NS)

2.8.2 SEDIMENTABLE HIGH MOLECULAR WEIGHT MULTIMERS OF E4 CONTRIBUTE TO THE ENHANCEMENT OF THE INFECTION RATE

E4 FORMS SEDIMENTABLE STRUCTURES THAT ENHANCE THE LENTIVIRAL INFECTION

The EM analysis showed that the E4 protein preparations were not homogenous and consist of a wide variety of different structures. However, this microscopic technique did not allow a quantification of the proportion of E4 that assembles into fibrils or remains as a monomeric protein. In face of the fact that amyloid formation is unnecessary for E4 activity, it is important to define to which extent monomeric or small multimeric forms of E4 influence the infection.

To address this question, the sedimentation properties of E4 were examined. Unlike monomeric protein, high molecular weight fibrils can be easily pelleted using centrifugation with forces as low as 10,000 × g (Mok and Howlett 2006). E4dN was centrifuged for 15 min at 13,000 rpm (15,000 × g). The supernatant was collected and the pellet was resuspended in PBS to its initial volume. Both fractions were analyzed using immunoblotting with the α-RPE4 antibody to check for the presence of the E4dN protein. The effects of the supernatant and the resuspended pellet on the lentiviral infection rate were tested in parallel. Untreated (unfractionated) E4dN was used as a positive control.

Centrifugation of E4dN for 15 min at 13,000 rpm led to the accumulation of a clearly visible protein pellet. Very low amounts of E4 were detected in the supernatant and most of the protein was present in the pellet, indicating the formation and sedimentation of high molecular weight structures (Fig. 38A). The supernatant did not enhance the infection rate, while the resuspended pellet increased the lentiviral infection with an efficiency comparable to unfractionated E4 protein (Fig. 38B). This effect was dose-dependent.

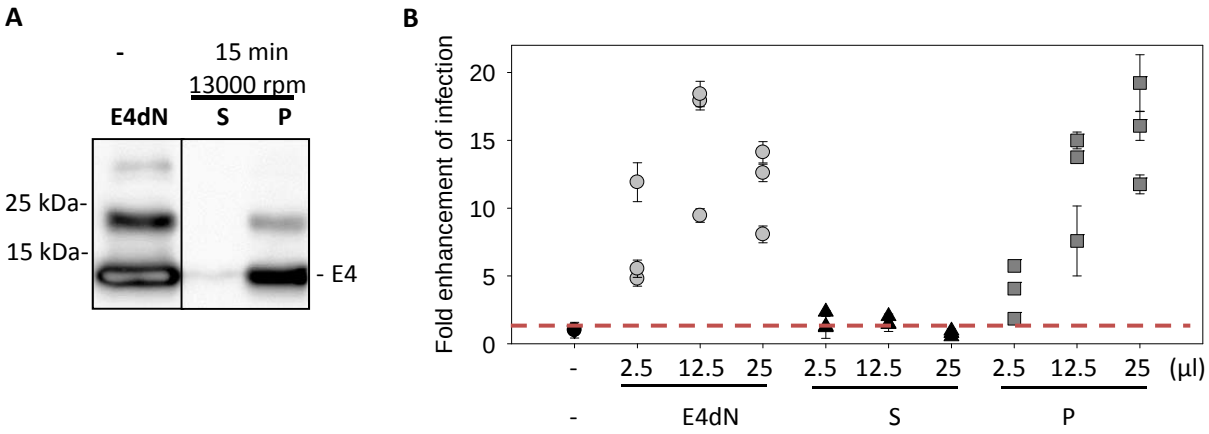

Figure 38: Sedimentable E4dN multimers enhance the lentivirus infection.
E4dN was centrifuged for 15 min at 13,000 rpm. The pellet was resuspended in refolding buffer to its initial volume. As the protein concentration could not be determined in the supernatant corresponding volumes of E4dN untreated (E4dN), supernatant (S) and resuspended pellet (P) were used.
(A) Immunoblot analysis with an α-RPE4 antibody.
(B) Fractions obtained from (A) were used for infection analysis. SupT1 CCR5 cells were infected with VSV-G-pseudotyped lentiviral vector in the presence or absence of uncentrifuged E4dN, supernatant (S) and resuspended pellet (P). GFP expression was measured after 72 h using FACS. Fold enhancement of infection was calculated relative to the number of cells infected with virus without E4 (arbitrarily set as 1.0) Each dot/triangle/square represents the mean of one independent experiment performed in triplicates (error bars reflect the SD).

This experiment showed that E4dN forms insoluble multimers that can be almost completely sedimented after centrifugation for 15 min at 13,000 rpm. Due to the protein size and centrifugation speed applied, this indicates that, at least for E4dN, monomers or dimers are not present in substantial amount after protein refolding. The resuspended pellet enhanced the infection rate to the same extent as unfractionated E4, indicating that insoluble, sedimentable, high molecular weight multimers, mediate the enhancement of the lentiviral infection.

E4 VARIANTS FORM MULTIMERS LARGER THAN 100 KDA

Size exclusion filtration was used to characterize the size of protein multimers formed by different E4 variants. Membranes with a pore size of 30 kDa or 100 kDa were used, enabling the separation of monomers, dimers, or tetra- to octamers, respectively. Protein preparations were filtered through the membranes. Filtrate (F), containing protein below the indicated cut-off size, and supernatant (S), containing protein above the indicated cut-off size, were aspirated and resuspended to their initial volumes.

Immunoblot analysis of the obtained fractions revealed that all E4 variants formed multimers bigger than 100 kDa. For E4 variants with partial (E4dC) and complete (E4d70) deletion of the multimerization domain, tetramers to octamers were also detected. These forms were more abundant for E4d70 compared to E4dC. The mutant corresponding to the calpain-cleaved form of E4 with a C-terminal deletion (E4dNdC) formed all described forms of multimers. Additionally, the E4dNdC preparation also contained monomers and dimers (Fig. 39A). As described before (Fig. 11), bands corresponding to denaturation-resistant multimers were observed in immunoblot analysis of the E4dC, E4d70 and E4ala.

It appears that E4WT and E4dN exist in solution predominantly in the form of multimers larger than 100 kDa, as no smaller forms were detected. Partial deletion of the multimerization domain led to the appearance of multimers smaller than decamers (100 kDa) but bigger than dimers (above 30 kDa). The abundance of these multimers increased with complete deletion of the multimerization domain. The E4dNdC variant was detected in the filtrate and supernatant fractions of all size cut-offs, indicating the presence of monomers, dimers, small multimers and large polymers. These observations suggest that deletion of the multimerization domain indeed interferes with the formation of E4 multimers. At the same time, neither the deletion of the central charged domain, nor substitution of all positively charged amino acids with alanine had any quantitative effect on the formation of E4 high molecular weight structures (Fig. 39A).

The effect of supernatants and filtrates on the lentiviral infection rate was tested. Only the E4 variants that had considerable enhancing effect (E4WT, E4dN, E4dC and E4dNdC) were analyzed. All fractions containing protein enhanced the lentiviral infection rate (Fig. 39B). Differences in the strength of the E4 effect were most likely caused by differences in the respective protein amounts. When tested in functional analysis, all detected forms of E4dCdN, even fractions containing monomers or dimers, enhanced the infection rate. It can be hypothesized that either monomers or dimers also have the ability to enhance the lentiviral infection rate or a re-aggregation of the protein took place rapidly.

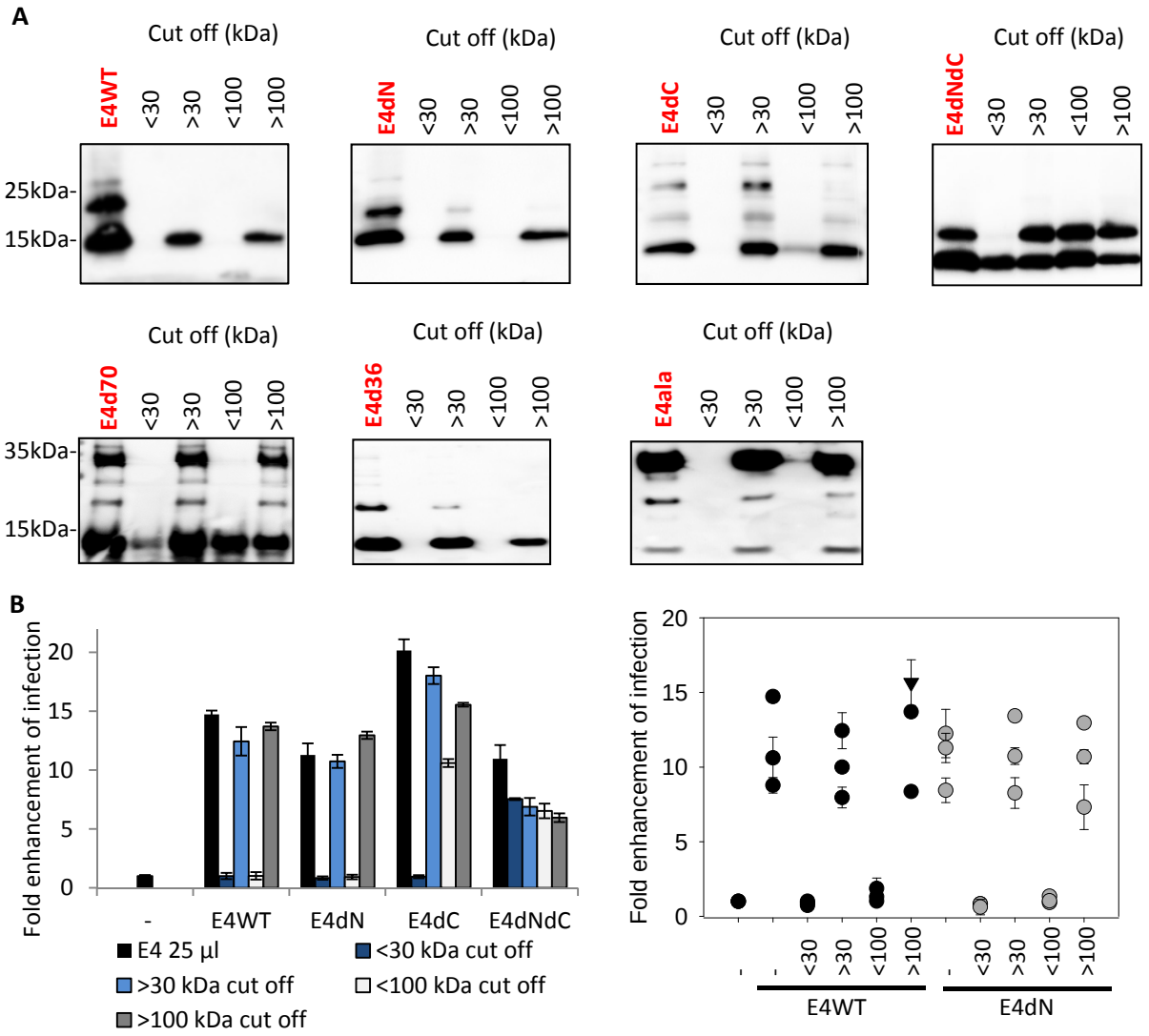

Figure 39: E4 variants form high molecular weight multimers that enhance the lentiviral infection rate.
(A) Protein solutions of E4 variants were filtered through membranes with 30 kDa or 100 kDa cut-offs and analyzed by immunoblot using an α-RPE4 antibody. To account for changes in volume, caused by the filtration procedure half of the untreated E4 volume was loaded.
(B) SupT1 CCR5 cells were infected with VSV-G-pseudotyped lentiviral vectors in the presence or absence of unfiltrated E4 or fractions with different molecular cut-offs (20 µl). GFP expression was measured after 72 h using flow cytometry. Fold enhancement of infection was calculated relative to the number of cells infected with virus without E4 (arbitrarily set as 1.0). Results of a single experiment with error bars corresponding to the SD of three replicates (left). Diagram shows results of 3 independent experiments. Each dot represents the mean of one independent experiment performed in triplicates (error bars reflect the SD). Numbers below horizontal axis indicate size of cut-off (right).

Next, the dynamic of the E4dNdC structures was analyzed. E4dNdC was filtered through a 30 kDa membrane and incubated for 30 min at 37°C. Samples of both filtrate and supernatant were filtered again through a membrane of the same pore size. After incubation of the filtrate, E4 structures both bigger and smaller than 30 kDa were detected (Fig. 40A). This indicates that the E4dNdC fraction containing monomers and dimers possessed the ability to assemble into larger multimers. The presence of high molecular weight multimers supports the possibility that re-multimerization of E4dNdC in the fraction below 30 kDa is responsible for the enhanced lentiviral infection in the

previous experiment. The fraction containing protein assemblies larger than 30 kDa could, with time, also partially pass through the membrane, indicating a release of smaller multimers (Fig. 40A).

After centrifugation for 15 min at 13,000 rpm, conditions that led to complete precipitation of E4dN, E4dNdC was detected both in the pellet and the supernatant (Fig. 40B), indicating the presence of small, unpelletable multimers or monomers.

These findings indicate that multimers of E4dNdC are relatively dynamic, unstable structures that undergo continuous rearrangements, with assembly and disassembly of the larger multimers. The E4dNdC fraction smaller than 30kDa re-assemble quickly, forming larger multimers, while the fraction larger than 30 kDa disassembled, continuously releasing monomers and dimers. The other tested E4 variants appear to be more stable, with predominantly high molecular weight structures larger than 100 kDa.

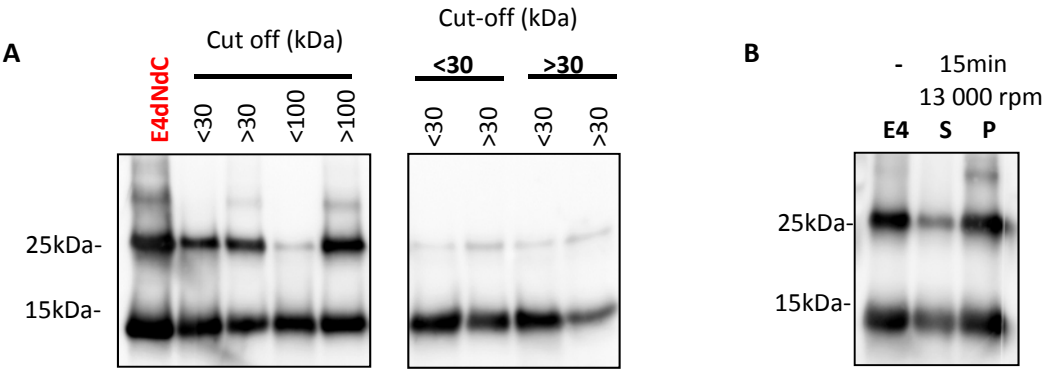

Figure 40: E4dNdC multimers are dynamic structures.
Immunoblot analysis was performed using an α-RPE4 antibody.
(A) The E4dNdC protein preparation was filtered through membranes with a molecular weight cut-off of 30 kDa and 100 kDa (left). Fractions above and below 30 kDa were incubated for 30 min at 37°C and filtered again through a membrane with a 30 kDa cut-off (right).
(B) E4dNdC was centrifuged for 15 min at 13,000 rpm. The pellet was resuspended in refolding buffer to the initial volume. E4dNdC untreated (E4); supernatant (S); resuspended pellet (P).

It is technically challenging to determine whether small E4 multimers can mediate the enhancement of infection because of their swift assembly into larger multimers. Nevertheless, we attempted to test the influence of E4 forms up to octamers on the lentiviral infection rate. E4dNdC was filtered through a membrane with a molecular weight cut-off of 30 kDa. The supernatant and filtrate were mixed with VSV-G-pseudotyped lentiviral vector and immediately added to SupT1 CCR5 cells.

Compared with untreated E4dNdC, which increased the infection rate up to 20-fold, and the resuspended pellet, which also increased the infection rate to the same degree, the filtrate containing fresh protein below 100 kDa only marginally enhanced the lentiviral infection, up to 4-fold (Fig. 41). The amount of protein in both fractions was comparable (Fig. 39 and 40), so the much weaker augmentation of the infection with the filtrate was not caused by differences in the E4 concentration. It is rather plausible that filtration temporarily removed high molecular weight structures, which are most likely necessary for the E4 effect. The observed low enhancement of infection rate may be a consequence of rapid E4dNdC re-assembly into multimers. Alternatively, it is

possible that even smaller E4 multimers below 100 kDa can enhance the lentiviral infection rate to a very low degree.

Because of the unstable nature of E4dNdC assemblies and the lack of a mutant that does not form multimers, the relative contribution of small E4 multimers to lentivirus transduction enhancement cannot be accurately assessed.

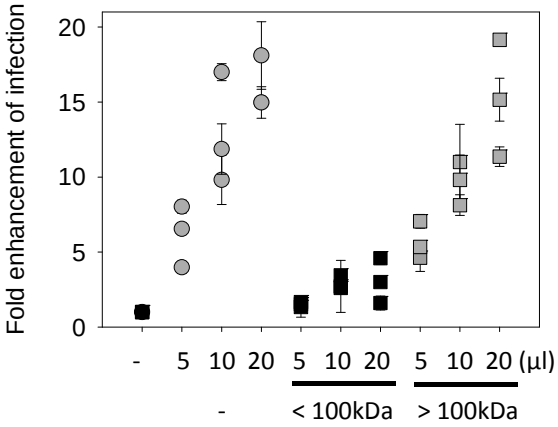

Figure 41: The E4dNdC fraction below 100 kDa does not strongly enhance the lentiviral infection rate.
The E4dNdC protein solution was filtered through membranes with a 100 kDa cut-off. SupT1 CCR5 cells were infected with VSV-G-pseudotyped lentiviral vector in the presence or absence of unfiltered E4 or fractions above/below the 100 kDa cut-off. As the protein concentration could not be determined due to experimental settings corresponding volumes of tested solutions were used. GFP expression was measured after 72 h using FACS. Fold enhancement of infection was calculated relative to the number of cells infected with virus without E4 (arbitrarily set as 1.0) Each dot/square represents the mean of one independent experiment performed in triplicates (error bars reflect the SD).

2.8.3 E4 ENHANCES THE VIRUS SEDIMENTATION VELOCITY

From previous experiments it is clear that E4 forms sedimentable, high molecular weight structures with a positive charge. As a next step, the interaction of E4 multimers with virus particles was analyzed. E4dN was pre-incubated with VSV-G-pseudotyped lentiviral vector for 15 min at 37°C and centrifuged for 15 min at 13,000 rpm (treatment resulting in almost complete sedimentation of E4dN (Fig. 38)). The supernatant (S) was removed and the pellet was resuspended in PBS to the initial volume (P). SupT1 CCR5 cells were infected with S or P. Our standard infection conditions were used as a positive control. To exclude sedimentation of virus particles in the absence of E4, the virus stock was centrifuged for 15 min at 13,000 rpm. No visible virus pellet (VP) was formed and no infection was detected. Collected virus supernatant (VS) led to the infection of the same number of cells as non-centrifuged virus stock (V) (Fig. 42).

The redissolved E4-virus pellet increased the lentiviral infection with an efficiency comparable to the control. Importantly, when E4 was pre-incubated with virus and centrifuged, the supernatant showed no infectivity (Fig. 42). This result suggests that E4 and viral particles interact in solution and that the virus is “pulled down” with E4 into the pellet during centrifugation.

The E4-containing pellet and E4-free supernatant were tested by RT-PCR for the presence of lentivirus RNA. E4dN or E4ala were pre-incubated with virus for 15 min at 37°C and then centrifuged for 15 min at 13,000 rpm. In parallel, VSV-G-pseudotyped lentivirus without E4 (-) was centrifuged. RNA was extracted from the samples and RT-PCR was performed with primers specific for GFP (reporter gene present in VSV-G-pseudotyped lentivirus). The pWPXL plasmid encoding for GFP was used as a positive control. In the E4dN pellet, a 120 bp fragment of the expected size was detected. The supernatant did not contain any amplified product (Fig. 42B), indicating the absence of viral RNA.

In the control sample without E4, GFP RNA was present only in the supernatant indicating that the virus alone cannot be pelleted. Finally, in samples pretreated with E4ala, viral RNA was detected in both the pellet and supernatant (Fig. 42B).

After E4 pre-incubation with VSV-G-pseudotyped lentivirus, only the E4-containing pellet fraction mediated an enhancement of the lentiviral infection rate. Moreover RT-PCR showed a complete absence of viral RNA in the supernatant. As described in the appendix, pre-incubation of E4 with virus in a small volume enhances the E4-mediated augmentation of infection (see 5.3.6 -5.3.8), suggesting that direct interaction of E4 with the virus is needed for its effect. It is likely that E4 strongly binds to the virions, forming E4-virus complexes, consequently enhancing virus sedimentation velocity. A positive charge is required for this effect, since the E4ala mutant was unable to completely "pull down" the virus.

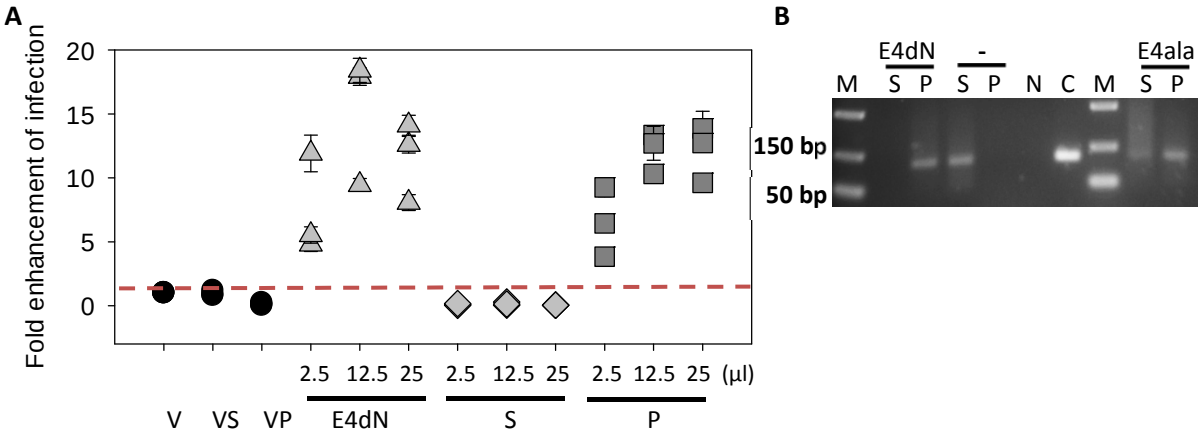

Figure 42: HPV16 E4 multimers enhance the virus sedimentation velocity.
(A) E4dN was pre-incubated for 15 min with VSV-G-pseudotyped vectors and centrifuged for 15 min at 13,000 rpm. SupT1 CCR5 cells were infected with the supernatant (S) or the resuspended pellet (P). Since the protein concentration could not be determined due to experimental settings corresponding volumes of tested solutions were used. As a control to exclude sedimentation of virus particles at the applied experimental conditions, virus stock was centrifuged and cells were infected with the virus pellet (VP) or the virus supernatant (VS). GFP expression was measured after 72 h using flow cytometry. Fold enhancement of infection was calculated relative to the number of cells infected with virus without E4 (arbitrarily set as 1.0) Each dot/square represents the mean of one independent experiment performed in triplicates (error bars reflect the SD).
(B) RT-PCR amplified product visualized on agarose gel. RNA extracted from pellet (P) and supernatant (S) was reverse transcribed to cDNA and amplified with GFP primers. 10 ng pWPXL DNA was used as template for the positive control (C); DNA size marker (M). Negative control with no template (N).

2.9 HPV16 E4 PROTEIN IS TAKEN UP BY CELLS

Amyloidogenic Alzheimer peptides can be taken up from the extracellular space and stored in the lysosomal compartment of cells (Hu et al. 2009, Kandimalla et al. 2009). Therefore, the possibility of a similar mechanism for internalization of E4 was tested.

HeLa cells were incubated with E4WT or E4dN with or without virus overnight and subsequently washed. Cells were fixed 72 h post-treatment. Several different staining approaches were used. First, nuclei were visualized with DAPI. Phalloidin conjugated with TRITC was used to stain the actin cytoskeleton. As described before (Fig. 10), E4 possesses an observable autofluorescence with an excitation of 488 nm. Therefore, this property of the protein was exploited in preliminary experiments for E4 detection. Cells were visualized using confocal microscopy. To exactly determine the localization of E4, Z-stacks were taken and used to construct an orthogonal view as well as a 3D model.

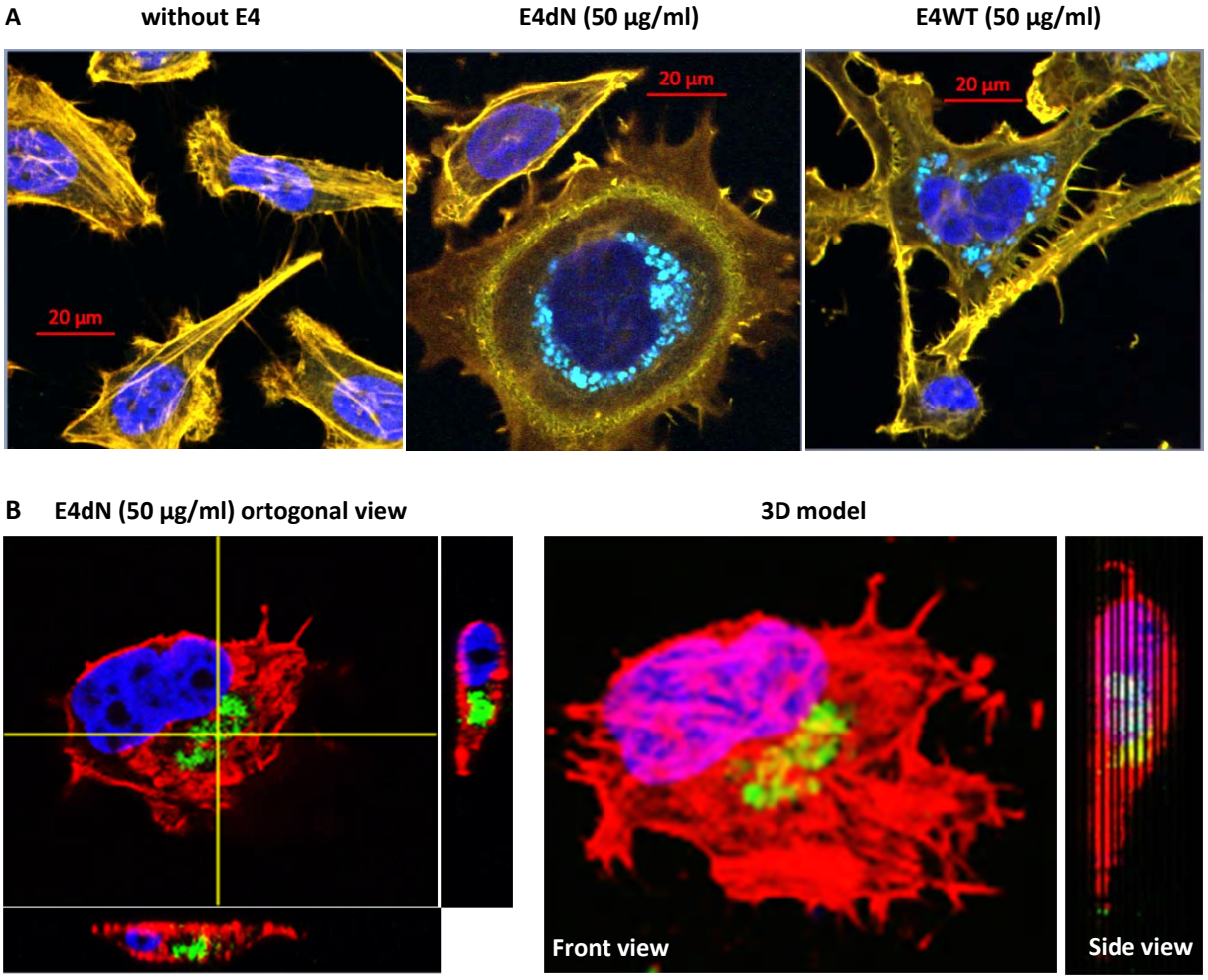

Figure 43: HPV16 E4 is taken up by cells.
HeLa cells were treated with E4WT or E4dN overnight, washed and fixed after 72 h. Nuclei were stained with DAPI (blue) and actin with phalloidin-TRITC (orange-red). E4 autofluorescence is shown (blue/green).

Large amounts of both E4dN and E4WT were repeatedly detected within the actin cytoskeleton (Fig. 43), indicating a *bona fide* uptake into cells. E4 formed perinuclear aggregates resembling aggresomes (Fig. 43). In some preparations, E4 also adhered to the outer site of cellular membranes.

To confirm that the autofluorescence signal was E4-specific, the protein localization was tested with specific antibodies against E4. E4 was visualized with an Alexa Fluor 647 labeled secondary antibodies which can be detected at a wavelength where E4 has no autofluorescence and does not overlap with other used dyes. Co-localization of the autofluorescence signal with the α-RPE4 signal confirmes that assemblies were indeed constituted of E4 protein accumulated to tremendously high amounts inside the cells (Fig. 44A).

Uptake of high amounts of E4 resulted in the formation of large structures whose accumulation in some cases led to a displacement of the nucleus (Fig. 44A). These structures had a visible actin coating (Fig. 44B), which is one of the features of aggresomes.

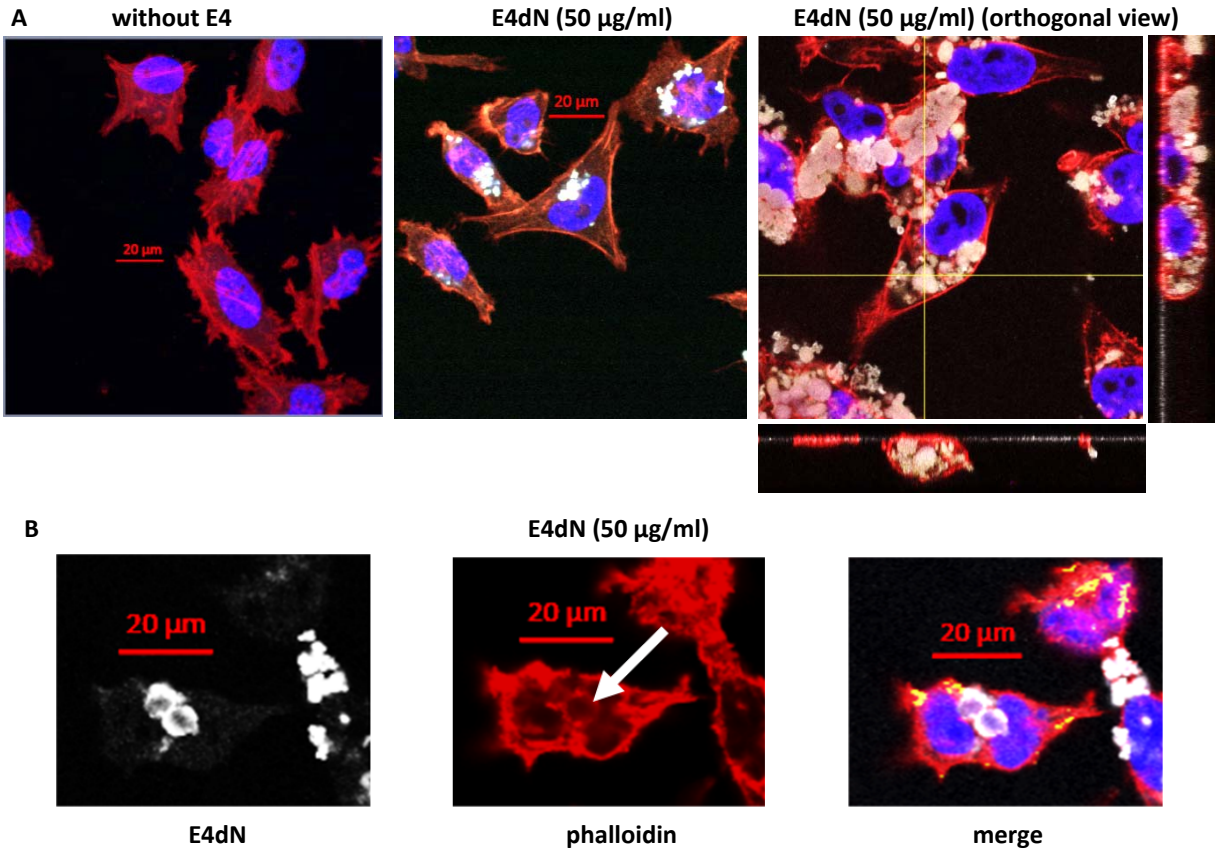

Figure 44: Taken up E4 is stored in form of vacuolar-like structures.
HeLa cells were treated with E4dN overnight, washed and fixed after 72 h. Nuclei were stained with DAPI (blue), actin with phalloidin-TRITC (red), and E4 was detected using rabbit polyclonal antibody against E4 (white). Arrow indicates an actin coated E4 vesicle.

Next, the presence of E4 in lentivirus-infected cells was tested. Therefore, HeLa cells were infected with VSV-G-pseudotyped lentivirus pre-incubated with E4. We readily observed uninfected cells containing E4, cells expressing GFP (marker indicating lentivirus infection) but without E4, and cells with both E4 and GFP. The low percentage of infection combined with high levels of E4 found in

around 50% - 80% of the cells, depending on the experimental conditions, made it impossible to determine if there is any direct connection between E4 internalization and the increase of virus infection rate (Fig. 45A).

The internalization of two other proteins, E7 and L1, was also analyzed. HeLa cells were incubated overnight in the presence of E4, L1 or E7, washed and visualized using confocal microscopy after 72 h. Proteins were detected using an α-His-tag antibody. Compared to E4, only small amounts of E7 could be found inside the cells. L1 formed perinuclear structures similar to E4, although to a lesser extent (Fig. 45B).

To test when E4 internalization occurs, a time-course experiment was performed. Cells were incubated with E4dN and fixed after 2, 6, 24 and 48 h. Microscopic analysis showed that E4 was internalized as early as 2 h post-treatment with E4 (Fig. 45C), supporting the idea that E4 may assist virus internalization.

In summary, HPV16 E4 is internalized by cells and stored in large perinuclear aggregates encapsulated by the actin cytoskeleton. Protein up take occurs within 2 h and it is possible that E4 enters the cells together with the virus. Other tested proteins, E7 and L1, were also internalized, although they do not accumulate to the same degree as E4 in the cells.

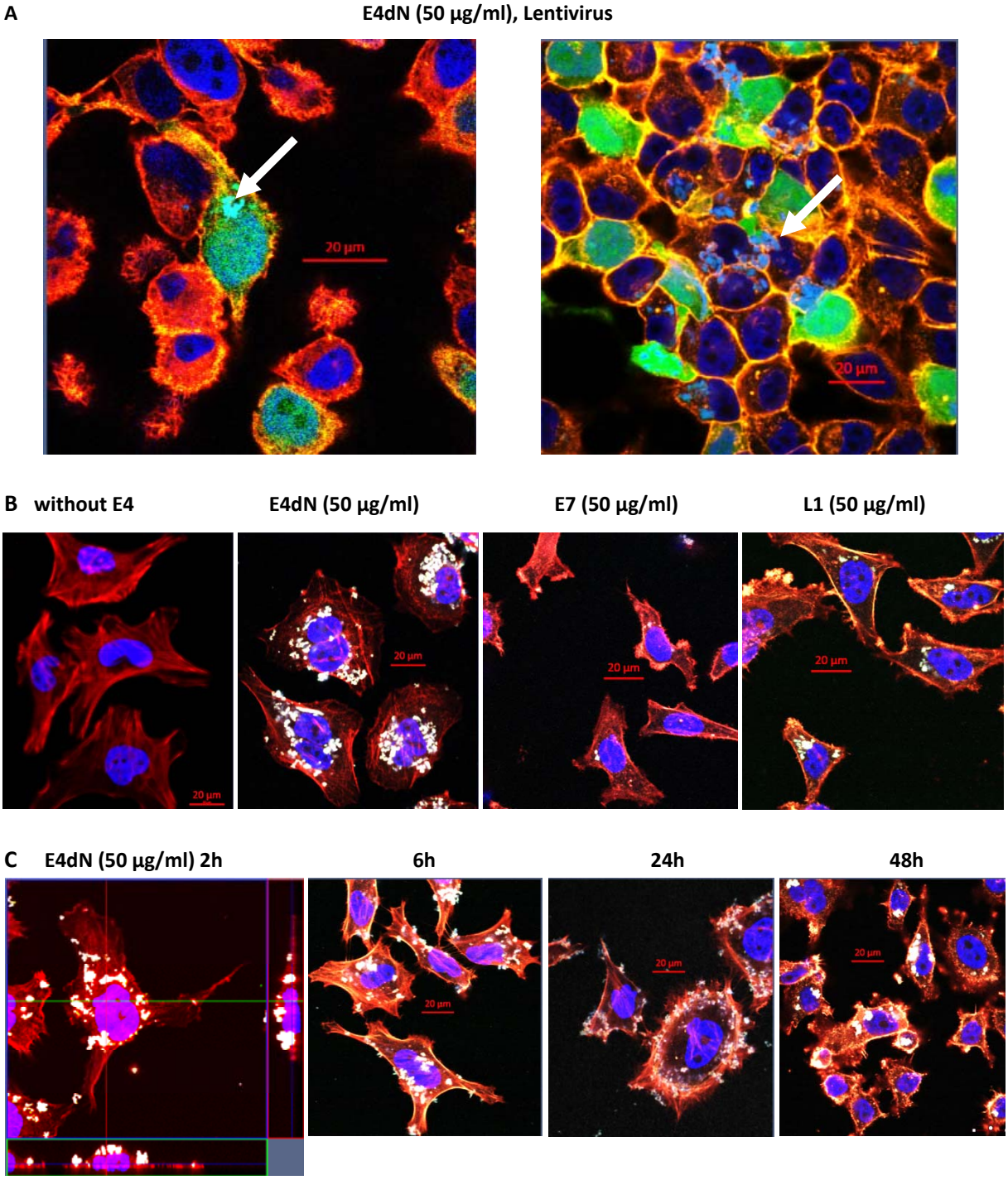

Figure 45: HPV16 E4 is internalized by cells within 2 h.
(A) HeLa cells were infected with VSV-G-pseudotyped lentiviral vector (lentivirus) in the presence of E4dN overnight, washed and fixed after 72 h. Nuclei were stained with DAPI (blue), actin with phalloidin-TRITC (red), autofluorescence was used to visualize E4 which is indicated with an arrow. GFP-expressing, lentivirus-infected cells are green.
(B) HeLa cells were treated overnight with E4dN, E7 or L1 and fixed after 72 h. Nuclei were stained with DAPI (blue), actin, with phalloidin-FRITC (red), E4, E7 and L1 were detected with an α-His-tag antibody (white).
(C) HeLa cells were treated with E4dN and fixed after 2, 6, 24 or 48 h. Nuclei were stained with DAPI (blue), actin, with phalloidin-FRITC (red), E4, E7 and L1 were detected with an α-His-tag antibody (white) .

2.10 E4 STRONGLY ENHANCES THE INFECTION RATE OF HIV AND OTHER VIRUSES

Following the proof-of-principle presented in this work, the observed E4 function was confirmed in an HIV-1 context, as well as for other enveloped viruses, in cooperation with the group of Prof. Oliver Keppler at Frankfurt University.

In this set of experiments, it was shown that:
(I) Various E4 variants, including E4WT and E4dN, strongly enhance the HIV-1 infection rate by a factor up to 100-fold.
(II) As observed in our data, the E4 effect was dose-dependent and highest at concentrations between 50 - 100 µg/ml. Moreover, the maximum concentration present with the virus prior to infection, not the final protein concentration, determined the increase in the infection rate.
(III) Enhancement of infection was best observed at low infection units.
(IV) E4 appeared to be a general enhancer of the HIV infection, increasing the infection rate of both primary virus isolates as well as different lab strains of HIV-1 and HIV-2. Furthermore, E4 augments infection of various cell types expressing the appropriate HIV receptor and co-receptors, including the cell lines TZM, Jurkat, and SupT1 CCR5 and primary cells such as macrophages and activated $CD4^+$ T lymphocytes.
(V) From an epidemiological standpoint, it is relevant that E4 also enhanced the infection rate of other enveloped viruses, herpex simplex virus type 1 (HSV-1) and 2 (HSV-2) up to 12- and 6-fold, respectively. Surprisingly, E4 also increased the infection by adenovirus, which is a non-enveloped virus.
(VI) Finally, E4 enhanced the HIV-1 infection rate at the point of virus attachment to cells and cell fusion. This process was still dependent on Env-mediated HIV entry and other canonical milestones of the viral life cycle, such as attachment, CD4 binding, CXCR4 binding, exposure of fusion peptide, uncoating, reverse transcription, trafficking, nuclear import, and integration.

Results of our colleagues in Prof. Oliver Keppler's group strongly supported and complemented our findings. The VSV-G-pseudotyped vector used in this project proved to be an excellent model, accurately predicting the E4 effect on enveloped viruses, including HIV. All key findings concerning the E4 concentration and infection conditions were, indeed, strong confirmed by the HIV-1 model.

CHAPTER 3

DISCUSSION AND CONCLUSIONS

3.1 E4 AS A FACTOR ENHANCING THE TRANSMISSION OF HIV-1

A growing number of epidemiological studies show a strong, positive association between a primary HPV infection and HIV-1 acquisition. In face of evidence accumulated from many countries and various population groups, HPV is currently proposed as a cofactor for HIV infection (Auvert et al. 2010, Averbach et al. 2010, Chin-Hong et al. 2009, Houlihan et al. 2012, Lissouba et al. 2013, Smith et al. 2010, Smith-McCune et al. 2010, Veldhuijzen et al. 2010). In contrast, no studies have been conducted to explain this association, no mechanism of HPV - HIV direct crosstalk is known, and all proposed hypotheses of indirect crosstalk of those two pathogens remain highly speculative. The work presented here shows, for the first time, a possible mechanism of an HPV-mediated enhancement of HIV infection.

HIV-1 is mainly acquired through sexual contact (up to 90% of the cases), with around 2.3 million people being infected each year (UNAIDS/WHO AIDS epidemic update 2013). The main factor preventing a global HIV pandemic is the surprisingly low rate of virus transfer. Sexual transmission of HIV is described as a bottleneck process, where HIV viral particles must overcome a large number of anatomic and physiologic host barriers. These viral infection inhibitors include the impenetrable physical barrier of intact epithelium, mucus that supports virus capture and removal, physiologically acidic pH that inactivates virions, presence of innate immune cells and inhibitory chemokines and cytokines, and finally limited availability of target cells (Haase 2005, Keele and Estes 2011, Miller et al. 2005, Plummer et al. 1991, Zhang et al. 1999). As a result, the chance of acquiring HIV-1 is between 0.0007 and 0.0082 per coital act, depending on the serostatus of the carrier (Boily et al. 2009, Wawer et al. 2005).

Since the virus has a very low probability of establishing a productive infection in target cells on its own, it is suggested that additional enhancers of infection are necessary for adequate HIV propagation. The need to identify factors influencing the HIV transmission rate is currently strongly emphasized. Notably, all agents that enhance a lentiviral transmission are a potential target for preventive intervention and, perhaps in the future, will aid to control a global HIV pandemic (Haase 2005, Keele and Estes 2011, Miller et al. 2005, Plummer et al. 1991, Zhang et al. 1999).

3.1.1 E4 STRONGLY ENHANCES THE LENTIVIRAL INFECTION RATE

In this study, VSV-G-pseudotyped lentivirus was used as a model for enveloped viruses (including HIV) to investigate the influence of the HPV E4 protein on the lentiviral infection rate. Taken together, E4 was a very potent enhancer of the infection rate. Pre-treatment of lentivirus with HPV16 E4dN, corresponding to the E4 calpain-cleaved fragment (Khan et al. 2011, McIntosh et al. 2008), increased lentiviral transduction up to 40-fold. This was observed for both adherent and suspension cells, indicating a certain level of cell-type independence. The highest increase of infection was observed for the SupT1 CCR5 cell line, derived from T lymphocytes, the natural target of HIV-1 (Fior 2012, Gay et al. 2012, Miller and Shattock 2003).

In vitro functional analysis of amyloidogenic peptides requires a detailed characterization of all preparation conditions to ensure reproducible formation of fibrils. On one hand, the protein has to be protected from aggregation that can occur in the absence of cellular chaperons. On the other

hand, the native fold of the protein has to be destabilized and non-covalent interactions between protein monomers need to be promoted to form amyloids (Chiti et al. 2001, Chiti et al. 1999, Jahn et al. 2006). Hence, it was first necessary to optimize the E4 handling conditions. The HPV E4 protein is described to form amyloids both *in vitro* and *in vivo* (Knight et al. 2004, McIntosh et al. 2008). Although we were unable to confirm the presence of mature fibrils in later experiments, E4 was treated like an amyloidogenic peptide in the design of all experimental conditions. In initial experiments, differences in the activity between different protein stocks were observed. It was proposed that those inconsistences were caused by the formation of different protein structures that, in case of amyloids, strongly depends on the preparation conditions (Chiti et al. 2001, Chiti et al. 1999, Eisenberg and Jucker 2012, Pedersen et al. 2010, Fezoui et al. 2000, Jahn et al. 2006, Toyama and Weissman 2011). Therefore, the preparation settings (including time, temperature and handling of E4) were optimized to yield stable, reproducible and highly active E4 protein stocks. Furthermore, infection conditions were modified to maximize the E4-mediated enhancement of infection. The highest effect was observed when E4 variants were dispersed by sonication and pre-incubated with virus in a small volume at 37°C for at least 15 min. In this regard, E4 behaved very similarly to SEVI, which requires an analogous pre-incubation step (Munch et al. 2007). Moreover, as with SEVI (Munch et al. 2007) and other amyloidogenic peptides (Zhang et al. 2014), it was observed that the maximal protein concentration during virion pre-incubation rather than the final protein amount determines the magnitude of the enhancement.

3.1.2 HPV16 E4 STRONGLY ENHANCES THE INFECTION RATE OF HIV AND OTHER VIRUSES

The model used in this study was further confirmed by our collaboration partners from the group of Prof. Oliver Keppler at Frankfurt University.

Both, E4WT and E4dN, greatly increased the HIV-1 infection by more than two orders of magnitude. All factors described in this work to influence the E4-mediated enhancement of infection the rate, found confirmation in the HIV-1 model. These are for example, a dependence on protein concentration and a stronger enhancement of infection rate with a lower number of viral infectious units. Most importantly, E4 was established to be a very potent enhancer of several virus infections, increasing the infection rate of HIV-1, HIV-2 (including primary virus isolates and different lab strains), HSV-1, HSV-2 and adenoviruses in various cell lines and primary cells (Prof. Oliver Keppler, personal communication). Nevertheless, E4 appears not to be a universal enhancer of viral infection as we did not observe any effect on the HPV transduction (see 3.3).

The relatively higher enhancement of the HIV-1 infection compared to the effect on our model of VSV-G-pseudotyped lentivirus may be a consequence of the greater efficiency with which the lentivirus vector infects the cells. In line, Wojtowicz et al. (2002) suggested that the augmentation of infection by Aβ is better observed for viruses with poorer cell infection efficiency and in the absence of other enhancing factors (Wojtowicz et al. 2002).

Our findings that E4 increases the infection rate of different viruses argues for a common mechanism. Moreover, the enhancement of infection of primary cells by different primary HIV-1 isolates opens the intriguing possibility that the here-described role of E4 could be a relevant *in vivo* mechanism.

3.1.3 E4 AND PRIMARY HIV-1 INFECTION

A crucial finding of this study is that the conditions described for the E4-mediated enhancement of infection are compatible with a typical HIV-1 infection event *in vivo*. The primary infection is established by only a few HIV virus particles, termed founder or transmitted viruses (Keele et al. 2008, Parker et al. 2013, Shaw and Hunter 2012). It is described that the number of HIV-1 virions transmitted during a sexual intercourse is usually subinfectious (Gray et al. 2001) and the HIV viral load in semen is as low as 50 copies in 1 ml of ejaculate, resulting in the deposit of as few as 200 viral particles in the female genital tract per coital act (Gupta et al. 1997, Osborne et al. 2011). Notably, Munch and colleagues (2007) showed that viral doses in this order of magnitude are insufficient to establish a productive HIV-1 infection in an *ex vivo* tonsillar model or in a peripheral blood mononucleated cell (PBMC) culture, in the absence of additional enhancers of infection (Munch et al. 2007).

Our results show that the E4-mediated increase of the infection rate is most prominent at a very low number of infectious units, below a control infection rate of 0.02%, which resembles the conditions found *in vivo*. This renders the contribution of E4 to virus transmission highly relevant if further confirmed in *in vivo* models.

3.1.4 *IN VIVO* E4 CONCENTRATION AND ACCESSIBILITY OF HIV-1 TARGET CELLS

Another important point is whether the protein concentrations needed for the E4 enhancement of infection can be reached *in vivo*. As described in this work, the E4 effect was strongly dose-dependent and the efficiency of enhancing lentiviral infection rates reached a peak at concentrations between 50 - 100 µg/ml.

Expression of HPV E4 is mostly studied in cervical neoplasia biopsies and CIN lesions. In clinical material, both *E4* mRNA and protein can be readily detected, though the amount and frequency differs between studies (Crum et al. 1989, Durst et al. 1992, Onda et al. 1993, Palefsky et al. 1991). Data from expression of E4 in raft cultures *in vitro* confirmed that E4 accumulates to very high levels in the uppermost cells of the epithelium. Moreover, it is postulated that E4 is the most abundant product of a HPV infection (Brown et al. 2004, Bryan et al. 1998, Griffin et al. 2012, McIntosh et al. 2010, Pray and Laimins 1995, Supchokpul et al. 2011, Roberts et al. 1993, Wilson et al. 2005). In fact, the amount of E4 in the corneal layer of the epithelium seems to exceed that of keratin in HPV-positive tissue sections (McIntosh et al. 2010). Additional reports that E4 is detected in high amounts in the mucosa of HPV-infected cervical and anorectal tissue was provided by our collaboration partners (Prof. Oliver Keppler, personal communication).

Further indication for the high E4 abundance comes from observations that HPV E4 is highly expressed in the epithelium of individuals infected with cutaneous HPV types (Borgogna et al. 2012, Borgogna et al. 2014). Here, E4 may account for as much as one-third of the total protein expressed in HPV-driven skin warts (Breitburd and Croissant 1987).

Likely, HPV E4 is not only present in high amounts in superficial squamous cells, but it also accumulates on the outer surface of the epithelium. Both E4-induced cytokeratin collapse (McIntosh

et al. 2010) and death of terminally differentiated cells in the upper part of epithelium (Hackemann et al. 1968) should result in massive release of E4. Amyloids are highly resistant to degradation (Chiti et al. 1999, Eisenberg et al. 2012, Nilsson 2004, Pedersen et al. 2010) and it is well-established that they can accumulate in high amounts in the extracellular space (Knauer et al. 1992). One example is a clinical manifestation is reactive systemic amyloidosis. The disease-causing acute-phase reactant serum amyloid A protein (SAA) can accumulate in serum to concentrations as high as 50 µg/ml (Gillmore et al. 2001). Apparently there are no efficient mechanisms for amyloid removal from the organism. Considering the postulated amyloid properties and expression pattern of E4, we hypothesize that in an *in vivo* scenario, E4 could come in contact with HIV-1 on the surface of the anogenital epithelium at functionally relevant concentrations.

An additional and important point that should be addressed is whether E4 comes into contact with HIV-1 target cells. Both E4 and the virus meet on the surface of the epithelium, but on the other hand, lymphocytes reside in much deeper layers of the mucosa, in the stroma (Nishibu et al. 2006, Miller and Shattock 2003, Shen et al. 2011). However, the integrity of the cervical epithelium is often compromised during sexual intercourse, exposing the subepithelium and providing access to immune cells (Fraser et al. 1999, Jones et al. 2003). Moreover, HPV on its own can promote the exposure of immune cells by creation of microabrasions during infection. In addition to the development of dysplastic lesions in some persistent infections with high-risk HPV types (Longworth and Laimins 2004), HPV E6 mediates the disruption of cellular tight junctions (Kranjec and Banks 2011) and E7 causes the downregulation of the epithelial adhesion molecule E-cadherin (Laurson et al. 2010). The final outcome is a disruption of the epithelial integrity, which could open access for HIV-1 infection. Hence, E4 fibrils, released from the upper layers of the epithelium, can access DCs, macrophages and lymphocytes in the stroma and, in principle, subsequently increase HIV-1 transmission.

3.1.5 E4 ENHANCES THE LENTIVIRAL INFECTION UNDER ACIDIC CONDITIONS

Amyloid structure and properties are largely influenced by environmental conditions in which fibrils are formed and deposited (Chiti et al. 2001, Chiti et al. 1999, Eisenberg and Jucker 2012, Pedersen et al. 2010, Fezoui et al. 2000, Jahn et al. 2006, Toyama and Weissman 2011). *In vivo*, E4 forms in the female reproductive tract, an environment characterized by low pH, ranging between 3.8 and 6 (Linhares et al. 2011, Witkin et al. 2007). These acidic conditions mediate the inactivation of sexually transmitted viruses, including HIV-1 (Aldunate et al. 2013, Tevi-Benissan et al. 1997). The ability of E4 to promote lentiviral infection was not reduced for protein prepared at acidic pH. Thus, our findings indicate that the physiological pH of the female reproductive tract should not impair E4 function in terms of an enhancement of HIV-1 transmission. This idea is further supported by studies showing that acidic pH actually enhances amyloid fibril formation and accumulation (Barrow and Zagorski 1991, Chiti et al. 1999, Lai et al. 1996, Srinivasan et al. 2003) it is even suggested that low pH is a prerequisite for the formation of certain types of amyloids

3.1.6 COMPARISON OF THE E4 EFFECT WITH OTHER ENHANCERS OF THE LENTIVIRAL INFECTION

Many enhancers of retroviral gene transfer have been developed for laboratory purposes, including protamine sulfate and polybrene. They are widely and routinely used to increase the transduction rate of a number of different cell lines with a wide range of viral vectors (Cornetta and Anderson 1989, Seitz et al. 1998). The effect of polybrene, a compound that enhances retrovirus transduction by increasing receptor-independent virus absorption, is the best studied (Denning et al. 2013, Davis et al. 2002).

E4dN was observed to be a remarkably robust enhancer of lentiviral infection. It increased lentiviral transduction four times higher than polybrene used at its standard concentration recommended by previous studies (Denning et al. 2013, Davis et al. 2002). In a study by Wurm and colleagues (2010), the effect of SEVI was also compared with enhancers of retrovirus transduction, like polybrene. Similarly to our observations with E4, the SEVI-mediated increase of infection rate was three times more efficient than that of commercially available compounds (Wurm et al. 2010).

Accordingly, it was shown here that E4dN and SEVI have a comparable strength in augmenting the lentiviral infection at a similar concentration range. In contrast to an earlier report by Wojtowicz et al. (2002), however, we did not detect an appreciable effect of $A\beta_{40}$ on the lentiviral infection. $A\beta_{40}$ was not structurally analyzed in this study and therefore we cannot formally exclude that the lack of activity may simply reflect improper refolding. When Munch and colleagues (2007) tested the effect of Alzheimer amyloids on the HIV-1 infection, they were also unable to detect any enhancement, but again the presence of amyloid fibrils was not confirmed (Munch et al. 2007). One hypothesis is that preparation of $A\beta_{40}$ and its handling in order to form functional fibrils is technically demanding, as is the case for many amyloidogenic peptides.

Thus, the comparative analysis between known enhancers of enveloped virus infection classifies E4 as a potent factor for infection augmentation, similarly to SEVI, with better performance than synthetic cationic compounds like polybrene.

Although the magnitude of the observed augmentation by E4 and SEVI was comparable, their effects and outcome *in vivo* may differ. The relevance of the effect of SEVI and SEM on HIV-1 transmission *in vivo* is still being discussed. It has been shown that SEM cleavage by PSA leads to rapid degradation and solubilization of semen coagulum (Lilja et al. 1987). Similarly, SEVI undergoes proteolytic degradation in seminal plasma (Martellini et al. 2011). Importantly, SEVI had no drastic effect on simian immunodeficiency virus vaginal transmission in a rhesus macaques model (Munch et al. 2013). Moreover, semen itself is known to have an inhibitory effect on the HIV-1 infection. Its antiviral activity is mainly mediated by two factors: (I) oxygen radicals, to which the lipids of the HIV envelope are highly sensitive (Agarwal and Prabakaran 2005), and (II) the presence of cationic antimicrobial polypeptides, including lactoferrin, leukoprotease inhibitor and defensins (Doncel et al. 2011). Finally, semen plasma interferes with the HIV-1 attachment to its target cells, T-lymphocytes, macrophages, and DCs (Sabatte et al. 2007). Therefore, it remains unclear to which extent the amyloids present in semen enhance the HIV-1 transmission *in vivo.*

3.2 THE ABILITY TO ENHANCE LENTIVIRAL INFECTION IS PRESERVED AMONG E4 PROTEINS ACROSS DIFFERENT HPV TYPES

Epidemiological reports state that several HPV types, including the low-risk serotypes, are associated with higher HIV acquisition (Houlihan et al. 2012, Lissouba et al. 2013). In this study, it was established that E4 from high-risk HPV16, HPV18 and HPV58 and low-risk HPV11, HPV42 and HPV70 genotypes are all strong enhancers of the lentiviral infection rate. The tested types were chosen based on the prevalence and geographical distribution of the respective HPV genotypes. For example HPV11 is the most common cause of genital warts (Bruni et al. 2010, Denny et al. 2014). In addition, these types are postulated to be associated with HIV-1 acquisition in epidemiological studies (Auvert et al. 2010, Smith-McCune et al. 2010, Smith et al. 2010).

The E4 effect was observed for both full-length and calpain-cleaved forms of the protein. E4 from all tested types enhanced in this study lentiviral infection rate. This is interesting as there is very low E4 sequence homology between the different HPV types (Doorbar and Myers 1996, Doorbar 2013). This is in line with the epidemiological data indicating that the probability of infection does not depend on the type or the oncogenic potential of the virus (Houlihan et al. 2012).

Taken together, it appears that the E4-mediated augmentation of lentiviral infection is a broad phenomenon caused by the E4 protein of at least 6 different genotypes, and most likely of all HPV types, regardless of their oncogenic potential. This finding, combined with the high prevalence of a HPV infection - more than 80% of the population is infected with at least one HPV type during their lifetime (Bruni et al. 2010, de Sanjose et al. 2007), provide a possible explanation of the epidemiological data correlating HPV and HIV-1.

3.3 THE HPV E4 EFFECT ON THE INFECTION RATE OF HPV

We also addressed the question whether E4 is involved in HPV transmission and cell entry. No indication that HPV16 E4 may enhance the infection rate of HPV16, by which it is encoded or of other heterologous HPV types, like HPV18, was observed. This result is probably caused by the differences in the virus structures. Lentiviruses possess a negatively charged proteo-lipidic envelope that has been suggested to interact with amyloids (Munch et al. 2007, Wojtowicz et al. 2002). In contrast, HPVs are non-enveloped viruses, covered only by a protein capsid without an external cell-derived lipid membrane (Chen et al. 2000). If the mechanism of the E4-mediated enhancement of the infection rate is similar to that seen for other amyloids, it is plausible that the presence of an envelope is a prerequisite for an E4-virus interaction and consequent enhancement of infection. A possible alternative mechanism for the E4 effect on the infection with another non-enveloped virus – adenovirus – will be discussed later (see 3.4).

Similarly to our results, SEVI and the Alzheimer peptides $A\beta_{40}$ and $A\beta_{42}$ are believed to have no effect on the infection rate of non-enveloped viruses (Munch et al. 2007, Wojtowicz et al. 2002). Even polycation-based enhancers of the infection rate, which do not form an organized tertiary structure, such as poly-L-lysine, are recommended for the enhancement of the transduction of enveloped

viruses (Davis et al. 2002, Davis et al. 2004, Landazuri and Le Doux 2004, Landazuri and Le Doux 2006).

This data suggests that the potential of E4 to enhance the infection of viruses plays no role in the life cycle of HPV itself. Still, it cannot be excluded that, under *in vivo* conditions, the presence of E4 fibrils may create an advantageous environment for papillomavirus transmission and secondary infection. Therefore, this is an important issue for future research and it should be carefully analyzed, for example, in a keratinocyte raft tissue model (Anacker and Moody 2012).

3.4 MECHANISM OF THE E4-MEDIATED ENHANCEMENT OF THE LENTIVIRAL INFECTION RATE

3.4.1 FORMATION OF MATURE AMYLOID FIBRILS IS NOT ESSENTIAL FOR E4-MEDIATED ENHANCEMENT OF THE INFECTION RATE

Pinpointing the exact domain mediating the E4 effect on viral transduction proved to be challenging, as all tested protein variants increased the lentiviral infection rate to some degree. Therefore, functional and structural E4 studies were correlated to explain this phenomenon and to identify any common features amongst all E4 mutants, which could explain their ability to increase virus transduction.

Deletion of the N-terminal domain was described to mediate amyloid formation (McIntosh et al. 2008). In our studies, this E4dN variant had the strongest effect on the lentiviral infection rate. EM data showed that E4dN formed various high molecular weight structures such as thin filaments, ragged ribbon-like filaments of approximately 100 - 200 nm in length, assemblies of filaments and thick fibrils. These latter structures strongly resembled E4dN amyloid-like fibrils reported previously (McIntosh et al. 2008). However, they do not meet the structural requirements to be classified as amyloids, which should be straight and needle-like (Gras et al. 2011, Jimenez et al. 2001, Nielsen et al. 1999, Shirahama and Cohen 1967). Full-length E4 is not known to assemble into fibrils. It is suggested that the presence of the N-terminal domain masks the multimerization domain and hinders polymerization (Doorbar 2013, Khan et al. 2011, McIntosh et al. 2008). Nonetheless, E4WT from HPV16 and other HPV types still strongly increased the lentiviral infection rate. Structural analysis revealed that E4WT forms thick fibrils, fibril assemblies and protein assemblies similar to some of the structures found in E4dN samples. The multimerization domain consists of amino acids 66-92 (E4C) and is known to spontaneously assemble into short twisted fibers (McIntosh et al. 2008). This domain alone was sufficient to mediate the augmentation of infection, although the strength of enhancement was decreased approximately three-fold compared to E4dN. In our analysis, E4C formed a large amount of short, straight, rod-like filaments up to 100 nm long that assembled into a network. These filaments resembled published E4C structures (McIntosh et al. 2008). In previous studies the deletion of the E4 C-terminus (E4dC) resulted in a mutant that is unable to form amyloids and assembles only into multimers up to hexamers (Wang et al. 2004). Moreover, the E4dC mutant could not be detected by amyloid imaging probes (McIntosh et al. 2008). Surprisingly, in our hands, E4 mutants with a partial, as in E4dC and E4dNdC, and complete, as in E4d70, deletion of the multimerization domain enhanced the lentiviral infection rate. These mutants still formed multimers, as confirmed by SDS-PAGE in non-reducing conditions and at lower SDS concentrations. Finally,

despite the lack of the multimerization domain, E4dC was shown here in EM studies to form thin fibrils with features of pre-fibrils when compared with published data (Jimenez et al. 2001, Nielsen et al. 1999). The positively charged region encompassing amino acids 36-41 has been postulated to contribute to the overall E4 fibril organization (Doorbar 2013). Nevertheless, the deletion of this domain, as in E4d36, decreased but not abolished the E4-mediated enhancement of the infection rate. Again, this protein mutant formed multimers (summarized in Table 5).

All tested E4 variants also moderately enhanced ThT fluorescence, despite the lack of mature amyloid structures. ThT staining is routinely used as a "gold standard" for the detection of a cross-β-sheet protein conformation (Bruggink et al. 2012). ThT is known to bind strongly to amyloid fibrils (Khurana et al., 2005). Neverthelss, this dye can also stain cross-β-sheets forming already in pre-filaments, pre-fibrils or even in some non-structural protein aggregates (Biancalana and Koide 2010, Nilsson 2004). Moreover, SEVI enhanced ThT fluorescence stronger than E4 in the same concentration range. Therefore, it appears that mature amyloid fibrils are absent in the E4 solution and that positive ThT staining originates from cross-β-sheets present in filaments and fibrils. Lack of mature amyloid fibrils can be explained by *in vitro* protein preparation conditions. *In vivo*, E4 amyloid fibrils form inside cells (Khan et al. 2011, McIntosh et al. 2008), where protein folding is aided by a number of molecular chaperones (Tyedmers et al. 2010). Mature fibrils of some amyloids efficiently form only through interaction with such chaperones (Grenwald et al., 2010).

A number of studies have proposed that SEVI and the Alzheimer peptides -$A\beta_{40}$ and $A\beta_{42}$ enhance the enveloped viruses infection rate through the formation of mature amyloid fibrils (Arnold et al. 2012, Munch et al. 2007, Wojtowicz et al. 2002), but these findings still remain controversial. Munch and colleagues (2007) did not observe large fibrils in semen itself. Furthermore, freshly prepared SEVI solution acquired the ability to augment virus infection before the formation of amyloid fibrils was detected by ThT fluorescence (Munch et al. 2007). At the same time, Wojtowicz et al., (2002) postulated that short forms of fibrils are more effective in promoting HIV-1 transduction compared to long ones. Similarly, the amyloidogenic peptide P16 enhanced the infection rate of HIV-1 prior to the formation of fibrils (Zhang et al., 2014). As a result, it has been suggested that smaller aggregates may be more effective in increasing the infection rate than mature amyloids (Munch et al. 2007).

In this study, none of the deletions of functional domains of E4 designed to block amyloid formation was able to completely abolish the E4-mediated effect. Different types of structures were observed in EM analysis, most resembling either pre-filaments or pre-fibrils (Gras et al. 2011, Jimenez et al. 2001, Nielsen et al. 1999, Shirahama and Cohen 1967). Nonetheless, no mature fibrils were seen, in contrast to the SEVI samples. Taken together, these results indicate that mature amyloid formation is dispensable for the enhancement of infection.

3.4.2 ENHANCEMENT OF THE INFECTION RATE IS ASSOCIATED WITH THE PRESENCE OF HIGH MOLECULAR WEIGHT MULTIMERS

The extremely robust effect on the enhancement of the lentiviral infection rate observed for the E4 proteins of divergent sequence length and structure suggests that more general properties of E4 are responsible for its function. Detailed structural analysis showed that all E4 variants are able to assemble into high molecular weight multimers above 100 kDa, forming filaments, fibrils or

amorphous assemblies possessing different levels of organization. Deletion of the multimerization domain partially impaired formation of high molecular weight E4 structures and led to the presence of additional smaller multimers (E4dC, E4dNdC and E4d70) or even monomers or dimers (E4dNdC) (Table 5).

As discussed above, the formation of amyloid fibers does not appear to be a requirement for the E4-mediated enhancement of infection. We therefore hypothesize that this effect is dependent on the formation of high molecular weight structures. We found that E7, which forms mostly monomers and dimers (Clemens et al. 1995), had no detectable effect on the lentiviral infection rate. In contrast, a L1 mutant forming pentamers (which are the basic building block of the HPV capsid (Schadlich et al. 2009)) and L1 VLPs (Seitz et al. 2013), enhanced the lentiviral infection rate.

Table 5: Summary of the structure, charge and effect on the infection of all proteins tested in this study.

	SDS-PAGE	Low SDS	Turbidity/ Microscopic structures	Filtration 30 kDa and 100 kDa cut-off	Isoelectric Point	EM	Enhancement of infection [fold]
E4WT	M, D	Hexamer and high molecular weight multimers	**+/+**	E4> 100kDa	**9.14**	Fibrils/ assemblies	**15-20**
E4dN	M, D		**+/+**	E4> 100kDa	**8.8**	Filaments/ fibrils/ assemblies	**20-40**
E4dC	M, D, T, H		**+/+**	E4> 100kDa 100kDa> E4<30kDa	**9.14**	Filament/ non structural aggregates	10-15
E4dNdC	M, D		**+/+**	All forms	**8.8**	X	10-20
E4d70	M, D, T, H		**+/+**	All forms	**9.18**	X	5-10
E4d36	M, D		**+/+**	E4> 100kDa	**6.23**	X	5-10
E4ala	M, D, T, H		**+/+**	E4> 100kDa	**4.75**	X	1
E4C	X	+/+	X	X	**7.02**	Thin filaments	5-10
E4Cala	X	+/+	X	X	**6.25**	X	1-4
SEVI	X	+/+	X	X	**10.21**	Amyloid fibrils	**20**
L1	Ladder	+/+	X	X	**8.27**	X	5-10
E7	M	-/-	X	X	**4.77**	X	1

Monomer (M); dimer (D); trimer (T); tetra-pentamer (H), not tested (X). Positively and negatively charged polypeptides are marked in red and blue, respectively. Strong enhancers of the infection rate are underlined.

A similar effect has previously been described for high molecular weight polymers that do not form organized fibrillar structures and yet significantly increase the transduction of enveloped viruses (Davis et al. 2002, Davis et al. 2004, Landazuri and Le Doux 2004, Landazuri and Le Doux 2006). One example is poly-L-lysine (PLL), a group of homopolymers of different lengths made of lysine polypeptides. All PLLs have an identical charge/mass ratio, but the different lengths lead to a change in the charge/molecule ratio. Consequently, identical masses of the various PLLs always contain the same amounts of total charge but different numbers of molecules. PLLs enhance the transduction rate independent of both the viral envelope and cellular receptors. This effect is correlated with the

size of the polymer. High molecular weight PLLs (above 50 kDa) enhance virus adsorption almost 100 times more efficiently than small multimers (Davis et al. 2004, Landazuri and Le Doux 2004, Le Doux et al. 2001).

The observations for E4 are thus consistent with the mechanistic examples provided by synthetic polymers, where the enhancement of the lentiviral infection rate does not require the presence of an organized structure but rather high molecular weight multimers.

3.4.3 THE POSITIVE OF E4 CHARGE IS REQUIRED FOR THE E4 EFFECT ON INFECTION

Both, the cell surface and the lentivirus envelope, possess a negative charge, leading to considerable electrostatic repulsion between the cellular membrane and virions (Conti et al. 1991, Elul 1967, Ugolini et al. 1999). This study revealed that the positive charge of E4 is crucial for its ability to efficiently enhance lentiviral infection.

E4 variants possess neutral (E4C) or moderately acidic (E4WT) isoelectric points (Table 5). Pre-treatment of E4 with polyanionic compounds that block the charge decreased the infection rate back to control levels. This inhibition of the E4 effect could be observed for all E4 mutants, regardless of their sequence, structure and isoelectric point. Moreover, the L1-mediated enhancement of the infection rate was also blocked by polyanions, which argues that this effect is not protein-specific.

The necessity of a positive charge for E4 function is further supported by studying E4 alanine mutants. In E4ala and E4Cala, all positively charged amino acids were substituted with alanine, resulting in basic isoelectric points of 4.7 and 6.2, respectively. Although, these E4 variants assembled into macroscopically visible structures and E4ala formed high molecular weight multimers, neither of the alanine mutants had a strong effect on the lentiviral infection rate. The most plausible explanation is that E4 binds directly to both enveloped virions and membranes of the target cells, shielding electrostatic repulsion between them and in turn aiding virion fusion.

Similarly to our observations, studies on both SEVI and another region of PAP that enhances the lentiviral infection rate, PAP85-120, showed that the positive charge of fibrils is indispensable for the enhancement of the infection rate. Like in our experiments, the effect of SEVI and PAP85-120 on virions can be abolished in the presence of various polyanionic compounds, such as heparin, dextran sulfate, oversulfated heparin, and oversulfated chondroitin sulfate. It has been proposed that polyanions inhibit SEVI fibril attachment to the cell surface and/or to HIV-1 (Roan et al. 2009). The same effect is observed for semen, where addition of polyanionic compounds greatly decreases the enhancement of HIV-1 infectivity (Arnold et al. 2012, Roan et al. 2009).

In line with our findings, a SEVI mutant in which all lysines and arginines were replaced with alanine is still able to form amyloid fibrils but fails to bind virions or enhance the infection (Roan et al. 2009). Alanine mutants of other amyloidogenic peptides are also deficient in their ability to enhance the HIV-1 infection rate (Zhang et al., 2014).

Similar results have been obtained for synthetic, short, charged modular peptides which spontaneously assemble into fibrils. Amyloid-like fibrils formed by both positively and negatively

charged precursors have the same structure and spectroscopic properties, yet only fibrils formed by cationic peptides increased the lentiviral infection rate (Easterhoff et al. 2011).

Positive charge itself, without any structural requirement is sufficient to enhance enveloped viruses transduction, as seen with polybrene (Coelen et al. 1983, Davis et al. 2002, Davis et al. 2004, Denning et al. 2013, Landazuri and Le Doux 2004, Toyoshima and Vogt 1969). Likewise, it has been known for a long time that high molecular weight (> 100kDa) polycations such as poly-L-ornithine augment infection by retroviruses and herpesviruses (Toyoshima and Vogt 1969, Wallis and Melnick 1968).

The ability to enhance the infection rate via charge shielding without any organized structure appears to be a common property. Another positively charged protein reported to enhance HIV-1 transduction is RANTES (Regulated on Activation, Normal T-cell Expressed and Secreted, also known as CCL5). RANTES is a β-chemokine synthesized by T-lymphocytes with a pro-inflammatory function. At high concentrations, RANTES aggregates into multimers that enhance the HIV-1 infection rate through the binding of positively charged virus-RANTES multimers to negatively charged proteoglycans on the surface of the target cells (Appay and Rowland-Jones 2001, Trkola et al. 1999).

In agreement with the results presented here, an overall positive charge does not appear to be required for the augmentation of lentiviral transduction. Two of the tested E4 variants, the E4C and E4d36, have a neutral or even slightly basic pI and still enhanced the infection rate up to 10-fold. Studies on polymer-mediated enhancement of viral transduction indicate that the total charge plays a secondary role in augmentating the infection. The simultaneous addition of oppositely charged polymers with a resultant neutral net charge to virus stocks also enhances the transduction rate. (Landazuri and Le Doux 2004, Le Doux et al. 2001). It has been proposed that, even if the total charge is neutral, the acidic amino acids are still able to interact with the viral envelope, leading to the formation of high molecular weight complexes with viral particles (Zhang et al., 2014).

Surprisingly, the E4 multimerization domain itself (E4C), which possesses a neutral pI of 7.02 and just one positively charged amino acid, also increased lentiviral transduction. The E4C-mediated enhancement of the infection rate could only be partially inhibited by the addition of polyanions. Similarly, in case of SEVI and PAP85-120, polyanions had a strong but not completely suppressive effect on the augmentation of the infection rate (Arnold et al. 2012). Polyanion-mediated blocking of enhancers of viral infection depends on the concentration of the applied compounds. It is possible that E4C requires higher polyanion concentrations which, in turn, could nonspecifically interfere with infection, making the results difficult to interpret. Indeed, in HeLa cells, pre-treatment of E4C with heparin lead to a complete abrogation of the infection rate enhancement. However, at the same time heparin also decreased the infection in the absence of E4 to 0.7 fold (Julia Bulkescher, personal communication).

We reasoned whether the pI of an E4 variant could be used to predict the magnitude of the E4 effect on the infection rate. However, this does not seem to be the case. For example, E4d70 has a higher pI than E4dN but nevertheless has an activity almost four times lower. The difference between the two E4 variants lies mostly in the structures formed in solution (Table 5). By comparing all E4 variants, SEVI, E7 and L1, we propose that the E4-mediated enhancement of the infection rate may be linked to the ability of the protein to form larger complexes with a positive charge. Nevertheless,

it appears that the magnitude of the effect depends on the structure of the E4 multimers rather than merely on pI of the monomeric protein.

3.4.4 HIGH MOLECULAR WEIGHT MULTIMERS OF E4 CONTRIBUTE TO THE E4-MEDIATED AUGMENTATION OF INFECTION BY CAPTURING VIRAL PARTICLES AND ENHANCING THEIR SEDIMENTATION VELOCITY

Transport of retroviruses to target cells, a major rate-limiting step of infection, has a very poor efficiency (Chuck et al. 1996). We observed that high molecular weight E4 multimers could be pelleted and, when resuspended, enhanced lentiviral infection rate. Smaller multimers (E4dNdC < 100 kDa) have a very weak effect. Moreover, when E4 multimers were incubated with lentivirus, they strongly bound to the viral particles, leading to sedimentation of E4-virion complexes. It has been established that E4dN structures can pull-down bound virions. This strongly enhances sedimentation velocity of viruses. A similar mechanism is proposed for virus-polycation aggregation and co-precipitation (Davis et al. 2004, Landazuri and Le Doux 2004, Le Doux et al. 2001). Polymers appear to form high molecular weight complexes with virus particles, mediating their flocculation via an increase in the effective particle diameter. This promotes retrovirus sedimentation and transport to cells that conventionally proceed by diffusion, a slow process during which viruses decay and lose their bioactivity (Davis et al. 2004, Landazuri and Le Doux 2004, Le Doux et al. 2001). Accordingly, the E4 mutant carrying no positively charged amino acids was unable to pull down virus, indicating again that both the positive charge and the formation of high molecular weight structures are required for the enhancement of the infection rate.

Based on the results presented here, a mechanistic model for the E4-mediated enhancement of the infection rate, consisting of 4 steps, can be proposed (Fig. 46). First, E4 interacts with the negatively charged viral envelope, leading to the formation of E4-virus complexes. Next, because of their relatively high molecular weight, E4-virus complexes co-sediment onto cells (Fig. 46A). Cells have a negative charge due to the composition of their lipid membrane (Devaux 1991, Li et al. 2014, Op den Kamp 1979, Yeung et al. 2008) and, in epithelial cells, the presence of a glycocalyx. Glycocalyx is a negatively charged layer on the cell surface several hundred nanometers thick, mostly composed of sulfated proteoglycans, hyaluronan, glycoproteins, and plasma protein. It is also found in the cervical epithelium (Chavez and Anderson 1985, Constantinescu et al. 2003, Pries et al. 2000, Swaminathan Iyer et al. 2012). During the sexual transmission of HIV-1, the shielding of negative charge from the glycocalyx is possibly one of the most important transmission-limiting steps.

In the third step, the electrostatic attraction occurs between E4 assemblies and the negatively charged cellular membrane. In the absence of E4, electrostatic repulsion between virions and cells discourages binding (Fig. 46B). Finally, E4 shields negative charges on the cell surface, facilitating virus absorption and receptor-mediated entry (Fig. 46C).

Anionic compounds inhibit this process by sequestering E4, preventing aggregation with the virus and charge shielding (Fig. 46D). Studies suggest that the apparent low frequency of ‘‘infectious’’ HIV-1 virions is caused by a very poor efficiency of virus-cell interactions (Thomas et al., 2007). The presence of E4 can help overcome this early ‘‘bottleneck’’ for infection, by supporting HIV-1 attachment to genital surfaces.

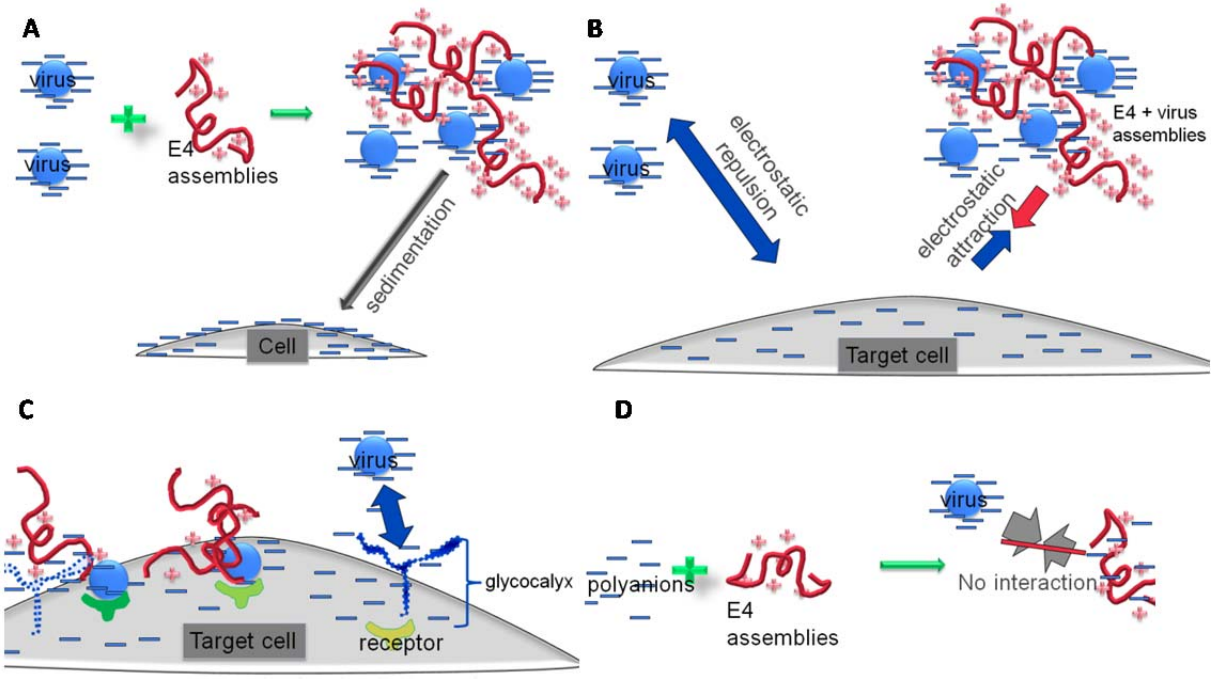

Figure 46: Schematic model for the E4-mediated enhancement of the infection rate.
(A) Positively charged E4 assemblies bind to negatively charged enveloped viruses. E4-virus complexes sediment onto cells. **(B)** The presence of positively charged domains in E4 leads to electrostatic attraction between E4-virus assemblies and the cell surface. **(C)** E4 shields the negative charge of the cell surface and the glycocalyx, allowing interactions of the virus with the receptor. **(D)** Polyanions block the E4-mediated effect by neutralizing the positive charge of E4 assemblies.

3.5 CONSEQUENCE OF E4 TAKE UP BY CELLS

We observed that E4 was very efficiently taken up by cells, leading to protein accumulation in form of vacuolar-like structures. This process was surprisingly fast, within the first 2 h, implying that E4 and the virus enter the cells at the same time. We could not determine whether E4 and virus enter the cell together or if these two events occurs independent of each other.

Frequently, large E4 deposits surrounded by an actin cage were observed. Actin filaments are known to play an important role in endosomal and lysosomal trafficking (Taunton et al. 2000, van Deurs et al. 1995). Therefore, we suggest that positively charged E4 is taken up by cells but, because of its size and high abundance, cannot be degraded by the lysosome and is instead deposited in aggresomes. This form of storage was previously observed for some amyloids and other misfolded proteins (Dehvari et al. 2012, Tyedmers et al. 2010, Viswanathan et al. 2011). Compared to E4, very low amounts of E7 and L1 were detected in cells upon addition to the cell culture medium. It is possible that other proteins are not internalized as efficiently as E4. Alternatively, this could be due to the inability of E7 and L1 to form high molecular weight structures and aggregates. In this case they would likely be more efficiently degraded by the lysosome system.

Endocytosis of amyloids by cells occurs both *in vivo* and *in vitro*. It has been demonstrated that Alzheimer amyloidogenic peptides can be taken up from the extracellular space and stored in the lysosomal compartment of the cells. Furthermore, $A\beta_{40}$ is internalized to some extent by neurons via

passive diffusion (Hu et al. 2009, Kandimalla et al. 2009). This makes us speculate that E4 amyloids found *in vivo* in HPV-infected cervical epithelium, smaller multimers and monomeric full-length proteins can be internalized by adjacent cells. Whether internalization of E4-virus complexes aids lentiviral transmission still needs to be established. Lentiviruses require specific receptors and co-receptors for entry (Berger et al. 1999, Clapham and McKnight 2002, Overbaugh et al. 2001) and, in the case of SEVI, $A\beta_{40}$ and $A\beta_{42}$ the presence of fibrils does not bypass the requirement for the specific HIV-1 receptors (Munch et al. 2007, Wojtowicz et al. 2002). Moreover, E4 appears to enhance the infection even before entry of the virus into cells (Prof. Oliver Keppler, personal communication). Hence, it is rather possible that, in case of lentiviruses, E4 take up and viral entry are unrelated and just occur in parallel.

We observed that E4 also enhances the infection rate of adenoviruses (Prof. Oliver Keppler, personal communication). This was surprising, as adenoviruses are non-enveloped viruses (Rux et al. 2003, Nemerow et al. 2009). Adenoviruses can enter cells via receptor-mediated endocytosis (Meier and Greber 2004, Li et al. 1998a, Li et al. 1998b). Thus it is possible that, in case of adenovirus infection, virions might be endocytosed together with E4 protein aggregates, entering cells in form of large infectious complexes. In agreement, it was shown that some charged polymers can augment adenovirus entry into cells both *in vivo* and *in vitro* (Dodds et al. 1999, Fasbender et al. 1997).

3.6 INDIRECT CROSSTALK BETWEEN HPV AND HIV-1

Indirect interactions between HPV and HIV-1 have been previously proposed. They are mostly based on possible alternations of the HIV-1 infection site by the presence of HPV (Herfs et al. 2011, Syrjanen 2011).

One of the most widely discussed indirect interaction suggests the recruitment and activation of HIV target cells, such as epithelial Langerhans cells and T-lymphocytes by HPVs (Nicol et al. 2005). However, it is known that HPV mostly evades an efficient immune response (Deligeoroglou et al. 2013, Kobayashi et al. 2008). For example, expression of the HPV oncogenes leads to disturbances in Toll-like receptor signaling, which in turn impairs the antigen presentation by Langerhans cells and decreases activation of CD4+ cells activation (DeCarlo et al. 2012, Guess and McCance 2005). Moreover, HPV can directly and indirectly interfere with the migration and function of macrophages, natural killer cells and T-helper cells (Garcia-Iglesias et al. 2009, Hacke et al. 2010).

Another hypothesis suggests that HPV upregulates expression of pro-inflammatory cytokines (Clerici et al. 1997, Peghini et al. 2012), which could favor HIV replication (Herfs et al. 2011). Some reports show elevated cytokine levels in HPV-infected women (Scott et al. 2013). Nevertheless, it is suspected that persistent HPV infections result in silencing of cytokine the production by innate immune cells (Scott et al. 2013)Kanodia et al., 2007, Scott et al. 2013). Moreover, in undifferentiated keratinocytes, HPV16 and HPV18 strongly downregulate the expression of pro-inflammatory and chemotactic cytokines (Karim et al., 2007).

The studies discussed above indicate that during persistent HPV presence the virus infection site is rather depleted of immune cells and therefore unlikely to enhance the infection by HIV in this manner. Conversely, during acute HPV infection the virus is cleared by immune cells, the migration of

which may increase access of HIV-1 target cells (Scott et al. 2001). This scenario corresponds with epidemiological data where an acute, non-persisting HPV infection correlated with a higher risk of HIV acquisition (Averbach et al. 2010, Smith-McCune et al. 2010). Finally it is most likely that a disturbance of the epithelial integrity by HPV infections (discussed in 3.1) can also contribute to indirect interaction between HPV and HIV.

3.7 THE POSSIBLE ROLE OF E4 IN OTHER SEXUALLY TRANSMITTED INFECTIONS

We have observed that E4 is a very general enhancer of lentiviral infection. HPV16 E4 increased the infection rates not only of various strains of HIV-1 and HIV–2, but also of HSV-1 and HSV-2 (Prof. Oliver Keppler, personal communication). Combined with the results presented here from VSV-G-pseudotyped lentivirus as a general model for enveloped virus infection, it appears that E4 may augment the infection rate of a large group of sexually transmitted pathogens. These may include, in addition to HIV and HSV, hepatitis B virus (HBV) - a main agent for hepatitis B, and Molluscum contagiosum virus (MCV), which causes warts on the skin and mucous membranes. Both HBV and MCV are sexually transmitted enveloped viruses (Alter et al. 1986, Kingsley et al. 1990, Porter et al. 1989, Zichichi et al. 2012) .

We showed that E4 enhances the infection rate of enveloped viruses in a manner similar as previously reported for SEVI, $A\beta_{40,}$ and $A\beta_{42}$. The hypothesis that E4 may be a more general enhancer of STIs corroborates the results of Wojtowicz et al., (2002). They showed that Alzheimer amyloids enhance the infection rate of multiple HIV-1 isolates, HSV, and viruses pseudotyped with the envelope glycoproteins of VSV and amphotrophic Moloney leukemia virus (A-MuLV). The role of SEVI in enhancing the infection by different viruses has also been reported (Munch et al. 2007). In addition to a strong augmentation of HIV-1 infection, SEVI enhances the transduction of lentiviral and gammaretroviral vectors pseudotyped with VSV-G, Gibbon ape leukemia virus (GALV), RD-114 - a retrovirus isolated in 1971 from a human tumor cell line and foamy virus envelopes (Wurm et al. 2010). Furthermore, SEVI elevates the infection rate of xenotropic murine leukemia virus-related virus (XMRV, Hong et al. 2009) and human cytomegalovirus (HCMV, Tang et al. 2013).

The effect of amyloid fibrils may possibly not be limited to viral transmission. Bacterial vaginosis is a synergic polymicrobal syndrome caused by a large group of pathogens including *Gardnerella vaginalis*, *Mobiluncus, Bacteroides*, and *Mycoplasma* and *Candida albicans* (Fredricks et al. 2005). The development of a bacterial infection in the reproductive tract requires the formation of biofilms, which is accelerated by the presence of adhesion surfaces and molecules (Chandra et al. 2001, Swidsinski et al. 2005, Swidsinski et al. 2010). Bacterial lipopolysaccharides are known to have a strong negative charge at physiological pH levels and bacterial cells therefore possess a pI between 2 and 5 (Harden and Harris 1953, Rijnaarts et al. 1995). This makes bacteria good candidates for interactions with positively charged high molecular weight multimers. Indeed, SEVI has been shown to interact with Gram-negative (*Escherichia coli, Neisseria gonorrhoeae*) and Gram-positive (*Staphylococcus aureus*) bacteria (Easterhoff et al. 2013). Amyloid fibrils bind to bacteria and form sedimentable aggregates although, in this case, SEVI-bacteria assemblies have been observed to enhance the immune response and infection clearance (Easterhoff et al. 2013). The ability of charged fibrils to enhance infection with mycoplasma, sexually transmitted bacteria lacking a cell wall (Jensen

2004), can be even more prominent. Using liposomes as a model, $A\beta_{40}$ and $A\beta_{42}$ amyloid fibrils were shown to stimulate their association with cells (Wojtowicz et al. 2002).
The function of the HPV E4 protein in the enhancement of viral and bacterial sexually transmitted diseases cannot be underestimated. Our study implies that HPV E4 may be an important cofactor in the acquisition of many sexually transmitted pathogens. Further work is required to establish whether E4 from cutaneous HPV types has a similar potential to influence infection. If so, the list of pathogens for which HPV infection is an important cofactor would further expand significantly.

3.8 PERSPECTIVES

HIV treatment still remains non-curative and only delays progression of the disease than attain full recovery (Ebrahim and Mazanderani 2013, Passaes and Saez-Cirion 2014). Development of a preventive vaccine has been unsuccessful so far (Fauci et al. 2008). For these reasons, all cofactors that enhance HIV transmission urgently need to be studied. Knowledge of the molecular mechanism underlying the higher infection rates by HIV and other pathogens in HPV-positive individuals is a first step for new preventive treatments and novel prophylactic approaches.

Relevantly, a modeling study has predicted that more than half of the HIV sexual transmissions can be attributed to a much greater susceptibility of individuals infected with anogenital pathogens. There are reports proposing treatment of curable STIs as a feasible way to control HIV epidemics (Steen et al. 2009, White et al. 2008). It has already been suggested that the HPV vaccine can strongly contribute to HIV prevention by decreasing HPV prevalence (Lissouba et al. 2013, Rositch et al. 2013, van der Loeff et al. 2011). Nevertheless, HPV vaccination currently protects only from two HR-HPV types, HPV16 and HPV18, or four types, HPV16, HPV18 and two additional LR-HPV types 6 and 11 with some cross-protectivity to other HPV types (Tovar et al. 2008). Although prospective studies predict that HPV vaccines will strongly decrease the occurrence of the HPV types used in the vaccine (Garnett et al. 2006), they will have limited impact on other HPV types. Here, it has been clearly shown that E4 from various, possibly all, HPV types has the potential to strongly augment the infection rate of lentivuses, including HIV. Therefore, current vaccines will not be sufficient to abolish the observed E4-mediated enhancement of HIV infection.

E4 has been described to form amyloids *in vivo.* Therefore, it is plausible that compounds which are able to disrupt the formation of E4 fibrils and oligomers, inhibit amyloid growth by targeting and blocking the ends of fibrils, and/or disturb the structure of pre-existing fibrils may prove useful in blocking the E4-mediated effect. These approaches are currently being developed for the treatment of amyloidosis such as Alzheimer's disease and in the future may prove useful in blocking the E4-mediated effect (Eisenberg and Jucker 2012, Hardy and Selkoe 2002).

An alternative method could be based on testing already existing compounds for their potency in blocking E4. Characterization of SEVI and SEMs as strong enhancers of HIV-1 infection led to a concentrated focus on developing compounds that could interfere with amyloid-mediated effects. Inhibitors of an amyloid-mediated enhancement of infection have been designed. Many of them are derived from the amyloid imaging agent ThT. They are small molecular compounds that attach to the generic cross-β-sheet structure of amyloids, subsequently sterically inhibiting fibril interactions with viral particles. For example, BTA-EG6, a hexaethylene glycol derivate of ThT, strongly binds along the

amyloid fibril axis, reducing semen-mediated and specific SEVI-mediated enhancement of the HIV-1 infection rate in a dose-dependent manner (Arnold et al. 2012, Olsen et al. 2010). This approach could be applied to block E4, as this protein also binds to ThT.

Aside from ThT-based inhibitors, other compounds have been shown to strongly decrease the amyloid-mediated enhancement of lentivirus infection. These include TFmix gel (Yang et al. 2012), the theaflavins TF1, TF2a, TF2b, and TF3, extracted from black tea (Grelle et al. 2011), or zinc and copper ions, which affect SEVI fibrillation kinetics (Sheftic et al. 2012).

Given a relatively similar mechanism of action, we propose that substances blocking the SEVI-mediated enhancement of infection will have a similar effect on E4. This should allow decreasing the E4-mediated effect on HIV transmission. One of the possible approaches would be to use microbicides and virucides in combination with compounds that block E4. This inhibition of both, the virus and cofactors present in host mucosa, could in theory be a highly effective targeted strategy in preventing HIV transmission.

In addition, the high magnitude of the E4-mediated enhancement of enveloped viral infection rate may have a completely alternative usage. Retrovirus-mediated gene transfer is one of the best-known and most routinely used techniques for mammalian cells transduction (Miller and Rosman 1989). Moreover, retroviral vectors have also been developed for the treatment of cancer and genetic diseases (Drumm et al. 1990, Roth et al. 1996). The infection rate of target cells is often the limiting step for virus-based gene therapy (Kotani et al. 1994). We suggest that the effect described here will be useful in enhancing the efficiency of retrovirus-mediated gene delivery. This approach has several advantages over existing ones. First, E4 had a stronger effect on the enhancement of infection than the commonly used polybrene. Secondly, E4 can be highly expressed and purified *in vitro*. Lastly, most people come into contact with E4 at some point during their life without any known adverse effects. The high potency of E4 in enhancing enveloped virus infection and its relatively low cytotoxicity makes it a valid candidate for research or as a therapeutic enhancer of virus-vector infection rate.

Finally, the observed co-sedimentation of E4 and virus particles could be exploited for virus stock preparations. Currently, the most commonly used techniques to concentrate and purify viral vectors include ultracentrifugation and ultrafiltration. Those methods have significant drawbacks, including low throughput and long procedures, resulting in the inactivation of virus particles (Burns et al. 1993, Paul et al. 1993). Formation of an E4-retrovirus complex may be used for rapid, highly efficient concentration of viral vectors. Pelleted particles can be resuspended in the medium of choice, removing undesired impurities originating from virus preparation. This E4-based approach can be easily scaled-up, producing a virus stock that is not only concentrated and purified but also with enhanced transduction properties.

3.8 OUTLOOK

The work presented here showed for the first time that HPV E4 has a potent effect on increasing infection with lentiviruses, including HIV. The mechanism for E4-mediated enhancement of lentiviral infection rates was investigated. We conclude that both charge and the formation of high molecular weight multimers are necessary prerequisites for this effect. However, several open questions remain to be answered.

First, further work is required to assess the level of E4 expression in anogenital tracts of HPV-infected individuals. Moreover, the amount of E4 release on the surface of mucosa should be analyzed, including the prevalence of calpain-cleaved E4. Contrary to previous work (Khan et al. 2011, McIntosh et al. 2008), we did not observe mature amyloid structure formation in any of the E4 variants, while pre-filaments and pre-fibrils dominated. Therefore, the presence or absence of amyloid fibrils *in vivo* should be investigated.

Secondly, the E4 effect on other sexually transmitted infections should be further investigated. As discussed above, the mechanism of E4 function makes it a potential enhancer of a large group of different pathogens, including viruses and possibly bacteria.

Thirdly, in the present study, we did not obtain evidence that the formation of amyloid fibrils is essential for E4-mediated enhancement of lentiviral infection. On one hand, E4 mutants with a deletion of the multimerization domain were still able to enhance the infection rate and L1, which forms only pentamers, also increased infection. On the other hand, E4dN displayed the strongest effect on infection, four times higher than E4dC on average. Further analysis of the E4 structure/function relation is an important issue for future research.

Fourthly, the similarities between the mechanisms of action of E4 and SEVI suggest the possibility that both proteins could be blocked in a similar way. Further studies should therefore focus on testing agents known to block SEVI in order to evaluate their influence on E4. This may prove to be an important step in interfering with E4, blocking the E4-mediated increase of the HIV infection rate, and stherby contributing to the control of the HIV pandemic.

CHAPTER 4

MATERIALS AND METHODS

4.1 REAGENTS AND PEPTIDES

REAGENTS

Molecular biology grade reagents were used where possible. Otherwise, the purest available materials were chosen. All standard reagents were obtained from the following companies: AppliChem (Darmstadt, Germany), Applied Biosystems (Carlsbad, CA, USA), Bio-Rad (Munich, Germany), BD Biosciences (Heidelberg, Germany), Braun AG (Melsungen, Germany), Carl Roth (Karlsruhe, Germany), Cell Signaling Technology (Danvers, USA), Clontech Laboratories (Mountain View, USA), Epicentre (Illumina, Madison, USA), Eurofins MWG (Ebersberg, Germany), Fermentas (St. Leon-Roth, Germany), GE Healthcare (Buckinghamshire, UK), GERBU Biotechnik GmbH (Heidelberg, Germany), Gibco BRL (Eggenstein, Germany), Invitrogen (Carlsbad, CA, USA), Merck (Darmstadt, Germany), Millipore (Bedford, MA, USA), New England Biolabs (Frankfurt, Germany), PEQLAB Biotechnologie GmbH (Erlangen, Germany), Promega (Madison, WI, USA), Qiagen (Hagen, Germany), Roche Diagnostics (Mannheim, Germany), Santa Cruz (Santa Cruz, CA, USA), Sigma-Aldrich (Munich, Germany), Thermo Fisher Scientific (Lafayette, CO, USA).

MEDIA, ANTIBIOTICS AND GENERAL SOLUTIONS

All solutions and media used for work with bacteria and for protein purification/preparation were prepared with water for injection purposes (B. Braun, Melsungen, Germany) or double distilled water (ddH_2O). The solutions were either autoclaved for 20 min at 121°C or sterilized by filtration through a 0.22 µm filter (MILLIPORE, Billerica, MA, USA). The pH was adjusted using a 761 Calimatic pH meter (Knick, Berlin, Germany). Culture agar plates and media were stored at 4°C. All solutions, if not indicated otherwise, were kept at room temperature (RT).

POLYPEPTIDES

The SEVI peptide sequence (GIHKQKEKSRLQGGVLVNEILNHMKRATQIPSYKKLIMY) was synthesized by Celtek Peptides (Franklin, USA).

The amyloid β protein fragment 1-40 (DAEFRHDSGYEVHHQKLVFFAEDVGSNKGAIIGLMVGGVV) was purchased from Sigma-Aldrich (Munich, Germany).

The HPV16 E4 fragment 66 - 92 (QWTVLQSSLHLTAHTKDGLTVIVTLHP) and the corresponding alanine mutant (QWTVLQSSLHLTAHTADGLTVIVTLHP) were synthesized by Peptide Specialty Laboratories GmbH (Heidelberg, Germany).

4.2 MOLECULAR BIOLOGY TECHNIQUES

4.2.1 TRANSFORMATION OF BACTERIA

ESCHERICHIA COLI STRAINS

Plasmid DNA propagation and cloning were performed using the *recA E. coli* TG2 strain *Δ(lac-pro) thi supE* [Res$^-$ Mod$^-$ (k)] F'(*traD36, proA$^+$B$^+$ lacI^{q}ZΔM15* (Benen et al. 1989, Gibson 1984).

Protein overexpression was performed in *E. coli* M15 *nal^s str^s rif^s thi$^-$ lac$^-$ ara$^+$ gal$^+$ mtl$^-$ f recA$^+$ uvr$^+$ lon$^+$* (Beckwith 1964, Villarejo and Zabin 1974). Protein expression was driven by a *lac* promoter and induced by isopropyl-β-D-thiogalactopyranoside (IPTG).

CULTIVATION AND CONSERVATION OF *E. COLI* STRAINS

E. coli were cultured at 37°C in lysogeny broth (LB) (Sambrook and Russell 2001). Bacteria were grown either in liquid medium on a shaking platform or on agar plates containing 1.5% Bacto agar. For long term storage of transformed *E. coli* strains, 5 ml overnight bacteria cultures in LB medium with appropriate antibiotics were mixed 1:1 (v/v) with glycerol, then were aliquoted and frozen at −80°C.

LB medium

Bacto tryptone	1%
yeast extract	0.5%
NaCl	170 mM
pH	7.0

CHEMICALLY COMPETENT BACTERIA

Chemically competent *E. coli* were prepared using magnesium-enriched transformation media. Bacterial strains were grown in liquid LB medium until they reached an OD_{600} of 0.3 - 0.4. Cells were pelleted by centrifugation (3 min, 10,000 x g, 4°C) and gently resuspended in transformation buffer. Aliquots were flash-frozen in liquid nitrogen and stored at -80°C until further use.

Transformation buffer

In LB:	
polyethylene glycol 8000	10%
DMSO	5%
$MgCl_2$	50 mM
glycerol	15%
pH	6.5

TRANSFORMATION OF BACTERIA WITH PLASMID DNA

Competent bacteria were transformed using the heat shock transformation procedure as previously described (Hanahan 1983). Appropriate *E. coli* strains (100 µl of competent bacteria) were thawed on

ice and mixed with 20 - 100 ng plasmid DNA. Cells were further incubated on ice for 45 - 90 min. Heat shock was performed at 42°C for 45 sec, followed by 1 min incubation on ice. 1 ml LB medium without antibiotics was added and bacteria were shaken for 90 min at 37°C. Transformed bacteria were subsequently plated on LB agar plates or cultured in 50 ml liquid LB medium supplemented with the appropriate antibiotic(s) for selection.

4.2.2 DNA PREPARATION

PREPARATION OF PLASMID DNA

Transformed bacteria were shaken overnight at 37°C in LB medium. Smaller amounts of plasmid DNA were purified from *E. coli* TG2 using the Plasmid Miniprep or Midiprep Kits (Qiagen, Hilden, Germany) according to the manufacturer's protocols.

PREPARATION OF PLASMID DNA BY ALKALINE LYSIS WITH SDS

Large-scale preparations of closed circular plasmid DNA (ccDNA) were obtained using the maxi preparation protocol followed by purification via equilibrium centrifugation in a continuous cesium chloride (CsCl)/ethidium bromide gradient (Sambrook and Russell, 2001). In specific, a pellet from a 200 ml overnight bacterial culture was resuspended in solution I and lysed with freshly prepared solution II. Solution III was added to neutralize the alkaline pH. Samples were centrifuged (5 min, 27,000 × g, 4°C) to pellet genomic DNA and coagulated protein. After centrifugation, plasmid DNA was precipitated by adding ethanol at a final concentration of 70%, followed by centrifugation (10 min, 15,000 x g, 4°C). The pellet was resuspended in 1x TE buffer (1 M Tris, 0.5 M EDTA, pH 8.0) and supplemented with 100 µl ethidium bromide solution (10 mg/ml). The DNA was transferred to a PA Ultracrimp tube (Sorvall, Asheville, NC USA). Next the tube was filled with CsCl solution and centrifuged in an OTD75B Sorvall Ultracentrifuge (Sorvall, Asheville, NC USA) at 220,000 × g for 16 h at RT. The lowest red-colored band containing the ccDNA was harvested. To remove ethidium bromide, repeated extractions with water-saturated 1-butanol were performed. Plasmid DNA in the aqueous phase was precipitated with ethanol that was added to a final concentration of 70%, followed by centrifugation (10 min, 15,000 x g, 4°C). Purified DNA was resuspended in TE buffer and stored at -20°C.

Solution I		**Solution II**		**Solution III**		**CsCl solution**	
glucose	50 mM	SDS	1%	potassium acetate	3 M	bromide ethidium	10 mg
Tris	25 mM	NaOH	0.2 M	acetic acid	11.5%	TE	41ml
EDTA	10 mM					CsCl	44 g
pH	7.6						

4.2.3 POLYMERASE CHAIN REACTION (PCR)

DNA was amplified using the polymerase chain reaction (PCR). E4 sequences were amplified from the plasmid pGEX16E4tag, which contains the sequence for the full-length E1^E4 HPV16 protein. Reaction conditions and components are summarized in Table 6. The annealing temperature was calculated and adjusted for each primer pair. The elongation time required for every predicted

amplification product was calculated based on a DNA polymerization rate of 1000 bp/min. Primers used for the generation of all constructs are listed in Table 7.

Table 6: PCR reaction conditions and components.

Components	
DNA template	100 ng
10x Pfu buffer	10 µl
10 mM dNTPs	2 µl
Forward primer	25 pM
Reverse primer	25 pM
Pfu polymerase	2.5 U
ddH_2O	to total volume of 100 µl

	Temperature	Time	Number of cycles
Initial denaturation	94°C	3 min	1
Annealing	Prime-specyfic	30 sec	30
Elongation	72°C	30 sec	
Denaturation	94°C	30 sec	
Final annealing	58°C	30 sec	1
Final elongation	72°C	5 min	1

Table 7: Primer pairs for the cloning of E4 variants.

Primer Name	Sequence (5'-3')	Restriction enzyme
E4WT -for	AGAGGATCCATGGCTGATCCTGCAGCAG	BamHI
E4WT-rev	ATGCAAGCTTCTAGAATTCTATGGGTGTAGTGTTACTATTACAG	HindIII
E4dN(d2-17) -for	AGAGGATCCATGAGCACTTGGCCAACCACCC	BamHI
E4dN(d2-17)-rev	AGTCAAGCTTCTATTATGGGTGTAGTGTTACTATTACA	HindIII
E4dN'(d2-5) -for	AGAGGATCCATGGCAGCAACGAAG	BamHI
E4dN'(d2-5)-rev	AGTCAAGCTTTTATGGGTGTAGTGTTACTATTACA	HindIII
E4dC(d87-92) -for	AGAGGATCCATGGCTGATCCTGCAGCAG	BamHI
E4dC(d87-92) -rev	ATGCAAGCTTCTATACGAATTCTAAGTTAATCCGTCCTTTGTGTGA	HindIII
E4dC'(d86-92) -for	AGAGGATCCATGGCTGATCCTGCAGCAG	BamHI
E4dC'(d86-92) -rev	ATGCAAGCTTCTAGAATTCTAAGTTAATCCGTCCTTTGTGTGA	HindIII
E4dNdC (d2-17d87-92)-for	AGAGGATCCATGAGCACTTGGCCAACCACCC	BamHI
E4dNdC (d2-17d87-92)-rev	ATGCAAGCTTCTATACGAATTCTAAGTTAATCCGTCCTTTGTGTGA	HindIII
E4d70(d70-92) -for	AGAGGATCCATGGCTGATCCTGCAGCAG	BamHI
E4d70(d70-92)-rev	AGTCAAGCTTTTAGAGCACTGTCCACTGAGTC	HindIII
E4d36(d36-41) –for internal	AGAGGATCCATGGCTGATCCTGCAGCAG	BamHI
E4d36(d36-41) –rev internal	AGTCAAGCTTTTATGGGTGTAGTGTTACTATTACA	HindIII
E4d36(d36-41) –for external	GCCTTGGGCACTATCCAGCGACCAAGATCAGA	-
E4d36(d36-41) –rev external	GTCGCTGGATAGTGCCCAAGGCGACGGCTT	-

Restriction site is underlined.

4.2.4 ENZYMATIC MODIFICATION OF DNA

ETHANOL PRECIPITATION

DNA was isolated using ethanol precipitation. DNA in solution was mixed 1:2 (v/v) with 100% ethanol. NaCl was added to a final concentration of 200 µM. Samples were incubated for 10 min at -70°C and then centrifuged for 30 min at 15,000 × g at 4°C. The pellet was washed with 70% ethanol, centrifuged for 5 min at 15,000 × g, dried and resuspended in TE buffer.

DNA CONCENTRATION MEASUREMENT

DNA concentrations were determined by measuring absorbance at 260 nm using a NanoDrop ND-1000 (Thermo Fisher Scientific, Wilmington, DE, USA).

CLEAVAGE OF DOUBLE-STRANDED DNA WITH RESTRICTION ENDONUCLEASES

Restriction endonucleases were purchased from Fermentas or New England Biolabs and used according to the manufacturer's guidelines. 5 - 10 µg or 500 ng DNA were used for preparative or analytical digestion, respectively. Digestion reaction conditions are summarized in Table 8. In case of restriction enzyme buffer incompatibility, DNA digestion was performed in successive cleavage reaction steps.

Table 8: Components and conditions for cleavage of dsDNA with restriction endonucleases.

dsDNA cleavage	
Plasmid DNA	0.5-10 µg
10x reaction buffer	2 µl
10x BSA	2 µl
Restriction enzyme	1 U/1 µg DNA
H_2O	To a total volume of 20 µl
Temperature	37°C
Time	1-1.5 h

DEPHOSPHORYLATION OF 5' ENDS OF DNA

To avoid recirculation of linearized plasmid vector after digestion with restriction enzymes, the 5'-terminus of digested DNA was dephosphorylated using calf intestine alkaline phosphatase (CIP) (New England Biolabs, Frankfurt, Germany). Components and conditions of the dephosphorylation reaction are described in Table 9.

Table 9: Components and conditions of the dephosphorylation reaction.

DNA dephosphorylation	
plasmid DNA	0.5-10 µg
10x reaction buffer	5 µl
10x BSA	0.5 µl
CIP	30 U/100 ng DNA
TE buffer	To a total volume of 50 µl
Temperature	37°C
Time	1-1.5 h

DNA LIGATION

Digested and purified (see chapter 4.2.5) inserts were cloned into linearized (digested, dephosphorylated and purified) vectors. For the ligation of cohesive DNA ends, T4 DNA ligase (Fermentas, St. Leon-Roth, Germany) was used. Reaction components are summarized in Table 10. Ligation was performed for 2 h at 21°C or overnight at 12°C in a water bath. T4 DNA ligase was inactivated by incubation of the reaction mixture at 65°C for 10 min.

Table 10: DNA ligation reaction conditions and components

DNA ligation	
Vector	50 - 100 ng
Insert	5-10 x molar excess of vector
10x reaction buffer	2 µl
T4 DNA ligase	10 U

4.2.5 DNA AGAROSE GEL ELECTROPHORESIS

Size separation of DNA fragments by horizontal gel electrophoresis was performed for analytical purposes and purification. DNA mixed with 6x DNA loading dye was loaded onto a 1% - 3% agarose gel supplemented with 0.5 µg/ml of peqGREEN DNA/RNA dye (Peqlab, Erlangen, Germany). Samples were run in electrophoresis chambers (Peqlab, Erlangen, Germany) filled with TAE electrophoresis buffer. A gel documentation system (Intas Science Imaging Instruments, Göttingen, Germany) and UV light were used to visualize separated DNA bands.

6x DNA loading dye	
bromophenol blue	30% (w/v)
glycerol	0.25% (w/v)

TAE electrophoresis buffer	
Tris	40 mM
sodium acetate	5 mM
EDTA	1 mM
pH	7.8

DNA FRAGMENT PURIFICATION

Fragments of appropriate size, as determined by electrophoresis, were excised from an agarose gel and eluted using the QIAquick Gel Extraction Kit (Qiagen, Hilden, Germany), following the manufacturer's protocol.

4.3 PLASMIDS AND CLONING STRATEGY

4.3.1 BACTERIAL EXPRESSION VECTORS

pQcH6 and pQE_8 were used for overexpression of hexahistidine tag (6xHis)-tagged fusion proteins in bacteria. Target sequences were inserted into a multiple cloning site (MCS) of vectors using BamHI and HindIII.

E4WT, E4dN' and E4dN variants were cloned into pQcH6. In this vector expression of the target sequence is regulated by an IPTG-inducible *lac* promoter. Proteins are expressed with a C-terminal 6xHis-tag. The vector constitutively expresses β-lactamase, which confers ampicillin resistance. This plasmid was a kind gift from Prof. Hanswalter Zentgraf.

All E4 constructs, E7 and L1 were cloned into pQE_8. In this vector expression of the target sequence is regulated by an IPTG-inducible lac promoter. Proteins are expressed with an N-terminal 6xHis-tag. The vector constitutively expresses β-lactamase, which confers ampicillin resistance. This vector was purchased from Qiagen.

4.3.2 CLONING STRATEGY

Two different cloning strategies were used. Inserts were either (I) amplified using PCR (see 4.2.3) or (II) subcloned by excision via restriction digestion and ligated into the appropriate target vector by cohesive ends (see 4.2.4).

In the first approach, the insert was amplified by PCR using primers containing the appropriate restriction sites. Both, vector and inserts, were digested with restriction endonucleases to yield cohesive ends. The 5'-ends of the vector were dephosphorylated to prevent recirculation. After gel electrophoresis and purification of DNA, the insert and vector were ligated using T4 DNA ligase and transformed into *E. coli* (see 4.2.1).

In the second approach, the insert was cleaved from its parent plasmid with restriction endonucleases. All subsequent steps were performed as described above.

Transformed *E. coli* were grown on LB agar plates supplemented with the appropriate selection antibiotic(s). Several colonies were grown in liquid LB supplemented with antibiotics for analysis. Pasmid DNA was extracted using the Qiagen MiniPrep kit and subsequent analysis was performed by restriction digest and sequencing.

4.3.3 SITE-DIRECTED MUTAGENESIS

The E4d36-41 construct was created using two-step PCR-based targeted mutagenesis. Briefly, the E4WT sequence was used as a template for two separate PCR reactions with either "E4d36-41 –forward internal" and "E4d36-41 –reverse external primers" or "E4d36-41 –forward external" and "E4d36-41 –reverse internal" primers (Table 11). PCR products were separated by agarose gel electrophoresis and extracted (see 4.2.5). The two PCR products were then mixed 1:1 (v/v) and used

as template for a second round of PCR using only the internal primers. The resulting product was ligated into the target vector by cohesive end ligation (see 4.3.2).

Table 11: Primer pairs for E4d36-41 cloning.

Primer Name	Sequence (5'-3')	Restriction site
E4d36-41 –for internal	AGAGGATCCATGGCTGATCCTGCAGCAG	BamHI
E4d36-41 –rev internal	AGTCAAGCTTTTATGGGTGTAGTGTTACTATTACA	HindIII
E4d36-41 –for external	GCCTTGGGCA^CTATCCAGCGACCAAGATCAGA	-
E4d36-41 –rev external	GTCGCTGGATAG^TGCCCAAGGCGACGGCTT	-

Restriction sites are underlined. ^ indicates a deletion.

4.3.4 CLONING CONTROL AND SEQUENCING

Verification of the successful cloning product was performed by restriction analysis. Digested fragments were separated using agarose gel electrophoresis and controlled for the correct vector and insert sizes. Construct sequences were confirmed by Sanger sequencing by Eurofins MWG (Ebersberg, Germany). Sequences were analyzed using the Basic Local Alignment Search Tool (BLAST, NCBI, USA).

4.4 RNA PREPARATION AND ANALYSIS

4.4.1 RNA EXTRACTION AND RT-PCR ANALYSIS

RNA EXTRACTION

RNA was extracted using the RNA MasterPure™ Complete RNA Purification Kit Epicentre (Illumina, Madison, USA) according to the manufacturer's guidelines.

REVERSE TRANSCRIPTION PCR (RT-PCR)

To generate complementary cDNA from a VSV-G-pseudotyped lentiviral RNA template, reverse transcription was performed using the ProtoScript® Taq RT-PCR Kit (New England Biolabs, Frankfurt, Germany). 10 - 1000 µg purified RNA was incubated with 100 pM of primer $dT_{23}VN$ and 10 nM of dNTP mix in a final volume of 16 µl for 5 min at 70°C. After cooling on ice, 2 µl 10X RT Buffer, 20 U murine RNase Inhibitor, 10 U M-MuLV reverse transcriptase and nuclease-free water were added to a final volume of 20 µl. Reverse transcription was performed for 1 h at 42°C. The enzyme was inactivated by heating of the reaction mixture to 80°C for 5 min. The resulting cDNA product was stored at –20°C until further use.

In the next step obtained cDNA was amplified. PCR components and conditions are described in Table 12.

Table 12: cDNA PCR components and conditions.

Components			
DNA template			5 µl of RT reaction product
Taq 2X Master Mix			12.5 µl
dNTP			20 nM
Forward primer 5'-ACTGGGTGCTCAGGTAGTG-3'			5 pM
Reverse primer 5'-GACTGGGTGCTCAGGTAGTG-3'			5 pM
ddH_2O			To total volume of 25 µl
Reaction conditions			
	Temperature	Time	Number of cycles
Initial denaturation	94°C	3 min	1
Annealing	58°C	30 sec	20
Elongation	68°C	30 sec	
Denaturation	94°C	30 sec	
Final annealing	58°C	30 sec	1
Final elongation	58°C	10 min	1

4.5 PROTEIN EXPRESSION

4.5.1 SELECTION OF CLONES WITH HIGH E4 EXPRESSION

E4 variants were expressed in *E. coli* M15 (see 4.3.2). Bacteria transformed with the appropriate constructs (see 4.2.1) were streaked on LB agar plates supplemented with appropriate antibiotics for selection and grown overnight at 37°C. 5 - 10 colonies were then picked from the plates, inoculated in 20 ml LB supplemented with the appropriate selection antibiotics and shaken at 37°C until an OD_{600} of 0.6 was reached. Protein expression was induced by adding IPTG at a final concentration of 1.2 mM. To evaluate protein expression, cells were incubated at 37°C and samples were collected every 30 min from 2 h to 4 h post-induction or after overnight culture. To estimate the expression level of the E4 variants, 30 µl of bacterial culture were mixed with 10 µl protein loading buffer. Samples were boiled for 5 min at 96°C and analyzed using SDS-PAGE and immunoblotting (see 4.7.2 and 4.7.3).

4.5.2 LARGE-SCALE PROTEIN EXPRESSION IN *E.COLI*

Bacterial colonies expressing high levels of E4 protein were inoculated in 50 ml LB with the appropriate antibiotic and grown overnight at 37°C. This starter culture was added to 1 l Terrific Broth (TB) supplemented with 100 ml of K_3PO_4 buffer and appropriate antibiotics. Bacteria were grown at 37°C until an OD_{600} of ~0.6 was reached. Protein expression was induced by adding IPTG to a final concentration of 1.2 mM. Proteins were expressed either for 3 h at 37°C or overnight at RT.

Terrific Broth	
peptone	1.2%
yeast extract	2.4%
glycerol	0.4%

K_3PO_4 buffer	
KH_2PO_4	0.17 M
K_2HPO4	0.72 M
pH	7.0

4.5.3 PROTEIN EXTRACTION FROM INCLUSION BODIES

To extract protein from *E. coli*, cells were centrifuged (30 min, 2,000 × g, 4°C) and resuspended in lysis buffer. Cells were lysed by stirring at 4°C overnight. Bacterial lysates were stored at -20°C until further use. Protein inclusion bodies were solubilized using a French pressure cell press (FP) (SMC, Stuttgarg, Germany). FP was cooled at 4°C overnight and kept on ice during all procedures to prevent protein denaturation. The press system was washed sequentially with 50 ml 20% ethanol, 75 ml 0.5 M NaOH, and 75 ml 10 mM HCl and equilibrated using lysis buffer. Cell lysate was passed through the press several times with a pressure reaching 1,000-1,500 bar until the solution cleared. Samples were centrifuged for 45 min at 17,000 × g at 4°C. Resulting supernatant containing the extracted protein was mixed 1:1 (v/v) with glycerol and stored at -20°C.

Lysis buffer

NaH_2PO_4	100 mM
Tris·Cl	10 mM
guanidine·HCl,	6 M
β-mercaptoethanol	70 µM
pH	8.0

4.5.4 PROTEIN PURIFICATION USING NICKEL AFFINITY CHROMATOGRAPHY

6xHis-tagged E4 protein variants were purified using nickel affinity chromatography. A XK16/20 column (GE Healthcare, Buckinghamshire, UK) was filled with 10 - 20 ml of Ni-NTA agarose beads (Qiagen, Hagen, Germany), washed with two column volumes (CV) of ddH_2O and left to sediment by gravity. A peristaltic pump (Pharmacia Fine Chemicals, Piscataway, USA) was used to control the correct flow rate in all subsequent steps. The resin was equilibrated with four CV of buffer A at a flow rate of 1 - 2 ml/min. Bacterial lysate was passed through the column at a flow rate of 0.5 ml/min. The amount of protein in elution fractions was controlled measuring the absorbance at 280 nm using an Econo UV Monitor cell reader (Bio-Rad, Berkeley, USA). The column was washed with buffers B, C and D until no proteins were detected. The E4 protein was eluted using buffer E until the A_{280} value of the eluate was similar to that of the wash buffer. 1 ml protein fractions were collected and 10 µl of 5 mM NaOH were added to each fraction to neutralize the low pH. The column was equilibrated with buffer F and washed with two CV of ddH_2O. Samples from the bacterial lysate and each purification step and fraction were analyzed for their protein content by SDS–PAGE and immunoblotting (see 4.7.2). Collected samples were stored in 8 M urea at -20°C until refolding.

A buffer		**B buffer**	**C buffer**	**D buffer**	**E buffer**
NaH_2PO_4	100 mM		NaH_2PO_4	100 mM	
Tris·Cl	10 mM		Tris·Cl	10 mM	
guanidine HCl	6 M		urea	8 M	
pH	8.0	pH 8.0	pH 6.3	pH 5.7	pH 4.2

F Buffer

Guanidine HCl	8 M
Acetic acid	0.2 M

The Ni-NTA resin was reused for purification of identical recombinant proteins after regeneration. The column was washed with an ethanol gradient (increasing 0-100% and then decreasing 100-0%) in steps of 25%, followed by ddH_2O at a flow rate of 1-2 ml/min for 20 min/step. Nickel was removed by washing with 100 mM EDTA. The resin was recharged using 6 - 10 CV 100 mM $NiSO_4$. For longer storage, the column was filled with 0.02% sodium azide and stored at 4°C.

4.5.5 PROTEIN PURIFICATION USING COBALT CHROMATOGRAPHY

Cobalt affinity chromatography was performed by filling a XK16/20 column (GE Healthcare, Buckinghamshire, UK) with HIS-Select Cobalt Affinity Gel (Sigma-Aldrich, Munich, Germany). The column was washed with two CV of ddH_2O and equilibrated with four CV of equilibration buffer. Samples were loaded onto the column at a flow rate of 2 – 10 CV/h. The column was washed with wash buffer at a flow rate of 5 - 15 CV/h until the A_{280} value of the eluate was similar to that of the wash buffer. The E4 protein was eluted from the column using elution buffer at a flow rate of 2 - 10 CV/h. 1 ml fractions were collected and stored in 8 M urea at -20°C until refolding.

Equilibration/Wash Buffer	
Sodium phosphate	0.1 M
Urea	8 M
pH	8.0

Elution Buffer	
Sodium phosphate	0.1 M
Urea	8M
Imidazole	250 mM
pH	8.0

4.5.6 PROTEIN REFOLDING

Protein concentrations were determined by measuring the absorbance at 280 nm using a NanoDrop ND-1000 (Thermo Fisher Scientific, Rockford, IL USA). Prior to refolding, purified E4 protein was concentrated using an ULTRAFREE Centrifugal Filter Device (Millipore, Bedford, MA, USA), following the manufacturer's guidelines. As a first step, the protein was diluted to a desired final concentration in refolding buffer, filtered through a 0.22 µm filter (MILIPORE, Billerica, MA, USA) and transferred to a dialysis bag (Thermo Fisher Scientific, Rockford, IL USA). Refolding in dialysis buffer was performed with agitation over three days at 4°C. During that time, the dialysis buffer was changed several times. Alternatively in the last step, E4 was dialyzed into PBS. Refolded protein was stored in 100 µl aliquots at -20°C.

Refolding Buffer	
NaCl	100 mM
phosphate	50 mM
2-mercaptoethanol or DTT	2 mM
EDTA	5 mM
pH	7.0

PBS	
NaCl	0.137 mM
KCl	2.7 mM
Na_2HPO_4	4.3 mM
KH_2PO_4	1.4 mM
pH	7.0

PROTEIN CONCENTRATION DETERMINATION

To determine the final concentration of the refolded E4 protein variants, 1 µl protein was mixed with 1 µl of serial dilutions of a BSA standard (Thermo Fisher Scientific, Rockford, IL USA) and visualized using SDS-PAGE and Instant Blue staining (see 4.7.2). The relative band intensity was determined

using BioID software from PEQLAB. Protein concentrations were interpolated from a BSA standard curve using Microsoft Excel.

ISOELECTRIC POINT PREDICTION

The isoelectric point of proteins was predicted *in silico* using Compute pI/Mw (www.expasy.org).

4.6 CELLULAR BIOLOGY TECHNIQUES

4.6.1 CELL LINES AND CELL CULTURE

Stocks of mammalian cell lines were stored in liquid nitrogen. To initiate a cell culture, frozen stocks were thawed in a 37°C water bath. Thawed cells were diluted in 10 ml of appropriate growth medium (Table 14) containing 10% FCS and centrifuged for 3 min at 800 × g. The pellet was resuspended in growth medium.
To freeze cells for longer storage, harvested cells were centrifuged for 3 min at 800 × g. Growth medium was removed and the pellet was resuspended in freezing medium. 1 ml aliquots were dispensed into sterile cryovials and stored at -80°C. For long-term storage, cryovials were transferred from -80°C to liquid nitrogen.

Freezing medium

Appropriate cell culture medium	70%
DMSO	10%
FCS	20%

Cells were cultured in cell culture flasks or dishes (Greiner Bio-One, Frickenhausen, Germany) at 37°C and 5% CO_2 atmosphere in appropriate culture medium supplemented with 10% heat inactivated (45 min, 60°C) fetal bovine serum (FCS) (PAA Laboratories, GE Healthcare, Buckinghamshire, UK), 100 U/ml penicillin, 100 µg/ml streptomycin, and 2 mM L-Glutamine (all three Sigma-Aldrich, Munich, Germany). Adherent cells were split at 1:5 to 1:10 ratios after reaching 80% - 90% confluency. Adherent cells were detached from the culture vessel by incubating the cells in trypsin-EDTA solution (Invitrogen, Carlsbad, CA, USA). Suspension cell lines were passaged every 3 - 4 days. Details of used cell lines are summarized in Table 13.

Table 13: Cell lines.

Cell line	Origin	Culture medium	Source
Cos7	Transformed African green monkey kidney fibroblasts	DMEM	ATCC CRL-1651
HeLa	Huma HPV18 positive cervix epithelial adenocarcinoma	DMEM	ATCC CCL-2
HeLaT	Derivative of HeLa stably expressing the large T antigen of Simian virus 40 (SV40)	DMEM	kind gift of Prof. Martin Müller
HEK293T	Derivative of HEK293 (human embryonic kidney) stably expressing the large T antigen of SV40	DMEM	ATCC CRL-11268
SupT1 CCR5	Human, Caucasian, pleural effusion T-cell lymphoma expressing HIV-1 coreceptor CCR5	RPMI	ATCC CRL-1942

ATCC catalogue numbers (American Type Cell Culture Collection, Rockville, MD USA) references are given.

4.6.2 CYTOTOXICITY ASSAY

Cytotoxicity was determined using WST-1 reagent (Roche Diagnostics, Mannheim, Germany). The WST-1 assay is based on the water soluble tetrazolium salt (WST-1), which is reduced to a dark yellow-colored formazan by cellular dehydrogenases. The amount of formazan produced is directly correlated to the cell number. $1.5x10^3$ cells/well were seeded in a 96-well plate to a final volume of 100 µl culture medium and cells were grown overnight at 37°C. The medium was exchanged and appropriate concentrations of the compounds to be tested were added. After 72 h of treatment, 10 µl WST-1 dye solution was added to each well and gently mixed. Plates were incubated for 15 – 30 min at 37°C. The medium was pipetted vigorously and absorbance was measured using a Multiskan™ GO Microplate Spectrophotometer (Thermo Fisher Scientific, Lafayette, CO, USA) at 420 - 480 nm with a reference wavelength of 600 nm. The percentage of viable cells was calculated dividing average absorbance of experimental results by average absorbance of the control.

4.6.3 TRANSFECTION OF DNA BY CALCIUM CO-PRECIPITATION

The calcium phosphate co-precipitation method by Chen and Okayama (1987) (Chen and Okayama 1987) was used to transiently transfect cells with plasmid DNA. The day before transfection, cells were seeded in 6 or 10 cm plates and incubated overnight until a confluency of 70 - 80% was reached. On the day of transfection, the culture medium was exchanged. The transfection mixture was freshly prepared prior to usage, incubated for 15 min at RT and then added slowly drop-wise to the cell culture. After 16 - 18 h incubation at 35°C in 3% CO_2, cells were washed twice and incubated in the appropriate medium at 37°C in 5% CO_2 until harvest.

Transfection mixture

	per 3 ml of medium
Plasmid DNA	6 µg
0.25 M $CaCl_2$	150 µl
2x BES buffer (25 mM BES (N,N-bis-(2-hydroxyethyl)-2-aminoethane sulfonic acid), 280 mM NaCl, 1.5 mM Na_2HPO_4, pH 6.95)	150 µl

4.6.4 GENERATION OF VSV-G-PSEUDOTYPED LENTIVIRAL VECTOR

To generate VSV-G-pseudotyped lentivirus stocks, HEK293T cells seeded in 10 cm plates were transfected using calcium phosphate co-precipitation (see 4.6.3) with plasmids described in Table 14. 72 h post-transfection, the supernatant was harvested. To concentrate the virus stocks, the supernatant was layered onto a 20% sucrose cushion in 1x PBS and centrifuged in a Sorvall Ultracentrifuge (Sorvall, Asheville, NC USA) at 40,000 × g for 2 h at 4°C. The pellet was resuspended in PBS and filtered through a 0.45 µm filter (MILLIPORE, Billerica, USA). Aliquots (1 - 2 ml) were stored at -80 °C.

Table 14: Plasmids used for the generation of lentiviral (VSV-G-pseudotyped) vectors.

Name	Description	per ml medium
pWPXL	transfer vector plasmid [EF1-alpha promoter-driven GFP expression]	1 µg
VSV – G	envelope plasmid	0.3 µg
ΔR8.91	packaging plasmid	0.6 µg
pADVANTAGE	enhancer of transient protein expression by increasing translation initiation	0.1 µg

DETERMINATION OF VSV-G-PSEUDOTYPED LENTIVIRUS STOCK INFECTION UNITS

To quantify the lentivirus stock infection titer, 0.7 x 10^5 HeLa cells per well were seeded in a 24-well plate. On the following day, cells were infected with 1:10 serial dilutions of the virus stock, beginning with 200 µl, (in duplicate) and incubated at 37°C in 5% CO_2. The medium was changed 16 - 18 h after infection. 72 h post infection, cells were trypsinized and analyzed by flow cytometry (see 4.8). The percentage of GFP positive cells was used to calculate the number of infection units as follows:

Number of infected cells = average % of infected cells * number of cells seeded/100 %

This result was extrapolated to obtain the number of infectious units (IU) per ml.

4.6.5 LENTIVIRAL TRANSDUCTION

VSV-G-pseudotyped lentiviral vectors were used for transduction of adherent or suspension cells.

In case of adherent cells, 0.7x10^5 HeLa cells per well were seeded in a 24-well plate in 450 µl of the appropriate medium. On the following day, 50 - 200 IU of VSV-G-pseudotyped lentivirus in the final volume of 50 µl were added to cells. Medium was changed after overnight incubation and cells were grown at 37°C in 5% CO_2 until further analysis.

For transduction of suspension cells, 2.5x10^5 SupT1 CCR5 cells per well were seeded in a U-bottom 96-well plate in 150 µl of appropriate medium and directly mixed with 50 - 200 IU of VSV-G-pseudotyped lentivirus in the final volume of 50 µl. Spin infection was performed by centrifuging the plate for 120 min at 800 x g. Medium was changed immediately after the spin infection and cells were grown at 37°C in 5% CO_2 until futher analysis.

Polybrene (Sigma-Aldrich, Munich, Germany) was used to enhance transduction efficiency in some experiments. Briefly, virus stock was mixed with polybrene before transduction at a final concentration of 8 µg/ml medium, added to cells and spread evenly. All further steps were performed as described above.

4.7 BIOCHEMICAL METHODS

4.7.1 PREPARATION OF PROTEIN SAMPLES FOR WESTERN BLOT ANALYSIS

The Bradford protein assay was used to measure the concentration of the protein sample. 1 µl protein extract was added to 1 ml of a Bradford working solution (1:5 (v/v) dilution of Bio-Rad Dye reagent concentrate (Bio-Rad, Munich, Germany), in ddH_2O). The solution was vortexed briefly and incubated for 2 min at RT. Absorbance was measured at 595 nm by spectrophotometry (GeneQuant, Munich, Germany) and the protein concentration was calculated using a BSA standard curve. After quantification of the protein concentration, appropriate amounts of 4x protein loading buffer and RIPA buffer were added to reach a final concentration of 4 µg/µl. Samples were boiled for 5 min at 96°C and stored at -80°C until further analysis.

Loading buffer (4x)

Tris-HCl pH 6.87	0.25 mM
SDS	8% SDS
glycerol	40%
β-mercaptoethanol	20%
bromophenol blue	0.008%

For non-reducing denaturing conditions, buffer without β-mercaptoethanol was used.
For non-reducing and non-denaturing conditions, buffer without β-mercaptoethanol and an appropriately lower (2- or 5- fold) SDS concentration was used.

4.7.2 SDS-PAGE

Modified sodium dodecyl sulfate (SDS) polyacrylamide gel electrophoresis (SDS-PAGE) was used to separate proteins according to their molecular weight. Gels with a stacking layer (5% acrylamide, 0.47 M Tris, pH 6.7) on top of a running gel (12.5% acrylamide, 3 M Tris, pH 8.9) were used (AUSUBEL, 2002). For low percentage SDS gels, all solutions and gels contained a respectively lower SDS concentration (2 or 5 times less). 10 µl protein solution and 3 µl of a broad band protein marker (peqGOLD Prestained Protein Marker IV, PEQLAB Biotechnologie GmbH, Erlangen, Germany) were loaded onto the gel and separated at 100 V in Tris-glycine running buffer supplemented with 0.5 ml of NuPAGE® Antioxidant (Thermo Fisher Scientific, Lafayette, CO, USA).

Tris-glycine running buffer

Tris	25 mM
Glycine	250 mM
SDS	0.1%
pH	8.6

4.7.3 WESTERN BLOT

Proteins separated by SDS-PAGE were transferred from the gels onto an Immobilon-P 0.45 µm PVDF (polyvinylidene fluoride) membrane (Millipore, Bedford, MA, USA) using semi-dry transfer. The membrane was activated in 100% methanol for 1 min. Whatman blotting paper, the membrane and

gels were equilibrated in Towbin transfer buffer for 10 min. A wet sandwich was assembled as follow: four Whatman paper, membrane, gel, four Whatman paper (from bottom (anode) to top (cathode)). Transfer was performed in the Trans-Blot® SD Semi-Dry Electrophoretic Transfer Cell (Bio-Rad) for 1 h at a voltage of 15 – 20 V.

For protein detection unspecific binding of antibodies was blocked by incubation of the membrane in PBS-T milk solution (PBS with 0.1% Tween-20 (v/v), 5% (w/v) non-fat dry milk powder, 1% (w/v) BSA) for 1.5 h. Membranes were incubated overnight with primary antibodies or specific serum (Table 15) at 4°C with mild shaking. To wash excess antibodies, the membranes were incubated three times (10 min each) in PBS-T milk solution and washed twice with PBS-T (10 min each). Membranes were incubated with the appropriate secondary antibodies for 1 h at RT. Before detection, the membrane was washed three times with PBS-T milk solution, twice with PBS-T and once in PBS (10 min each).

Towbin transfer buffer

Tris pH 8.3	2.5 mM
glycine	192 mM
methanol	20% (v/v)

Table 15: List of primary and secondary antibodies used for enzyme-linked immunodetection in Western blots.

Primary antibody	specification	source
α-11	Rabbit polyclonal #AB9234	Millipore
α-OC	Rabbit polyclonal #AB2286	Millipore
α-HPV16 E1/E4 (α-TVG 402)	Mouse monoclonal #sc-53324	Santa Cruz
α-His	Mouse monoclonal	Prof. Zentgraf (DKFZ, Heidelberg)
α-HA	Rat mAb Clone 3F10/12CA5, 1867423	Roche
α-E4	Rabbit polyclonal Or mouse monoclonal	Prof. Keppler (Uni Frankfurt)

Secondary antibody	specification	source
Goat α-mouse	HRP-conjugate	Promega
Goat α-rabit	HRP-conjugate	Promega

4.7.4 ENZYME-LINKED IMMUNODETECTION OF PROTEINS

Signals from horseradish peroxidase (HRP)-conjugated secondary antibodies were detected using enhanced chemiluminescence (ECL). ECL detection reagents 1 and 2 (GE Healthcare, Buckinghamshire, UK), were mixed at a ratio of 1:1 (v/v) and applied onto the membrane. After 1 min of incubation, light emission was detected with an image acquisition system (Vilber Lourmat, Eberhardzell, Germany). The relative intensity of bands was analyzed using BioID software (Vilber Lourmat).

4.7.5 COOMASSIE BRILLIANT BLUE STAINING

Polyacrylamide gels used for protein separation were washed in ddH_2O for 1 h at RT with agitation and stained with Instant Blue protein stain (Expedeon, Cambridgeshire, United Kingdom) for 3 h at RT

or overnight at 4°C. Gels were rinsed several times with ddH_2O until excess dye was removed. Images were documented in a gel documentation system (Intas Science Imaging Instruments, Göttingen, Germany) via white light illumination.

4.8 FLOW CYTOMETRY-BASED DETERMINATION OF CELL TRANSDUCTION

The percentage of virus-infected cells was determined based on GFP expression by flow cytometry 72 h post infection. Adherent cells were detached from culture plates using trypsin-EDTA solution. For suspension cells, the culture medium was aspirated. All subsequent steps were identical. Cells were centrifuged (3 min, 1,000 × g), washed twice with PBS, fixed with 2% paraformaldehyde (PFA) for 30 min at RT. Cells were then washed once with PBS, resuspended in PBS, filtered through an 85 µm SEFAR Nitex nylon mesh (Sefar, Heiden, Switzerland) and analyzed immediately. GFP fluorescence signal of 20,000 cells per sample was measured with a FACSCalibur Flow Cytometer (BD Biosciences, Heidelberg, Germany) using CellQuest Pro software (BD Biosciences). Apoptotic cells were excluded. FlowJo software (Tree Star, Ashland, OR) was used for quantification of GFP expressing cells. Samples were prepared as technical duplicates or triplicates.

4.9 FLUORESCENCE AND IMMUNOFLUORESCENCE MICROSCOPY

For analysis of cellular protein expression by fluorescence microscopy, two different approaches were used. Proteins were visualized either directly by expression of GFP or GFP-fusion proteins or indirectly by fluorophore-coupled antibody labeling. In both cases, cells grown on coverslips were washed with PBS, fixed for 30 min in 4% PFA and washed three times in PBS. Slides were incubated at RT in a wet incubation chamber. All subsequent steps were performed while avoiding exposure to light.

In the first approach, slides were incubated with 30 µl DAPI solution in PBS for 30 min at RT, washed five times in PBS and analyzed by microscopy. In the second approach, fixed coverslips were incubated with 35 µl of the primary antibody in milk solution (5% (w/v) milk in PBS) for 1 h, rinsed five times in PBS and washed twice for 10 min in PBS. 40 µl of the secondary antibody solution (antibody and DAPI in 5% milk in PBS) were added and incubated for 30 min. The primary antibodies used for microscopy are the same as those used for Western blot analysis (Table 15). Secondary antibodies used for immunofluorescence analysis are itemized in Table 16. Slides were washed five times in PBS, once in ddH_2O to remove residual salt and once in 100% ethanol. After drying, cells were embedded in VectaShield H-1000 mounting medium (Vectro Laboratories, Burligame CA, USA). Cy3, DAPI and FITC signals were detected using a Vanox-T AH-2 epifluorescence microscope (Olympus, Hamburg, Germany). Pictures were captured with an F-Viewer camera. For analysis, analySIS^B software (both Soft Imaging System, Olympus) was used.

Table 16: Secondary antibodies used for immunofluorescence analysis.

Secondary antibody	specification	source
Goat α-mouse	Cy3-conjugate	Jackson ImmunoResearch, Suffolk, UK
Goat α-rabbit	Cy3-conjugate	Jackson ImmunoResearch, Suffolk, UK

4.10 CONFOCAL MICROSCOPY ANALYSIS

To analyze E4 (and other proteins uptake by cells) $0.2x10^5$ HeLa cells per well were seeded on glass coverslips in 24-well plates in 450 µl DMEM supplemented with 10% FCS and antibiotics. The next day, proteins to be analyzed (final concentration 50 - 100 µg/ml) were added to the cells. Following overnight incubation, cells were washed twice and further incubated in fresh medium. The medium was then removed and cells were washed three times in PBS and incubated for 5 min in PBS. Coverslips were fixed in 4% PFA for 15 min at RT and washed three times (5 min each) with PBS. Cells were stored for up to two weeks in PBS at 4°C.

For staining, coverslips were washed for 5 min in PBS and permeabilized using 0.2% Triton X-100 in PBS for 5 min at RT. The respective protein was detected using either an E4- or 6xHis-specific antibody (Table 15) or unspecific E4 autofluorescence was utilized. For antibody detection, coverslips were incubated with 40 µl of primary antibody in milk solution (5% (w/v) milk in PBS) for 1 h, washed five times in PBS and incubated in PBS twice for 10 min. The secondary antibody solution was prepared by diluting phalloidin-TRITC #P1951 (Sigma-Aldrich, Munich, Germany) 1:5,000 in PBS and adding appropriate amounts of secondary antibody (Table 17). 40 µl of secondary antibody solution was added to coverslips followed by incubation for 30 min. Slides were washed five times in PBS (3 min each), once in ddH_2O and then air-dried. Nuclear staining was performed by embedding stained coverslips in VECTASHIELD Mounting Medium with DAPI (VECTOR LABORATORIES, Accent Park, United Kingdom). Samples were analyzed using a Zeiss LSM 700 or Leica TCS SP5 confocal microscope. For analysis, ZEN software (Carl Zeiss Microscopy) or FIJI (Open Source image processing package) were used.

Table 17: Secondary antibodies used for immunofluorescence analysis in confocal microscopy.

Secondary antibody	Specification	Source
Goat α-mouse	Alexa Fluor 647-conjugate	Thermo Fisher Scientific
Goat α-rabbit	Alexa Fluor 647-conjugate	Thermo Fisher Scientific

4.11 ELECTRON MICROSCOPY

For negative staining of protein samples, carbon-coated copper grids (300 mesh) were glow-discharged and placed on Parafilm. 10 µl of the E4 solution (1 - 500 ng/ml) in refolding buffer was placed on the grid and incubated for 10 min at RT. To remove excess solution, grids were carefully placed on the surface of water drops (sample side facing down). Grids were washed five times in PBS for 2 min each at RT and seven times in ultrapure ddH_2O for 2 min each at RT. Two different staining methods were used. For the first technique, samples were fixed with glutaraldehyde for 30 min at RT. Grids were washed once with ddH_2O and excess liquid was removed. Staining was performed by incubating the samples with a 2% aqueous solution of uranyl acetate for 30 min. For the second technique, samples were fixed using methylcellulose on ice. First, grids were shortly incubated three times in ultrapure ddH_2O, washed twice with cold contrast solution and incubated in contrast solution for 10 min at 0°C. Stained grids were air-dried at RT for 10 min and then stored at RT. Samples were imaged at the DKFZ Microscopy Core Facility using a Zeiss EM 912 electron microscope at 80 kV. The magnification indicator was routinely monitored by using a grating replica.

Contrast solution
uranyl acetate (3%)
methylcellulose (2%)

4.12 THIOFLAVIN T SPECTROSCOPIC ASSAY

Thioflavin T (ThT) (Sigma-Aldrich, Munich, Germany) stock solution (2.5 mM) was prepared by dissolving ThT in phosphate buffer and filteration through a 0.22 µm syringe filter (Khurana et al., 2005). 45 µl protein solution in refolding buffer (1 mg/ml) were mixed with ThT stock solution to a final concentration of 16 µg/ml and incubated for 1 h at 4°C. ThT fluorescence was detected using an Infinite™ 200 Quad-4 Monochromator™ microplate reader (TECAN, Männedorf, Switzerland). Fluorescence intensity was measured with an excitation wavelength of 440 nm and emission wavelength of 482 nm. Data was analyzed using Magellan™ data analysis software (TECAN, Männedorf, Switzerland).

Phosphate buffer

phosphate	10mM
NaCl	150mM
pH	7.0

4.13 DATA ANALYSIS

Statistical analysis was performed using Sigma Plot software (Systat Software Inc., San Jose, CA). Each experiment was repeated at least twice with samples in technical duplicates or triplicates. Original data sets were tested with a normality test (Shapiro-Wilk) and an equal variance test. Upon passing both tests, data sets were analyzed using the t-test. Otherwise, data sets were analyzed with the Mann-Whitney rank-sum test. A result was considered statistically significant if the two-tailed p-value was smaller than 5%. Significance was determined at the following levels: (*) $p < 0.05$, (**) $p < 0.01$, (***) $p < 0.005$.

CHAPTER 5

APPENDIX

5.1 OPTIMIZATION OF E4 EXPRESSION

The conditions for the expression of E4 protein variants were tested and optimized. In the first step, three E4 variants were examined: the E4 wild type (E4WT), E4d17-92 (E4dN) and E4d2-5 (E4dN') (Table 1). The E4 constructs were expressed from a lactose-inducible promoter with a C-terminal hexahistidine tag (6xHis-tag).

The 6xHis-tag was chosen as it is, with 0.8 kDa, the smallest tag with the least effect on the overall protein charge. The *in silico* Compute pI/Mw tool predicted a pI of 8.80 for E4dN without the 6xHis-tag and 8.81 with the tag. In addition, tHis-tag allows for efficient purification (Terpe 2003). E4 protein expression was evaluated in small-scale (5 ml) *E. coli* M15 cultures. For each construct, four to ten different bacterial clones were tested. Protein expression was induced with IPTG (1 mM) and cells were incubated at 37°C for 3 h. Subsequently, samples were collected and the protein content was analyzed by immunoblot using an α-His-tag antibody (Fig. 47A).

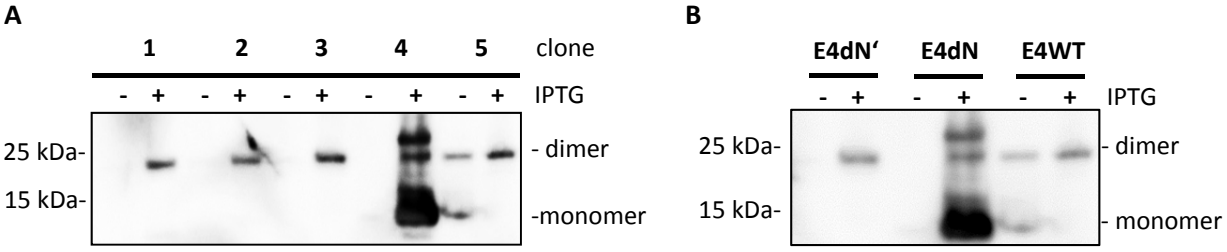

Figure 47: E4 expression.
After selection, single colonies were picked, grown in liquid culture until an OD_{600} of ~0.6 was reached and induced with 1 mM IPTG. Expression was carried out for 3 h at 37°C. Bacterial cultures were lysed by boiling for 5 min at 96°C in loading buffer (4x). Immunoblot analysis was performed using an α-His-tag antibody. Monomeric and dimeric forms of the protein are indicated.
(A) Example of screening for bacterial clones with high E4 expression. *E. coli* M15 were transformed with pQcH6 containing C-terminal 6xHis-tag E4WT under the control of a lactose-inducible promoter.
(B) Expression of different E4 variants. *E. coli* M15 were transformed with pQcH6 containing C-terminal 6xHis-tag E4WT, E4dN and E4dN' under the control of a lactose-inducible promoter.

For preparative protein production, bacterial clones with the highest E4 expression were selected. To obtain larger amounts of proteins for further experiments, bacterial cultures were scaled up to 1 L. In initial preparations, the yield obtained for the HPV16 E4 proteins was relatively low (Fig. 47B). Therefore, experimental conditions were further modified. Time, temperature and expression medium were tested and the best conditions were defined. Overnight expression at room temperature with IPTG (1.2 mM) led to an increase of E4 expression. However, upon chemical cell lysis with guanidine, the amount of E4WT protein obtained was insufficient for purification (Fig. 48A).

The major bottleneck of *in vitro* protein expression is the formation of inclusion bodies (Palmer and Wingfield 2012). E4 has previously been described to be expressed in bacteria in form of insoluble aggregates (McIntosh et al. 2008). Therefore, freeze-thaw cycles and a french pressure cell (FP) were utilized to disrupt cells and solubilize proteins. This led to a drastic increase in the amount of E4 detected in lysates, which in principle should have been suitable for further preparation (Fig. 48B).

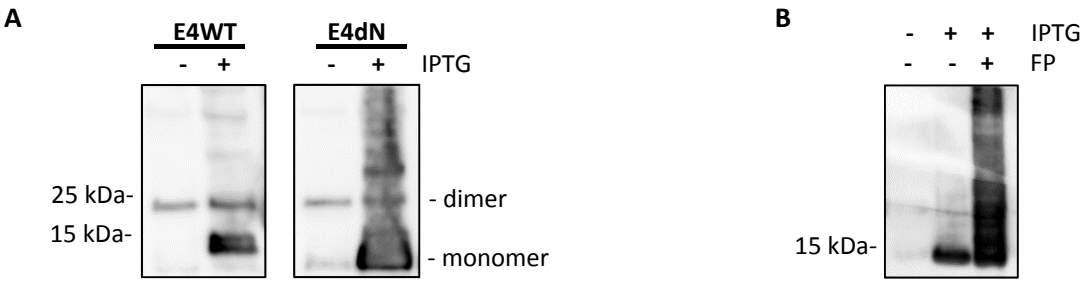

Figure 48: Optimization of E4 expression and extraction conditions.
(A) E4WT and E4dN were expressed in *E. coli M15* after induction with IPTG (1.2 mM) overnight at RT.
(B) Extraction of protein from inclusion bodies resulted in enrichment of E4WT protein lysates. *E. coli M15* lysates were freeze-thawed and the protein was extracted from inclusion bodies using a french pressure cell (FP). Immunoblot analysis was performed using an α-His-tag antibody.

5.2 OPTIMIZATION OF E4 PURIFICATION

To purify E4, immobilized metal ion affinity chromatography was used, exploiting the binding of the 6xHis-tag to ion triads (Cheung et al. 2012). The E4WT protein with the 6xHis-tag on the C-terminus bound weakly to nickel (Fig. 49A). Based on the E4 structure (McIntosh et al. 2008), it was proposed that, in the full-length protein, the C-terminus may be buried inside a hairpin structure and is thus inaccessible for binding. This hypothesis was supported by the observation that, in SDS-PAGE analysis, E4 was regularly detected in form of a band twice the size of the monomer, indicating that E4 still forms dimers in the presence of high concentrations of urea and reducing conditions. Therefore, some intra- and inter- molecular interactions persist, even in denaturing conditions.

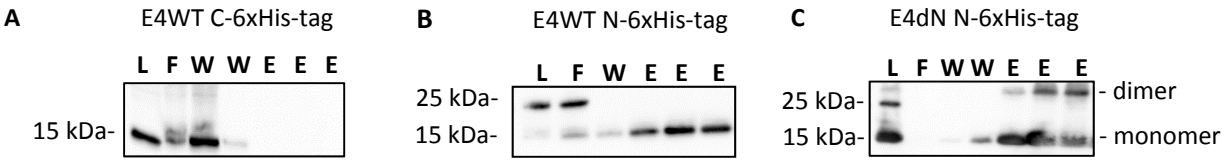

Figure 49: Position of the 6xHis-tag influences the efficiency of HPV16 E4 protein purification.
The HPV16 E4WT and E4dN with C- or N-terminal 6xHis-tag were purified using nickel affinity chromatography. Lysate (L); flow-through (F); washing steps (W); elution fractions (E). Immunoblot analysis was performed using an α-His-tag antibody.

E4WT, E4dN, and all subsequent mutants were subcloned with an N-terminal 6xHis-tag. This considerably improved protein binding (Fig. 49 B and C). Resins for protein purification (nickel vs. cobalt), buffers and elution conditions (pH step gradient vs. imidazole gradient) were tested and improved. The highest protein yield was obtained by means of nickel affinity chromatography with washing steps done using a pH step gradient of urea buffer. The elution conditions were optimized for each protein variant. Differences in binding to the NI-NTA resin between the E4 variants were observed, with mutants lacking the N-terminal domain generally binding stronger. An alanine (E4ala) mutant depleted of all positively charged amino acids bound very weakly and purification required an additional pH adjustment and increased nickel resin capacity. Both E7 and L1 bound moderately well to the column. The optimization of the purification conditions for all variants resulted in a high yield of E4 as described in Table 18.

Table 18: Summary of N-terminally 6xHis-tagged E4 variants expression and purification results.

Name	Expression yield	Amount of protein purified
E4WT	Expressed overnight at RT (protein concentration remains very low after 3 – 5 h expression)	~10-15 mg per column
E4dN	Highly expressed even after 3 h at 37°C	~30-40 mg per column
E4dN'	Not expressed in *E.coli*	X
E4dC'	Expressed overnight at RT but at low levels	~1-2 mg per column
E4dC	Expressed overnight at RT	~4-5 mg per column
E4dNdC	Expressed overnight at RT	~5-10 mg per column
E4ala	Highly expressed overnight at RT	~2 mg per column
E4d70	Expressed overnight at RT but at low levels	~3-5 mg per column
E4d36	Expressed overnight at RT	~4-8 mg per column
E7	Highly expressed overnight at RT	~5-10 mg per column
L1	Well-expressed overnight at RT	~5-10 mg per column

Purity of the prepared protein fractions was assessed by SDS-PAGE and immunoblotting, confirming the absence of bacterial protein contamination (Fig. 50).

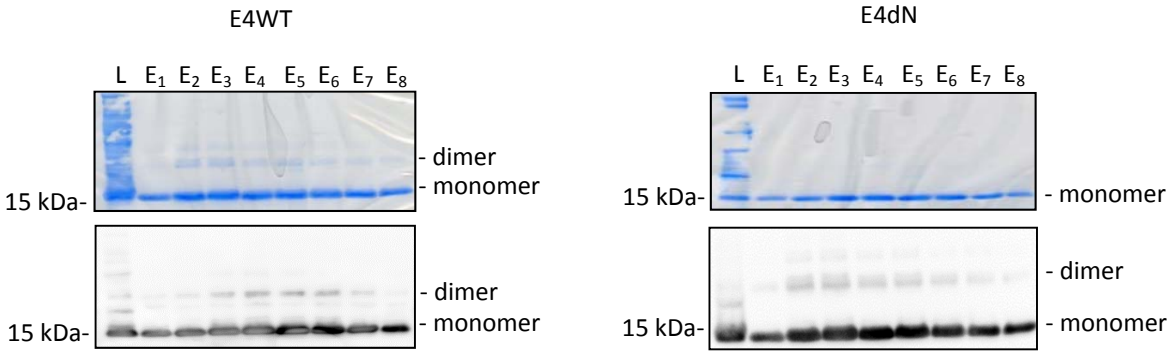

Figure 50: Confirmation of E4 purity.
The HPV16 E4WT (left) and E4dN (right) variants were purified using nickel affinity chromatography. Lysate (L); eight elution fractions (E_1 - E_8). The analysis was done using SDS-PAGE and Instant Blue staining (upper panels) and immunoblotting with an α-His-tag antibody (lower panels).

5.3 OPTIMIZATION OF E4 PREPARATION CONDITIONS

Amylogenic protein refolding conditions can strongly influence the structure of the fibrils formed and the equilibrium between monomers, protofilaments and mature fibrils (Chiti et al. 2001, Chiti et al. 1999, Jahn et al. 2006). For these reasons, the influence of protein preparation and handling settings on the observed E4 effect were analyzed.

5.3.1 TEMPERATURE OF REFOLDING INFLUENCES E4 ACTIVITY

Different refolding temperatures were compared (4°C, RT, 36°C). Dialysis at a temperature above 4°C led to rapid protein precipitation. Protein precipitates were difficult to resuspend and only marginally enhanced the lentiviral infection rate when compared with protein refolded at 4°C (Fig. 51). Therefore, all following protein stocks were prepared at 4°C.

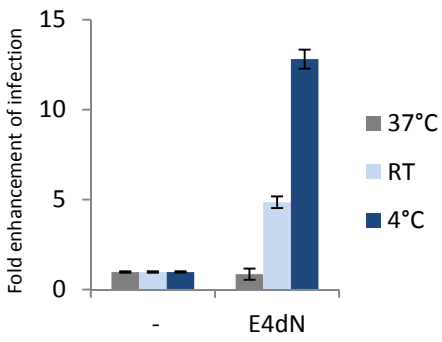

Figure 51: E4 refolded at 4°C has the highest activity in enhancing the lentiviral infection rate.
E4dN was refolded at 37°C, RT or 4°C for 1 week. SupT1 CCR5 cells were infected with VSV-G-pseudotyped lentiviral vector in the absence (-) or the presence of E4dN (100 µg/ml). GFP expression was measured 72 h post-infection using flow cytometry. Fold enhancement of infection was calculated relative to the number of cells infected with virus without E4 (arbitrarily set as 1.0). Results of a single representative experiment are shown. Error bars reflect the SD of two replicates.

5.3.2 FILTRATION INCREASES E4 ACTIVITY

It is suggested that filtration of amyloidogenic peptides during early stages of refolding leads to the removal of pre-aggregated proteins, formation of more homogenous fibrils, and the production of highly reproducible amyloid stocks (Posada et al. 2012). Therefore, after dilution in refolding buffer, E4 was filtered through a 0.22 µm filter, followed by dialysis. Filtered E4 enhanced the lentiviral infection rate stronger than unfiltered E4 (Fig. 52). This additional step also led to more reproducible results and lower deviation between stocks.

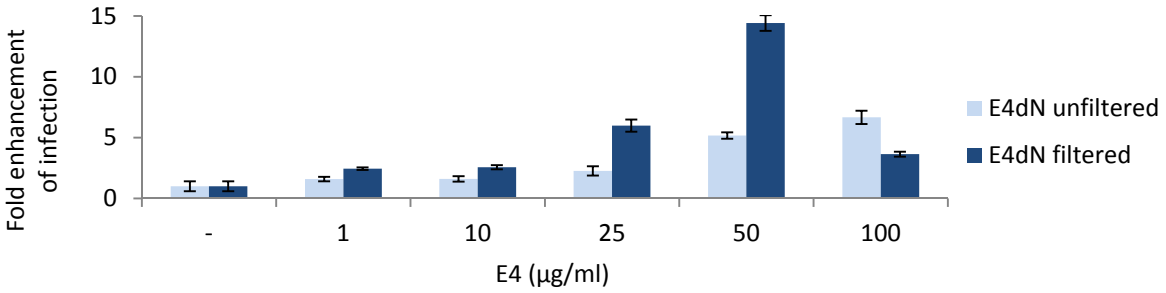

Figure 52: Filtration before E4 dialysis increases the E4-mediated enhancement of the lentiviral infection.
E4dN diluted in refolding buffer was filtered through 0.22 µm filters and dialyzed. SupT1 CCR5 cells were infected with VSV-G-pseudotyped lentiviral vector in the absence (-) or the presence of E4dN. GFP expression was measured 72 h post infection using flow cytometry. Fold enhancement of infection was calculated relative to the number of cells infected with virus without E4 (arbitrarily set as 1.0). The results of a single representative experiment are shown. Error bars reflect the SD of two replicates.

5.3.3 E4 REFOLDS INTO ITS FUNCTIONAL FORM WITHIN THREE DAYS

The kinetics of amyloid formation is complex and differs considerably between different amyloid precursors. Some fibrils need weeks for proper formation, while others assemble within days or even hours (Chiti et al. 2001, Jahn et al. 2006). Therefore, the influence of refolding time on E4 activity was tested. First, the protein was refolded for one, two or three weeks. No significant change in the resulting enhancement of infection was observed (Fig. 53). In addition, protein refolded for just three days was tested. This short time was sufficient for a strong, 10-fold enhancement of the infection (Fig. 53).

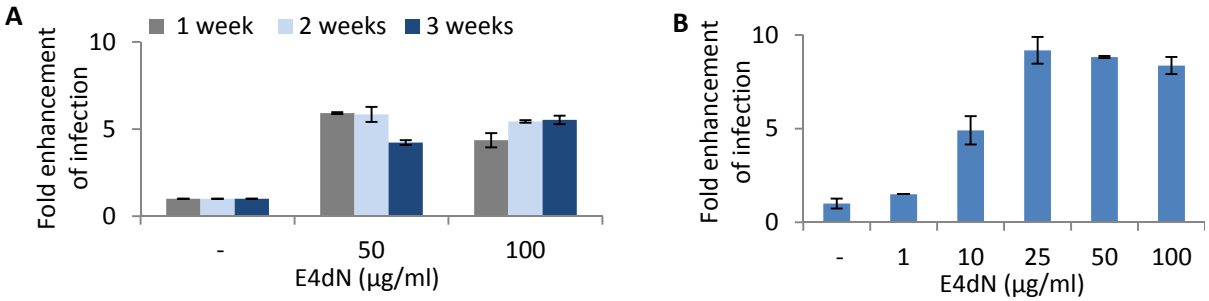

Figure 53: Refolding of E4 for three days is sufficient to induce the E4-mediated effect.
E4dN was refolded for 1, 2 or 3 weeks **(A)** or 3 days **(B)** at 4°C. HeLa cells were infected with VSV-G-pseudotyped lentiviral vector in the absence (-) or the presence of E4dN. GFP expression was measured 72 h post-infection using flow cytometry. Fold enhancement of infection was calculated relative to the number of cells infected with virus without E4 (arbitrarily set as 1.0). The results of single representative experiment are shown. Error bars reflect the SD of two replicates.

5.3.4 CONFIRMATION OF E4 STABILITY DURING STORAGE

Protein stability largely depends on the storage conditions and can considerably affect protein activity (Lowe 1984). Storage conditions can lead to protein degradation by oxidation and deamination or result in the formation of aggregates (Cleland et al. 1993). Thus, the activity of E4 after storage in different conditions was functionally tested. Defining an optimal storage temperature may pose a problem since frozen protein aliquots tend to be more stable but the process of freezing itself may lead to protein damage and major structural changes (Chi et al. 2003). To test the protein stability, E4 was refolded and stored for 1 week either at 4°C or -20°C. The influence of the prepared protein stocks on the lentiviral infection rate was then compared. It was observed that storage at lower temperatures resulted in a more active protein stock (Fig. 54A).

Moreover, E4 kept for longer than one year at -20 °C was also tested. E4 did not lose its activity during the long storage time and still enhanced the infection rate up to 10-fold (similar to the fresh stock) (Fig. 54B). We also tested whether the E4 protein can be thawed and frozen again without loss of activity. Three freeze-thaw cycles compared to one freeze-thaw cycle (15 min at RT, -20°C overnight) resulted in a drastic decrease of protein activity (Fig. 54C).

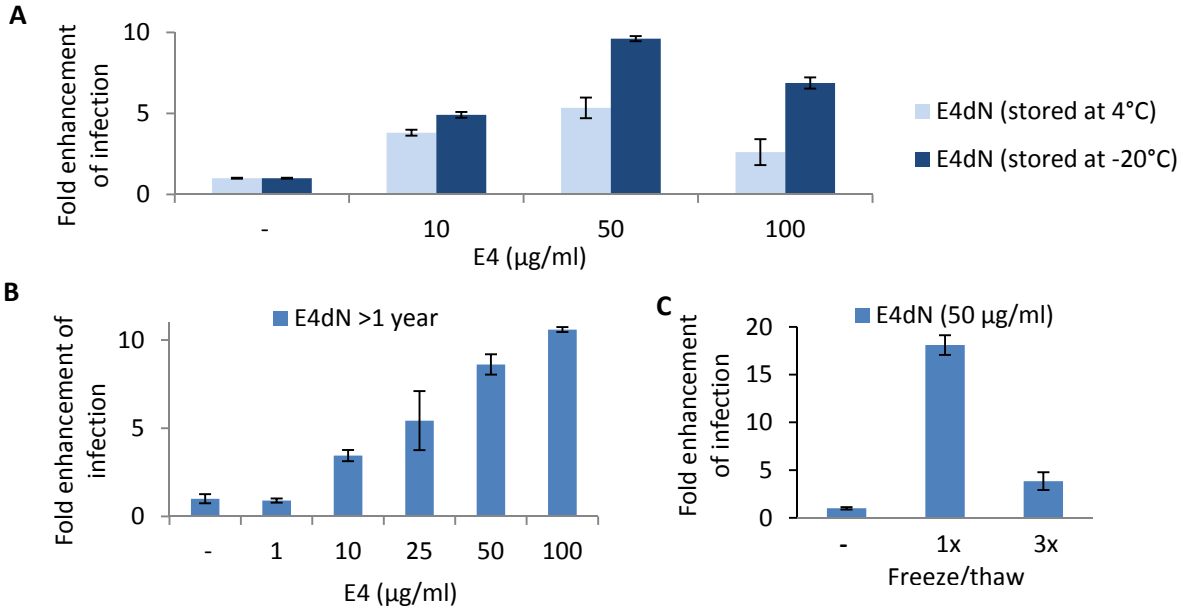

Figure 54: E4 protein stability varies as a result of different storage conditions.
SupT1 CCR5 cells were infected with VSV-G-pseudotyped lentiviral vector in the absence (-) or the presence of E4. GFP expression was measured 72 h post-infection using flow cytometry. Fold enhancement of infection was calculated relative to the number of cells infected with virus without E4 (arbitrarily set as 1.0). The results of single representative experiment are shown. Error bars reflect the SD of three replicates. **(A)** E4 was stored at 4°C or at -20°C for one week. **(B)** E4 was stored for more than 1 year at -20°C. **(C)** E4 was frozen and thawed the indicated number of times.

5.3.5 DISPERSION OF THE E4 PRIOR TO ITS USE ENHANCES ITS EFFECT ON THE INFECTION

Sonication of proteins can lead to better protein dispersion and solubilization (Stathopulos et al. 2004) but also may induce the formation of aggregates that resemble amyloid fibrils (Milto et al. 2013, Ohhashi et al. 2005, Stathopulos et al. 2004). Upon refolding, E4 formed a turbid solution, which precipitated to the bottom of the tube over time. Therefore, it was tested whether sonication could enhance solubilization of those structures. During microscopy analysis, sonified E4 still formed visible assemblies, but appeared to have a finer structure. Sonication of E4 before its application increased the infection rate two-fold (Fig. 55). This effect could be mediated by dispersion of the largest protein complexes, allowing for coverage of wider surfaces or changing the sedimentation properties of E4.

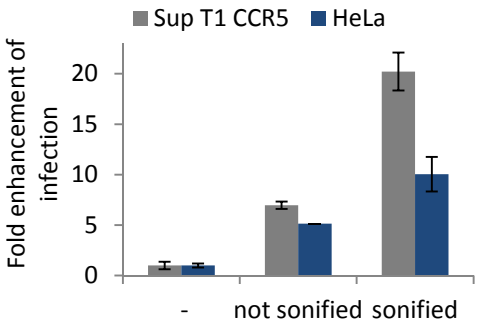

Figure 55: Sonication of E4 before its use increases the E4-mediated enhancement of the lentivirus infection.
SupT1 CCR5 or HeLa cells were infected with VSV-G-pseudotyped lentivirus in the absence (-) or the presence of E4dN (100 µg/ml) with or without sonication. GFP expression was measured 72 h post-infection using flow cytometry. Fold enhancement of infection was calculated relative to the number of cells infected with virus without E4 (arbitrarily set as 1.0). The results of one representative experiment are shown. Error bars reflect the SD of three replicates.

5.3.6 PRE-INCUBATION OF E4 WITH THE VIRUS INCREASES THE INFECTION RATE

Next, the influence of the time of pre-incubation on the infection rate was analyzed. It was observed that pre-incubation of E4 with the virus generally enhances the infection rate, with the highest enhancement when E4 was pre-incubated with the virus for 15- 45 min (Fig. 56).

This result possibly reflects the fact that the E4-mediated enhancement of the infection rate requires direct contact of the virus with the protein assemblies and the pre-incubation step allows for more stable E4-virus interactions. Correspondingly, in the case of SEVI a pre-incubation step of protein with virions has also been used before infecting cells (Munch et al. 2007).

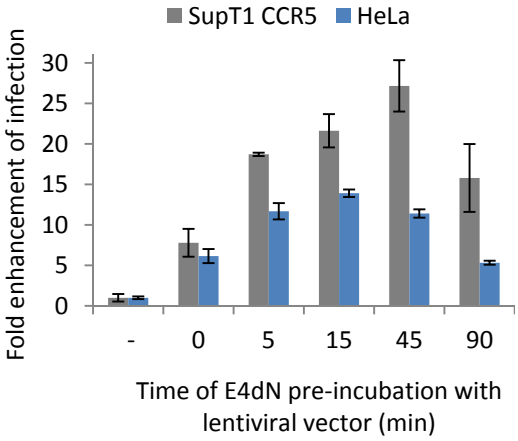

Figure 56: E4 pre-incubation with the lentivirus increases the infection rate.
E4dN (100 µg/ml) was pre-incubated with lentivirus for the indicated length of time before adding to the cells. SupT1 CCR1 or HeLa cells were infected with VSV-G-pseudotyped lentiviral vector in the absence (-) or the presence of E4dN. GFP expression was measured 72 h post infection using flow cytometry. Fold enhancement of infection was calculated relative to the number of cells infected with virus without E4 (arbitrarily set as 1.0). The results of a representative experiment are shown. Error bars reflect the SD of two replicates.

5.3.7 PRE-INCUBATION OF E4 WITH THE VIRUS AT 37°C INCREASES THE INFECTION RATE

The influence of temperature on E4-lentivirus contact was also tested. E4 was pre-incubated with the virus for 15 min at RT or at 37°C. Interaction at 37 °C led to a moderate increase in the E4-mediated enhancement of the infection rate (Fig. 57).

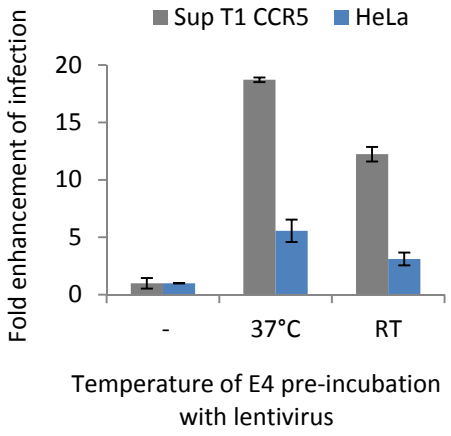

Figure 57: E4 pre-incubation with the lentivirus at higher temperature moderately increases the infection rate.
E4dN (100 µg/ml) was pre-incubated with lentivirus for 15 min at 37°C or at (RT). SupT1 CCR1 or HeLa cells were infected with VSV-G-pseudotyped lentiviral vector in the absence (-) or the presence of E4dN. GFP expression was measured 72 h post infection using flow cytometry. Fold enhancement of infection was calculated relative to the number of cells infected with virus without E4 (arbitrarily set as 1.0). The results of a representative experiment are shown. Error bars reflect the SD of three replicates.

5.3.8 THE E4 EFFECT DEPENDS ON THE MAXIMAL PROTEIN CONCENTRATION PRESENT WITH VIRUS

Different infection schemes were tested to analyze whether contact of E4 with the virus before infection is required. E4 was mixed with the virus and incubated for 15 min at 37°C (E4 + V) or added to cells in parallel with the virus without a pre-incubation step (E4/V). Alternatively, cells were either pre-treated with E4 for 15 min and subsequently infected with lentivirus (E4 + C) or incubated with virus for 15 min before E4 addition (V + C). The best results were observed when E4 was pre-incubated with the virus, lower efficacy was seen when E4 was mixed with virus and directly added on cells. The lowest increase in the lentiviral infection rate was measured when E4 was pre-incubated with cells or added after the virus (Fig. 58A).

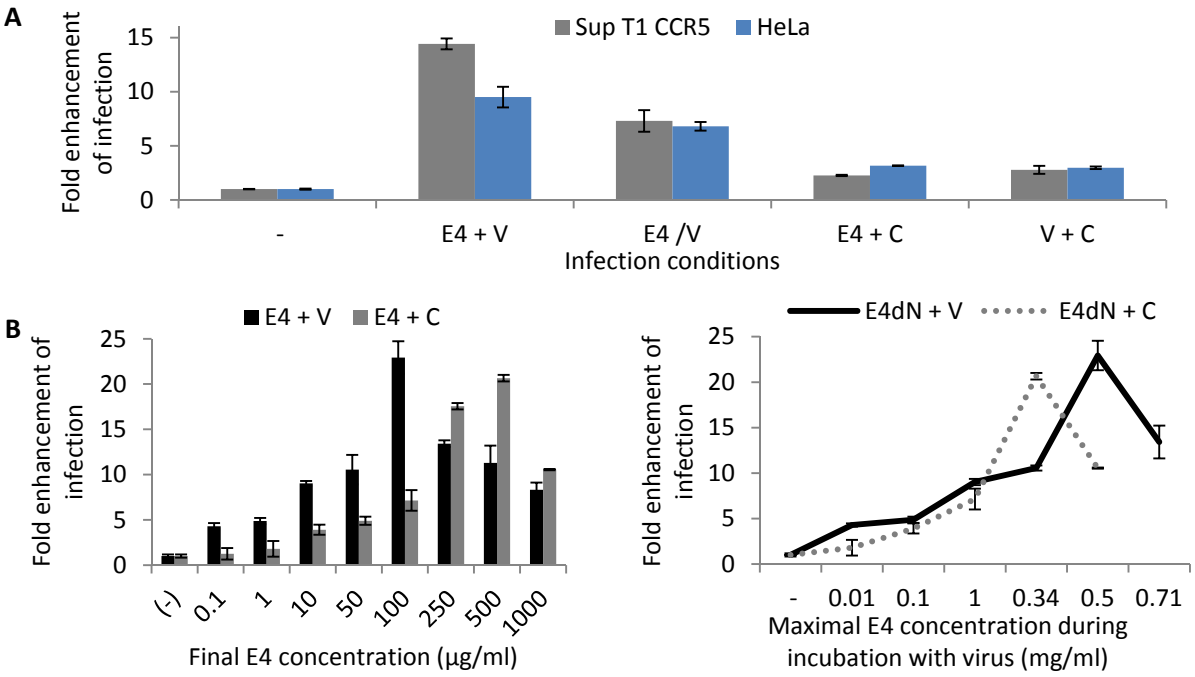

Figure 58: The E4 effect depends on the maximal protein concentration present with the virus prior to infection.
(A) SupT1 CCR5 cells or HeLa cells were infected with VSV-G-pseudotyped lentiviral vector in the absence (-) or the presence of E4dN (E4) (50 µg/ml). The virus was pre-incubated with E4dN for 15 min (E4 + V); E4dN was mixed with the virus and directly added to the cells (E4/V); E4dN was added to the cells and incubated for 15 min before virus addition (E4 + C); virus was added to the cells incubated for 15 min before E4dN addition (V + C).
(B) SupT1 CCR5 cells were infected in the absence (-) or the presence of E4dN (E4). An increasing amount of protein was either pre-incubated with the virus for 15 min (E4 + V) in a small volume or added to the cells (E4 + C). The diagram presents the final concentration of E4 (left panel) in the cell culture volume or the recalculated, maximal concentration of E4 present together with the virus (right panel).
GFP expression was measured 72 h post-infection using flow cytometry. Fold enhancement of infection was calculated relative to the number of cells infected with virus without E4 (arbitrarily set as 1.0). The results of a representative experiments are shown. Error bars reflect the SD of three replicates.

Because the E4 effect strongly depends on the protein concentration, it was checked whether the lower increase in the infection rate caused by E4 pre-incubation with cells instead of virus is simply the result of protein dilution by adding it to a cell culture medium. Either cells, or the virus were pre-

incubated with an increasing amount of E4 before infection. The protein concentrations were re-calculated to convert the data into the maximal E4 concentration present together with the virus. Indeed it was observed that the E4 effect depends on the maximal protein concentration present together with virus prior to infection rather than the final amount of E4 during infection (Fig. 59B). The drop in enhancement (Fig. 59B) at high E4 concentrations resembles the one observed in previous experiments (Fig. 14).

5.4 THE E4-MEDIATED INFECTIVITY ENHANCEMENT IS INDEPENDENT OF FETAL CALF SERUM

To test whether additional protein cofactors are required for the E4-mediated enhancement, cells were infected in the presence or absence of fetal calf serum (FCS). Before infection, HeLa or SupT1 CCR5 cells were washed twice and transferred to medium with or without FCS. Cells infected in the absence of FCS were grown without serum until detection of GFP expression.

Importantly, a lack of cell proliferation caused by serum starvation should not have any effect on the enhancement of infection because the percentages of infected cells rather than absolute numbers are compared.

No significant difference between the E4-mediated enhancement of the infection rate of both cell lines in the absence or presence of serum was observed (Fig. 59). We therefore conclude that the E4-mediated enhancement of the lentiviral infection does not require a serum cofactor.

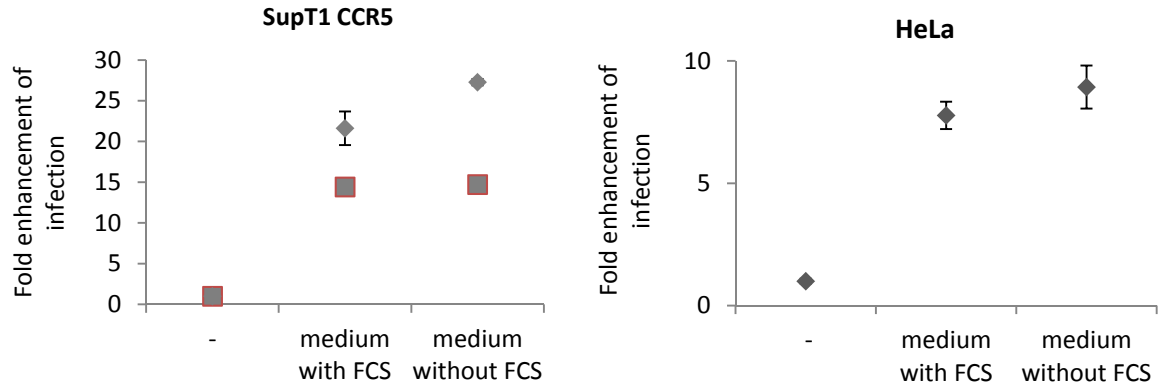

Figure 59: The E4-mediated infectivity enhancement is independent of fetal calf serum.
(A) SupT1 CCR5 cells and **(B)** HeLa cells were infected with VSV-G-pseudotyped lentiviral vector in the absence (-) or presence of E4dN (100 µg/ml) in serum-free medium or medium supplemented with 10% FSC. GFP expression was measured 72 h post-infection using flow cytometry. Fold enhancement of infection was calculated relative to the number of cells infected with virus without E4 (arbitrarily set as 1.0). Each dot represents mean of one independent experiment. Error bars reflect the SD of technical replicates.

INDEX

LIST OF FIGURES

LIST OF TABLES

ABBREVIATIONS

6xHis-tag	hexahistidine tag
aa	amino acid
Aβ	β-amyloids
A MuLV	amphotrophic Moloney leukemia virus
AIDS	Acquired Immunodeficiency Syndrome
APP	Amyloid Precursor Protein
ATP	Adenosine triphosphate
BLAST	Basic Local Alignment Search Tool
BSA	bovine serum albumin
ccDNA	closed circular DNA
CDK	Cyclin dependent kinase
ccDNA	circular covalent DNA
cDNA	complementary DNA
CIN	cervical intraepithelial neoplasia
CMV	Cytomegalovirus
CV	column volumes
DAPI	4',6-diamidino-2-phenylindole
DNA	Deoxyribonucleic Acid
E4-DBP	E4-DEAD box protein
E. coli	*Escherichia coli*
e.g.	exempli gratia
ECL	enhanced chemiluminescence
EM	electron microscopy
ERK	Extracellular signal-Regulated Kinase
et al.	et alii
FACS	fluorescence activated cell sorting
FP	french pressure cell
GALV	Gibbon ape leukemia virus
GFP	green fluorescent protein
HA	hemagglutinin
HDAC	histone deacetylase
HIV	human immunodeficiency virus
HPV	human papilloma virus

HSPG	heparan sulfate proteoglycans
HSV-1	herpes simplex virus type 1
HSV-2	herpes simplex virus type 2
HR	high-risk
HRP	horseradish peroxidase
IPTG	isopropyl-β-D-thiogalactopyranoside
IU	infectious units
JNK	c-Jun N-terminal kinase
LB	Lysogeny Broth
LCR	long control region
LR	low-risk
LTR	long terminal repeat
M	main
MAPK	mitogen-activated protein kinase
Mcm	mini-chromosome maintenance
MCS	Molluscum contagiosum virus
MCV	multiple cloning site
MHC	major histocompatibility complex
mRNA	messenger RNA
MTOC	microtubule organizing center
N	non-M/non-O
ND10	nuclear dot 10
Ni-NTA	nickel-nitrilotriacetic acid
nef	Negative Factro
NP40	Nonidet P 40
O	outlier
ORF	open reading frame
PAP	prostatic acid phosphatase
PBMC	peripheral blood mononucleated cell
PBS	Phosphate Buffered Saline
PCR	Polymerase Chain Reaction
PFA	paraformaldehyde
pH	potential hydrogen
pI	isoelectric point

PLL	poly-L-lysine
pRb	retinoblastoma protein
PSA	prostate-specific antigen
Ras	Rat sarcoma
RATNES	Regulated on Activation, Normal T-cell Expressed and Secreted
rev	Regulator of Expression of viral proteins
RNA	Ribonucleic Acid
RLF	replication licensing factors
RT	room temperature
RT-PCR	Reverse Transcription real-time PCR
SAPK	stress-activated protein kinase
SDS	Sodium Dodecyl Sulfate
SDS-PAGE	Sodium Dodecyl Sulfate Polyacrylamide Gel Electrophoresis
SEM	semenogelin
SEVI	Semen derived Enhancer of Virus Infection
ssRNA	single-stranded RNA
STI	sexually transmited infections
SV40	Simian Virus 40
T-Ag	T-antigen (of SV40)
tat	Tat Transactivator of expression
TB	Terrific Broth
TAR	Transactivation Response Element
ThT	Thioflavin T
URR	upstream regulatory region
vif	Viral Infectivity Factor
v/v	volume/volume
w/v	weight/volume
WT	wild type
XMLV	xenotropic murine leukemia virus-related virus

Abbreviations for one letter codes of nucleotides and amino acids as well as chemical compounds were used according to the system of the International Union of Pure and Applied Chemistry (IUPAC) and the International Union of Biochemistry (IUB).

BIBLIOGRAPHY

AGARWAL A AND PRABAKARAN SA. 2005. Mechanism, measurement, and prevention of oxidative stress in male reproductive physiology. Indian J Exp Biol 43: 963-974.

ALDUNATE M, TYSSEN D, JOHNSON A, ZAKIR T, SONZA S, MOENCH T, CONE R AND TACHEDJIAN G. 2013. Vaginal concentrations of lactic acid potently inactivate HIV. J Antimicrob Chemother 68: 2015-2025.

ALFSEN A, YU H, MAGERUS-CHATINET A, SCHMITT A AND BOMSEL M. 2005. HIV-1-infected blood mononuclear cells form an integrin- and agrin-dependent viral synapse to induce efficient HIV-1 transcytosis across epithelial cell monolayer. Mol Biol Cell 16: 4267-4279.

ALTER MJ, AHTONE J, WEISFUSE I, STARKO K, VACALIS TD AND MAYNARD JE. 1986. Hepatitis B virus transmission between heterosexuals. JAMA : the journal of the American Medical Association 256: 1307-1310.

ANACKER D AND MOODY C. 2012. Generation of organotypic raft cultures from primary human keratinocytes. Journal of visualized experiments : JoVE.

ANTZUTKIN ON, LEAPMAN RD, BALBACH JJ AND TYCKO R. 2002. Supramolecular structural constraints on Alzheimer's beta-amyloid fibrils from electron microscopy and solid-state nuclear magnetic resonance. Biochemistry 41: 15436-15450.

APPAY V AND ROWLAND-JONES SL. 2001. RANTES: a versatile and controversial chemokine. Trends in immunology 22: 83-87.

ARNOLD F ET AL. 2012. Naturally occurring fragments from two distinct regions of the prostatic acid phosphatase form amyloidogenic enhancers of HIV infection. Journal of virology 86: 1244-1249.

AUVERT B, LISSOUBA P, CUTLER E, ZARCA K, PUREN A AND TALJAARD D. 2010. Association of oncogenic and nononcogenic human papillomavirus with HIV incidence. J Acquir Immune Defic Syndr 53: 111-116.

AVERBACH SH, GRAVITT PE, NOWAK RG, CELENTANO DD, DUNBAR MS, MORRISON CS, GRIMES B AND PADIAN NS. 2010. The association between cervical human papillomavirus infection and HIV acquisition among women in Zimbabwe. Aids 24: 1035-1042.

BARROW CJ AND ZAGORSKI MG. 1991. Solution structures of beta peptide and its constituent fragments: relation to amyloid deposition. Science (New York, NY) 253: 179-182.

BAYER P, KRAFT M, EJCHART A, WESTENDORP M, FRANK R AND ROSCH P. 1995. Structural studies of HIV-1 Tat protein. Journal of molecular biology 247: 529-535.

BECKWITH JR. 1964. A DELETION ANALYSIS OF THE LAC OPERATOR REGION IN ESCHERICHIA COLI. Journal of molecular biology 8: 427-430.

BELL I, MARTIN A AND ROBERTS S. 2007. The E1circumflexE4 protein of human papillomavirus interacts with the serine-arginine-specific protein kinase SRPK1. Journal of virology 81: 5437-5448.

BENEN JA, VAN BERKEL WJ, VAN DONGEN WM, MULLER F AND DE KOK A. 1989. Molecular cloning and sequence determination of the lpd gene encoding lipoamide dehydrogenase from Pseudomonas fluorescens. Journal of general microbiology 135: 1787-1797.

BERGANT MARUSIC M, OZBUN MA, CAMPOS SK, MYERS MP AND BANKS L. 2012. Human papillomavirus L2 facilitates viral escape from late endosomes via sorting nexin 17. Traffic (Copenhagen, Denmark) 13: 455-467.

BERGER EA, MURPHY PM AND FARBER JM. 1999. Chemokine receptors as HIV-1 coreceptors: roles in viral entry, tropism, and disease. Annu Rev Immunol 17: 657-700.

BIANCALANA M AND KOIDE S. 2010. Molecular mechanism of Thioflavin-T binding to amyloid fibrils. Biochim Biophys Acta 1804: 1405-1412.

BITAN G, KIRKITADZE MD, LOMAKIN A, VOLLERS SS, BENEDEK GB AND TEPLOW DB. 2003. Amyloid beta -protein (Abeta) assembly: Abeta 40 and Abeta 42 oligomerize through distinct

pathways. Proceedings of the National Academy of Sciences of the United States of America 100: 330-335.
BODILY J AND LAIMINS LA. 2011. Persistence of human papillomavirus infection: keys to malignant progression. Trends Microbiol 19: 33-39.
BOILY MC, BAGGALEY RF, WANG L, MASSE B, WHITE RG, HAYES RJ AND ALARY M. 2009. Heterosexual risk of HIV-1 infection per sexual act: systematic review and meta-analysis of observational studies. Lancet Infect Dis 9: 118-129.
BOMSEL M. 1997. Transcytosis of infectious human immunodeficiency virus across a tight human epithelial cell line barrier. Nature medicine 3: 42-47.
BORGOGNA C ET AL. 2014. Improved detection reveals active beta-papillomavirus infection in skin lesions from kidney transplant recipients. Modern pathology : an official journal of the United States and Canadian Academy of Pathology, Inc.
BORGOGNA C ET AL. 2012. Characterization of beta papillomavirus E4 expression in tumours from Epidermodysplasia Verruciformis patients and in experimental models. Virology 423: 195-204.
BREITBURD F, O. AND CROISSANT GO. 1987. Expression of human papillomavirus type- 1 E4 gene products in warts. Cance rCells Cold Spring Harbor Laboratory Press 5: 115–122.
BRILLARD-BOURDET M, REHAULT S, JULIANO L, FERRER M, MOREAU T AND GAUTHIER F. 2002. Amidolytic activity of prostatic acid phosphatase on human semenogelins and semenogelin-derived synthetic substrates. Eur J Biochem 269: 390-395.
BROWN DR, BROWN CR AND LEHR EE. 2004. Intracellular expression patterns of the human papillomavirus type 59 E1/E4 protein in COS cells, keratinocytes, and genital epithelium. Intervirology 47: 321-327.
BRUGGINK KA, MULLER M, KUIPERIJ HB AND VERBEEK MM. 2012. Methods for analysis of amyloid-beta aggregates. J Alzheimers Dis 28: 735-758.
BRUNI L, DIAZ M, CASTELLSAGUE X, FERRER E, BOSCH FX AND DE SANJOSE S. 2010. Cervical human papillomavirus prevalence in 5 continents: meta-analysis of 1 million women with normal cytological findings. The Journal of infectious diseases 202: 1789-1799.
BRYAN JT, FIFE KH AND BROWN DR. 1998. The intracellular expression pattern of the human papillomavirus type 11 E1--E4 protein correlates with its ability to self associate. Virology 241: 49-60.
BRYAN JT, HAN A, FIFE KH AND BROWN DR. 2000. The human papillomavirus type 11 E1E4 protein is phosphorylated in genital epithelium. Virology 268: 430-439.
BUCK CB, CHENG N, THOMPSON CD, LOWY DR, STEVEN AC, SCHILLER JT AND TRUS BL. 2008. Arrangement of L2 within the papillomavirus capsid. Journal of virology 82: 5190-5197.
BUCK CB, THOMPSON CD, PANG YY, LOWY DR AND SCHILLER JT. 2005. Maturation of papillomavirus capsids. Journal of virology 79: 2839-2846.
BURD EM. 2003. Human papillomavirus and cervical cancer. Clin Microbiol Rev 16: 1-17.
BURNS JC, FRIEDMANN T, DRIEVER W, BURRASCANO M AND YEE JK. 1993. Vesicular stomatitis virus G glycoprotein pseudotyped retroviral vectors: concentration to very high titer and efficient gene transfer into mammalian and nonmammalian cells. Proceedings of the National Academy of Sciences of the United States of America 90: 8033-8037.
CAPULE CC, BROWN C, OLSEN JS, DEWHURST S AND YANG J. 2012. Oligovalent amyloid-binding agents reduce SEVI-mediated enhancement of HIV-1 infection. J Am Chem Soc 134: 905-908.
CHANDRA J, KUHN DM, MUKHERJEE PK, HOYER LL, MCCORMICK T AND GHANNOUM MA. 2001. Biofilm formation by the fungal pathogen Candida albicans: development, architecture, and drug resistance. Journal of bacteriology 183: 5385-5394.
CHAVEZ DJ AND ANDERSON TL. 1985. The glycocalyx of the mouse uterine luminal epithelium during estrus, early pregnancy, the peri-implantation period, and delayed implantation. I. Acquisition of Ricinus communis I binding sites during pregnancy. Biology of reproduction 32: 1135-1142.

CHEN C AND OKAYAMA H. 1987. High-efficiency transformation of mammalian cells by plasmid DNA. Molecular and cellular biology 7: 2745-2752.
CHEN XS, GARCEA RL, GOLDBERG I, CASINI G AND HARRISON SC. 2000. Structure of small virus-like particles assembled from the L1 protein of human papillomavirus 16. Mol Cell 5: 557-567.
CHEUNG RC, WONG JH AND NG TB. 2012. Immobilized metal ion affinity chromatography: a review on its applications. Appl Microbiol Biotechnol 96: 1411-1420.
CHI EY, KRISHNAN S, RANDOLPH TW AND CARPENTER JF. 2003. Physical stability of proteins in aqueous solution: mechanism and driving forces in nonnative protein aggregation. Pharm Res 20: 1325-1336.
CHIN-HONG PV ET AL. 2009. Anal human papillomavirus infection is associated with HIV acquisition in men who have sex with men. Aids 23: 1135-1142.
CHITI F, BUCCIANTINI M, CAPANNI C, TADDEI N, DOBSON CM AND STEFANI M. 2001. Solution conditions can promote formation of either amyloid protofilaments or mature fibrils from the HypF N-terminal domain. Protein Sci 10: 2541-2547.
CHITI F, WEBSTER P, TADDEI N, CLARK A, STEFANI M, RAMPONI G AND DOBSON CM. 1999. Designing conditions for in vitro formation of amyloid protofilaments and fibrils. Proceedings of the National Academy of Sciences of the United States of America 96: 3590-3594.
CHOO KB, PAN CC AND HAN SH. 1987. Integration of human papillomavirus type 16 into cellular DNA of cervical carcinoma: preferential deletion of the E2 gene and invariable retention of the long control region and the E6/E7 open reading frames. Virology 161: 259-261.
CHUCK AS, CLARKE MF AND PALSSON BO. 1996. Retroviral infection is limited by Brownian motion. Human gene therapy 7: 1527-1534.
CLAPHAM PR AND MCKNIGHT A. 2002. Cell surface receptors, virus entry and tropism of primate lentiviruses. J Gen Virol 83: 1809-1829.
CLELAND JL, POWELL MF AND SHIRE SJ. 1993. The development of stable protein formulations: a close look at protein aggregation, deamidation, and oxidation. Crit Rev Ther Drug Carrier Syst 10: 307-377.
CLEMENS KE, BRENT R, GYURIS J AND MUNGER K. 1995. Dimerization of the human papillomavirus E7 oncoprotein in vivo. Virology 214: 289-293.
CLERICI M, MEROLA M, FERRARIO E, TRABATTONI D, VILLA ML, STEFANON B, VENZON DJ, SHEARER GM, DE PALO G AND CLERICI E. 1997. Cytokine production patterns in cervical intraepithelial neoplasia: association with human papillomavirus infection. J Natl Cancer Inst 89: 245-250.
COELEN RJ, JOSE DG AND MAY JT. 1983. The effect of hexadimethrine bromide (polybrene) on the infection of the primate retroviruses SSV 1/SSAV 1 and BaEV. Arch Virol 75: 307-311.
CONGER KL, LIU JS, KUO SR, CHOW LT AND WANG TS. 1999. Human papillomavirus DNA replication. Interactions between the viral E1 protein and two subunits of human dna polymerase alpha/primase. The Journal of biological chemistry 274: 2696-2705.
CONSTANTINESCU AA, VINK H AND SPAAN JA. 2003. Endothelial cell glycocalyx modulates immobilization of leukocytes at the endothelial surface. Arterioscler Thromb Vasc Biol 23: 1541-1547.
CONTI C, MASTROMARINO P, RICCIOLI A AND ORSI N. 1991. Electrostatic interactions in the early events of VSV infection. Res Virol 142: 17-24.
CORDIN O, BANROQUES J, TANNER NK AND LINDER P. 2006. The DEAD-box protein family of RNA helicases. Gene 367: 17-37.
CORNETTA K AND ANDERSON WF. 1989. Protamine sulfate as an effective alternative to polybrene in retroviral-mediated gene-transfer: implications for human gene therapy. Journal of virological methods 23: 187-194.
CRUM CP, SYMBULA M AND WARD BE. 1989. Topography of early HPV 16 transcription in high-grade genital precancers. The American journal of pathology 134: 1183-1188.
CULP TD, BUDGEON LR, MARINKOVICH MP, MENEGUZZI G AND CHRISTENSEN ND. 2006. Keratinocyte-secreted laminin 5 can function as a transient receptor for human

papillomaviruses by binding virions and transferring them to adjacent cells. Journal of virology 80: 8940-8950.

CUMMING SA, CHEUN-IM T, MILLIGAN SG AND GRAHAM SV. 2008. Human papillomavirus type 16 late gene expression is regulated by cellular RNA processing factors in response to epithelial differentiation. Biochem Soc Trans 36: 522-524.

DARNELL GA, SCHRODER WA, ANTALIS TM, LAMBLEY E, MAJOR L, GARDNER J, BIRRELL G, CID-ARREGUI A AND SUHRBIER A. 2007. Human papillomavirus E7 requires the protease calpain to degrade the retinoblastoma protein. The Journal of biological chemistry 282: 37492-37500.

DAVIS HE, MORGAN JR AND YARMUSH ML. 2002. Polybrene increases retrovirus gene transfer efficiency by enhancing receptor-independent virus adsorption on target cell membranes. Biophysical chemistry 97: 159-172.

DAVIS HE, ROSINSKI M, MORGAN JR AND YARMUSH ML. 2004. Charged polymers modulate retrovirus transduction via membrane charge neutralization and virus aggregation. Biophys J 86: 1234-1242.

DAVY CE, AYUB M, JACKSON DJ, DAS P, MCINTOSH P AND DOORBAR J. 2006. HPV16 E1--E4 protein is phosphorylated by Cdk2/cyclin A and relocalizes this complex to the cytoplasm. Virology 349: 230-244.

DAVY CE ET AL. 2005. Human papillomavirus type 16 E1 E4-induced G2 arrest is associated with cytoplasmic retention of active Cdk1/cyclin B1 complexes. Journal of virology 79: 3998-4011.

DAVY CE, JACKSON DJ, WANG Q, RAJ K, MASTERSON PJ, FENNER NF, SOUTHERN S, CUTHILL S, MILLAR JB AND DOORBAR J. 2002. Identification of a G(2) arrest domain in the E1 wedge E4 protein of human papillomavirus type 16. Journal of virology 76: 9806-9818.

DE VILLIERS EM, FAUQUET C, BROKER TR, BERNARD HU AND ZUR HAUSEN H. 2004. Classification of papillomaviruses. Virology 324: 17-27.

DECARLO CA, ROSA B, JACKSON R, NICCOLI S, ESCOTT NG AND ZEHBE I. 2012. Toll-like receptor transcriptome in the HPV-positive cervical cancer microenvironment. Clin Dev Immunol 2012: 785825.

DEHVARI N, MAHMUD T, PERSSON J, BENGTSSON T, GRAFF C, WINBLAD B, RONNBACK A AND BEHBAHANI H. 2012. Amyloid precursor protein accumulates in aggresomes in response to proteasome inhibitor. Neurochem Int 60: 533-542.

DELIGEOROGLOU E, GIANNOULI A, ATHANASOPOULOS N, KAROUNTZOS V, VATOPOULOU A, DIMOPOULOS K AND CREATSAS G. 2013. HPV infection: immunological aspects and their utility in future therapy. Infect Dis Obstet Gynecol 2013: 540850.

DENNING W, DAS S, GUO S, XU J, KAPPES JC AND HEL Z. 2013. Optimization of the transductional efficiency of lentiviral vectors: effect of sera and polycations. Mol Biotechnol 53: 308-314.

DENNY L ET AL. 2014. Human papillomavirus prevalence and type distribution in invasive cervical cancer in sub-Saharan Africa. International journal of cancer Journal international du cancer 134: 1389-1398.

DEVAUX PF. 1991. Static and dynamic lipid asymmetry in cell membranes. Biochemistry 30: 1163-1173.

DODDS E, PIPER TA, MURPHY SJ AND DICKSON G. 1999. Cationic lipids and polymers are able to enhance adenoviral infection of cultured mouse myotubes. J Neurochem 72: 2105-2112.

DONCEL GF, JOSEPH T AND THURMAN AR. 2011. Role of semen in HIV-1 transmission: inhibitor or facilitator? Am J Reprod Immunol 65: 292-301.

DOORBAR J. 2013. The E4 protein; structure, function and patterns of expression. Virology 445: 80-98.

DOORBAR J, CAMPBELL D, GRAND RJ AND GALLIMORE PH. 1986. Identification of the human papilloma virus-1a E4 gene products. Embo j 5: 355-362.

DOORBAR J, CONERON I AND GALLIMORE PH. 1989. Sequence divergence yet conserved physical characteristics among the E4 proteins of cutaneous human papillomaviruses. Virology 172: 51-62.

DOORBAR J ET AL. 2000. The E1E4 protein of human papillomavirus type 16 associates with a putative RNA helicase through sequences in its C terminus. Journal of virology 74: 10081-10095.

DOORBAR J, MEDCALF E AND NAPTHINE S. 1996. Analysis of HPV1 E4 complexes and their association with keratins in vivo. Virology 218: 114-126.

DOORBAR J AND MYERS G. 1996. The E4 protein, . G L Myers et al (ed), The human papillomaviruses 1996 Compendium Los Alamos National Laboratory: p. III58-III80.

DOORBAR J, PARTON A, HARTLEY K, BANKS L, CROOK T, STANLEY M AND CRAWFORD L. 1990. Detection of novel splicing patterns in a HPV16-containing keratinocyte cell line. Virology 178: 254-262.

DOROSKO SM AND CONNOR RI. 2010. Primary human mammary epithelial cells endocytose HIV-1 and facilitate viral infection of CD4+ T lymphocytes. Journal of virology 84: 10533-10542.

DRUMM ML, POPE HA, CLIFF WH, ROMMENS JM, MARVIN SA, TSUI LC, COLLINS FS, FRIZZELL RA AND WILSON JM. 1990. Correction of the cystic fibrosis defect in vitro by retrovirus-mediated gene transfer. Cell 62: 1227-1233.

DURST M, GLITZ D, SCHNEIDER A AND ZUR HAUSEN H. 1992. Human papillomavirus type 16 (HPV 16) gene expression and DNA replication in cervical neoplasia: analysis by in situ hybridization. Virology 189: 132-140.

DYSON N, HOWLEY PM, MUNGER K AND HARLOW E. 1989. The human papilloma virus-16 E7 oncoprotein is able to bind to the retinoblastoma gene product. Science (New York, NY) 243: 934-937.

EASTERHOFF D, DIMAIO JT, DORAN TM, DEWHURST S AND NILSSON BL. 2011. Enhancement of HIV-1 infectivity by simple, self-assembling modular peptides. Biophys J 100: 1325-1334.

EASTERHOFF D ET AL. 2013. Semen-derived enhancer of viral infection (SEVI) binds bacteria, enhances bacterial phagocytosis by macrophages, and can protect against vaginal infection by a sexually transmitted bacterial pathogen. Antimicrobial agents and chemotherapy 57: 2443-2450.

EBRAHIM O AND MAZANDERANI AH. 2013. Recent Developments in Hiv Treatment and Their Dissemination in Poor Countries. Infectious disease reports 5: e2.

EISENBERG D AND JUCKER M. 2012. The amyloid state of proteins in human diseases. Cell 148: 1188-1203.

EISENBERG D, JUCKER M AND JUCKER M. 2012. The amyloid state of proteins in human diseases. Cell 148: 1188-1203.

ELUL R. 1967. Fixed charge in the cell membrane. J Physiol 189: 351-365.

EMERMAN M AND MALIM MH. 1998. HIV-1 regulatory/accessory genes: keys to unraveling viral and host cell biology. Science (New York, NY) 280: 1880-1884.

FASBENDER A, ZABNER J, CHILLON M, MONINGER TO, PUGA AP, DAVIDSON BL AND WELSH MJ. 1997. Complexes of adenovirus with polycationic polymers and cationic lipids increase the efficiency of gene transfer in vitro and in vivo. The Journal of biological chemistry 272: 6479-6489.

FAUCI AS ET AL. 2008. HIV vaccine research: the way forward. Science (New York, NY) 321: 530-532.

FAVRE M, BREITBURD F, CROISSANT O AND ORTH G. 1977. Chromatin-like structures obtained after alkaline disruption of bovine and human papillomaviruses. Journal of virology 21: 1205-1209.

FELSANI A, MILEO AM AND PAGGI MG. 2006. Retinoblastoma family proteins as key targets of the small DNA virus oncoproteins. Oncogene 25: 5277-5285.

FEZOUI Y, HARTLEY DM, HARPER JD, KHURANA R, WALSH DM, CONDRON MM, SELKOE DJ, LANSBURY PT, JR., FINK AL AND TEPLOW DB. 2000. An improved method of preparing the amyloid beta-protein for fibrillogenesis and neurotoxicity experiments. Amyloid 7: 166-178.

FINNEN RL, ERICKSON KD, CHEN XS AND GARCEA RL. 2003. Interactions between papillomavirus L1 and L2 capsid proteins. Journal of virology 77: 4818-4826.

FIOR J. 2012. An initial in vitro investigation into the potential therapeutic use of SupT1 cells to prevent AIDS in HIV-seropositive individuals. PloS one 7: e37511.

FLEMING DT AND WASSERHEIT JN. 1999. From epidemiological synergy to public health policy and practice: the contribution of other sexually transmitted diseases to sexual transmission of HIV infection. Sex Transm Infect 75: 3-17.

FOLEY J, HILL SE, MITI T, MULAJ M, CIESLA M, ROBEEL R, PERSICHILLI C, RAYNES R, WESTERHEIDE S AND MUSCHOL M. 2013. Structural fingerprints and their evolution during oligomeric vs. oligomer-free amyloid fibril growth. J Chem Phys 139: 121901.

FOTI M, MANGASARIAN A, PIGUET V, LEW DP, KRAUSE KH, TRONO D AND CARPENTIER JL. 1997. Nef-mediated clathrin-coated pit formation. The Journal of cell biology 139: 37-47.

FOUCHIER RA, BROUWER M, BROERSEN SM AND SCHUITEMAKER H. 1995. Simple determination of human immunodeficiency virus type 1 syncytium-inducing V3 genotype by PCR. J Clin Microbiol 33: 906-911.

FRANKEL AD AND YOUNG JA. 1998. HIV-1: fifteen proteins and an RNA. Annual review of biochemistry 67: 1-25.

FRASER IS ET AL. 1999. Variations in vaginal epithelial surface appearance determined by colposcopic inspection in healthy, sexually active women. Human reproduction (Oxford, England) 14: 1974-1978.

FREDRICKS DN, FIEDLER TL AND MARRAZZO JM. 2005. Molecular identification of bacteria associated with bacterial vaginosis. The New England journal of medicine 353: 1899-1911.

FREEMAN EE, WEISS HA, GLYNN JR, CROSS PL, WHITWORTH JA AND HAYES RJ. 2006. Herpes simplex virus 2 infection increases HIV acquisition in men and women: systematic review and meta-analysis of longitudinal studies. Aids 20: 73-83.

FRENCH KC AND MAKHATADZE GI. 2012. Core sequence of PAPf39 amyloid fibrils and mechanism of pH-dependent fibril formation: the role of monomer conformation. Biochemistry 51: 10127-10136.

FU L, VAN DOORSLAER K, CHEN Z, RISTRIANI T, MASSON M, TRAVE G AND BURK RD. 2010. Degradation of p53 by human Alphapapillomavirus E6 proteins shows a stronger correlation with phylogeny than oncogenicity. PloS one 5.

GALLO RC ET AL. 1984. Frequent detection and isolation of cytopathic retroviruses (HTLV-III) from patients with AIDS and at risk for AIDS. Science (New York, NY) 224: 500-503.

GARCIA-IGLESIAS T, DEL TORO-ARREOLA A, ALBARRAN-SOMOZA B, DEL TORO-ARREOLA S, SANCHEZ-HERNANDEZ PE, RAMIREZ-DUENAS MG, BALDERAS-PENA LM, BRAVO-CUELLAR A, ORTIZ-LAZARENO PC AND DANERI-NAVARRO A. 2009. Low NKp30, NKp46 and NKG2D expression and reduced cytotoxic activity on NK cells in cervical cancer and precursor lesions. BMC Cancer 9: 186.

GARNETT GP, KIM JJ, FRENCH K AND GOLDIE SJ. 2006. Chapter 21: Modelling the impact of HPV vaccines on cervical cancer and screening programmes. Vaccine 24 Suppl 3: S3/178-186.

GAY V, MOREAU K, HONG SS AND RONFORT C. 2012. Quantification of HIV-based lentiviral vectors: influence of several cell type parameters on vector infectivity. Arch Virol 157: 217-223.

GIBSON TJ. 1984. Studies on the Epstein-Bar virus genome. Ph.D., Cambridge University.

GILLMORE JD, LOVAT LB, PERSEY MR, PEPYS MB AND HAWKINS PN. 2001. Amyloid load and clinical outcome in AA amyloidosis in relation to circulating concentration of serum amyloid A protein. Lancet 358: 24-29.

GOTTLIEB MS, SCHROFF R, SCHANKER HM, WEISMAN JD, FAN PT, WOLF RA AND SAXON A. 1981. Pneumocystis carinii pneumonia and mucosal candidiasis in previously healthy homosexual men: evidence of a new acquired cellular immunodeficiency. The New England journal of medicine 305: 1425-1431.

GRAS SL, WADDINGTON LJ AND GOLDIE KN. 2011. Transmission electron microscopy of amyloid fibrils. Methods in molecular biology (Clifton, NJ) 752: 197-214.

GRASLUND S ET AL. 2008. Protein production and purification. Nat Methods 5: 135-146.

GRAY RH, WAWER MJ, BROOKMEYER R, SEWANKAMBO NK, SERWADDA D, WABWIRE-MANGEN F, LUTALO T, LI X, VANCOTT T AND QUINN TC. 2001. Probability of HIV-1 transmission per coital

act in monogamous, heterosexual, HIV-1-discordant couples in Rakai, Uganda. Lancet 357: 1149-1153.
GREENWALD J AND RIEK R. 2010. Biology of amyloid: structure, function, and regulation. Structure 18: 1244-1260.
GRELLE G, OTTO A, LORENZ M, FRANK RF, WANKER EE AND BIESCHKE J. 2011. Black tea theaflavins inhibit formation of toxic amyloid-beta and alpha-synuclein fibrils. Biochemistry 50: 10624-10636.
GRIFFIN H ET AL. 2012. E4 antibodies facilitate detection and type-assignment of active HPV infection in cervical disease. PloS one 7: e49974.
GROSS G, PFISTER H, HAGEDORN M AND GISSMANN L. 1982. Correlation between human papillomavirus (HPV) type and histology of warts. J Invest Dermatol 78: 160-164.
GUESS JC AND MCCANCE DJ. 2005. Decreased migration of Langerhans precursor-like cells in response to human keratinocytes expressing human papillomavirus type 16 E6/E7 is related to reduced macrophage inflammatory protein-3alpha production. Journal of virology 79: 14852-14862.
GUPTA P, MELLORS J, KINGSLEY L, RIDDLER S, SINGH MK, SCHREIBER S, CRONIN M AND RINALDO CR. 1997. High viral load in semen of human immunodeficiency virus type 1-infected men at all stages of disease and its reduction by therapy with protease and nonnucleoside reverse transcriptase inhibitors. Journal of virology 71: 6271-6275.
HAASE AT. 2005. Perils at mucosal front lines for HIV and SIV and their hosts. Nature reviews Immunology 5: 783-792.
HACKE K, RINCON-OROZCO B, BUCHWALTER G, SIEHLER SY, WASYLYK B, WIESMULLER L AND ROSL F. 2010. Regulation of MCP-1 chemokine transcription by p53. Mol Cancer 9: 82.
HACKEMANN M, GRUBB C AND HILL KR. 1968. The ultrastructure of normal squamous epithelium of the human cervix uteri. Journal of ultrastructure research 22: 443-457.
HANAHAN D. 1983. Studies on transformation of Escherichia coli with plasmids. Journal of molecular biology 166: 557-580.
HARDEN V AND HARRIS J. 1953. The isoelectric point of bacterial cells. J Bacteriol 65: 198 –202.
HARDY J AND SELKOE DJ. 2002. The amyloid hypothesis of Alzheimer's disease: progress and problems on the road to therapeutics. Science (New York, NY) 297: 353-356.
HERFS M, HUBERT P, MOUTSCHEN M AND DELVENNE P. 2011. Mucosal junctions: open doors to HPV and HIV infections? Trends Microbiol 19: 114-120.
HLADIK F AND MCELRATH MJ. 2008. Setting the stage: host invasion by HIV. Nature reviews Immunology 8: 447-457.
HONG S ET AL. 2009. Fibrils of prostatic acid phosphatase fragments boost infections with XMRV (xenotropic murine leukemia virus-related virus), a human retrovirus associated with prostate cancer. Journal of virology 83: 6995-7003.
HOULIHAN CF, LARKE NL, WATSON-JONES D, SMITH-MCCUNE KK, SHIBOSKI S, GRAVITT PE, SMITH JS, KUHN L, WANG C AND HAYES R. 2012. Human papillomavirus infection and increased risk of HIV acquisition. A systematic review and meta-analysis. Aids 26: 2211-2222.
HOWLEY PM. 1996. Papillomaviridae: the viruses and their replication. In B N Fields, D M Knipe, and P M Howley (ed), Fields virology

Lippincott-Raven Publishers, Philadelphia, Pa

p. 947-978. .
HU X, CRICK SL, BU G, FRIEDEN C, PAPPU RV AND LEE JM. 2009. Amyloid seeds formed by cellular uptake, concentration, and aggregation of the amyloid-beta peptide. Proceedings of the National Academy of Sciences of the United States of America 106: 20324-20329.
HUBBERT NL, SEDMAN SA AND SCHILLER JT. 1992. Human papillomavirus type 16 E6 increases the degradation rate of p53 in human keratinocytes. Journal of virology 66: 6237-6241.

HUGHES FJ AND ROMANOS MA. 1993. E1 protein of human papillomavirus is a DNA helicase/ATPase. Nucleic acids research 21: 5817-5823.

ITO M, BABA M, SATO A, PAUWELS R, DE CLERCQ E AND SHIGETA S. 1987. Inhibitory effect of dextran sulfate and heparin on the replication of human immunodeficiency virus (HIV) in vitro. Antiviral Res 7: 361-367.

JAHN TR, PARKER MJ, HOMANS SW AND RADFORD SE. 2006. Amyloid formation under physiological conditions proceeds via a native-like folding intermediate. Nat Struct Mol Biol 13: 195-201.

JENSEN JS. 2004. Mycoplasma genitalium: the aetiological agent of urethritis and other sexually transmitted diseases. Journal of the European Academy of Dermatology and Venereology : JEADV 18: 1-11.

JIMENEZ JL, TENNENT G, PEPYS M AND SAIBIL HR. 2001. Structural diversity of ex vivo amyloid fibrils studied by cryo-electron microscopy. Journal of molecular biology 311: 241-247.

JOHNSON KM, KINES RC, ROBERTS JN, LOWY DR, SCHILLER JT AND DAY PM. 2009. Role of heparan sulfate in attachment to and infection of the murine female genital tract by human papillomavirus. Journal of virology 83: 2067-2074.

JONES JS, ROSSMAN L, HARTMAN M AND ALEXANDER CC. 2003. Anogenital injuries in adolescents after consensual sexual intercourse. Academic emergency medicine : official journal of the Society for Academic Emergency Medicine 10: 1378-1383.

KAJITANI N, SATSUKA A, YOSHIDA S AND SAKAI H. 2013. HPV18 E1^E4 is assembled into aggresome-like compartment and involved in sequestration of viral oncoproteins. Front Microbiol 4: 251.

KANDIMALLA KK, SCOTT OG, FULZELE S, DAVIDSON MW AND PODUSLO JF. 2009. Mechanism of neuronal versus endothelial cell uptake of Alzheimer's disease amyloid beta protein. PloS one 4: e4627.

KANTOR R ET AL. 2005. Impact of HIV-1 subtype and antiretroviral therapy on protease and reverse transcriptase genotype: results of a global collaboration. PLoS medicine 2: e112.

KAYED R ET AL. 2007. Fibril specific, conformation dependent antibodies recognize a generic epitope common to amyloid fibrils and fibrillar oligomers that is absent in prefibrillar oligomers. Mol Neurodegener 2: 18.

KEELE BF AND ESTES JD. 2011. Barriers to mucosal transmission of immunodeficiency viruses. Blood 118: 839-846.

KEELE BF ET AL. 2008. Identification and characterization of transmitted and early founder virus envelopes in primary HIV-1 infection. Proceedings of the National Academy of Sciences of the United States of America 105: 7552-7557.

KHAN J, DAVY CE, MCINTOSH PB, JACKSON DJ, HINZ S, WANG Q AND DOORBAR J. 2011. Role of calpain in the formation of human papillomavirus type 16 E1^E4 amyloid fibers and reorganization of the keratin network. Journal of virology 85: 9984-9997.

KIM RH, YOCHIM JM, KANG MK, SHIN KH, CHRISTENSEN R AND PARK NH. 2008. HIV-1 Tat enhances replicative potential of human oral keratinocytes harboring HPV-16 genome. Int J Oncol 33: 777-782.

KINES RC, THOMPSON CD, LOWY DR, SCHILLER JT AND DAY PM. 2009. The initial steps leading to papillomavirus infection occur on the basement membrane prior to cell surface binding. Proceedings of the National Academy of Sciences of the United States of America 106: 20458-20463.

KINGSLEY, RINALDO AND LYTER. 1990. Sexual transmission efficiency of hepatitis B virus and human immunodeficiency virus among homosexual men. Critical care nurse 10: 43.

KLODMANN J, LEWEJOHANN D AND BRAUN HP. 2011. Low-SDS Blue native PAGE. Proteomics 11: 1834-1839.

KNAUER MF, SOREGHAN B, BURDICK D, KOSMOSKI J AND GLABE CG. 1992. Intracellular accumulation and resistance to degradation of the Alzheimer amyloid A4/beta protein. Proceedings of the National Academy of Sciences of the United States of America 89: 7437-7441.

KNIGHT GL, GRAINGER JR, GALLIMORE PH AND ROBERTS S. 2004. Cooperation between different forms of the human papillomavirus type 1 E4 protein to block cell cycle progression and cellular DNA synthesis. Journal of virology 78: 13920-13933.

KOBAYASHI A, WEINBERG V, DARRAGH T AND SMITH-MCCUNE K. 2008. Evolving immunosuppressive microenvironment during human cervical carcinogenesis. Mucosal Immunol 1: 412-420.

KONIG R ET AL. 2008. Global analysis of host-pathogen interactions that regulate early-stage HIV-1 replication. Cell 135: 49-60.

KORENROMP EL, WHITE RG, ORROTH KK, BAKKER R, KAMALI A, SERWADDA D, GRAY RH, GROSSKURTH H, HABBEMA JD AND HAYES RJ. 2005. Determinants of the impact of sexually transmitted infection treatment on prevention of HIV infection: a synthesis of evidence from the Mwanza, Rakai, and Masaka intervention trials. The Journal of infectious diseases 191 Suppl 1: S168-178.

KOTANI H, NEWTON PB, 3RD, ZHANG S, CHIANG YL, OTTO E, WEAVER L, BLAESE RM, ANDERSON WF AND MCGARRITY GJ. 1994. Improved methods of retroviral vector transduction and production for gene therapy. Human gene therapy 5: 19-28.

KRANJEC C AND BANKS L. 2011. A systematic analysis of human papillomavirus (HPV) E6 PDZ substrates identifies MAGI-1 as a major target of HPV type 16 (HPV-16) and HPV-18 whose loss accompanies disruption of tight junctions. Journal of virology 85: 1757-1764.

LAI Z, COLON W AND KELLY JW. 1996. The acid-mediated denaturation pathway of transthyretin yields a conformational intermediate that can self-assemble into amyloid. Biochemistry 35: 6470-6482.

LANDAZURI N AND LE DOUX JM. 2004. Complexation of retroviruses with charged polymers enhances gene transfer by increasing the rate that viruses are delivered to cells. The journal of gene medicine 6: 1304-1319.

LANDAZURI N AND LE DOUX JM. 2006. Complexation with chondroitin sulfate C and Polybrene rapidly purifies retrovirus from inhibitors of transduction and substantially enhances gene transfer. Biotechnol Bioeng 93: 146-158.

LANGFORD SE, ANANWORANICH J AND COOPER DA. 2007. Predictors of disease progression in HIV infection: a review. AIDS research and therapy 4: 11.

LAURSON J, KHAN S, CHUNG R, CROSS K AND RAJ K. 2010. Epigenetic repression of E-cadherin by human papillomavirus 16 E7 protein. Carcinogenesis 31: 918-926.

LE DOUX JM, LANDAZURI N, YARMUSH ML AND MORGAN JR. 2001. Complexation of retrovirus with cationic and anionic polymers increases the efficiency of gene transfer. Human gene therapy 12: 1611-1621.

LEDERMAN MM, OFFORD RE AND HARTLEY O. 2006. Microbicides and other topical strategies to prevent vaginal transmission of HIV. Nature reviews Immunology 6: 371-382.

LI E, STUPACK D, BOKOCH GM AND NEMEROW GR. 1998a. Adenovirus endocytosis requires actin cytoskeleton reorganization mediated by Rho family GTPases. Journal of virology 72: 8806-8812.

LI E, STUPACK D, KLEMKE R, CHERESH DA AND NEMEROW GR. 1998b. Adenovirus endocytosis via alpha(v) integrins requires phosphoinositide-3-OH kinase. Journal of virology 72: 2055-2061.

LI L, SHI X, GUO X, LI H AND XU C. 2014. Ionic protein-lipid interaction at the plasma membrane: what can the charge do? Trends Biochem Sci 39: 130-140.

LILJA H, OLDBRING J, RANNEVIK G AND LAURELL CB. 1987. Seminal vesicle-secreted proteins and their reactions during gelation and liquefaction of human semen. The Journal of clinical investigation 80: 281-285.

LINHARES IM, SUMMERS PR, LARSEN B, GIRALDO PC AND WITKIN SS. 2011. Contemporary perspectives on vaginal pH and lactobacilli. Am J Obstet Gynecol 204: 120.e121-125.

LISSOUBA P, VAN DE PERRE P AND AUVERT B. 2013. Association of genital human papillomavirus infection with HIV acquisition: a systematic review and meta-analysis. Sex Transm Infect 89: 350-356.

LONGWORTH MS AND LAIMINS LA. 2004. Pathogenesis of human papillomaviruses in differentiating epithelia. Microbiol Mol Biol Rev 68: 362-372.
LOWE CR. 1984. Protein purification: Principles and practice. Cell Biochemistry and Function 2: 63-63.
MAJI SK, WANG L, GREENWALD J AND RIEK R. 2009. Structure-activity relationship of amyloid fibrils. FEBS Lett 583: 2610-2617.
MARTELLINI JA, COLE AL, SVOBODA P, STUCHLIK O, CHEN LM, CHAI KX, GANGRADE BK, SORENSEN OE, POHL J AND COLE AM. 2011. HIV-1 enhancing effect of prostatic acid phosphatase peptides is reduced in human seminal plasma. PloS one 6: e16285.
MCINTOSH PB, LASKEY P, SULLIVAN K, DAVY C, WANG Q, JACKSON DJ, GRIFFIN HM AND DOORBAR J. 2010. E1--E4-mediated keratin phosphorylation and ubiquitylation: a mechanism for keratin depletion in HPV16-infected epithelium. J Cell Sci 123: 2810-2822.
MCINTOSH PB ET AL. 2008. Structural analysis reveals an amyloid form of the human papillomavirus type 16 E1--E4 protein and provides a molecular basis for its accumulation. Journal of virology 82: 8196-8203.
MCINTYRE MC, RUESCH MN AND LAIMINS LA. 1996. Human papillomavirus E7 oncoproteins bind a single form of cyclin E in a complex with cdk2 and p107. Virology 215: 73-82.
MEIER O AND GREBER UF. 2004. Adenovirus endocytosis. The journal of gene medicine 6 Suppl 1: S152-163.
MILLER AD AND ROSMAN GJ. 1989. Improved retroviral vectors for gene transfer and expression. BioTechniques 7: 980-982, 984-986, 989-990.
MILLER CJ ET AL. 2005. Propagation and dissemination of infection after vaginal transmission of simian immunodeficiency virus. Journal of virology 79: 9217-9227.
MILLER CJ AND SHATTOCK RJ. 2003. Target cells in vaginal HIV transmission. Microbes Infect 5: 59-67.
MILLER MD, FARNET CM AND BUSHMAN FD. 1997. Human immunodeficiency virus type 1 preintegration complexes: studies of organization and composition. Journal of virology 71: 5382-5390.
MILTO K, BOTYRIUTE A AND SMIRNOVAS V. 2013. Amyloid-like fibril elongation follows michaelis-menten kinetics. PloS one 8: e68684.
MOK YF AND HOWLETT GJ. 2006. Sedimentation velocity analysis of amyloid oligomers and fibrils. Methods Enzymol 413: 199-217.
MUNCH J ET AL. 2007. Semen-derived amyloid fibrils drastically enhance HIV infection. Cell 131: 1059-1071.
MUNCH J, SAUERMANN U, YOLAMANOVA M, RAUE K, STAHL-HENNIG C AND KIRCHHOFF F. 2013. Effect of semen and seminal amyloid on vaginal transmission of simian immunodeficiency virus. Retrovirology 10: 148.
MUNIYAN S, CHATURVEDI NK, DWYER JG, LAGRANGE CA, CHANEY WG AND LIN MF. 2013. Human prostatic Acid phosphatase: structure, function and regulation. Int J Mol Sci 14: 10438-10464.
NAKAHARA T, NISHIMURA A, TANAKA M, UENO T, ISHIMOTO A AND SAKAI H. 2002. Modulation of the cell division cycle by human papillomavirus type 18 E4. Journal of virology 76: 10914-10920.
NAKAHARA T, PEH WL, DOORBAR J, LEE D AND LAMBERT PF. 2005. Human papillomavirus type 16 E1circumflexE4 contributes to multiple facets of the papillomavirus life cycle. Journal of virology 79: 13150-13165.
NASSERI M, HIROCHIKA R, BROKER TR AND CHOW LT. 1987. A human papilloma virus type 11 transcript encoding an E1--E4 protein. Virology 159: 433-439.
NEMEROW GR, PACHE L, REDDY V AND STEWART PL. 2009. Insights into adenovirus host cell interactions from structural studies. Virology 384: 380-388.
NICOL AF, FERNANDES AT, GRINSZTEJN B, RUSSOMANO F, JR ES, TRISTAO A, PEREZ MDE A, NUOVO GJ, MARTINEZ-MAZA O AND BONECINI-ALMEIDA MDA G. 2005. Distribution of immune cell subsets and cytokine-producing cells in the uterine cervix of human papillomavirus (HPV)-infected women: influence of HIV-1 coinfection. Diagn Mol Pathol 14: 39-47.

NIELSEN EH, NYBO M AND SVEHAG SE. 1999. Electron microscopy of prefibrillar structures and amyloid fibrils. Methods Enzymol 309: 491-496.
NILSSON MR. 2004. Techniques to study amyloid fibril formation in vitro. Methods 34: 151-160.
NISHIBU A, WARD BR, JESTER JV, PLOEGH HL, BOES M AND TAKASHIMA A. 2006. Behavioral responses of epidermal Langerhans cells in situ to local pathological stimuli. J Invest Dermatol 126: 787-796.
OHHASHI Y, KIHARA M, NAIKI H AND GOTO Y. 2005. Ultrasonication-induced amyloid fibril formation of beta2-microglobulin. The Journal of biological chemistry 280: 32843-32848.
OLSEN JS, BROWN C, CAPULE CC, RUBINSHTEIN M, DORAN TM, SRIVASTAVA RK, FENG C, NILSSON BL, YANG J AND DEWHURST S. 2010. Amyloid-binding small molecules efficiently block SEVI (semen-derived enhancer of virus infection)- and semen-mediated enhancement of HIV-1 infection. The Journal of biological chemistry 285: 35488-35496.
ONDA T, KANDA T, ZANMA S, YASUGI T, WATANABE S, KAWANA T, UEDA K, YOSHIKAWA H, TAKETANI Y AND YOSHIIKE K. 1993. Association of the antibodies against human papillomavirus 16 E4 and E7 proteins with cervical cancer positive for human papillomavirus DNA. International journal of cancer Journal international du cancer 54: 624-628.
OP DEN KAMP JA. 1979. Lipid asymmetry in membranes. Annual review of biochemistry 48: 47-71.
OSBORNE BJ, SHETH PM, KOVACS C, MAZZULLI T AND KAUL R. 2011. Impact of collection method on assessment of semen HIV RNA viral load. PloS one 6: e23654.
OVERBAUGH J, MILLER AD AND EIDEN MV. 2001. Receptors and entry cofactors for retroviruses include single and multiple transmembrane-spanning proteins as well as newly described glycophosphatidylinositol-anchored and secreted proteins. Microbiol Mol Biol Rev 65: 371-389, table of contents.
PALEFSKY JM, WINKLER B, RABANUS JP, CLARK C, CHAN S, NIZET V AND SCHOOLNIK GK. 1991. Characterization of in vivo expression of the human papillomavirus type 16 E4 protein in cervical biopsy tissues. The Journal of clinical investigation 87: 2132-2141.
PALMER I AND WINGFIELD PT. 2012. Preparation and extraction of insoluble (inclusion-body) proteins from Escherichia coli. Curr Protoc Protein Sci Chapter 6: Unit6.3.
PARKER ZF ET AL. 2013. Transmitted/founder and chronic HIV-1 envelope proteins are distinguished by differential utilization of CCR5. Journal of virology 87: 2401-2411.
PASSAES CP AND SAEZ-CIRION A. 2014. HIV cure research: Advances and prospects. Virology 454-455c: 340-352.
PAUL RW, MORRIS D, HESS BW, DUNN J AND OVERELL RW. 1993. Increased viral titer through concentration of viral harvests from retroviral packaging lines. Human gene therapy 4: 609-615.
PEDERSEN JS, ANDERSEN CB AND OTZEN DE. 2010. Amyloid structure--one but not the same: the many levels of fibrillar polymorphism. Febs j 277: 4591-4601.
PEGHINI BC, ABDALLA DR, BARCELOS AC, TEODORO L, MURTA EF AND MICHELIN MA. 2012. Local cytokine profiles of patients with cervical intraepithelial and invasive neoplasia. Hum Immunol 73: 920-926.
PEH WL ET AL. 2002. Life cycle heterogeneity in animal models of human papillomavirus-associated disease. Journal of virology 76: 10401-10416.
PETRONE L, AMMENDOLIA MG, CESOLINI A, CAIMI S, SUPERTI F, GIORGI C AND DI BONITO P. 2011. Recombinant HPV16 E7 assembled into particles induces an immune response and specific tumour protection administered without adjuvant in an animal model. Journal of translational medicine 9: 69.
PFEFFERKORN CM, MCGLINCHEY RP AND LEE JC. 2010. Effects of pH on aggregation kinetics of the repeat domain of a functional amyloid, Pmel17. Proceedings of the National Academy of Sciences of the United States of America 107: 21447-21452.
PIM D AND BANKS L. 2010. Interaction of viral oncoproteins with cellular target molecules: infection with high-risk vs low-risk human papillomaviruses. APMIS : acta pathologica, microbiologica, et immunologica Scandinavica 118: 471-493.

PLUMMER FA ET AL. 1991. Cofactors in male-female sexual transmission of human immunodeficiency virus type 1. The Journal of infectious diseases 163: 233-239.

POPOVIC M, SARNGADHARAN MG, READ E AND GALLO RC. 1984. Detection, isolation, and continuous production of cytopathic retroviruses (HTLV-III) from patients with AIDS and pre-AIDS. Science (New York, NY) 224: 497-500.

PORTER CD, BLAKE NW, ARCHARD LC, MUHLEMANN MF, ROSEDALE N AND CREAM JJ. 1989. Molluscum contagiosum virus types in genital and non-genital lesions. The British journal of dermatology 120: 37-41.

POSADA D, TESSIER PM AND HIRSA AH. 2012. Removal versus fragmentation of amyloid-forming precursors via membrane filtration. Biotechnol Bioeng 109: 840-845.

PRAY TR AND LAIMINS LA. 1995. Differentiation-dependent expression of E1--E4 proteins in cell lines maintaining episomes of human papillomavirus type 31b. Virology 206: 679-685.

PRIES AR, SECOMB TW AND GAEHTGENS P. 2000. The endothelial surface layer. Pflugers Arch 440: 653-666.

RAJ K, BERGUERAND S, SOUTHERN S, DOORBAR J AND BEARD P. 2004. E1 empty set E4 protein of human papillomavirus type 16 associates with mitochondria. Journal of virology 78: 7199-7207.

REID SD, FIDLER SJ AND COOKE GS. 2013. Tracking the progress of HIV: the impact of point-of-care tests on antiretroviral therapy. Clin Epidemiol 5: 387-396.

RESING KA, AL-ALAWI N, BLOMQUIST C, FLECKMAN P AND DALE BA. 1993. Independent regulation of two cytoplasmic processing stages of the intermediate filament-associated protein filaggrin and role of Ca2+ in the second stage. The Journal of biological chemistry 268: 25139-25145.

RIJNAARTS, H.M. H, NORDE W, LYKLEMA J AND ZEHNDER AJB. 1995. The isoelectric point of bacteria as an indicator for the presence of cell surface polymers that inhibit adhesion. Colloids and Surfaces B: Biointerfaces 4: 191-197.

RILEY RR, DUENSING S, BRAKE T, MUNGER K, LAMBERT PF AND ARBEIT JM. 2003. Dissection of human papillomavirus E6 and E7 function in transgenic mouse models of cervical carcinogenesis. Cancer research 63: 4862-4871.

RIVERA-MOLINA YA, MARTINEZ FP AND TANG Q. 2013. Nuclear domain 10 of the viral aspect. World J Virol 2: 110-122.

ROAN NR ET AL. 2011. Peptides released by physiological cleavage of semen coagulum proteins form amyloids that enhance HIV infection. Cell Host Microbe 10: 541-550.

ROAN NR, MUNCH J, ARHEL N, MOTHES W, NEIDLEMAN J, KOBAYASHI A, SMITH-MCCUNE K, KIRCHHOFF F AND GREENE WC. 2009. The cationic properties of SEVI underlie its ability to enhance human immunodeficiency virus infection. Journal of virology 83: 73-80.

ROBERTS S, ASHMOLE I, GIBSON LJ, ROOKES SM, BARTON GJ AND GALLIMORE PH. 1994. Mutational analysis of human papillomavirus E4 proteins: identification of structural features important in the formation of cytoplasmic E4/cytokeratin networks in epithelial cells. Journal of virology 68: 6432-6445.

ROBERTS S, ASHMOLE I, JOHNSON GD, KREIDER JW AND GALLIMORE PH. 1993. Cutaneous and mucosal human papillomavirus E4 proteins form intermediate filament-like structures in epithelial cells. Virology 197: 176-187.

ROBERTS S, ASHMOLE I, ROOKES SM AND GALLIMORE PH. 1997. Mutational analysis of the human papillomavirus type 16 E1--E4 protein shows that the C terminus is dispensable for keratin cytoskeleton association but is involved in inducing disruption of the keratin filaments. Journal of virology 71: 3554-3562.

ROBERTS S, HILLMAN ML, KNIGHT GL AND GALLIMORE PH. 2003. The ND10 component promyelocytic leukemia protein relocates to human papillomavirus type 1 E4 intranuclear inclusion bodies in cultured keratinocytes and in warts. Journal of virology 77: 673-684.

ROBERTS S, KINGSBURY SR, STOEBER K, KNIGHT GL, GALLIMORE PH AND WILLIAMS GH. 2008. Identification of an arginine-rich motif in human papillomavirus type 1 E1;E4 protein

necessary for E4-mediated inhibition of cellular DNA synthesis in vitro and in cells. Journal of virology 82: 9056-9064.

ROSITCH AF, GRAVITT PE AND SMITH JS. 2013. Growing evidence that HPV infection is associated with an increase in HIV acquisition: exploring the issue of HPV vaccination. Sex Transm Infect 89: 357.

ROTH JA ET AL. 1996. Retrovirus-mediated wild-type p53 gene transfer to tumors of patients with lung cancer. Nature medicine 2: 985-991.

RUBBERT A, BEHRENS G AND OSTROWSKI M. 2011. Pathogenesis of HIV-1 Infection. HIV 2011, hivbook.

RUELAS DS AND GREENE WC. 2013. An integrated overview of HIV-1 latency. Cell 155: 519-529.

RUX JJ, KUSER PR AND BURNETT RM. 2003. Structural and phylogenetic analysis of adenovirus hexons by use of high-resolution x-ray crystallographic, molecular modeling, and sequence-based methods. Journal of virology 77: 9553-9566.

SABATTE J, CEBALLOS A, RAIDEN S, VERMEULEN M, NAHMOD K, MAGGINI J, SALAMONE G, SALOMON H, AMIGORENA S AND GEFFNER J. 2007. Human seminal plasma abrogates the capture and transmission of human immunodeficiency virus type 1 to CD4+ T cells mediated by DC-SIGN. Journal of virology 81: 13723-13734.

SAMBROOK JF AND RUSSELL DW. 2001. Molecular Cloning: A Laboratory Manual. Cold Spring Harbor Laboratory Press Vols 1,2 and 3: 2100 pp.

SARNGADHARAN MG, POPOVIC M, BRUCH L, SCHUPBACH J AND GALLO RC. 1984. Antibodies reactive with human T-lymphotropic retroviruses (HTLV-III) in the serum of patients with AIDS. Science (New York, NY) 224: 506-508.

SCHADLICH L, SENGER T, GERLACH B, MUCKE N, KLEIN C, BRAVO IG, MULLER M AND GISSMANN L. 2009. Analysis of modified human papillomavirus type 16 L1 capsomeres: the ability to assemble into larger particles correlates with higher immunogenicity. Journal of virology 83: 7690-7705.

SCHIFFMAN M, CASTLE PE, JERONIMO J, RODRIGUEZ AC AND WACHOLDER S. 2007. Human papillomavirus and cervical cancer. Lancet 370: 890-907.

SCOTT M, NAKAGAWA M AND MOSCICKI AB. 2001. Cell-mediated immune response to human papillomavirus infection. Clinical and diagnostic laboratory immunology 8: 209-220.

SCOTT ME, SHVETSOV YB, THOMPSON PJ, HERNANDEZ BY, ZHU X, WILKENS LR, KILLEEN J, VO DD, MOSCICKI AB AND GOODMAN MT. 2013. Cervical cytokines and clearance of incident human papillomavirus infection: Hawaii HPV cohort study. International journal of cancer Journal international du cancer 133: 1187-1196.

SEILHEIMER B, BOHRMANN B, BONDOLFI L, MULLER F, STUBER D AND DOBELI H. 1997. The toxicity of the Alzheimer's beta-amyloid peptide correlates with a distinct fiber morphology. J Struct Biol 119: 59-71.

SEITZ B, MOREIRA L, BAKTANIAN E, SANCHEZ D, GRAY B, GORDON EM, ANDERSON WF AND MCDONNELL PJ. 1998. Retroviral vector-mediated gene transfer into keratocytes in vitro and in vivo. American journal of ophthalmology 126: 630-639.

SEITZ H, SCHMITT M, BOHMER G, KOPP-SCHNEIDER A AND MULLER M. 2013. Natural variants in the major neutralizing epitope of human papillomavirus minor capsid protein L2. International journal of cancer Journal international du cancer 132: E139-148.

SEUBERT P ET AL. 1993. Secretion of beta-amyloid precursor protein cleaved at the amino terminus of the beta-amyloid peptide. Nature 361: 260-263.

SHAW GM AND HUNTER E. 2012. HIV transmission. Cold Spring Harb Perspect Med 2.

SHEFTIC SR, SNELL JM, JHA S AND ALEXANDRESCU AT. 2012. Inhibition of semen-derived enhancer of virus infection (SEVI) fibrillogenesis by zinc and copper. European biophysics journal : EBJ 41: 695-704.

SHEN R, RICHTER HE AND SMITH PD. 2011. Early HIV-1 target cells in human vaginal and ectocervical mucosa. Am J Reprod Immunol 65: 261-267.

SHIRAHAMA T AND COHEN AS. 1967. High-resolution electron microscopic analysis of the amyloid fibril. The Journal of cell biology 33: 679-708.

SIEGAL FP ET AL. 1981. Severe acquired immunodeficiency in male homosexuals, manifested by chronic perianal ulcerative herpes simplex lesions. The New England journal of medicine 305: 1439-1444.

SIPE JD, BENSON MD, BUXBAUM JN, IKEDA S, MERLINI G, SARAIVA MJ AND WESTERMARK P. 2010. Amyloid fibril protein nomenclature: 2010 recommendations from the nomenclature committee of the International Society of Amyloidosis. Amyloid 17: 101-104.

SMITH-MCCUNE KK ET AL. 2010. Type-specific cervico-vaginal human papillomavirus infection increases risk of HIV acquisition independent of other sexually transmitted infections. PloS one 5: e10094.

SMITH JS, MOSES S, HUDGENS MG, PARKER CB, AGOT K, MACLEAN I, NDINYA-ACHOLA JO, SNIJDERS PJ, MEIJER CJ AND BAILEY RC. 2010. Increased risk of HIV acquisition among Kenyan men with human papillomavirus infection. The Journal of infectious diseases 201: 1677-1685.

SRINIVASAN R, JONES EM, LIU K, GHISO J, MARCHANT RE AND ZAGORSKI MG. 2003. pH-dependent amyloid and protofibril formation by the ABri peptide of familial British dementia. Journal of molecular biology 333: 1003-1023.

STATHOPULOS PB, SCHOLZ GA, HWANG YM, RUMFELDT JA, LEPOCK JR AND MEIERING EM. 2004. Sonication of proteins causes formation of aggregates that resemble amyloid. Protein Sci 13: 3017-3027.

STEEN R, WI TE, KAMALI A AND NDOWA F. 2009. Control of sexually transmitted infections and prevention of HIV transmission: mending a fractured paradigm. Bull World Health Organ 87: 858-865.

SUPCHOKPUL A, CHANSAENROJ J, THEAMBOONLERS A, PAYUNGPORN S, KAMOLVARIN N, SAMPATHANUKUL P, JUNYANGDIKUL P, SWANGVAREES S, KARALAK A AND POOVORAWAN Y. 2011. E4 expression of human papillomavirus in cervical samples with different cytology categories. Southeast Asian J Trop Med Public Health 42: 1113-1118.

SWAMINATHAN IYER K, GAIKWAD RM, WOODWORTH CD, VOLKOV DO AND SOKOLOV I. 2012. Physical labeling of papillomavirus-infected, immortal, and cancerous cervical epithelial cells reveal surface changes at immortal stage. Cell Biochem Biophys 63: 109-116.

SWIDSINSKI A, DOERFFEL Y, LOENING-BAUCKE V, SWIDSINSKI S, VERSTRAELEN H, VANEECHOUTTE M, LEMM V, SCHILLING J AND MENDLING W. 2010. Gardnerella biofilm involves females and males and is transmitted sexually. Gynecologic and obstetric investigation 70: 256-263.

SWIDSINSKI A, MENDLING W, LOENING-BAUCKE V, LADHOFF A, SWIDSINSKI S, HALE LP AND LOCHS H. 2005. Adherent biofilms in bacterial vaginosis. Obstetrics and gynecology 106: 1013-1023.

SYRJANEN S. 2011. Human papillomavirus infection and its association with HIV. Adv Dent Res 23: 84-89.

TAKAHASHI KM, R. ET AND AL. 1990. Calpain substrate specificity, . Intracellular calcium-dependent proteolysis CRC Press, Inc., Boca Raton, FL.

: p. 55–74.

TAN CL ET AL. 2012. HPV-18 E2^E4 chimera: 2 new spliced transcripts and proteins induced by keratinocyte differentiation. Virology 429: 47-56.

TANG Q, ROAN NR AND YAMAMURA Y. 2013. Seminal plasma and semen amyloids enhance cytomegalovirus infection in cell culture. Journal of virology 87: 12583-12591.

TAUNTON J, ROWNING BA, COUGHLIN ML, WU M, MOON RT, MITCHISON TJ AND LARABELL CA. 2000. Actin-dependent propulsion of endosomes and lysosomes by recruitment of N-WASP. The Journal of cell biology 148: 519-530.

TERPE K. 2003. Overview of tag protein fusions: from molecular and biochemical fundamentals to commercial systems. Appl Microbiol Biotechnol 60: 523-533.

TEVI-BENISSAN C, BELEC L, LEVY M, SCHNEIDER-FAUVEAU V, SI MOHAMED A, HALLOUIN MC, MATTA M AND GRESENGUET G. 1997. In vivo semen-associated pH neutralization of cervicovaginal secretions. Clinical and diagnostic laboratory immunology 4: 367-374.

TOMMASINO M, ADAMCZEWSKI JP, CARLOTTI F, BARTH CF, MANETTI R, CONTORNI M, CAVALIERI F, HUNT T AND CRAWFORD L. 1993. HPV16 E7 protein associates with the protein kinase p33CDK2 and cyclin A. Oncogene 8: 195-202.

TOVAR JM, BAZALDUA OV, VARGAS L AND REILE E. 2008. Human papillomavirus, cervical cancer, and the vaccines. Postgraduate medicine 120: 79-84.

TOYAMA BH AND WEISSMAN JS. 2011. Amyloid structure: conformational diversity and consequences. Annual review of biochemistry 80: 557-585.

TOYOSHIMA K AND VOGT PK. 1969. Enhancement and inhibition of avian sarcoma viruses by polycations and polyanions. Virology 38: 414-426.

TRKOLA A, GORDON C, MATTHEWS J, MAXWELL E, KETAS T, CZAPLEWSKI L, PROUDFOOT AE AND MOORE JP. 1999. The CC-chemokine RANTES increases the attachment of human immunodeficiency virus type 1 to target cells via glycosaminoglycans and also activates a signal transduction pathway that enhances viral infectivity. Journal of virology 73: 6370-6379.

TSAKOGIANNIS D, RUETHER IG, KYRIAKOPOULOU Z, PLIAKA V, SKORDAS V, GARTZONIKA C, LEVIDIOTOU-STEFANOU S AND MARKOULATOS P. 2012. Molecular and phylogenetic analysis of the HPV 16 E4 gene in cervical lesions from women in Greece. Arch Virol 157: 1729-1739.

TSCHACHLER E, GROH V, POPOVIC M, MANN DL, KONRAD K, SAFAI B, ERON L, DIMARZO VERONESE F, WOLFF K AND STINGL G. 1987. Epidermal Langerhans cells--a target for HTLV-III/LAV infection. J Invest Dermatol 88: 233-237.

TYEDMERS J, MOGK A AND BUKAU B. 2010. Cellular strategies for controlling protein aggregation. Nat Rev Mol Cell Biol 11: 777-788.

UGOLINI S, MONDOR I AND SATTENTAU QJ. 1999. HIV-1 attachment: another look. Trends Microbiol 7: 144-149.

VAN DER LOEFF MF, NYITRAY AG AND GIULIANO AR. 2011. HPV vaccination to prevent HIV infection: time for randomized controlled trials. Sexually transmitted diseases 38: 640-643.

VAN DEURS B, HOLM PK, KAYSER L AND SANDVIG K. 1995. Delivery to lysosomes in the human carcinoma cell line HEp-2 involves an actin filament-facilitated fusion between mature endosomes and preexisting lysosomes. Eur J Cell Biol 66: 309-323.

VELDHUIJZEN NJ, VYANKANDONDERA J AND VAN DE WIJGERT JH. 2010. HIV acquisition is associated with prior high-risk human papillomavirus infection among high-risk women in Rwanda. Aids 24: 2289-2292.

VILLAREJO MR AND ZABIN I. 1974. Beta-galactosidase from termination and deletion mutant strains. Journal of bacteriology 120: 466-474.

VISWANATHAN J ET AL. 2011. Alzheimer's disease-associated ubiquilin-1 regulates presenilin-1 accumulation and aggresome formation. Traffic (Copenhagen, Denmark) 12: 330-348.

WALLIS C AND MELNICK JL. 1968. Mechanism of enhancement of virus plaques by cationic polymers. Journal of virology 2: 267-274.

WANG Q ET AL. 2004. Functional analysis of the human papillomavirus type 16 E1=E4 protein provides a mechanism for in vivo and in vitro keratin filament reorganization. Journal of virology 78: 821-833.

WANG Q, KENNEDY A, DAS P, MCINTOSH PB, HOWELL SA, ISAACSON ER, HINZ SA, DAVY C AND DOORBAR J. 2009. Phosphorylation of the human papillomavirus type 16 E1--E4 protein at T57 by ERK triggers a structural change that enhances keratin binding and protein stability. Journal of virology 83: 3668-3683.

WARD H AND RONN M. 2010. Contribution of sexually transmitted infections to the sexual transmission of HIV. Curr Opin HIV AIDS 5: 305-310.

WATKINS BA, CROWLEY R, DAVIS AE, LOUIE AT AND REITZ MS, JR. 1997. Syncytium formation induced by human immunodeficiency virus type 1 isolates correlates with affinity for CD4. J Gen Virol 78 (Pt 10): 2513-2522.

WATTS JM, DANG KK, GORELICK RJ, LEONARD CW, BESS JW, JR., SWANSTROM R, BURCH CL AND WEEKS KM. 2009. Architecture and secondary structure of an entire HIV-1 RNA genome. Nature 460: 711-716.

WAWER MJ ET AL. 2005. Rates of HIV-1 transmission per coital act, by stage of HIV-1 infection, in Rakai, Uganda. The Journal of infectious diseases 191: 1403-1409.

WHITE RG, ORROTH KK, GLYNN JR, FREEMAN EE, BAKKER R, HABBEMA JD, TERRIS-PRESTHOLT F, KUMARANAYAKE L, BUVE A AND HAYES RJ. 2008. Treating curable sexually transmitted infections to prevent HIV in Africa: still an effective control strategy? J Acquir Immune Defic Syndr 47: 346-353.

WILSON R, FEHRMANN F AND LAIMINS LA. 2005. Role of the E1--E4 protein in the differentiation-dependent life cycle of human papillomavirus type 31. Journal of virology 79: 6732-6740.

WILSON R, RYAN GB, KNIGHT GL, LAIMINS LA AND ROBERTS S. 2007. The full-length E1E4 protein of human papillomavirus type 18 modulates differentiation-dependent viral DNA amplification and late gene expression. Virology 362: 453-460.

WITKIN SS, LINHARES IM AND GIRALDO P. 2007. Bacterial flora of the female genital tract: function and immune regulation. Best Pract Res Clin Obstet Gynaecol 21: 347-354.

WOJTOWICZ WM, FARZAN M, JOYAL JL, CARTER K, BABCOCK GJ, ISRAEL DI, SODROSKI J AND MIRZABEKOV T. 2002. Stimulation of enveloped virus infection by beta-amyloid fibrils. The Journal of biological chemistry 277: 35019-35024.

WURM M, SCHAMBACH A, LINDEMANN D, HANENBERG H, STANDKER L, FORSSMANN WG, BLASCZYK R AND HORN PA. 2010. The influence of semen-derived enhancer of virus infection on the efficiency of retroviral gene transfer. The journal of gene medicine 12: 137-146.

YANG J, LI L, JIN H, TAN S, QIU J, YANG L, DING Y, JIANG ZH, JIANG S AND LIU S. 2012. Vaginal gel formulation based on theaflavin derivatives as a microbicide to prevent HIV sexual transmission. AIDS Res Hum Retroviruses 28: 1498-1508.

YEUNG T, GILBERT GE, SHI J, SILVIUS J, KAPUS A AND GRINSTEIN S. 2008. Membrane phosphatidylserine regulates surface charge and protein localization. Science (New York, NY) 319: 210-213.

YOSHIIKE Y, MINAI R, MATSUO Y, CHEN YR, KIMURA T AND TAKASHIMA A. 2008. Amyloid oligomer conformation in a group of natively folded proteins. PloS one 3: e3235.

ZHANG L ET AL. 2014. A novel modified peptide derived from membrane-proximal external region of human immunodeficiency virus type 1 envelope significantly enhances retrovirus infection. Journal of peptide science : an official publication of the European Peptide Society 20: 46-54.

ZHANG Z ET AL. 1999. Sexual transmission and propagation of SIV and HIV in resting and activated CD4+ T cells. Science (New York, NY) 286: 1353-1357.

ZHAO G ET AL. 2013. Mature HIV-1 capsid structure by cryo-electron microscopy and all-atom molecular dynamics. Nature 497: 643-646.

ZHU L, ZHANG XJ, WANG LY, ZHOU JM AND PERRETT S. 2003. Relationship between stability of folding intermediates and amyloid formation for the yeast prion Ure2p: a quantitative analysis of the effects of pH and buffer system. Journal of molecular biology 328: 235-254.

ZICHICHI L, MANISCALCO M AND . 2012. The challenges of a neglected STI: Molluscum contagiosum. Giornale italiano di dermatologia e venereologia : organo ufficiale, Societa italiana di dermatologia e sifilografia 147: 447-453.

ZUR HAUSEN H. 2009. Papillomaviruses in the causation of human cancers - a brief historical account. Virology 384: 260-265.

ZUSSMAN A, LARA L, LARA HH, BENTWICH Z AND BORKOW G. 2003. Blocking of cell-free and cell-associated HIV-1 transmission through human cervix organ culture with UC781. Aids 17: 653-661.